

DOCKET: A-98-49
Item: II-B1-25

**EDOCKET NO:
EPA-HQ-OAR-2009-0330**

**TECHNICAL SUPPORT DOCUMENT FOR SECTION 194.24
EVALUATION OF THE COMPLIANCE RECERTIFICATION ACTINIDE SOURCE
TERM, BACKFILL EFFICACY AND CULEBRA DOLOMITE DISTRIBUTION
COEFFICIENT VALUES (REVISION 1)**

U. S. Environmental Protection Agency
Office of Radiation and Indoor Air
Center for the Waste Isolation Pilot Plant
1301 L St. N.W.
Washington, DC 20005

November 2010

TABLE OF CONTENTS

Acronym and Abbreviation List	vii
Executive Summary and Report Outline	ix
1.0 Introduction.....	1
2.0 Geologic Setting, Salado Formation Mineralogy, and Brine Chemistry	3
2.1 Geologic Setting.....	3
2.2 Salado Mineralogy	3
2.3 Salado Formation and Castile Formation Brine Chemistry	4
3.0 Gas Generation.....	6
3.1 Iron Corrosion.....	6
3.2 Corrosion of Other Metals	9
3.3 Microbial Gas Generation.....	10
3.3.1 CCA PA, PAVT, and CRA-2004 PA Microbial Gas Generation.....	10
3.3.2 Microbial Gas Generation Evaluation during AMWTF Review	12
3.3.3 PABC04 Microbial Gas Generation	13
3.3.4 Microbial Gas Generation Review for MgO Planned Change Request.....	17
3.3.5 Microbial Gas Generation for the CRA-2009 PA.....	18
3.3.6 Microbial Gas Generation for the PABC09.....	20
3.4 Radiolysis.....	21
3.5 Conclusions Regarding WIPP Gas Generation.....	22
4.0 Backfill Efficacy	23
4.1 CCA PA Conceptual Model and Implementation	23
4.1.1 MgO Reactions in the Repository.....	23
4.1.2 Placement of MgO Backfill	24
4.2 Reviews of MgO Efficacy and Implementation Changes Prior to the CRA-2004 PA	25
4.3 CRA-2004 PA and PABC04 Review of MgO Backfill Efficacy	26
4.3.1 Characterization of Premier MgO.....	26
4.3.2 MgO Hydration and Carbonation Experiments	27
4.3.3 MgO Excess Factor Calculations.....	27
4.4 MgO Planned Change Request	28
4.5 CRA-2009 MgO Backfill Efficacy Review	31
4.6 Backfill Efficacy Conclusions	34
5.0 Actinide Oxidation States	35
5.1 Actinide Oxidation State Information Developed Before the PABC04.....	35
5.2 Actinide Oxidation State Information Developed AFTER the PABC04	38

5.2.1	Uranium	38
5.2.2	Neptunium.....	39
5.2.3	Plutonium.....	40
5.3	Radiolysis.....	43
5.4	Validity of Actinide Oxidation State Assumptions for the PABC09	44
6.0	Dissolved Actinide Source Term	45
6.1	CCA and PAVT Dissolved Actinide Source Term.....	45
6.1.1	FMT Code and Database	46
6.1.2	Oxidation-State Analogy	46
6.1.3	Uranium(VI) Solubility.....	46
6.1.4	CCA PA and PAVT Actinide Solubility Uncertainties	47
6.1.5	Effects of Organic Ligands on Actinide Solubilities	47
6.1.6	Actinide Solubility Calculations for the CCA PAVT.....	48
6.2	CRA-2004 PA Dissolved Actinide Source Term	48
6.2.1	FMT Code and Database	50
6.2.2	Salado Brine Formulation	50
6.2.3	Carbon Dioxide Buffering in the Absence of Significant Microbial Activity	50
6.2.4	Uranium(VI) Solubility.....	51
6.2.5	Actinide Solubility Uncertainties Used in PA	52
6.2.6	Temperature Effects on Actinide Solubilities.....	55
6.2.7	Effects of Organic Ligands on Actinide Solubilities	55
6.3	PABC04 Dissolved Actinide Source Term.....	58
6.3.1	FMT Code and Database	58
6.3.2	Salado Brine Formulation.....	59
6.3.3	Carbon Dioxide Buffering Reactions.....	59
6.3.4	Uranium(VI) Solubility.....	59
6.3.5	Actinide Solubility Uncertainties Used in PA	59
6.3.6	Organic Ligand Concentrations	61
6.3.7	Results of the PABC04 Actinide Solubility Calculations.....	61
6.4	CRA-2009 PA Dissolved Actinide Source Term	62
6.4.1	Waste Inventory	63
6.4.2	Minimum Brine Volume.....	65
6.4.3	Repository Chemical Conditions	65
6.4.4	Actinide Aqueous Speciation and Solubility Data.....	73
6.5	PABC09 Dissolved Actinide Source Term.....	100
6.5.1	FMT Code and Database	100
6.5.2	Chemical Conditions Assumptions.....	101
6.5.3	Organic Ligand Concentrations	101
6.5.4	Results of Actinide Solubility Calculations.....	101
6.5.5	Actinide Solubility Uncertainties.....	106
7.0	Colloidal Actinide Source Term	118

8.0	Total Mobilized Actinide Calculations for PA	124
9.0	Actinides Included in Performance Assessment Calculations.....	128
10.0	Culebra Dolomite Distribution Coefficients	129
10.1	Distribution Coefficients Used in the CCA PA and PAVT	129
10.2	Distribution Coefficients Used in the PABC04 and CRA-2009 PA.....	130
10.3	Distribution Coefficients used in the PABC09.....	132
11.0	Effects of Heterogeneous Waste Loading.....	133
12.0	Effects of Chemical Processes on Repository Water Balance.....	135
13.0	Summary and Conclusions	137
14.0	References.....	141

LIST OF TABLES

Table 2-1.	Brine A, GWB, and ERDA-6 Compositions	5
Table 3-1.	Inventories of Iron-Based Metals and Alloys in Waste and Steel Packaging Materials.....	6
Table 3-2.	Inventories of Aluminum, Lead and Other Metals and Alloys in Waste and Packaging Materials.....	10
Table 3-3.	Inundated Microbial Gas Generation Rates (WAS_AREA:GRATMICI) Used in PA	12
Table 3-4.	Humid Microbial Gas Generation Rates (WAS_AREA:GRATMICH) Used in PA	12
Table 6-1.	Ligand Concentrations Calculated for the CCA PAVT, PABC04 and PABC09	48
Table 6-2.	Actinide Solubility Calculations for the CCA PAVT, the PABC04 and the PABC09	49
Table 6-3.	High Ionic Strength Uranium Solubility Data Evaluated by EPA (2006c)	53
Table 6-4.	Cumulative Density Function Ranges Established by the PABC04 Actinide Solubility Uncertainty Analysis.....	60
Table 6-5.	Changes in Reported Ligand Inventories between the PABC04 and PABC09	64
Table 6-6.	Curium and Neptunium Inventory and Calculated Solubilities.....	65
Table 6-7.	Mass Balance Calculations Comparing Moles of Portlandite in Cement to Moles of Magnesium Available from Brine and Polyhalite, Minimum Brine Volume of 17,400 m ³	69
Table 6-8.	PABC09 Organic Ligand Concentrations and Concentrations Used in the Sensitivity Calculations by Brush and Xiong (2004) and Brush et al. (2008).....	71
Table 6-9.	Solid Americium Phases Predicted by FMT Modeling Calculations	86
Table 6-10.	PABC09 Actinide Solubility Modeling Results With and Without Organic Ligands.....	104
Table 6-11.	Aqueous Actinide Speciation, PABC-2009 FMT Calculations With and Without Organic Ligands*.....	105
Table 6-12.	Comparison of the Thorium(IV) and Americium(III) Solubility Uncertainty Distribution Statistics for the PABC04 and the PABC09.....	108
Table 6-13.	Comparison of Difference Values Calculated for the PABC09 and for Individual Investigations.....	108
Table 6-14.	Americium(III) PABC09 Uncertainty Distribution and Range of Difference Values Calculated for Excluded Data.....	112
Table 7-1.	Actinide Concentrations Associated with Mineral Fragment and Intrinsic Colloids.....	119
Table 7-2.	Proportionality Constants and Maximum Concentrations for Humic and Microbial Colloids.....	122
Table 8-1.	PABC09 Mean Dissolved and Colloidal Actinides	125

Table 8-2.	Recalculated Mean Dissolved and Colloidal Actinides Using Thorium Dissolved and Intrinsic Colloid Data of Altmaier et al. (2004) and Recalculated Mean Uncertainty Distribution Values	127
Table 10-1.	Comparison of Matrix K_d Values for the CCA PA and PAVT With Matrix K_d Values for the CRA-2004 PA, PABC04, CRA-2009 PA and PABC09.....	130

LIST OF FIGURES

Figure 6-1.	Solubility of $\text{ThO}_2 \cdot x\text{H}_2\text{O}(\text{am})$ in 0.1 M to 4 M NaCl with a Total Carbonate Concentration of 0.02 M.....	77
Figure 6-2.	Uranium(VI) Solubility Measured in Carbonate-Free Brine as a Function of pcH	80
Figure 6-3.	Neodymium(III) Solubility in Carbonate-Free 5 M NaCl	90
Figure 6-4.	Neodymium(III) Solubility in 5 M NaCl in the Presence of Carbonate from 0.00001 M to 0.01 M	90
Figure 6-5.	Neodymium(III) Solubility in 5 M NaCl at WIPP-Relevant pcH Values from 9 to 10 as a Function of Total Carbonate Concentration	91
Figure 6-6.	Neodymium Solubility Experiment Results in GWB without Carbonate and Carbonate Concentrations Bracketing Repository Conditions Compared to PABC09 Modeled Value without Organic Ligands, Khalili et al. (1994) Results and FMT-Predicted Concentrations	92
Figure 6-7.	Neodymium Solubility Experiment Results in ERDA-6 without Carbonate and Carbonate Concentrations Bracketing Repository Conditions Compared to the PABC09 Modeled Concentration without Organic Ligands and FMT-Predicted Concentrations	92
Figure 6-8.	Neodymium Solubility Experiment Results in 5 M NaCl and ERDA-6 with Carbonate Concentrations from 0 to 0.001 M, Undersaturation and Oversaturation Experiments.....	94
Figure 6-9.	Recalculated Uncertainty Distribution for +IV Actinide Solubilities.....	111
Figure 6-10.	Recalculated Uncertainty Distribution for +III Actinide Solubilities.....	116

ACRONYM AND ABBREVIATION LIST

AMWTF	Advanced Mixed Waste Treatment Facility
Brine A	Simulated Salado brine formulation
CCA	Compliance Certification Application
CCDF	Complementary cumulative distribution function
CFR	<i>Code of Federal Regulations</i>
CH	Contact handled
Ci	Curie
CPR	Cellulosics, plastics, and rubber
CRA	Compliance Recertification Application
CRA-2004	First Compliance Recertification Application, March 2004
CRA-2009	Second Compliance Recertification Application, March 2009
D	Difference value, $\log_{10}(\text{measured solubility}) - \log_{10}(\text{predicted solubility})$
DBR	Direct brine release
DOE	U.S. Department of Energy
DRZ	Disturbed rock zone
EDTA	Ethylenediaminetetraacetic acid
EEF	Effective Excess Factor
EF	Excess Factor
EEG	Environmental Evaluation Group
Eh	Oxidation/reduction potential
EPA	U.S. Environmental Protection Agency
ERDA-6	Simulated Castile brine formulation
EXAFS	Extended x-ray absorption fine structure
FMT	Fracture Matrix Transport code
FMT_021120.CHEMDAT	Thermodynamic database used for the CRA-2004 PA
FMT_050405.CHEMDAT	Thermodynamic database used for the PABC04 and PABC09
FMT_970407.CHEMDAT	Thermodynamic database used for the PAVT
GWB	Generic Weep Brine, simulated Salado brine formulation
H ₂ S	Chemical formula for hydrogen sulfide
K _d	Distribution coefficient
kPa	kilopascal
K _{sp} ⁰	Solubility product at zero ionic strength
LANL	Los Alamos National Laboratory
LIBD	Laser-induced breakdown detection
LOI	loss on ignition
m	molal, moles/kg solvent (H ₂ O)

M	molar, moles/liter
MB	Marker bed
meq	milliequivalent
MPa	megapascal
μ^0/RT	Standard chemical potential (dimensionless)
Pa	Pascal
PA	Performance assessment
PABC04	CRA-2004 Performance Assessment Baseline Calculations
PABC09	CRA-2009 Performance Assessment Baseline Calculations
PAVT	Performance Assessment Verification Testing
pH	Negative log of the hydrogen ion activity
pcH	Negative log of the hydrogen ion concentration, molar units
pmH	Negative log of the hydrogen ion concentration, molal units
PVC	Polyvinylchloride
RH	Remote handled
RSI	Institute for Regulatory Science
S_m	Measured solubility
SNL	Sandia National Laboratories
S_p	Solubility predicted by FMT calculations
STTP	Actinide Source-Term Waste Test Program
TRU	Transuranic waste
WIPP	Waste Isolation Pilot Plant
XAFS	X-ray absorption fine structure
XANES	X-ray absorption near-edge spectroscopy
XRD	X-ray diffraction

EXECUTIVE SUMMARY AND REPORT OUTLINE

The Waste Isolation Pilot Plant (WIPP) in southeastern New Mexico is an underground facility designed for the permanent disposal of defense-related transuranic (TRU) waste. The U.S. Department of Energy (DOE) operates the WIPP repository under the regulatory oversight of the U.S. Environmental Protection Agency (EPA). DOE submitted the Compliance Certification Application (CCA) to the EPA in 1996. After extensive review of the CCA and supplemental information provided by DOE, including additional performance assessment (PA) calculations referred to as Performance Assessment Verification Testing (PAVT), EPA certified that DOE had met the regulatory requirements and WIPP began accepting waste in March 1999.

DOE is required to submit a Compliance Recertification Application (CRA) every 5 years after the initial receipt of waste at WIPP, and the first CRA (CRA-2004) was submitted to EPA in March 2004 (DOE 2004). EPA reviewed the CRA-2004 and supplemental information provided by DOE, including PA calculations referred to as the CRA-2004 Performance Assessment Baseline Calculations (PABC04), and certified that DOE continued to meet WIPP regulatory requirements (EPA 2006a). DOE submitted the second CRA (CRA-2009) to EPA in March 2009 (DOE 2009). The CRA-2009 PA included the PABC04 actinide solubility calculations. EPA performed a completeness review of the CRA-2009 and in EPA Comment 1-23-1, EPA instructed DOE to perform a new PA to capture changes since the 2004 recertification (Cotsworth 2009a). This PA, the CRA-2009 Performance Assessment Baseline Calculations (PABC09) was performed by DOE and reviewed by EPA. This Technical Support Document summarizes EPA's review of chemistry-related issues important to PA, including actinide source term modeling, backfill efficacy and actinide transport in the Culebra Dolomite above the repository for the WIPP CRA-2009 and PABC09.

Section 1.0 provides a summary of WIPP certification and recertification activities since the CCA. This section also summarizes the regulatory requirements and important waste chemical characteristics and repository processes considered during certification and recertification. WIPP waste characteristics and components that have been identified as potentially affecting the chemistry of the system and repository releases include actinide solubilities and oxidation state distributions; formation of colloidal suspensions containing radionuclides; production of gas from the waste; ferrous metals inventory; cellulose, plastics and rubber (CPR) inventory; chelating agents (organic ligands) and oxyanions; and the activity of each isotope of the radionuclides present in the waste [40 CFR 194.24(b), EPA 1997b].

A summary of the geologic setting, mineralogy of the Salado Formation surrounding the repository and WIPP brine chemistry is provided in Section 2.0. The WIPP repository is excavated within the Salado Formation. The Salado Formation is a relatively thick bedded salt, composed mainly of layers of impure halite [NaCl], with interbedded layers of anhydrite [CaSO₄(s)], polyhalite [K₂MgCa₂(SO₄)₄ • 2H₂O(s)] and mudstone. The low permeability of the Salado Formation provides a significant hydrologic barrier between the repository and other, more transmissive water-bearing strata. The Disturbed Rock Zone (DRZ) is a more permeable, transitory region that forms within the Salado around the repository in response to repository excavation. The Salado Formation is underlain by the Castile Formation. The Castile Formation is mainly composed of thick beds of high-purity halite, alternating with thick beds of interlaminated carbonate and anhydrite. The Castile Formation has been significantly deformed

in some areas near the WIPP repository, and pressurized brines are associated with the deformed areas. The Salado Formation is overlain by the Rustler Formation. The Rustler formation is composed of evaporite layers, of which the Culebra Dolomite is the most significant to WIPP PA. The Culebra Dolomite, which is mostly composed of dolomite [$\text{CaMg}(\text{CO}_3)_2(\text{s})$] with small amounts of anhydrite or gypsum [$\text{CaSO}_4 \cdot 2\text{H}_2\text{O}(\text{s})$], is the most transmissive continuously saturated unit above the WIPP facility. It therefore provides the most direct pathway from the repository to the accessible environment, apart from releases directly to the surface.

Small quantities of intergranular and intragranular Salado brines are associated with the salt at the repository horizon. These brines are highly concentrated (ionic strengths up to 8 molar), with a composition of mostly sodium, magnesium, potassium, chloride and sulfate, and with smaller amounts of calcium, carbonate and borate. Two formulations of these Salado brines have been used in WIPP laboratory experiments and in PA calculations—Brine A and Generic Weep Brine (GWB) (Snider 2003b). Brine A was used in the CCA PAVT to simulate intergranular Salado brines. However, this formulation was replaced by GWB for the CRA-2004 PA, the PABC04, CRA-2009 PA and PABC09. Castile brine may enter the repository if a borehole that penetrates the repository also penetrates an area of pressurized brine in the underlying Castile Formation. The ERDA-6 brine composition has been used to represent the likely composition of Castile brine in laboratory experiments and all WIPP PA calculations. ERDA-6 brine has lower magnesium and chloride concentrations and a lower ionic strength than GWB.

Section 3.0 provides a review and discussion of the Gas Generation conceptual model and its implementation for WIPP PA. The Gas Generation conceptual model includes the assumptions that significant gas generation will occur in the repository through corrosion of ferrous metals and through microbial degradation of CPR. It also assumes that essentially all carbon dioxide [CO_2] will be removed from the gas phase by reaction with the magnesium oxide (MgO) backfill. The effects of corrosion of other metals such as lead and aluminum are insignificant to PA because of the small amount of gas production that is likely to occur relative to anoxic corrosion of iron-based metals. It is also assumed that radiolysis of water in the waste and brine, and radiation of plastics and rubber in the waste will not significantly affect the amounts of gas generated.

Corrosion of iron-based metals in the repository is assumed to occur principally through anoxic corrosion and cannot occur unless brine is present. The humid corrosion rate is assumed equal to zero and the inundated corrosion rate is assumed to be a function of both brine saturation and steel surface area. Anoxic corrosion of iron-based metals in the waste and waste containers produces hydrogen and the reaction products $\text{Fe}(\text{OH})_2 \cdot x\text{H}_2\text{O}(\text{s})$ and $\text{FeS}(\text{s})$. The anoxic corrosion rate parameters and implementation have not changed since the CCA PAVT was reviewed and approved. Since the CCA PAVT, reviews of the iron corrosion rate parameters and PA implementation have supported the conceptual model and approach used to model iron corrosion for WIPP PA. Consequently, the Gas Generation conceptual model assumptions related to iron corrosion and implementation of anoxic corrosion in the CRA-2009 PA and PABC09 remain adequate.

Microbial gas generation was implemented for the CCA PAVT and the CRA-2004 PA using microbial gas generation rates measured in short-term WIPP-specific experiments with cellulose. Significant microbial degradation of cellulose was assumed not to occur in 50% of the PA

realizations, with significant degradation of cellulose in 25% of the PA realizations and significant degradation of cellulose, plastics and rubber in the remaining 25% of the PA realizations. For the PABC04, the CRA-2009 PA and PABC09, an initial gas pressure was used to account for rapid initial microbial gas generation rates, with lower rates used to account for slower long-term microbial gas generation through CPR degradation. It was assumed that significant microbial degradation of cellulose could occur in all PA realizations. Because of uncertainty regarding microbial degradation of plastics and rubber, it was assumed that plastics and rubber degradation could only occur in only 25% of the PA realizations. Based on the available data that include WIPP-specific long-term degradation experiments, the current approach for modeling microbial gas generation rates is appropriate for PA.

Section 4.0 describes the MgO backfill included in the WIPP repository to control repository chemical conditions and minimize actinide solubilities in the postclosure repository. The MgO backfill was determined by EPA to meet the requirements for an engineered barrier. MgO reacts with water in the repository to create brucite $[\text{Mg}(\text{OH})_2(\text{s})]$, and brucite dissolution buffers brine pH to prevent low pH values that could increase actinide solubilities. Brucite also reacts with CO_2 produced by microbial degradation of CPR to form hydromagnesite $[\text{Mg}_5(\text{CO}_3)_4(\text{OH})_2 \cdot 4\text{H}_2\text{O}(\text{s})]$, controlling CO_2 fugacities at low levels that minimize actinide solubilities in repository brines. Hydromagnesite is expected to convert to magnesite $[\text{MgCO}_3(\text{s})]$, which is the more stable phase and which will control CO_2 fugacities at even lower levels.

Evaluation of the available data indicates that the MgO backfill will control CO_2 fugacities under inundated conditions and maintain chemical conditions in WIPP brines that limit actinide solubilities. The current emplacement plan ensures adequate amounts of MgO, because the quantities of CPR and MgO are monitored in each room of the repository during emplacement, and additional MgO is emplaced if necessary. Because of uncertainties in the rate at which hydromagnesite will convert to magnesite in the repository environment, it is assumed for PA that the brucite-hydromagnesite reaction will buffer CO_2 fugacity at levels consistent with relatively low actinide solubilities under inundated conditions. The MgO reactivity test results obtained by DOE have demonstrated that the current backfill material will adequately control chemical conditions in the repository. The MgO reactivity testing procedure should effectively detect any MgO shipments with inadequate percentages of reactive periclase $[\text{MgO}(\text{s})]$ plus lime $[\text{CaO}(\text{s})]$.

Section 5.0 provides a review of the expected actinide oxidation states in the repository environment. The actinide oxidation states assumed for PA have remained unchanged since the CCA. As part of the Chemical Conditions conceptual model, equilibrium is not assumed for oxidation-reduction (redox) reactions among the actinides. Actinide oxidation states were determined based on the assumption that reducing conditions would be established relatively quickly in the WIPP repository, combined with the results of a literature review and experimental investigations.

Americium(III), curium(III) and thorium(IV) are assumed to be the only stable oxidation states for these radionuclides. However, uranium, neptunium and plutonium may be present in different oxidation states in the expected repository environment. It has been assumed for PA that uranium may exist in either the +IV or +VI oxidation state. This assumption remains valid,

based on the available data. Uranium(IV) is likely to be the most stable oxidation state under the reducing conditions in the WIPP repository. However, uranium(VI) may persist because of the effects of complexation on uranium reduction. It is assumed that neptunium will be present in the WIPP repository in either the +IV or +V oxidation state. The available evidence indicates that neptunium will be most likely present in the +IV oxidation state. The assumption that neptunium may be present in the +V oxidation state in the WIPP repository brines is conservative, because of the greater solubility of neptunium(V) solid phases. However, because of the relatively small neptunium inventory, the assumption of higher neptunium solubility in half of the PA realizations is unlikely to affect PA results. The assumption that plutonium will be present in the less-soluble +III and +IV oxidation states, rather than the more-soluble +V and +VI oxidation states, continues to be supported by the available data. The plutonium(III) oxidation state may be stable or may metastably persist under anticipated WIPP repository conditions. Radiolytic effects on actinide oxidation states have been assumed to be mitigated by the effects of reducing materials, mainly iron metal, in the WIPP repository and the available data continue to support this assumption.

Americium, curium, neptunium, plutonium, thorium and uranium solubilities used in PA are discussed in Section 6.0. Actinides in the WIPP waste inventory may dissolve in brines that enter the repository, either as brine that flows into the repository from the DRZ in the Salado Formation, or brine that flows up a borehole that intersects both the repository and a pressurized brine region in the underlying Castile Formation. In the repository, it is assumed that the possible brine compositions can be represented by end-member Salado (Brine A or GWB) and Castile (ERDA-6) brine equilibrated with Salado minerals and MgO hydration and carbonation products. The solubilities of americium(III), thorium(IV) and neptunium(V) are calculated for WIPP repository conditions using the FMT code and database. The FMT code and database were revised between the CCA PAVT and the PABC04. The PABC04 versions of the code and database were used for the PABC09 actinide solubility calculations.

The Dissolved Actinide Source Term conceptual model includes the assumption that actinides in the same oxidation state will exhibit the same solubilities and aqueous speciation. Accordingly, the solubilities of curium(III) and plutonium(III) are assumed equal to the solubility calculated for americium(III) and the solubilities of uranium(IV), neptunium(IV) and plutonium (IV) are assumed equal to the calculated thorium(IV) concentration. Calculated neptunium(V) solubilities are used only for neptunium, because it is the only actinide predicted to be present in WIPP brines in the +V oxidation state. Because DOE has not developed an aqueous speciation and solubility model for uranium(VI), an upper-limit concentration of 10^{-3} M is assumed for PA. The organic ligands acetate, citrate, ethylenediaminetetraacetic acid (EDTA) and oxalate could affect actinide solubilities in the repository because these ligands are water soluble and present in significant quantities in the WIPP inventory. The effects of organic ligands on actinide solubilities were not included in the CCA PAVT actinide solubility calculations because it was assumed that other constituents, including transition metals in the waste and magnesium from the MgO backfill, would compete with the actinides for binding sites on the organic ligands. The effects of organic ligands on actinide solubilities were included in the PABC04 and PABC09 and it was determined that the solubilities of the +III actinides are influenced by the assumed concentration of EDTA. The concentrations of the +IV actinides are unaffected by organic ligands at the concentrations predicted for the repository. The solubility of neptunium(V) may be affected by oxalate and acetate, but the neptunium inventory is too small to affect repository

performance. The potential effects of organic ligands on uranium(VI) solubility in WIPP brines cannot be directly determined because DOE has not developed a high-ionic-strength model for the +VI actinides. However, evaluation of the available data regarding the complexation of uranium(VI) under anticipated WIPP repository conditions indicates that organic ligands are unlikely to significantly affect uranium(VI) solubilities in WIPP brines because of the formation of relatively stable uranium(VI)-carbonate species.

The actinide solubilities calculated for the PABC04 were also used for the CRA-2009 PA dissolved actinide source term. The PABC04 actinide solubilities did not take into account the effects of the most recent inventory data. Because the updated inventory data included larger amounts of organic ligands compared to previous inventories, new actinide solubility calculations were carried out for the PABC09. The updated organic ligand inventory data were used with a revised minimum brine volume to calculate the concentrations of organic ligand used in the PABC09 actinide solubility calculations.

DOE qualitatively reviewed recent literature data regarding actinide solubilities, but did not revise the FMT database for the CRA-2009 PA or PABC09 calculations. Recent data have indicated that thorium intrinsic colloids may form and that dissolved thorium concentrations in equilibrium with amorphous thorium hydroxide in the WIPP repository may be lower than currently predicted by FMT calculations. New data have also been developed indicating the formation of different aqueous thorium-carbonate species than those included in the FMT database. Review of these data indicates that the +IV actinide solubilities calculated for the PABC09 were adequate. However, because new data are available regarding aqueous thorium speciation, solubility and intrinsic thorium colloid formation, DOE should undertake a thorough analysis and update of the thorium aqueous speciation and solubility data in the FMT database prior to the CRA-2014 PA to comply with the requirement that compliance recertification applications contain updated geochemical information [40 CFR194.15(a)(1)].

DOE has reported the results of an investigation of the solubility of uranium(VI) solid phases in GWB and ERDA-6 brines in the absence of carbonate. The concentrations of uranium(VI) in carbonate-free GWB and ERDA-6 brines were lower than previously reported for carbonate-free 5 M NaCl brines by Díaz Arocas and Grambow (1998). However, because of the expected importance of carbonate complexation on uranium(VI) concentrations in brine under repository conditions, these experiments cannot be used to revise the existing 10^{-3} M estimated upper limit for the solubility of uranium(VI) for WIPP PA.

Although a solubility model has been developed for predicting the aqueous concentrations of neptunium(V) for PA, the inventory of neptunium-237 in the repository is relatively small and does not significantly affect repository performance. No additional WIPP-relevant data related to the solubility or speciation of neptunium(V) have been identified since the PABC04 and the existing FMT database is consistent with the available literature data.

DOE (2009) reported the results of a neodymium(III) solubility investigation as an analogue for the solubility of +III actinides in 5 M NaCl, GWB and ERDA-6 brines. EPA's review of the data indicated that the solid phases present in experiments conducted with carbonate are uncertain because the identity of the solid phase formed in the experiments were indirectly determined and FMT calculations performed to simulate experimental conditions predicted the

formation of $\text{NdOHCO}_3(\text{cr})$ and $\text{NaNd}(\text{CO}_3)_2 \cdot 6\text{H}_2\text{O}(\text{cr})$ in addition to $\text{Nd}(\text{OH})_3(\text{s})$, depending on pH and total carbonate concentrations. Experimental results in ERDA-6 brine at WIPP-relevant pH values and carbonate concentrations were approximately one order of magnitude higher than FMT-predicted concentrations under these conditions. This difference was attributed by DOE to complexation of the +III actinides by borate. Experimental results in GWB brine were not obtained at WIPP-relevant pH values, so it is impossible to determine the effects of borate complexation in GWB brine under WIPP-relevant conditions. Significant disagreement between measured and predicted concentrations at low pH values (6.60 to 7.97) in carbonate-free GWB indicates that the FMT model is not well parameterized under these conditions. The cause of this disagreement between the measured and predicted solubilities is uncertain, but is of limited relevance to PA because these lower pH conditions are not expected in the WIPP repository.

The results of the neodymium(III) solubility experiments indicate that in the absence of organic ligands, the concentrations of +III actinides in ERDA-6 brine and possibly in GWB brine may exceed the actinide solubilities predicted using the current FMT database. However, the predicted concentration in ERDA-6 brine calculated for the PABC09 in the presence of organic ligands is slightly higher than the concentrations measured by Borkowski et al. (2009) at pH 9.7. Brush et al. (2008) performed a sensitivity study that assessed the effects of higher +III actinide solubilities on WIPP repository performance. Brush et al. (2008) determined that higher +III actinide solubilities increased DBR and total repository releases, but the effects were most evident at low probabilities and WIPP performance complied with EPA containment requirements. The effects of borate complexation on the solubility of the III actinides indicated by the Borkowski et al. (2009) experimental results will be smaller than the effects of organic ligands considered by Brush et al. (2008). As a result, borate complexation of the +III actinides is expected to have insignificant effects on repository performance.

The calculated actinide solubilities used in the PABC04 and PABC09 are higher than the solubilities used in the CCA PAVT. The increased concentrations of the +III actinides are primarily caused by increased inventories of organic ligands. Smaller increases in the +IV actinide solubilities result from changes in the thorium(IV) data in the FMT database since the CCA PA. The assumed uranium(VI) concentration used in the PABC04 and PABC09 is specified by EPA based on a review of the available literature. The concentrations of thorium(IV) and neptunium(V) are predicted to be controlled by the solubilities of $\text{ThO}_2(\text{am})$ and $\text{KNpO}_2\text{CO}_3(\text{s})$, respectively, which have remained unchanged since the CCA PAVT. For the CCA PAVT, $\text{AmOHCO}_3(\text{cr})$ was predicted to be the solubility-controlling solid for the +III actinides. As a result of revisions to the FMT database between the CCA PAVT and the PABC04, $\text{Am}(\text{OH})_3(\text{s})$ has been predicted to be the solubility-controlling solid phase for the PABC04 and PABC09.

The calculated solubilities for the +III, +IV, and +V actinides are constant values, with associated uncertainties. The +III, +IV and +V actinide solubilities used in each PA realization are the products of the antilog of the sampled uncertainties multiplied by the calculated solubilities. The uranium(VI) solubility used for the PABC04 and PABC09 has been an upper-limit, fixed value of 10^{-3} M for all PA realizations, without an associated uncertainty. For the CRA-2009 PA, the uncertainty distributions for each oxidation state were sampled for each realization using the distributions developed for the PABC04. At EPA's request, DOE re-

evaluated the +III and +IV actinide solubility uncertainty distributions and sampled these revised distributions for the PABC09.

The mean and median of the PABC09 +IV actinide solubility uncertainty distribution were lower than the PABC04 values. During their evaluation of the +IV actinide solubility uncertainty distribution for the PABC09, DOE did not include data from a number of experimental solubility investigations for thorium in carbonate solutions. DOE also included some data from samples that did not undergo filtration or centrifugation to remove colloidal thorium from the solutions. Removing the unfiltered, uncentrifuged data and including high-ionic-strength thorium-carbonate solubility data in the uncertainty distribution data increased the mean and median of the +IV actinide solubility uncertainty distribution. Although the increased mean value for the +IV actinide solubility uncertainty distribution would increase mean releases relative to the mean releases calculated for the PABC09, these changes would be relatively small, would occur only at low probabilities where DBR is important and would not significantly affect repository compliance.

The mean of the PABC09 +III actinide solubility uncertainty distribution was slightly lower and the median was slightly higher compared to the values for the PABC04 uncertainty distribution. For the PABC09 +III actinide solubility uncertainty distribution determination, DOE excluded some solubility data because it was obtained prior to the specified time frame for a literature search for appropriate data, excluded other solubility data obtained at moderately alkaline pH values in WIPP brines and included data from a study that did not directly determine the identity of the solubility-controlling solid phases. Recalculation of the +III actinide solubility uncertainty distribution resulted in a slightly higher mean, median and maximum and a significantly higher minimum than the uncertainty distribution used in the PABC09. Because the mean of the recalculated uncertainty distribution is only slightly higher than the mean of the distribution sampled for the PABC09, the effects on mean repository releases would be small.

The WIPP colloidal actinide source term is summarized in Section 7.0. The Colloidal Actinide Source Term conceptual model was peer reviewed and found to be adequate prior to the CCA PA and PAVT. This conceptual model and its PA implementation were the same for the CCA PAVT, PABC04, CRA-2009 PA and PABC09. It has been assumed that four types of colloids can form in the WIPP repository, including microbial, humic, intrinsic and mineral fragment colloids. Actinide concentrations associated with microbial and humic colloids are based on proportionality constants with maximum values and these values have remained unchanged since the CCA PAVT. The concentrations of actinide intrinsic colloids and mineral fragment colloids used in PA are constant values based on the results of experimental investigations.

In the absence of evidence of the formation of actinide intrinsic colloids for radionuclides other than plutonium, the concentrations of thorium, uranium, neptunium and americium intrinsic colloids are set equal to zero. Recent thorium solubility investigations, however, have identified the existence of intrinsic thorium colloids in dilute solution and in brines. The potential effects of thorium intrinsic colloids are not expected to significantly affect total mobilized thorium concentrations calculated for PA. However, the new data regarding intrinsic thorium colloid formation should be considered prior to the CRA-2014 PA so that DOE continues to comply with the requirement that compliance recertification applications contain updated geochemical information [40 CFR194.15(a)(1)].

Experimental data have been recently reported indicating that mineral fragment colloids may form and mobilize thorium in $MgCl_2$ brines. Although the mineral-fragment colloids reported in the recent literature are not expected to be stable in WIPP brines, examination of the data used to develop the colloidal actinide source term model has shown that possible formation of mineral fragment colloids by MgO and its hydration and carbonation products under WIPP-relevant conditions has not been evaluated. Because colloids capable of transporting actinides have been demonstrated to form from reaction of MgO in brines under some conditions, this omission introduces some uncertainty into the colloidal actinide source term model. To minimize this uncertainty, DOE should evaluate the potential formation of mineral-fragment colloids from MgO hydration and carbonation under WIPP-relevant conditions before the CRA-2014 PA.

Section 8.0 provides a summary of calculations of the total mobilized actinides for PA. Using mean PABC09 dissolved actinide concentrations and solubility uncertainty parameters, mobilized actinides are dominated by colloidal actinides for americium(III), thorium(IV), uranium(IV), neptunium(IV), plutonium(IV) and neptunium(V) in both GWB and ERDA-6 brines. Plutonium(III) mobilized in GWB is dominated by the dissolved concentration, whereas in ERDA-6, the concentrations of plutonium(III) mobilized as colloidal species is higher than the dissolved concentration. The mobilized concentration of uranium(VI) is dominated by dissolved species for both GWB and ERDA-6. Thorium intrinsic colloid formation is unlikely to significantly affect repository performance because the WIPP inventory is dominated by isotopes of americium and plutonium. The higher mean for the recalculated +III actinide solubility uncertainty distribution increased total mobilized +III actinide concentrations by about a factor of two, but these higher concentrations would have relatively small effects on repository performance and only at low probabilities.

Section 9.0 summarizes the actinide elements and isotopes included in WIPP PA calculations. Not all radionuclides in the WIPP inventory are included in PA calculations because of computational and time constraints. Consequently, the number of radionuclides included in PA has been reduced according to an algorithm initially developed for the CCA. Calculations of releases through direct brine release (DBR) include isotopes of plutonium, americium, uranium, thorium, neptunium and curium. A smaller number of plutonium, americium, uranium and thorium isotopes are used to calculate releases by transport through the Culebra and Salado. The results of PA calculations indicate that radionuclide releases are dominated by plutonium and americium.

Distribution coefficient (K_d) values used to calculate radionuclide transport through the Culebra are described in Section 10.0. These distribution coefficients are based on the results of WIPP-specific sorption studies carried out on Culebra rock samples and pure dolomite. During selection of these K_d values for the CCA PA and CCA PAVT, it was assumed that relatively low organic ligand concentrations would have negligible effects on K_d values. Distribution coefficients used in the CCA PA and PAVT were changed slightly for the CRA-2004 PA because of errors in the masses of dolomite and in the brine density used to calculate the K_d values. These revised values were also used for the PABC04 and CRA-2009 PA. Because of higher predicted organic ligand concentrations for the PABC09, the ranges of K_d values used in the PABC09 were adjusted for the +III and +IV actinides. For these actinide oxidation states, the lower limits of the K_d distribution were decreased to be consistent with the lowest K_d values measured with relatively high concentrations of organic ligands in WIPP-specific experiments.

Section 11.0 examines the potential effects of the assumption of homogeneity used in actinide solubility modeling. This assumption is potentially significant because of heterogeneous waste loading that has occurred in the WIPP repository and use of a panel closure that makes it relatively unlikely that brine in contact with waste in one panel of the repository will contact brine in another panel. Because chemical equilibrium is assumed between brine and actinide solubility-controlling solids, heterogeneous distribution of the radionuclide inventory between the panels will not affect the calculated actinide solubilities. DOE has adequately accounted for the effects of possible heterogeneous distribution of organic ligands between panels in the actinide solubility calculations.

Section 12.0 addresses the effects of chemical processes on the repository water balance. Chemical processes that may affect the quantity of water in the repository include anoxic corrosion of iron-based metal, microbial degradation of CPR, MgO hydration to form brucite or hydromagnesite and dehydration of hydromagnesite to form magnesite. Anoxic corrosion is the only process included in calculations of the quantity of brine in the repository. Microbial production of water during CPR degradation, and consumption of water by MgO hydration and hydromagnesite persistence are likely to be important only when relatively large quantities of brine enter the repository. In addition, there is significant uncertainty associated with the probability of plastics and rubber degradation, which constitute approximately two thirds of the CPR carbon in the inventory. Consequently, a more detailed repository water balance is not practical at this time.

Section 13.0 summarizes the Agency's conclusions based on their review of chemistry issues related to the CRA-2009 and the PABC09. Review of the CRA-2009 (DOE 2009) and supporting information, including the results of the PABC09, indicates that DOE adequately addressed all chemistry issues relevant to repository performance. There are a number of uncertainties related to chemical processes that may affect radionuclide releases from the WIPP repository during the 10,000-year regulatory period that have been addressed for WIPP PA by making appropriately conservative, bounding assumptions. These uncertainties include:

- The rates at which plastics and rubber will degrade, including the effects of radiolytic processes on microbial degradation
- The availability of sulfate in Salado Formation minerals, including the amounts of sulfate minerals and the rates of sulfate transport to the waste in the repository, which results in uncertainties in the relative amounts of CPR degradation that may occur via sulfate reduction and methanogenesis
- Extrapolation of microbial degradation rates from short-term laboratory experiments to long-term repository conditions
- Hydromagnesite to magnesite conversion rate under repository conditions
- Oxidation states of plutonium, neptunium and uranium in the repository environment
- Effects of organic ligands on actinide solubilities and Culebra transport

During this review, a number of ongoing issues related to WIPP repository chemical processes have been identified for possible additional investigation prior to the CRA-2014:

- Lack of rate data for brucite carbonation under humid conditions
- Review, and if appropriate, incorporation of recent literature data into the FMT geochemical modeling database for the +III and +IV actinide solubility calculations
- Development of a uranium(VI) aqueous speciation and solubility model and incorporation of this model into the FMT database
- Critical re-evaluation of the thorium-carbonate aqueous speciation and $\text{ThO}_2(\text{am})$ solubility
- Revision of the uncertainty distributions for the +III and +IV actinide solubilities using the available literature data and a consistent, well-documented method for selecting experimental data included in the uncertainty evaluation
- Evaluation of possible thorium intrinsic colloid formation
- Evaluation of the formation of pseudocolloids in WIPP brines from MgO hydration and carbonation products and potential effects on total mobilized actinides
- Evaluation of the effects of microbial degradation of CPR, MgO hydration, hydromagnesite dehydration and FeS formation on the repository water balance

These issues were qualitatively addressed during this review where it was determined that their impact on PA is minor. However, it is anticipated that a more quantitative approach for addressing these issues will expedite the review of future recertification applications.

1.0 INTRODUCTION

The Waste Isolation Pilot Plant (WIPP) in southeastern New Mexico is an underground facility designed for the permanent disposal of transuranic (TRU) defense-related waste. The U.S. Department of Energy (DOE) operates the WIPP repository under the regulatory oversight of the U.S. Environmental Protection Agency (EPA). DOE submitted the Compliance Certification Application (CCA) to the EPA in 1996. After extensive review of the CCA and supplemental information provided by DOE, including additional performance assessment (PA) calculations referred to as Performance Assessment Verification Testing (PAVT), EPA certified that DOE had met the regulatory requirements and WIPP began accepting waste in March 1999.

DOE is required to submit a Compliance Recertification Application (CRA) every 5 years after the initial acceptance of waste at WIPP, and the first CRA (CRA-2004) was submitted to EPA in March 2004 (DOE 2004). EPA reviewed the CRA-2004 and supplemental information provided by DOE, including PA calculations referred to as the CRA-2004 Performance Assessment Baseline Calculations (PABC04), and certified that DOE continued to meet WIPP regulatory requirements (EPA 2006a). DOE submitted the second CRA (CRA-2009) to EPA in March 2009 (DOE 2009). The CRA-2009 PA included the actinide solubility and colloidal actinide source term calculations from the PABC04. EPA performed a completeness review of the CRA-2009 and in EPA Comment 1-23-1, EPA instructed DOE to perform a new PA to capture changes since the 2004 recertification (Cotsworth 2009a). This revised PA, the CRA-2009 Performance Assessment Baseline Calculations (PABC09), was performed by DOE and reviewed by EPA.

Waste characteristics and waste components must be analyzed and the results must be included in any certification application [40 CFR 194.24(b)]. Those waste characteristics and components that could affect releases must be incorporated into PA [40 CFR 194.32(a)]. All additional data collected since the most recent CCA or CRA must be included in the CRA [40 CFR 194.15(a)], including any geochemical information, analyses, or results of laboratory experiments that are relevant to the performance of the repository. WIPP waste characteristics and components that have been identified as potentially affecting the chemistry of the system and releases include actinide solubilities and oxidation state distributions; formation of colloidal suspensions containing radionuclides; production of gas from the waste; ferrous metals inventory; cellulose, plastics, and rubber (CPR) inventory; chelating agents (organic ligands) and oxyanions; and the activity of each isotope of the radionuclides present in the waste [40 CFR 194.24(b), EPA 1997b].

This Technical Support Document summarizes EPA's review of chemistry-related issues important to PA, including actinide source term modeling, backfill efficacy, and actinide transport in the Culebra Dolomite above the repository for the WIPP CRA-2009 and PABC09. The principal portions of CRA-2009 (DOE 2009) addressed during this review are Appendix SOTERM and its supporting references, portions of §194.44 and Appendix MgO and their supporting references, and portions of Appendix MASS and its supporting references. Information has also been obtained from DOE's responses to EPA's requests for additional information and from the results of reviews of chemistry-related issues carried out by EPA since the CCA.

Chemistry-related topics addressed in this report include Salado Formation mineralogy surrounding the repository and the chemistry of Salado and Castile brines (Section 2.0); gas generation caused by microbial degradation of CPR and anoxic corrosion of metals in the repository (Section 3.0); the ability of the magnesium oxide (MgO) backfill to control chemical conditions (Section 4.0); actinide oxidation states assumed in source term modeling (Section 5.0); dissolved actinide source term modeling (Section 6.0); colloidal actinide source term modeling (Section 7.0); PA calculations of total mobilized actinides (Section 8.0); an assessment of the actinides included in PA (Section 9.0); distribution coefficients (K_{ds}) used in PA to model the release of actinides by transport through the Culebra member of the Rustler Formation (Section 10.0); the effects of heterogeneous waste loading (Section 11.0); and the effects of chemical processes on repository water balance (Section 12.0).

The results of this review indicate that DOE has continued to improve its assessment of repository chemical processes as additional information has become available since the CCA PAVT and PABC04. There remains considerable uncertainty associated with a number of repository chemical processes, including:

- Whether significant microbial degradation of plastic and rubber will occur in the repository, potentially releasing CO_2
- The availability of sulfate from the Salado Formation that could limit methanogenesis and increase the production of CO_2 during microbial degradation of CPR
- The rate at which hydromagnesite $[\text{Mg}_5(\text{CO}_3)_4(\text{OH})_2 \cdot 4\text{H}_2\text{O}(\text{s})]^1$ will convert to magnesite $[\text{MgCO}_3]$ in the repository and consume additional CO_2 while releasing water
- The effects of organic ligands, such as ethylenediaminetetraacetic acid (EDTA), on actinide solubilities
- The solubility of uranium(VI)-bearing solid phases under repository conditions
- The effects of chemical processes, such as hydromagnesite conversion to magnesite, and CPR degradation on the repository water balance

DOE has appropriately accounted for many of these uncertainties by making bounding assumptions where appropriate. Consequently, modeling of repository chemical processes for the PABC09 remains adequately conservative.

¹ DOE has reported two compositions for hydromagnesite: hydromagnesite₅₄₂₄ $[\text{Mg}_5(\text{CO}_3)_4(\text{OH})_2 \cdot 4\text{H}_2\text{O}(\text{s})]$ and hydromagnesite₄₃₂₃ $[\text{Mg}_4(\text{CO}_3)_3(\text{OH})_2 \cdot 3\text{H}_2\text{O}(\text{s})]$ (DOE 2009, Appendix MgO, Section 4.2.1). Only the hydromagnesite₅₄₂₄ composition has been observed to form in WIPP-specific experiments and hydromagnesite₅₄₂₄ is the composition recognized by the International Mineralogical Association (<http://pubsites.uws.edu.au/ima-cnmmc/IMA2009-01%20UPDATE%20160309.pdf>). Consequently, all references to hydromagnesite in this document refer to the hydromagnesite₅₄₂₄ composition.

2.0 GEOLOGIC SETTING, SALADO FORMATION MINERALOGY, AND BRINE CHEMISTRY

WIPP repository chemical processes are influenced by the chemistry of the waste and by interaction of the waste with brines that may contact the waste and with the minerals in the Salado Formation that surrounds the repository. As a result, the geologic setting, Salado Formation mineralogy and the chemistry of brines that could contact the waste can affect actinide releases from the repository and subsequent transport. The Salado mineralogy and the chemistry of brines that may contact WIPP waste are described in the CRA-2009 (DOE 2009, Appendix SOTERM, Section 2.0) and in the CRA-2004 (DOE 2004, Section 6.0).

2.1 GEOLOGIC SETTING

The WIPP repository is excavated within the Salado Formation. The low permeability of the Salado Formation surrounding the WIPP repository provides a significant hydrologic barrier between the repository and other, more transmissive water-bearing strata. A more permeable, transitory region forms within the Salado around the repository in response to the stress field caused by repository excavation; this region is called the Disturbed Rock Zone (DRZ) (DOE 2004, Section 6.0). The DRZ is relatively thin compared to the thickness of the Salado Formation surrounding the repository (DOE 2004, Section 6.0).

The Salado Formation is underlain by the Castile Formation. The Castile Formation is mainly composed of thick beds of high-purity halite, alternating with thick beds of interlaminated carbonate and anhydrite [$\text{CaSO}_4(\text{s})$] (DOE 2004, Section 2.0). The Castile Formation has been significantly deformed in some areas near the WIPP repository and pressurized brines are associated with the deformed areas.

The Salado Formation is overlain by the Rustler Formation (DOE 2004, Section 2.0). This formation is composed of evaporite layers called, from bottom to top, the Los Medaños Member, the Culebra Dolomite Member, the Tamarisk Member, the Magenta Dolomite Member, and the Forty-Niner Member. The Culebra Dolomite is mostly composed of dolomite [$\text{CaMg}(\text{CO}_3)_2(\text{s})$], with small amounts of anhydrite or gypsum [$\text{CaSO}_4 \cdot 2\text{H}_2\text{O}(\text{s})$] (Lambert 1992). The Culebra Dolomite is the most transmissive continuously saturated unit above the WIPP facility. It therefore provides the most direct pathway from the repository to the accessible environment, apart from releases directly to the surface (DOE 2004, Section 2.0). As a consequence, this aquifer has been studied more extensively than other portions of the Rustler Formation (Lambert 1992; DOE 2004, Section 2.0). The Magenta Dolomite has lower transmissivity than the Culebra Dolomite, and is unfractured at the WIPP site (DOE 2004, Section 2.0).

2.2 SALADO MINERALOGY

In the area around WIPP, the Salado Formation is a thick bedded salt, composed mainly of layers of impure halite [NaCl], with interbedded layers of anhydrite, polyhalite [$\text{K}_2\text{MgCa}_2(\text{SO}_4)_4 \cdot 2\text{H}_2\text{O}(\text{s})$] and mudstone (Lambert 1992). These sulfate-bearing interbeds are called Marker Beds (MB). Within the Salado Formation, these beds are labeled using numbers that range from MB 100 near the top of the formation to MB 144 near the bottom (DOE 2004, Section 2.0).

Stein (1985) provided mineralogical analyses of drill core from the Salado Formation above and below the repository horizon. Based on x-ray diffraction (XRD) data, Stein (1985) identified quartz [SiO₂(s)], magnesite [MgCO₃(s)], anhydrite, gypsum, halite, polyhalite, bassanite [CaSO₄•0.5H₂O(s)], alkali feldspar [(Na,K)AlSi₃O₈(s)], and clay minerals in the Salado Formation. Brush (1990) used these data to calculate the average mineralogical composition of the Salado to use for geochemical modeling of the effects of different backfill additives. Because this XRD evaluation of the mineralogical composition was only semiquantitative, Brush (1990) assumed that halite constituted 93.2 wt% of the Salado Formation, with the remaining fraction composed of equal parts magnesite, anhydrite, gypsum and polyhalite (1.7 wt% each). Brush (1990) did not include clay minerals, feldspar and quartz in the assumed mineralogy because of the lack of Pitzer data for aqueous silica species for use in geochemical modeling. Bassanite was not included in the assumed mineralogy, because it was identified in only one sample.

2.3 SALADO FORMATION AND CASTILE FORMATION BRINE CHEMISTRY

Small quantities of intergranular and intragranular Salado brines are associated with the salt at the repository horizon. These brines are highly concentrated (ionic strengths up to 8 molar), with a composition of mostly sodium, magnesium, potassium, chloride and sulfate, and with smaller amounts of calcium, carbonate and borate. Two formulations of these Salado brines have been used in WIPP laboratory experiments and PA calculations—Brine A and Generic Weep Brine (GWB) (Snider 2003b). In the CCA PAVT, the Brine A formulation was used to simulate intergranular Salado brines. However, the GWB Salado brine formulation was used in the CRA-2004 PA. A detailed discussion of GWB brine and a comparison of this brine to Brine A were provided by Snider (2003b).

GWB was developed based on chemical analyses of intergranular fluids that seep into the WIPP excavations from the DRZ (Snider 2003b). DOE developed the GWB formulation because of the potential effects of magnesium concentrations in the brine on the modeled and experimental chemical behavior of the MgO backfill; the concentration of magnesium in GWB is lower than in Brine A (Table 2-1). Snider (2003b) verified the calculations supporting the formulation of GWB and compared the concentrations of major cations and anions in several WIPP brines. The comparison between GWB and Brine A indicated that GWB has higher boron, sodium, bromide, chloride and sulfate concentrations, and lower calcium, potassium and magnesium than Brine A. Brine A has a relatively low reported inorganic carbon concentration, whereas none was reported for GWB (Table 2-1). The ionic strength² of GWB is approximately 6.5 compared to approximately 5.9 for Brine A.

EPA (2006c) reviewed DOE's proposed use of the GWB brine formulation to model actinide solubilities for the CRA-2004 PA and concluded that the GWB formulation was adequately documented. EPA concurred with DOE that the GWB brine formulation more closely matches the composition of Salado intergranular brines than Brine A, and that use of the GWB formulation in place of Brine A for the CRA-2004 PA and future actinide solubility calculations

² Ionic strength (I) is defined by the equation $I = \frac{1}{2} \sum_i c_i Z_i^2$. This summation is carried out for all cations and anions in the solution, and c_i and Z_i are the concentrations and charges, respectively, of all ions in solution.

is appropriate. Only minor differences were observed in actinide solubility calculations carried out with GWB and Brine A.

Table 2-1. Brine A, GWB, and ERDA-6 Compositions

Component	Brine A	GWB	ERDA-6
Boron	0.020	0.155	0.063
Calcium	0.020	0.014	0.012
Potassium	0.770	0.458	0.097
Magnesium	1.44	1.00	0.019
Sodium	1.83	3.48	4.87
Bromide	0.010	0.026	0.011
Chloride	5.35	5.51	4.8
Sulfate	0.040	0.175	0.170
Total Inorganic Carbon	0.010	Not reported	0.016
pH	6.5	Not reported	6.17
Specific Gravity (kg/L)	1.2	1.2	1.216
Total Dissolved Solids (mg/L)	306,000	Not reported	330,000

All units are moles/L solution, unless otherwise specified.

Source: Brush and Xiong (2003a)

Castile brine may enter the repository if a borehole that penetrates the repository also penetrates an area of pressurized brine in the underlying Castile Formation. Borehole ERDA-6 encountered pressurized brine in the Castile Formation. The composition of this ERDA-6 brine has been used to represent the likely composition of Castile brine in laboratory experiments and all WIPP PA calculations (Table 2-1).

3.0 GAS GENERATION

The Gas Generation conceptual model includes the assumption that significant gas generation will occur in the repository from corrosion of ferrous metals and from microbial degradation of CPR. The Gas Generation conceptual model also includes the assumption that essentially all carbon dioxide [CO₂] will be removed from the gas phase by reaction with the MgO backfill (Wilson et al. 1996a). The Gas Generation conceptual model includes the assumption that radiolysis of water in the waste and brine, and radiation of plastics and rubber in the waste will not have significant effects on the amounts of gas generated (Wilson et al. 1996a and 1996b). It is assumed that corrosion of other metals that are present in the WIPP inventory, such as aluminum and lead, will not contribute significantly to gas generation rates.

The Gas Generation conceptual model implemented in WIPP PA is called the average stoichiometry model, to differentiate it from alternative gas generation conceptual models considered for the CCA (Wilson et al. 1996a). The current Gas Generation conceptual model is described in detail by SC&A (2008b, Section 2.0 and Appendix A.1).

3.1 IRON CORROSION

Relatively large quantities of reduced iron will be present in the repository in the form of steel waste containers and as iron-based alloys in the waste. The most recent inventory estimates of the densities of iron-based waste material and packaging materials in contact-handled (CH) and remote-handled (RH) waste are provided by Crawford et al. (2009, Tables 5-4 and 5-5). These densities, multiplied by the scaled volumes of CH and RH waste, indicate that over 51,000 metric tons of iron-based materials will be present in the repository at closure (Table 3-1).

Table 3-1. Inventories of Iron-Based Metals and Alloys in Waste and Steel Packaging Materials

Parameter	Density (kg/m ³)	Disposal Volume (m ³)	Mass (kg)
CH Waste Iron-Based Metal and Alloys	81	168,485 m ³	13,647,285
CH Steel Packaging Materials	190	168,485 m ³	32,012,150
RH Waste Iron-Based Metal and Alloys	170	7,079 m ³	1,203,430
RH Steel Packaging Materials	630	7,079 m ³	4,459,770
Repository Total			51,322,635

Source: Crawford et al. 2009

The Gas Generation conceptual model includes a number of assumptions related to iron corrosion (Wilson et al. 1996a and 1996b, SC&A 2008b):

- The small amounts of oxygen trapped in the repository immediately after closure will be consumed by oxidic corrosion or aerobic microbial degradation, and these processes will not generate a significant amount of gas
- Anoxic corrosion can occur in the repository as soon as the shafts are sealed
- Anoxic corrosion of steel in the repository cannot occur unless brine is present and in contact with the steel, and the corrosion rate is assumed to be a function of both brine saturation and steel surface area

- Carbon dioxide generated by microbial degradation of CPR will not passivate steel, because CO₂ will be consumed by reaction with the MgO backfill
- Hydrogen sulfide (H₂S) might passivate steel by forming FeS on the steel surfaces if H₂S is produced in sufficient quantities; however, reducing chemical conditions would continue to be maintained by the FeS

Anoxic corrosion of steel in the waste and waste containers produces hydrogen (H₂). The chemical reactions that represent the stoichiometry of anoxic corrosion of steel in the WIPP repository are:



In both the CRA-2004 (DOE 2004, Appendix PA, Attachment SOTERM-2.2.3) and CRA-2009 (DOE 2009, Appendix SOTERM-2.3.4), DOE listed additional iron corrosion reactions based on WIPP-specific experiments (Telander and Westerman 1993 and 1997):



Reactions (3) and (4) indicate that iron corrosion could produce magnetite [Fe₃O₄(s)] or siderite [FeCO₃(s)]. The possible occurrence of reaction (3) is important, because reaction (3) produces 1.33 moles of gas per mole of iron, whereas reactions (1) and (2) produce only one mole of gas per mole of iron. EPA previously considered whether inclusion of reactions (3) and (4) in the Gas Generation conceptual model is appropriate (SC&A 2008b). The available experimental data indicate that magnetite formation will not occur at the low temperatures expected in the WIPP repository. Siderite formation is not expected to be a significant process in the repository, because of the presence of the MgO backfill, which will control CO₂ fugacities at low levels. Consequently, reactions (1) and (2) describe the expected anoxic corrosion reactions in the WIPP repository (SC&A 2008b).

Gas generation by anoxic corrosion of steel is implemented in PA by assuming the humid corrosion rate is equal to zero, whereas the inundated corrosion rate is a sampled parameter (STEEL:CORRMCO2) uniformly distributed from zero to 3.17×10^{-14} m/sec (Fox 2008). The humid and inundated rate parameters were reviewed and approved by EPA (1998c) at the time of the CCA PAVT.

If the humid anoxic corrosion rate is zero, the equation used to calculate the anoxic steel corrosion gas generation rate can be simplified (DOE 2009, Appendix PA-4.2.5):

$$q_{r\ gc} = R_{ci} S_{b,eff} D_s \rho_{Fe} X_C (\text{H}_2 | \text{Fe}) M_{H2} \quad (5)$$

Where:

$q_{r\ gc}$ = rate of gas production per unit volume of waste due to anoxic corrosion of iron-based metals (kg/m³/sec)

R_{ci} = corrosion rate under inundated conditions (m/sec)

$S_{b,eff}$	= effective brine saturation due to capillary action in the waste materials
D_s	= steel surface area per unit volume in the repository ($11.2 \text{ m}^2/\text{m}^3$), calculated from the parameters REFCON:ASDRUM ($6 \text{ m}^2/\text{drum}$), REFCON:DRROOM (6,800 drums/room), and REFCON:VROOM ($3,640 \text{ m}^3/\text{room}$) (Fox 2008)
ρ_{Fe}	= molar density of steel (moles/ m^3)
$X_C (\text{H}_2 \text{Fe})$	= stoichiometric coefficient for gas generation due to the corrosion of steel [1 mole H_2 per mole Fe, parameter STOIFX (Fox 2008)]
M_{H_2}	= molecular weight of H_2 [kg H_2 per mole H_2 , 2.02×10^{-3} , parameter REFCON:MW_H2 (Fox 2008)]

Thus, for each realization, the sampled anoxic corrosion rate is used to calculate anoxic corrosion gas generation as a function of the effective brine saturation.

MFG (2000) considered iron corrosion rates in the WIPP repository by evaluating WIPP-specific experimental data (Telander and Westerman 1997, Felmy et al. 2000) and natural analogue data. MFG (2000) concluded that iron corrosion would occur in the WIPP repository and maintain reducing conditions. Iron corrosion rates determined from natural analogue data were found to be similar to the corrosion rates used in WIPP PA.

DOE (Triay 2002) requested EPA approval for the disposal of compressed waste from the Advanced Mixed Waste Treatment Facility (AMWTF). During review of the AMWTF planned change request, EPA questioned whether higher iron surface areas expected in compressed waste would affect modeled releases from the repository because of increased anoxic corrosion and repository pressures (TEA 2004). This question arose because the iron surface area per drum (parameter REFCON:ASDRUM) has not changed since the CCA PA, even though a higher iron surface area per unit volume of waste is likely because compressed waste is included in the current inventory. DOE assessed the sensitivity of the PA results to changes in the assumed iron surface area and found that increased iron surface area and anoxic corrosion resulted in decreased overall gas production, with increased gas pressures during the first 2,500 years, followed by decreased gas pressures during later time periods (Stein and Zielinski 2004). Decreased overall gas production was predicted because higher initial gas pressures forced brine from the repository and decreased microbial gas production. DOE concluded that increased iron surface areas would not have significant effects on total repository releases, and EPA concurred with this conclusion (TEA 2004).

DOE is currently conducting experiments to investigate the solubilities of iron and lead in the presence of sulfide (Ismail et al. 2008, Roselle 2009). The goal of these experiments is to develop Pitzer parameters for the incorporation of iron(II), lead and sulfide into the geochemical modeling database used to predict brine chemistry in the repository. Inclusion of these data would allow for the quantitative assessment of the effects of iron and lead corrosion on brine chemistry. These experiments are being carried out using steel and lead coupons and synthetic WIPP brines (GWB and ERDA-6) that have been equilibrated with MgO (Roselle 2009). The

experimental matrix includes the presence and absence of organic ligands; fully inundated, partially submerged and humid atmosphere conditions; and varying concentrations of CO₂ in the atmosphere. Experiments with H₂S are planned but have not yet commenced. Only initial 6-month results from the corrosion experiments have been reported (Roselle 2009). Because the experimental results are preliminary, they have not been used in WIPP PA calculations.

The anoxic corrosion rate parameters and implementation have not changed since the PAVT was reviewed and approved by EPA (1998e). Since the PAVT, reviews of the iron corrosion rate parameter and PA implementation have supported the conceptual model and approach used to model iron corrosion for WIPP PA (MFG 2000, TEA 2004). Consequently, the Gas Generation conceptual model assumptions related to iron corrosion and implementation of anoxic corrosion in the CRA-2009 PA and PABC09 remain adequate.

3.2 CORROSION OF OTHER METALS

DOE (2009, Appendix SOTERM-2.3.5) addressed the potential effects of lead corrosion on repository chemistry, but did not address the effects on gas generation of the corrosion of metals in the WIPP inventory, such as lead and aluminum. It was determined during peer review of the Gas Generation conceptual model that the quantities of aluminum in the repository will be too small to cause significant gas generation (Wilson et al. 1996a, 1996b, 1997a, 1997b). Whether this assumption continues to be true can be assessed by comparing the quantities of iron in the most recent WIPP inventory (Table 3-1) with the quantities of other metals (Table 3-2). The quantity of iron in the WIPP repository at closure will be much greater than the quantities of other metals, such as aluminum and lead. Because relatively large variations in iron surface areas have been shown to have little effect on modeled repository releases (Stein and Zielinski 2004, TEA 2004), the effects of relatively small amounts of gas production from anoxic corrosion of other metals are also likely to be insignificant to repository performance.

DOE submitted a planned change request to allow use of shielded containers for disposal of RH waste. Because lead is used in the container shielding, use of these containers for RH waste disposal would be likely to increase the amounts of lead in the repository. However, EPA has determined that the potential effects of shielded container use will be considered separately from the CRA-2009 (Cotsworth 2009a).

Table 3-2. Inventories of Aluminum, Lead and Other Metals and Alloys in Waste and Packaging Materials

Parameter	Density (kg/m ³)	Disposal Volume (m ³)	Mass (kg)
CH Waste Aluminum-Based Metal and Alloys	1.5	168,485 m ³	252,728
RH Waste Aluminum-Based Metal and Alloys	10	7,079 m ³	10,790
Repository Total Aluminum-Based Metal and Alloys			323,518
CH Waste Other Metal and Alloys	5.1	168,485 m ³	859,274
RH Waste Other Metal and Alloys	28	7,079 m ³	198,212
Repository Total Other Metal and Alloys			1,057,486
CH Lead Packaging Materials	0.0	168,485 m ³	0
RH Lead Packaging Materials	3.5	7,079 m ³	24,777
Total Lead Packaging Materials			24,777
Total Lead, Aluminum-Based Metals and Alloys and Other Metal and Alloys			1,405,781

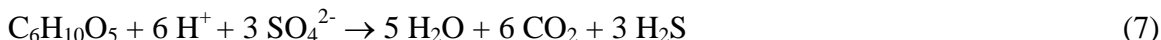
Source: Crawford et al. 2009

3.3 MICROBIAL GAS GENERATION

Cellulosics, plastics and rubber are present in WIPP waste and in waste emplacement and packaging materials. Microbial gas generation in the WIPP repository can occur because microbes are likely to be naturally present at the repository horizon or introduced with the waste. As these microbes utilize CPR materials as a carbon source, production of CO₂ could acidify repository brines or increase the solubility of actinides by carbonate complexation. To control chemical conditions and limit the possible effects of acidic conditions and carbonate complexation on actinide solubilities, MgO backfill is included in the repository to react with CO₂ and maintain mildly alkaline conditions with low CO₂ fugacity consistent with relatively low actinide solubilities (Section 4.0).

3.3.1 CCA PA, PAVT, and CRA-2004 PA Microbial Gas Generation

The same conceptual model was used for microbial gas generation in the WIPP repository for the CCA-PA, PAVT and CRA-2004 PA. In this conceptual model, it was assumed that microbial degradation of CPR may occur in the repository and produce methane [CH₄] and CO₂. The major pathways for microbial degradation of CPR are predicted to include the following reactions:



where C₆H₁₀O₅ is the chemical formula for cellulose monomer. In reactions (6) and (7), one mole of CO₂ is produced for each mole of organic carbon consumed. However, reaction (8) produces only 0.5 moles of CO₂ per mole of organic carbon consumed. Reactions (6) to (8) are predicted to proceed sequentially according to the energy yield of the reactions (Wang and Brush 1996). As the denitrification and sulfate-reduction reactions [reactions (6) and (7), respectively] proceed, DOE predicted that they would consume the limited amounts of nitrate [NO₃⁻] and sulfate [SO₄²⁻] in the WIPP waste inventory and produce limited quantities of nitrogen [N₂] and

hydrogen sulfide [H₂S]. In both the CCA and the CRA-2004, DOE predicted that the methanogenesis reaction (8) would be the dominant reaction pathway and, consequently, that approximately half of the CPR carbon consumed would be converted to CO₂ (DOE 1996, Appendix SOTERM, Section 8.2.2; DOE 2004, Appendix PA, Attachment SOTERM, Section 2.2.2).

DOE assumed that microbial consumption of CPR could be limited by the long-term viability of microbes in the repository, and uncertainty associated with whether microbes would consume plastics and rubbers was also considered important in development of the conceptual model. The rate of microbial gas generation was assumed to be dependent on brine saturation in DOE's conceptual model (DOE 2004, Appendix PA, Attachment MASS). It was assumed that CO₂ will be removed from the repository brines and gas phase by reaction with the MgO backfill, so CO₂ generated from CPR degradation will not significantly affect repository gas pressures. The effects of CPR degradation on the amount of brine in the repository are uncertain, so they are not accounted for in PA. It was also assumed that gas generation will take place homogeneously throughout the repository, because of the assumed homogeneous distribution of waste.

Microbial gas production was assumed to occur at a rate dependent on the availability of brine. Significant microbial gas production was assumed to occur in only half the realizations for the CCA PA, PAVT and CRA-2004 PA because of uncertainties associated with microbial processes. In one half of the realizations in which significant microbial consumption of CPR occurred (one quarter of all realizations), only cellulose was assumed to be consumed by microbial activity. In the remaining half of the realizations with significant microbial consumption of CPR (one quarter of all realizations), all CPR materials, including plastics and rubber, were assumed to be consumed by microbial activity (DOE 2004, Section 6.4.3.3).

The ranges of microbial gas generation rates used for the CCA PA, the CCA PAVT and the CRA-2004 PA were determined using initial results from inundated and humid condition microbial degradation experiments with cellulose (Francis and Gillow 1994; Wang and Brush 1996; DOE 2004, Appendix PA, Attachment PAR). The rates were determined from experiments that did not contain bentonite.³ A gas-generation rate was calculated in BRAGFLO from the humid and inundated rates based on the effective liquid saturation (DOE 2004, Section 6.4.3.3). Gas-generation rates for plastics and rubber are assumed equal to the rate for cellulose; the larger average carbon content by weight for plastics is accounted for by multiplying the mass of plastics by a factor of 1.7 for calculation of the gas generation rate (Wang and Brush 1996).

EPA (1998d) reviewed microbial gas generation during their evaluation of DOE's Source Term Model in the CCA. In their review of the CCA, EPA noted the uncertainties associated with whether microbial communities capable of degrading CPR would be present in the hypersaline WIPP environment, and numerous factors that may limit microbial gas generation, including the concentrations of nutrient and toxic compounds and limitations imposed by temperature, salinity, Eh, pH and the availability of electron acceptors. EPA observed that it is generally difficult to estimate the rate and extent of slow processes, such as CPR degradation, over long time periods by extrapolating the results of short-term studies. EPA concluded that, based on the available

³ At the time the experiments began, bentonite was being considered for use as backfill material and was included in some experiments. Because the backfill does not contain bentonite, these experiments were not used in the determination of the microbial gas generation rates.

evidence at that time, DOE's approach to addressing the probability of significant microbial gas generation was adequate (EPA 1998d). EPA also noted that the CO₂ production rates used at that time (Tables 3-3 and 3-4) were likely to be conservative overestimates, and that addition of MgO backfill to the WIPP repository made the CO₂ production rates unlikely to be of significant concern.

Table 3-3. Inundated Microbial Gas Generation Rates (WAS_AREA:GRATMICI) Used in PA

(moles CO₂/kg cellulose/sec)

Performance Assessment	Minimum	Maximum	Reference
CCA/PAVT	3.17100×10^{-10}	9.51290×10^{-9}	DOE (1996)
CRA-2004 PA	3.17100×10^{-10}	9.51290×10^{-9}	DOE (2004)
PABC04	3.08269×10^{-11}	5.56921×10^{-10}	Nemer et al. (2005)
CRA-2009 PA and PABC09	3.08269×10^{-11}	5.56921×10^{-10}	Fox (2008)

Table 3-4. Humid Microbial Gas Generation Rates (WAS_AREA:GRATMICH) Used in PA

(moles CO₂/kg cellulose/sec)

Performance Assessment	Minimum	Maximum	Reference
CCA/PAVT	0.00	1.26840×10^{-9}	DOE (1996)
CRA-2004	0.00	1.26840×10^{-9}	DOE (2004)
PABC04	0.00	1.02717×10^{-9}	Nemer et al. (2005)
CRA-2009 PA and PABC09	0.00	1.02717×10^{-9}	Fox (2008)

3.3.2 Microbial Gas Generation Evaluation during AMWTF Review

At the time of the CCA PA, DOE assumed that all carbon in CPR could potentially be converted to CO₂ and used this assumption to calculate the amount of MgO required in the backfill. By the time of the AMWTF review, methanogenesis was observed in some of the microbial degradation experiments (Gillow and Francis 2003). DOE stated that methane generation in the experiments demonstrated that methanogenesis will occur in the WIPP repository environment, if microbial degradation of CPR occurs. DOE also assumed that only limited amounts of CPR degradation will take place through denitrification and sulfate reduction [reactions (6) and (7)] because of the relatively small amounts of sulfate and nitrate in the waste (Hansen et al. 2003a and 2003b). DOE stated that after sulfate and nitrate inventories in the waste are consumed, CPR degradation will either cease or will proceed through methanogenesis (reaction 8). Because methanogenesis produces only 0.5 moles of CO₂ for each mole of CPR carbon, CPR degradation through methanogenesis would significantly reduce the amount of CO₂ that could be produced and the amount of MgO needed to maintain the required chemical conditions in the repository.

TEA (2004) reviewed the information provided by DOE (Hansen et al. 2003a and 2003b; Kanney et al. 2004), and concluded that DOE's consideration of the sulfate available for CPR degradation by sulfate reduction did not adequately account for sulfate in the brine and sulfate-bearing minerals in the Salado Formation. EPA considered the available information and the

uncertainty associated with possible microbial processes in the repository, and directed DOE to continue calculating required quantities of MgO backfill by assuming all CPR carbon could be converted to CO₂ unless new and convincing evidence was provided that methanogenesis would occur in the WIPP repository (Cotsworth 2004a, Marcinowski 2004).

3.3.3 PABC04 Microbial Gas Generation

For the CRA-2004 PA, DOE made no changes to the CCA PA and PAVT microbial gas generation conceptual model assumptions, or to the sampled humid or inundated microbial gas generation rates (DOE 2004, Appendix PA, Attachment SOTERM). EPA's review of the CRA-2004 PA included an evaluation of additional experimental data related to microbial gas generation rates and reaction products (EPA 2006c). These data included results from WIPP-specific experiments that continued after approval of the CCA (Francis et al. 1997; Francis and Gillow 2000; Gillow and Francis 2001a, 2001b, 2002a, 2002b, and 2003), as well as additional experiments carried out under WIPP-relevant conditions (Felicione et al. 2001). The data review assessed both microbial degradation probabilities and gas generation rates.

3.3.3.1 Microbial Degradation Probabilities

EPA requested additional information from DOE regarding microbial degradation probabilities (Cotsworth 2004b). The response to this request (Detwiler 2004b) was based on an analysis by Brush (2004) of uncertainties originally considered by Brush (1995) for the CCA. The uncertainties considered in the evaluation of the probability of microbial degradation included whether: (1) microorganisms will be present in the repository when it is filled and sealed, (2) sterilization of the waste and other contents of the repository will prevent microbial activity, (3) microbes will survive for a significant fraction of the 10,000 years of repository performance, (4) sufficient water will be present, (5) sufficient quantities of biodegradable substances will be present, (6) sufficient electron acceptors will be present and available and (7) enough nutrients, especially nitrogen and phosphorous, will be present and available. EPA (2006c) determined that information developed since the CCA indicated an increased probability that microorganisms will be present in the repository when it is filled and sealed, that there is insufficient evidence that MgO will prevent microbial activity in the WIPP environment, that some new evidence was available making long-term viability of microbes appear more probable than at the time of the CCA and that the amount of nutrients, specifically phosphate, in the inventory had increased, making the microbial degradation of cellulose in the repository appear more likely.

DOE evaluated the potential effects of a higher probability of significant degradation of CPR on microbial gas generation rates by comparing gas volumes and repository pressures for realizations with and without significant microbial activity using BRAGFLO simulation results from the CRA-2004 PA (Detwiler 2004b). The gas generation rate and repository pressure at early times was larger for realizations with significant microbial activity, as was the maximum cumulative gas generation and repository pressure over the 10,000-year regulatory period. The maximum cumulative gas generation and the range in the amount of gas generated for the realizations with significant microbial activity was approximately 1.4 to 1.5 times the values observed for realizations without significant microbial activity (Detwiler 2004b).

The effects of the increased assumed probability of microbial degradation of CPR were assessed by comparing total radionuclide mobilization for microbial and non-microbial realizations, based on PANEL output for Scenarios S1 and S3 (Detwiler 2004b). For Scenario S1 (undisturbed- no drilling intrusions, Salado brine), the range of mobilized radionuclides was similar for the microbial and non-microbial realizations, although the central tendency appeared higher for the microbial realizations. For Scenario S3 (single drilling intrusion at 1,000 years into excavated area, pressurized brine is penetrated, Castile brine), the range of mobilized concentrations for the microbial realizations were higher than for non-microbial realizations. These higher mobilized concentrations could influence releases through the Culebra and direct brine releases (DBRs), because these release modes are associated with intrusions (Detwiler 2004b).

For microbial and non-microbial realizations, DOE compared releases through the Culebra, DBRs, spall releases, and total releases to assess the possible effects of microbial activity (Detwiler 2004b). The comparison indicated that releases through the Culebra were minimally affected, most likely because the probability of such releases is low and not sensitive to microbial activity. Higher releases were observed in microbial realizations for DBRs and for spall releases. However, total releases were only slightly higher for microbial realizations than non-microbial realizations, because of the importance of cuttings and cavings to total releases, and cuttings and cavings should not be significantly affected by microbial activity (Detwiler 2004b).

EPA (2006c) concluded that the overall balance of information developed since the CCA indicated that microbial degradation of cellulosic materials may be more likely than previously assumed and that this higher probability would be likely to increase calculated releases from the repository. Results from DOE's experiments indicated that rubber materials may be microbially degraded in the WIPP repository environment. On the other hand, no evidence was found in the DOE experiments of microbial degradation of polyethylene or PVC. Based on this information, EPA (2006c) concluded that the probability of significant microbial degradation of cellulosic materials should be higher than assumed for the CCA PA, PAVT, and the CRA-2004 PA, and directed DOE to assume that microbial degradation of cellulose would occur in all realizations (Cotsworth 2005). Because only limited degradation of rubber materials was observed and no degradation of plastics was observed, there was no evidence that the probabilities of plastics or rubber degradation assumed for the CCA PA and PAVT should be revised.

The parameter WAS_AREA:PROBDEG is a sampled function used by BRAGFLO to indicate whether microbial gas generation occurs and what type of material degrades (Nemer 2005). DOE updated this parameter for the PABC04 to reflect the increased probability (0.75) of microbial degradation of only cellulose materials, and the unchanged probability (0.25) of microbial degradation of all CPR materials. EPA (2006b) found that these changes to WAS_AREA:PROBDEG are consistent with the available data and were an adequate response to EPA's request that significant microbial degradation should be assumed to occur in all PABC04 realizations.

3.3.3.2 Microbial Gas Generation Rates

Wang et al. (2003) recalculated inundated and humid microbial gas generation rates using lower, longer-term CO₂ generation rates from the WIPP-specific experiments that continued after the

CCA PA and PAVT. Although Wang et al. (2003) stated that these lower rates were more representative of rates likely to occur in the WIPP repository, the higher CCA PA and PAVT microbial gas generation rates were used in the CRA-2004 PA.

Because of the higher probability assumed for microbial degradation in the PABC04, DOE believed it was important to revise the microbial gas generation rates to account for rate data that had become available since the CCA PA and PAVT (Nemer et al. 2005). DOE used a two-step process to simulate microbial gas production rates in the WIPP repository for the PABC04 and the CRA-2009 PA (Nemer et al. 2005, DOE 2009). The initially rapid rates of microbial gas production were simulated by increasing the initial pressure in the BRAGFLO input file. This “precharging” of the repository gas pressure was combined with the use of lower gas generation rates determined from long-term experimental data.

Nemer et al. (2005) described the derivation of the microbial gas generation rates used in the PABC04 and CRA-2009 PA. The microbial gas generation data were obtained from experiments summarized by Francis et al. (1997) and Gillow and Francis (2002a, 2003). The microbial production of CO₂ as a function of time in these experiments took place at relatively high rates at the beginning of the experiments, but CO₂ production typically slowed after about 1.5 years. The exact causes of these slowing rates are not known. However, this type of bacterial growth curve is commonly encountered because of limitations on resources, such as nutrients or readily-degradable substrate, or because of increasing concentrations of metabolites. The microbial gas generation rates were modeled by obtaining a least-squares fit of two linear functions to the reported mean values for the CO₂ gas generation data. In this manner, both a short-term and a long-term rate were determined for each experimental dataset. A minimum of three data points were included in each short-term or long-term fit to the data. The best fit was determined by choosing the result with the smallest residual between the observed and fitted values of CO₂ produced as a function of time (Nemer et al. 2005).

None of the data considered by Nemer et al. (2005) were from experiments that included bentonite, which is consistent with DOE’s previous determination of microbial gas generation rates (see Section 3.3.1). Samples from initially aerobic experiments were also not considered; Wang and Brush (1996) justified the use of data only from initially anaerobic experiments by noting that the WIPP repository was expected to become anoxic shortly after closure. Nemer et al. (2005) used the 95% upper confidence limit and 95% lower confidence limit about the mean slope values to determine the maximum and minimum possible rates for inundated and humid conditions (Tables 3-3 and 3-4). EPA (2006b) reviewed the derivation of the humid and inundated microbial gas generation rates and found that they were reasonable and adequately supported by the available experimental data.

3.3.3.3 PABC04 and CRA-2009 PA Implementation of Microbial Gas Generation Rates

Nemer and Stein (2005) described the implementation of the revised microbial gas generation rates in BRAGFLO for the PABC04; this implementation was also used for the CRA-2009 PA. The two zero-order microbial gas generation rates for humid (WAS_AREA:GRATMICH) and inundated (WAS_AREA:GRATMICI) conditions were determined as described by Nemer et al. (2005), with units converted to those used by BRAGFLO (moles C/kg cellulose/sec) and accounting for the dissolution of CO₂ in water for the inundated rates. The rates used in the

different PAs are compared in Tables 3-3 and 3-4. The revised inundated long-term microbial gas generation rate used in the PABC04, CRA-2009 PA and PABC09 is more than an order of magnitude lower than the previous rate. The revised humid long-term microbial gas generation rate is only slightly lower than the previous humid rate.

Because DOE believed the humid rate should be lower than the inundated rate, the sampled humid and inundated rates were compared within BRAGFLO for the PABC04. If the sampled humid rate exceeded the sampled inundated rate, the humid rate was set equal to the inundated rate. Stein and Nemer (2005) did not provide information on the likely effects of assuming that the humid rate would always be lower than the inundated rate. However, because the maximum inundated and humid rates differ by only about a factor of two (Tables 3-3 and 3-4), it is likely that the humid rates used in BRAGFLO were not significantly reduced by this assumption.

The revised microbial gas generation rates were based on long-term experimental data. Therefore, gas generation during the early stages of the repository was accounted for in BRAGFLO for the PABC04, by assuming a fixed amount of gas was present in the repository at the beginning of the calculations (Nemer et al. 2005, Appendix B). The amount of gas in the repository was assumed to be equivalent to the amount of gas generated per gram of cellulose at the point where the relatively rapid short-term rate changed to the slower long-term rate in the nutrient and nitrate-amended inundated experiments; these experiments were used to evaluate the maximum long-term inundated rate.

This amount of gas initially present in the repository because of rapid early microbial gas generation rates equaled 181 $\mu\text{mole/g}$ cellulose (Nemer et al. 2005). This value was converted to the total moles of gas in the repository, based on the equivalent amounts of cellulose in the CRA-2004 PA inventory (Nemer et al. 2005, Appendix B) and the microbial gas generation model of Wang and Brush (1996). This amount of gas was then converted to a pressure value of 26.714 kPa, using the ideal gas equation and the volume and temperature of the repository. This additional pressure was assumed to be generated immediately upon closure, resulting in an initial total repository pressure of 128.039 kPa (Nemer et al. 2005, Stein and Nemer 2005). Use of the CRA-2004 PA inventory to calculate the initial pressure generated by microbial gas generation for the PABC04 resulted in a slightly smaller initial pressure than would have been calculated using the PABC04 inventory. The differences in the CPR inventory between the CRA-2004 inventory (Nemer et al. 2005) and the PABC04 inventory (Fox 2008, Nemer and Clayton 2008) were relatively small, approximately 3% in terms of equivalent moles of carbon. Consequently, the difference between the calculated initial pressures using the two inventories is less than 1 kPa. At EPA's direction, DOE changed the probability of microbial degradation to account for new evidence regarding the presence and viability of microbes capable of degrading CPR in the WIPP repository. The revised probability parameters resulted in microbial gas generation in all realizations for the PABC04 (Section 3.3.3.1). However, DOE asserted that uncertainties remained regarding the viability of microbes in the repository, because of different conditions in the repository compared to the conditions in the experiments (Nemer et al. 2005). DOE therefore introduced an additional sampled parameter, WAS_AREA: BIOGENFC. This parameter, which has a uniform distribution from 0 to 1, was multiplied by the sampled humid and inundated microbial gas generation rates to reduce the rates from the experimentally determined long-term rates.

The uncertainties listed by DOE as justification for this rate reduction were:

- Whether microbes will survive for a significant fraction of the 10,000-year regulatory period
- Whether sufficient water will be present
- Whether sufficient quantities of biodegradable substrate will be present
- Whether sufficient electron acceptors will be present and available
- Whether enough nutrients will be present and available

EPA (2006b) noted that these factors had already been considered and, in fact, assessment of many of these uncertainties had resulted in a decision to increase the probability of significant microbial degradation for WIPP PA (Cotsworth 2005). However, EPA (2006b) concluded that because of the inherent uncertainties associated with extrapolating experimentally measured microbial gas generation rates to repository conditions, it was reasonable to add an uncertainty factor to these rates.

DOE reported that implementation of lower long-term microbial gas generation rates reduced both the rate of pressurization and the pressure in the undisturbed repository (Nemer et al. 2005, Leigh et al. 2005a). This implementation also resulted in slightly higher brine saturation for the undisturbed repository. For the disturbed repository, pressures are relatively unchanged by the different microbial gas generation rates, but the brine saturation is higher using the lower long-term rates. Higher brine saturation may lead to increased flow up the borehole and DBR of radionuclides. Therefore, lower microbial gas generation rates may have had some previously unanticipated effects, in that the likelihood of DBR of radionuclides was increased. However, the frequency and volume of spillings releases were decreased in the PABC04 compared to the CRA-2004 PA because of lower gas pressures (Leigh et al. 2005a). Because the releases from the repository are controlled by cuttings and cavings except at low probability (Leigh et al. 2005a), these differences in spillings and DBR are unlikely to significantly affect overall repository performance.

DOE's implementation of an initially rapid microbial gas generation rate, followed by slower long-term rates, is more likely to be representative of future repository conditions. Assuming a rapid initial rate followed by slower long-term rates is more consistent with the experimental data and with general patterns of microbial processes. A consequence of this change is likely to be longer persistence of microbial gas-generating processes and higher brine saturations in both the disturbed and undisturbed repository scenarios.

3.3.4 Microbial Gas Generation Review for MgO Planned Change Request

At DOE's request, an expert panel was convened by the Institute for Regulatory Science (RSI) to consider issues associated with the MgO backfill and microbial degradation of CPR in the WIPP repository (RSI 2006). The expert panel recommended that an expert elicitation panel be formed to determine the likely extent of degradation of CPR materials and to determine if the amounts of MgO currently placed in the repository could be safely reduced. To address the potential need for an expert elicitation panel related to gas generation from CPR, EPA carried out a review to

identify technical questions and uncertainties related to gas generation from CPR degradation (SC&A 2006). This review included the potential CO₂-generating microbial degradation reactions that could occur within the repository and the extent to which these reactions could occur.

SC&A (2006) performed a review of WIPP-specific data and a survey of the scientific literature regarding gas generation from CPR degradation under WIPP repository conditions. SC&A (2006) concluded that uncertainties in CPR inventories in the WIPP should be addressed before changes in the MgO backfill engineered barrier were made. SC&A (2006) evaluated the potential effects of radiolysis, and found that additional information should be obtained related to the radiolytic degradation of CPR, along with the potential interactions of radiolytic and microbial processes. SC&A (2006) concluded that cellulose could potentially be completely degraded in the repository environment over the 10,000-year regulatory period, but that more investigation of radiolytic and microbial degradation of plastics and rubber would be required to assess likely extents of degradation of these materials.

EPA regulations require that expert judgment should not be substituted for available experimental data or data that could be obtained from a reasonable set of experiments (40 CFR 194.26). The results of the review by SC&A (2006) indicated that literature data are available that might reduce the uncertainties associated with the extent of CPR degradation in the WIPP repository and improve understanding of WIPP's future performance. SC&A (2006) concluded that the use of expert judgment to assess the likely extent of CPR degradation in the WIPP repository would require further justification from DOE that included an in-depth analysis of the available data.

3.3.5 Microbial Gas Generation for the CRA-2009 PA

Implementation of microbial gas generation for the CRA-2009 was essentially the same as for the PABC04. The initial gas pressure in the repository resulting from the short-term, rapid microbial degradation of CPR was assumed to be equal to the pressure of 128.039 kPa calculated by Nemer et al. (2005) for the PABC04 using the CRA-2004 PA inventory (Nemer and Clayton 2008). The long-term rates used in the CRA-2009 PA were the same as the rates used in the PABC04 (Tables 3-3 and 3-4).

The microbial gas generation rate is calculated using the following equation (DOE 2009, Appendix PA-4.2.5; Nemer et al. 2005):

$$q_{r\text{ gm}} = (R_{\text{mi}} S_{\text{b,eff}} + R_{\text{mh}} S_{\text{g}}^*) D_{\text{c}} y (\text{H}_2 | \text{C}) M_{\text{H}_2} B_{\text{fc}} \quad (9)$$

Where:

- $q_{r\text{ gm}}$ = rate of microbial gas production per unit volume of waste (kg/m³/sec)
- R_{mi} = rate of CO₂ production from cellulose biodegradation under inundated conditions (moles C consumed/kg C₆H₁₀O₅/sec)
- R_{mh} = rate of CO₂ production from biodegradation under humid conditions (moles C consumed/kg C₆H₁₀O₅/sec)
- $S_{\text{b,eff}}$ = effective brine saturation due to capillary action in the waste materials

S_g^*	= 1 - $S_{b,eff}$ if $S_{b,eff} > 0$ = 0 if $S_{b,eff} = 0$
D_c	= mass concentration of cellulose in the repository (kg biodegradable material/m ³ disposal volume)
$y(H_2 C)$	= average stoichiometric factor for microbial gas generation of cellulose, i.e., moles of H ₂ generated per mole of carbon consumed by microbial action (moles H ₂ /mole C)
M_{H_2}	= molecular weight of H ₂ (kg H ₂ per mole H ₂)
B_{fc}	= variable representing uncertainty related to long-term microbial degradation of CPR (BIOGENFC)

The variable D_c is the initial CPR inventory, with the mass of plastics increased by a factor of 1.7 to account for the higher average carbon concentration per kg of plastic (Wang and Brush 1996). The modeled microbial gas generation rate is zero-order with respect to the mass of CPR.

The sampled humid and inundated rates were compared within BRAGFLO for the PABC04. If the sampled humid rate exceeded the sampled inundated rate, the humid rate was set equal to the inundated rate. For the CRA-2009 PA, DOE determined that changing the higher sampled humid rate to equal the inundated rate introduced a small error into the sensitivity analysis, because the regression analysis was based on the sampled values rather than the lower conditional values for the humid rate. Consequently, DOE applied a conditional relationship for the CRA-2009, so that the sampled inundated rate is used as the maximum value for humid rate sampling (DOE 2009, Section 23.11.5; Kirchner 2008). The effects of this change on predicted repository performance are small.

DOE (2009 CRA, Appendix PA-2009, Section 7.1.1) attributed slower changes in repository pressure after 2,000 years to cessation of room closure, slowing of brine inflow and consumption of CPR. To understand whether complete consumption of CPR contributes to slower changes in repository pressure after 2,000 years, EPA requested that DOE provide information regarding whether the slower rates of microbial degradation assumed for the CRA-2009 resulted in the persistence of CPR in the PA realizations (Cotsworth 2009a, Comment 1-C-3). Moody (2009a) provided a graph of the fraction of initial CPR remaining in the repository over time for the undisturbed scenario. This graph demonstrated that for most realizations, 70% or more of the initial CPR remained in the undisturbed repository at the end of the 10,000-year period of performance. Nemer and Clayton (2008, Figures 6-65 and 6-66) illustrated the fraction of cellulose remaining versus time for all realizations in Replicate R1, Scenarios S2 and S4, which are disturbed repository scenarios. These figures show that, in the vast majority of disturbed realizations, undegraded CPR also remained at the end of the 10,000-year period of performance. The persistence of CPR in the repository under most conditions is a reasonable result, because of the likely resistance to rapid microbial degradation of plastics and rubber and potential limitations on the amounts of brine in the repository.

During review of the CRA-2009 PA, EPA requested additional information from DOE regarding whether it was reasonable to assume that plastic and rubber degradation, in the 25% of realizations where it occurred, will take place at the same rate as cellulose degradation when normalized to the assumed carbon content of the CPR (Cotsworth 2009a, Comment 1-C-4). EPA

noted that this assumption may no longer be appropriate, based on WIPP-specific experimental results showing essentially no plastic degradation and limited degradation of rubber (Gillow and Francis 2003), evaluations of literature data regarding plastics and rubber degradation process that have become available since the PABC04 (SC&A 2006), and evidence from the PABC04 that lower microbial gas generation rates resulted in a slight increase in releases. EPA accordingly requested that DOE consider the possible effects on PA of lower microbial gas generation rates from plastics and rubber degradation.

DOE noted in their response that there is a high level of uncertainty regarding the rates of degradation of plastics and rubber over the 10,000-year repository period of performance (Moody 2009a). DOE explained that this uncertainty is addressed in PA by only modeling significant degradation of plastics and rubber in 25% of the realizations, and by the use of a lower bound of zero for the sampled microbial degradation rate range. DOE stated that the effects on releases for lower microbial degradation rates implemented for the PABC04 were not calculated, and that Nemer and Stein (2005) showed very little difference between the CRA-2004 PA and PABC04 intermediate results. DOE further stated that they do not believe that reduction in gas generation rates increases releases. DOE also noted that reducing the rates of plastic and rubber degradation would likely have only minor effects on the gas volumes generated, because on average, gas generation rates from iron corrosion are three times greater than from CPR degradation, and plastics and rubber degradation is modeled to occur in only 25% of the realizations.

DOE's conclusions regarding the lack of effect of lower microbial gas generation rates differ from the conclusions drawn by EPA (2006b) during review of the PABC04. Higher releases were calculated at low probability for the PABC04 than for the CCA PAVT, which EPA (2006b) found were caused by increased DBRs. These higher DBRs were believed by EPA (2006b) to be primarily due to higher brine saturations resulting from lower microbial gas generation rates, and to changes in the PABC04 that increased actinide solubilities. Although DOE and EPA appear to have reached different conclusions regarding potential effects on releases of lower gas generation rates from microbial degradation of plastic and rubber in the WIPP inventory, comparison of the results of the CCA PAVT and PABC04 shows that large decreases in microbial gas generation rates had relatively small effects on repository releases and only at low probabilities. Consequently, although the relatively high microbial gas generation rates used for plastic and rubber in the CRA-2009 PA may not be consistent with the available data, it is likely that reducing these rates would have insignificant effects on repository releases. Consequently, the assumption that microbial gas generation from plastic and rubber degradation will occur at the same rate as from cellulose degradation remains adequate for the purposes of PA.

3.3.6 Microbial Gas Generation for the PABC09

No changes were made to the implementation of microbial gas generation or to microbial gas generation rate parameters for the PABC09. The initial gas pressure in the repository resulting from the short-term, rapid microbial degradation of CPR was assumed equal to the pressure of 128.039 kPa calculated by Nemer et al. (2005) for the PABC04 using the CRA-2004 PA inventory (Nemer and Clayton 2008). Based on the inventory used for the PABC09 (Crawford et al. 2009), the total amount of CPR carbon in the repository is estimated to be 1.063×10^9 moles, which is virtually unchanged from the value of 1.069×10^9 moles used by Nemer

et al. (2005). Consequently, the initial pressure used in the PABC09 remains appropriate. The long-term gas generation rates used in the PABC09 were the same as the rates used in the PABC04 (Tables 3-3 and 3-4), because no additional data have been identified that would justify modifying these rates.

3.4 RADIOLYSIS

The Gas Generation Conceptual model includes the assumption that radiolysis of water in the waste and brine and radiation of plastics and rubber in the waste will not have significant effects on the amounts of gas generated (SC&A 2008b). In their initial evaluation of the Gas Generation conceptual model, the CCA Peer Review Panel found that possible radiolytic hydrogen and oxygen gas generation from wetted and dissolved actinides and gas generation from radiolysis of cellulose and plastics had not been adequately evaluated (Wilson et al. 1996a). DOE supplied additional information about radiolytic gas generation in the CCA (DOE 1996). DOE's reasoning for assuming negligible radiolytic gas generation was based on their determination that radiolysis of brine, cellulose and plastics would result in a maximum two-fold to three-fold increase in total gas generation. Because gas pressures above 12.7 MPa would be vented into the interbeds, maximum gas pressures that had been calculated without radiolysis would not be increased. The Peer Review Panel accepted DOE's conclusion that radiolysis would not be an important source of gas generation in WIPP (Wilson et al. 1996b).

This assumption that radiolytic processes will not significantly influence overall rates of gas generation has remained unchanged since the CCA. However, because lower microbial gas generation rates are now used in PA, it is no longer certain that radiolytic gas generation will be relatively insignificant. Radiolysis effects in WIPP are addressed in CRA-2009 (DOE 2009, Appendix SOTERM-2.4.2). However, this discussion did not provide information on potential rates of gas generation through radiolysis of water or CPR in WIPP. SC&A (2006) carried out a preliminary review of WIPP-specific data, as well as literature data regarding radiolytic gas generation from CPR. SC&A (2006) concluded that there is some evidence indicating that radiolytic gas production may occur in the WIPP repository, but whether radiolytic gas generation would affect repository performance was not determined.

At the time of the CCA PA, PAVT and CRA-2004 PA, it was assumed that higher gas generation rates would result in the overestimation of repository releases because of increased spallings releases. However, EPA (2006b) found that evidence developed during review of the CRA-2004 PA and PABC04 indicates that lower gas generation rates may slightly increase repository releases from DBR at low probabilities because of higher brine saturation. This evidence was developed during implementation of lower microbial gas generation rates, as described in Section 3.3.3.3 (Nemer et al. 2005, Leigh et al. 2005a). Leigh et al. (2005a) reported that mean spallings releases were lower and DBRs were higher in the PABC04 than in the CRA-2004 PA. Leigh et al. (2005a) also reported higher mean total releases at low probabilities for the PABC04 than for the CRA-2004 PA. The lower spallings releases were attributed to lower microbial gas generation rates. EPA (2006b) found that higher releases through DBRs were due partly to higher brine saturation, because of lower microbial gas generation rates, but also to increased actinide solubilities used in the PABC04.

The effects of radiolytic gas generation are likely to be encompassed by the range of microbial gas generation rates. Regardless of the source of variations in gas generation rates from CPR, whether microbial or radiolytic, the available evidence indicates that effects on repository releases should be negligibly small and only observable at low probabilities (see Section 3.3.5).

3.5 CONCLUSIONS REGARDING WIPP GAS GENERATION

The conceptual model assumptions and implementation of gas generation by anoxic corrosion of iron-based metals and alloys have remained unchanged since the CCA PAVT. The available data continue to support the conceptual model and approach.

The microbial gas generation rates used for the CRA-2009 PA and PABC09 were the same rates as used for the PABC04. These rates were based on WIPP-specific microbial gas generation experiments carried out with cellulose. Consequently, these rates are appropriate for modeling gas generation rates from degradation of cellulosic materials, but may overestimate gas generation rates from the degradation of plastics and rubber. DOE accounted for the uncertainties regarding the rates of plastic and rubber degradation in the WIPP repository environment by assuming it occurs in only 25% of the realizations. Based on the available data, the current approach for modeling microbial gas generation rates is appropriate for PA.

4.0 BACKFILL EFFICACY

Magnesium oxide backfill was included in the WIPP repository design to control repository chemical conditions and thereby minimize actinide solubilities in the postclosure repository (DOE 1996, Appendix BACK, Section 1). DOE selected MgO as an engineered barrier based on an analysis described in the CCA (DOE 1996, Appendix EBS), and EPA determined that MgO met the requirements for an engineered barrier (40 CFR Part 194.44).

4.1 CCA PA CONCEPTUAL MODEL AND IMPLEMENTATION

Expected performance of the MgO backfill was described in the CCA (DOE 1996, Appendices BACK and SOTERM). Additional information was provided by DOE during the EPA's review of the CCA (EPA 1997c). The MgO chemical reactions and their ability to control chemical conditions in WIPP brines were addressed in the Chemical Conditions conceptual model, which was peer-reviewed and accepted for the CCA (Wilson et al. 1996a, 1996b, 1997a, 1997b).

4.1.1 MgO Reactions in the Repository

Magnesium oxide backfill is expected to control actinide solubilities in brine within the post-closure repository by consuming CO₂ produced by microbial degradation of CPR and by buffering brine pH at moderately alkaline values (approximately 8 to 10). MgO will initially react with brine to form brucite [Mg(OH)₂(s)]:



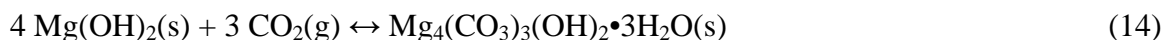
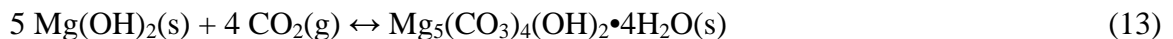
and brucite dissolution is expected to buffer brine pH in the repository:



Microbial degradation of CPR will produce CO₂, which can react with brucite to form magnesium-carbonate phases such as magnesite:



hydromagnesite, for which two chemical formulas have been reported:



or nesquehonite [MgCO₃•3H₂O(s)]:



Because of the high energy of hydrolysis of the magnesium ion, magnesite does not precipitate directly from low-temperature solutions. Instead, metastable formation of hydrated magnesium carbonate phases, such as hydromagnesite and nesquehonite, are more likely to occur. Because

these phases are not thermodynamically stable under repository conditions, they are expected to eventually dehydrate to form magnesite, for example:



At equilibrium in the repository, magnesite is expected to be the most stable magnesium-carbonate phase (EPA 1998d).

The reaction of brucite to form magnesium-carbonate in the repository will control the CO_2 partial pressure. In the CCA PA, DOE assumed that the brucite-magnesite reaction (12) would control CO_2 partial pressure (DOE 1996, Appendix SOTERM). EPA (1998d) reviewed experimental data on magnesium-carbonate formation in WIPP brines (SNL 1997) and found that nesquehonite formed initially in the experiments, but nesquehonite converted within a few days to a solid phase with a composition similar to proto-hydromagnesite [$\text{MgCO}_3 \cdot \text{Mg}(\text{OH})_2 \cdot 4\text{H}_2\text{O}(\text{s})$]. Hydromagnesite formation was observed in other scoping experiments (SNL 1997). There was no evidence of hydromagnesite conversion to magnesite in the experiments reviewed by EPA (1998d).

Based on a review of the literature, EPA (1998d) developed the following conceptualization of the sequence and time scales of reactions between infiltrating brine and MgO backfill in the WIPP repository:

1. Rapid reaction of MgO with brine to produce brucite (hours to days)
2. Rapid carbonation of brucite to produce nesquehonite and possibly hydromagnesite (hours to days)
3. Rapid conversion of nesquehonite to hydromagnesite (days to weeks)

Slow conversion of hydromagnesite to magnesite (hundreds to thousands of years)

EPA (1998d) found that brucite in combination with the different magnesium carbonates buffered CO_2 fugacities at different values, with the highest value observed for nesquehonite, intermediate values for the two different forms of hydromagnesite and the lowest fugacities for magnesite. Higher CO_2 fugacities generally increase actinide solid solubilities, because of the formation of aqueous actinide-carbonate complexes. Verification calculations indicated that predicted actinide concentrations did not significantly change when the different reported compositions of hydromagnesite [either $\text{Mg}_5(\text{CO}_3)_4(\text{OH})_2 \cdot 4\text{H}_2\text{O}(\text{s})$ or $\text{Mg}_4(\text{CO}_3)_3(\text{OH})_2 \cdot 3\text{H}_2\text{O}(\text{s})$] were assumed to form (EPA 1998d). Errors in the thermodynamic database used for the CCA PA were corrected for the CCA PAVT (EPA 1998d). Because of the database errors, the actinide solubilities predicted for the CCA PA using the brucite-magnesite buffer were higher than the actinide solubilities calculated for the CCA PAVT using the brucite-hydromagnesite buffer (EPA 1998d).

4.1.2 Placement of MgO Backfill

Magnesium oxide (MgO) emplaced in the repository is obtained from the supplier in a dry granular form (WTS 2003). This form was selected to minimize dusting in case of a premature bag rupture, ensure sufficient permeability for access of brine for reaction, reduce possible

entrainment of MgO in brine flow and provide sufficient density so adequate amounts can be placed in the repository (DOE 1996, Appendix BACK, Section 2; DOE 2004, Appendix BARRIERS, Section 2.2). Adequate reactivity of supplied MgO has been tested using a laboratory procedure (Krumhansl et al. 1997; WTS 2003).

Initially, MgO was placed in the repository in 4,200-pound supersacks and 25-pound minisacks. The supersacks were placed on top of various combinations of waste containers (Standard Waste Boxes, 7-packs of 55-gallon drums, ten-drum overpacks, 4-packs of 85-gallon overpack drums, and 3-packs of 100 gallon drums), whereas the minisacks were placed among the waste containers and between the waste containers and the sides of the disposal rooms. The MgO supersacks are constructed of woven polypropylene material and are designed to provide a barrier to atmospheric moisture and CO₂ (WTS 2003). The supersacks are provided with a plastic support sheet, which remains under the supersacks after placement on the waste containers (WTS 2003).

At the time of the CCA, DOE calculated the required amount of MgO by assuming that all CPR carbon in the repository could be converted to CO₂; DOE determined that the amount of MgO required to react with this amount of CO₂ would be 43,700 tons (EPA 1997c). The MgO Excess Factor⁴ (EF) is defined as:

$$EF = \frac{M_{MgO}}{M_{CO_2}} \quad (17)$$

Where:

M_{MgO} = total moles of emplaced MgO
 M_{CO_2} = the maximum possible number of moles of CO₂ that could be generated by microbial consumption of all carbon in the CPR

An appropriate EF was included in the engineered barrier design by setting the amount of MgO at 85,000 tons. This quantity was based on the density of the MgO, the volume of the backfill packages, and the amount of space available in the repository for the backfill. The amount of MgO backfill in the CCA provided an EF of 1.95 (EPA 1997c).

4.2 REVIEWS OF MgO EFFICACY AND IMPLEMENTATION CHANGES PRIOR TO THE CRA-2004 PA

The Actinide Source-Term Waste Test Program (STTP) experiments were designed to provide data on the concentrations of actinides, actinide-containing colloids, complexing agents, and other chemical reactants in simulated WIPP brine in contact with candidate backfill materials and actual TRU wastes (Villareal 1996, Villareal et al. 2001). MgO slurry was added to one experiment carried out at a CO₂ partial pressure of 60 bars to test the ability of the MgO to control chemical conditions. However, the MgO did not buffer the pH of this experiment in the slightly alkaline range predicted by the Chemical Conditions conceptual model. EPA reviewed the results of the STTP experiments and concerns regarding the efficacy of the MgO engineered

⁴ The MgO Excess Factor was originally called the MgO Safety Factor by EPA.

barrier expressed by the Environmental Evaluation Group (EEG), and determined that the STTP experiment with MgO was not relevant to repository conditions because of the high CO₂ partial pressure (SC&A 2000). EPA also reviewed the uncertainty regarding the persistence of nesquehonite in the repository and concluded that no new evidence had been developed since the CCA to demonstrate that the MgO backfill would not behave as previously predicted. (TEA 2000, TEA 2001).

DOE requested EPA's approval to eliminate the MgO minisacks to enhance worker safety; EPA approved this change in January 2001 (DOE 2004, Appendix BARRIERS; EPA 2001a and 2001b). Elimination of the MgO minisacks decreased the EF to 1.67 (EPA 2001a).

EPA addressed the MgO EF during their review of DOE's request for AMWTF waste disposal at WIPP (Marcinowski 2004). This review was required because of the higher CPR densities in AMWTF waste and the potential effects on the amounts of MgO required to maintain an adequate EF (see Section 3.3.2) (TEA 2004). Because of the potential availability of sulfate in brines and in Salado minerals such as anhydrite, it is possible that all CPR degradation could take place by denitrification and sulfate reduction [reactions (6) and (7)]. EPA approved DOE's request to dispose of AMWTF compressed waste at WIPP, subject to the conditions that DOE maintain the MgO EF of 1.67 by adding extra MgO backfill with the compressed waste and that the MgO EF would be calculated on a room-by-room basis assuming that all CPR carbon in the waste could be converted to CO₂ (Marcinowski 2004).

4.3 CRA-2004 PA AND PABC04 REVIEW OF MgO BACKFILL EFFICACY

EPA (2006c) evaluated additional information related to MgO backfill efficacy during their review of the CRA-2004 PA and PABC04. This information included characteristics of the MgO used in the repository at that time, results from ongoing experiments related to MgO hydration and carbonation reactions, and calculations of the excess quantities of MgO in the repository.

4.3.1 Characterization of Premier MgO

At the time of the CRA-2004, WIPP MgO backfill was obtained from Premier Chemicals. Premier MgO was generated using a different process, had a different texture, and contained higher percentages of potentially reactive impurities than the MgO from National Magnesia Chemicals initially used as WIPP backfill (Bryan and Snider 2001b). Premier MgO was manufactured from mined sedimentary magnesite that was calcined to expel all CO₂ (DOE 2004, Appendix BARRIERS-2.3.1). This material was characterized by XRD and found to contain primarily periclase [MgO], along with minor phases, such as forsterite [Mg₂SiO₄(s)], lime [CaO(s)], monticellite [CaMgSiO₄(s)], spinel [MgAl₂O₄(s)] and ulvospinel [FeTi₂O₄(s)]. Periclase and lime, which are expected to be reactive, made up approximately 90 wt% of the Premier MgO, with the unreactive constituents forming the remaining 10 wt% (Snider 2003a). Particle-size analysis was carried out for two batches of Premier MgO (Bryan and Snider 2001a; DOE 2004, Appendix BARRIERS, Section 2.3.1). The particle-size distribution of these two batches varied considerably; one batch had a bimodal distribution, with most MgO falling into the higher or lower size ranges, whereas the other batch had a single distribution of particle sizes centered at the middle of the range.

4.3.2 MgO Hydration and Carbonation Experiments

DOE reported a number of MgO hydration and carbonation experiments (Bryan and Snider 2001a; Zhang et al. 2001; Snider 2001; Bryan and Snider 2001b; Snider 2002; Snider 2003a; Snider and Xiong 2002; Xiong and Snider 2003; DOE 2004, Appendix BARRIERS). These experiments included hydration experiments under humid conditions, using a range of relative humidities and at temperatures up to 90°C. Inundated hydration experiments were carried out using deionized water, sodium chloride [NaCl] solutions and GWB and ERDA-6 brines at temperatures up to 90°C. The hydration products in deionized water, NaCl solutions, and ERDA-6 brine were identified as brucite using XRD. However, in experiments with GWB brine, a magnesium-chloride-hydroxide hydrate phase formed initially (Snider 2002). This phase was identified by XRD and scanning electron microscope examination as “phase 5” $[\text{Mg}_3(\text{OH})_5\text{Cl}\cdot 4\text{H}_2\text{O}]^5$ (DOE 2004, Appendix BARRIERS-2.3.2.1). In longer-term experiments, there was XRD evidence that this material was slowly being replaced by brucite (Snider 2003a; DOE 2004, Appendix BARRIERS-2.3.2.1).

Magnesium oxide (MgO) carbonation experiments were carried out under inundated conditions at CO₂ concentrations that ranged from atmospheric conditions up to 5%, using deionized water, 4 M NaCl, GWB brine, and ERDA-6 brine. Nesquehonite formation [reaction (15)] was only observed at the highest CO₂ partial pressure, and nesquehonite apparently was being replaced by hydromagnesite as these experiments progressed (DOE 2004, Appendix BARRIERS-2.3.2.2). In all GWB and ERDA-6 inundated experiments with Premier MgO at atmospheric CO₂ partial pressures, hydromagnesite was the only magnesium-carbonate phase detected.

EPA (2006c) reviewed the MgO hydration and carbonation experiments. Based on this review, EPA concluded that DOE had adequately accounted for information developed since the CCA in their consideration of the magnesium-carbonate phases most likely to control pH and CO₂ fugacities in the WIPP repository. The formation of brucite and possibly a magnesium-chloride-hydroxide hydrate phase is likely to control pH in the repository. Based on the experimental results, nesquehonite formation, if it occurs, appears to be transient and hydromagnesite is likely to be the most important magnesium-hydroxycarbonate phase in the repository during the regulatory time period.

4.3.3 MgO Excess Factor Calculations

The MgO EF calculations for the CRA-2004 were performed during the same time period as the AMWTF review of issues associated with the CPR microbial degradation reactions and effects on the MgO EF (see Section 3.3.2). Consequently, EPA’s requirement that DOE should assume all CPR carbon could be completely converted to CO₂ was not included in these calculations. In addition, when calculating the amount of CPR in the repository for the CRA-2004 PA, DOE did not take into account the CPR materials external to the waste containers, such as shrink wrap placed around the 55-gallon drum 7-packs or the support sheets and packaging materials used for the MgO supersacks (Cotsworth 2004b, Comment G-2). EPA pointed out that the MgO EF had not been appropriately computed for the 2004 CRA (Cotsworth 2004b, Comment C-23-5). EPA

⁵ This magnesium hydroxychloride is referred to as “phase 5” in the cement industry, and this term is adopted for consistency with other WIPP documents (e.g., Xiong et al. 2010a).

reiterated the condition that DOE must maintain a 1.67 MgO EF on a room-by-room basis, and requested that DOE provide a plan for implementing this condition (Cotsworth 2004b, Comment G-4). DOE responded that the necessary measures would be implemented to ensure that the required amounts of MgO are emplaced within the repository, and provided the emplacement plan requested by EPA (Detwiler 2004a, Detwiler 2004d).

Under the MgO emplacement plan, DOE monitors the amounts of MgO backfill and CPR during their emplacement in each room to ensure that the required MgO EF of 1.67 is maintained on a room-by-room basis (Detwiler 2004a). During review of the CRA-2004 PA, EPA (2006c) noted that waste loading in Panel 1 demonstrated that waste placement in the repository is likely to be heterogeneous, and that tight panel seals could prevent brine mixing between panels. EPA (2006c) concurred with DOE's plan to emplace enough MgO in each room of each panel to ensure an adequate EF under heterogeneous waste loading conditions.

Because the AMWTP compressed waste contains higher than average concentrations of CPR, DOE was required to emplace additional MgO. Consequently, in addition to the one supersack per stack of waste that had previously been used in WIPP, the DOE began emplacing additional MgO supersacks on racks placed in the repository to achieve the required EF in each room. Each rack contains five supersacks identical to those placed on top of the waste containers and spans the same vertical distance normally occupied by the waste containers. Thus, emplacement of additional MgO in the repository has used space normally occupied by CH waste (DOE 2009, Section 44.6.1.2).

4.4 MgO PLANNED CHANGE REQUEST

DOE submitted a Planned Change Request to EPA to reduce the MgO EF from the approved value of 1.67 to 1.20 (Moody 2006). Because of the importance of MgO as the only engineered barrier for WIPP, EPA requested additional information about the uncertainties related to MgO effectiveness, the size of these uncertainties and their potential impacts on WIPP's long-term performance (Gitlin 2006). DOE responded with an analysis of the uncertainties associated with the effectiveness of MgO and provided an assessment of the effects of these uncertainties on the calculation of required MgO quantities (Vugrin et al. 2006). Vugrin et al. (2006) divided these uncertainties into four categories:

- Uncertainties in the quantity of CPR that will be consumed
- Uncertainties associated with the quantities of CO₂ produced by microbial degradation of CPR
- Uncertainties related to the amount of MgO available to react with CO₂
- Uncertainties in the moles of CO₂ consumed per mole of available MgO, and in the moles of CO₂ that could be consumed by reaction with other materials

To evaluate the uncertainties associated with the performance of the MgO backfill, Vugrin et al. (2006) defined the Effective Excess Factor (EEF) as:

$$EEF = \frac{(m \times M_{MgO})}{(g \times M_c)} \times r \quad (18)$$

Where:

- g = uncertainty in the moles of CO₂ produced per mole of consumed organic carbon
- m = uncertainty in the moles of MgO available for CO₂ consumption
- M_c = total moles of organic carbon in the emplaced CPR reported by DOE
- r = uncertainty in the moles of CO₂ consumed per mole of emplaced MgO

Vugrin et al. (2006) addressed the uncertainties associated with the parameters in equation (18). During their review of the proposed change in the MgO EF, EPA requested additional information that was provided by DOE during technical exchange meetings in September 2006, January 2007 and May 2007. DOE then provided a revised report describing the uncertainties associated with the MgO EF in the repository (Vugrin et al. 2007).

Uncertainty in the CPR inventory masses was accounted for by Vugrin et al. (2007) using the results of an evaluation by Kirchner and Vugrin (2006). The results of this study indicated that the mean CPR quantity in a disposal room should equal the sum of the CPR quantities reported by DOE for the individual containers. This study also demonstrated that the standard deviation would be relatively small, because of the random nature of the differences between the reported and actual inventory contents. Because of uncertainty regarding the long-term degradation of CPR, Vugrin et al. (2006, 2007) made the bounding assumption that all CPR could degrade during the 10,000-year WIPP regulatory period.

SC&A (2008a) observed that the reported masses of CPR in the inventory must be converted to moles of carbon to determine the amount of CO₂ that could be produced by CPR degradation. These calculations require assumptions regarding the chemical composition of the CPR. Assumptions summarized by Wang and Brush (1996) have been used in the past to perform these calculations. Vugrin et al. (2006, 2007) did not consider the possible effects of these assumptions on the EEF. Assumptions regarding the compositions of the CPR were used by SC&A (2008a) to develop reasonable upper-range and lower-range estimates of the moles of carbon in the CPR inventory. Using these values, it was determined that the estimated moles of CPR carbon in the inventory ranged from 0.97 to 1.09 times the value calculated using the Wang and Brush (1996) assumptions. SC&A (2008a) stated that this range should be included in the EEF calculations as an uncertain parameter with a uniform distribution.

Vugrin et al. (2006, 2007) assumed that sufficient sulfate was present in the waste, brines and Salado minerals for complete degradation of all CPR carbon in the repository through sulfate reduction and denitrification. As a consequence, it was assumed that each mole of organic carbon consumed would produce a mole of CO₂. Because of the lower CO₂ yield from methanogenic CPR degradation, this assumption conservatively bounds the uncertainties related to the microbial reactions that may degrade CPR in the repository.

SC&A (2008a) concluded that the MagChem 10 WTS-60 MgO from Martin Marietta Magnesia Specialties, Inc. (Martin Marietta MgO), currently being used as backfill, has been reasonably well characterized. Preliminary hydration data provided by Wall (2005) indicated the Martin

Marietta MgO will likely hydrate and carbonate more rapidly than MgO from previous suppliers (National Magnesia Chemicals and Premier Chemicals). Deng et al. (2006) used chemical analysis results, loss on ignition (LOI), thermogravimetric tests and assumptions regarding the chemical composition of the nonreactive phases in the MgO to calculate the amounts of reactive periclase and lime in Martin Marietta MgO samples. The results indicated that the Martin Marietta MgO contained 96 ± 2 (1σ) mole percent reactive periclase plus lime, with periclase making up 95 mole % and lime making up 1 mole % of the Martin Marietta MgO. SC&A (2008a) noted that the results reported by Deng et al. (2006) were based on analysis of eight samples from a single shipment (shipment SL2980076). Although limited data were available at that time regarding potential variability of the physical and chemical properties of the Martin Marietta MgO, SC&A (2008a) concluded on the basis of information regarding the manufacturing processes and feedstock that this MgO would be expected to meet the performance specification of 96 ± 2 mole % reactive periclase plus lime included in the EEF calculations of Vugrin et al. (2007). However, SC&A (2008a) noted that the reactivity test (Krumhansl et al. 1997) included in the MgO specifications at that time (WTS 2005) was unlikely to be sufficient to ensure adequate reactivity of the materials in each MgO shipment, so an improved reactivity test was necessary.

The MgO backfill can react with brine and thereby control repository chemical conditions only if the brine and MgO remain in physical contact. There is no evidence that significant physical segregation of MgO by room roof collapse will occur. Similarly, the MgO supersacks appear very likely to rupture and expose MgO to any brine that enters the repository. An analysis presented by Clayton and Nemer (2006) of loss of MgO with brine from the repository was consistent with previous evaluations of the effects of drilling events on repository performance, and the effects of MgO loss to brine are likely to be relatively small. A very small fraction of the MgO appears likely to carbonate before emplacement, and this fraction was accounted for in the EEF calculation. Only a small amount of MgO dissolved in Salado brine is likely to enter the repository and react with CO_2 , reducing the required amount of MgO; this effect was conservatively omitted from the calculations. Formation of impermeable rims of reaction products on individual periclase grains and impermeable reaction rinds on the masses of MgO in the repository would have the potential to limit the availability of MgO for complete reaction. The possible formation of such reaction rims on individual periclase grains or impermeable rinds on masses of MgO was previously considered by the CCA Conceptual Models Peer Review Panel (Wilson et al. 1996a, 1996b, 1997a, 1997b). The Panel concluded that formation of magnesium-carbonate reaction products would not inhibit the access of brine to the surfaces of the MgO, and would not render any of the MgO unavailable for reaction with brine and CO_2 . SC&A (2008a) determined that no new data had been developed since the time of the peer review to contradict this assumption, and concluded that it was reasonable to assume that essentially all MgO in the backfill will be available for reaction with brine and CO_2 . Kanney and Vugrin (2006) evaluated aqueous diffusion of CO_2 in the repository; their results indicated that the gases and liquids in the repository will be sufficiently well mixed to permit contact and reaction of the MgO with brine and CO_2 .

Upon reaction with brine, periclase in the backfill is expected to hydrate to brucite. In the presence of CO_2 under WIPP repository conditions, hydromagnesite is expected to form initially from the brucite, with eventual reaction to form the more stable magnesite phase. The rate at which hydromagnesite will convert to magnesite is important, because it affects the moles of

CO₂ consumed per mole of MgO reacted during the 10,000-year repository regulatory period, which in turn affects the EEF calculation. SC&A (2008a) examined the available experimental and natural analogue data that indicated the hydromagnesite to magnesite reaction rate could be relatively slow, so this reaction may not be complete during the WIPP repository regulatory period. Vugrin et al. (2007) accordingly used an uncertain variable with a uniform distribution to represent the moles of CO₂ consumed per mole of reacted MgO. This variable ranged from 0.8 (hydromagnesite only) to 1.0 (magnesite only).

Significant amounts of CPR degradation by sulfate reduction would require dissolution of sulfate minerals in the Salado Formation, including anhydrite, gypsum and polyhalite. Dissolution of these solid phases would release relatively large quantities of calcium ion into the brine. Elevated calcium concentrations would in turn be expected to cause calcium-carbonate precipitation and increased net consumption of CO₂ per mole of MgO in the backfill. DOE carried out EQ3/6 geochemical computer code calculations to estimate the proportions of CO₂ that would be consumed by magnesite or hydromagnesite and calcium carbonate precipitation (Brush et al. 2006). However, limitations in the EQ3/6 database resulted in modeling calculations that inadequately represented repository conditions. Because of the difficulties associated with quantifying the amount of calcium-carbonate solids that would precipitate, a limiting assumption was made for the EEF calculation that no calcium carbonate precipitation would occur. This is undoubtedly a conservative, bounding assumption, and will lead to an underestimation of the EEF.

Vugrin et al. (2007) calculated a mean EEF of 1.03, with a standard deviation of 0.0719. SC&A (2008a) found that incorporating the effects of uncertainty associated with the chemical composition of the CPR reduced the EEF to 1.00, with a standard deviation of 0.078. This EEF might seem to indicate that if the EF is reduced to 1.20, the average amount of MgO in a disposal room would equal the quantity required to react with CO₂. The EEF calculation, however, includes a number of conservative assumptions, including the assumptions that all CPR will degrade, all carbon in the CPR will react to form CO₂, and carbonate minerals other than hydromagnesite or magnesite will not precipitate, including calcite, iron carbonates, or lead carbonates. SC&A (2008a) determined that given these conservative, bounding assumptions, it was probable that if the EF was reduced to 1.20, the EEF in the disposal rooms will be greater than the mean bounding value of 1.00. Consequently, SC&A (2008a) determined that reduction of the EF to 1.20 would be expected to have no significant effects on repository chemistry.

After a review of the Planned Change Request to decrease the amount of MgO backfill emplaced at WIPP, which reduced the MgO EF from 1.6 to 1.2, and supporting documentation, EPA concluded that the available data supported a 1.20 MgO EF (Reyes 2008). EPA approved this planned change, stipulating that DOE should continue to calculate and track both the CPR carbon disposed and the required MgO needed on a room-by-room basis. EPA also required DOE to annually verify the reactivity of the MgO and ensure that it is maintained at 96%, as assumed in DOE's supporting documentation.

4.5 CRA-2009 MGO BACKFILL EFFICACY REVIEW

The WIPP engineered barrier was described in CRA-2009, Section 44.6.1, Appendix MgO-2009, and Appendix SOTERM-2009, Section 2.3 (DOE 2009). Descriptions of the MgO supersacks

and their placement in the disposal system were provided in the CRA-2004 (DOE 2004, Section 3.3.1) and Section 44.6.1.2 of the CRA-2009 (DOE 2009).

The CRA-2009 included additional information regarding the Martin Marietta MgO now used as backfill at WIPP (DOE 2009, Appendix MgO-3.3.2). Deng et al. (2007) reported the results from characterization and accelerated inundated hydration testing of the MgO. The characterization and hydration results were obtained using samples from the same lot used by Deng et al. (2006). Particle-size analysis was carried out by sieving the Martin Marietta MgO through a series of sieves with openings of 2 mm (10 mesh) and less. The particle-size analysis results indicated that on average, 92.98% of the WTS-60 MgO passed through a 10-mesh sieve, and 17.9% passed through a sieve with openings of 0.075 mm (200 mesh).

Deng et al. (2007) reported results of hydration tests in deionized water at 70°C. These tests were designed to evaluate the potential influence of MgO particle size, stirring rate, and solid-to-liquid ratio. Deng et al. (2007) observed that the Martin Marietta MgO currently used at WIPP hydrated more quickly in deionized water at 70°C than the Premier MgO. Deng et al. (2007) also observed that diffusion mechanisms may be important for small MgO particle sizes, whereas surface area appeared to be an important control for the rate of hydration for larger MgO particle sizes. The results of the Deng et al. (2007) investigation were used to design long-term hydration and carbonation experiments.

Deng et al. (2009) described preliminary results from long-term MgO inundated hydration experiments using Martin Marietta MgO currently used as WIPP backfill. These experiments included two MgO to brine ratios (3 g/11 ml and 3.1g/77 ml), three brines (GWB, ERDA-6, and simplified GWB), and three particle-size ranges (as received, 1.0 to 2.0 mm, and less than 0.075 mm). All experiments were conducted at the predicted repository temperature of 28°C. Based on XRD examination, the MgO hydration reaction products were brucite in ERDA-6 brine and brucite plus phase 5 in GWB and simplified GWB brines. The results showed that MgO particle size affected the hydration rates, with more rapid hydration of smaller particles. The MgO hydration rate was faster in simplified GWB than in GWB or ERDA-6.

During their review of the CRA-2009, EPA requested that DOE provide additional characterization data for the Martin Marietta MgO that is currently used as WIPP backfill (Cotsworth 2009a, Comment 1-C-1). EPA noted that the information provided in the CRA-2009 was based on a single lot of this material, and questioned whether analysis of a single lot would be representative. EPA also questioned whether the reactivity test developed by Krumhansl et al. (1997) for MgO material acceptance was likely to reliably detect MgO with insufficient reactive periclase plus lime (Cotsworth 2009a, Comment 1-C-2). In response, DOE provided their revised procedure for MgO acceptance testing (Nemer 2008), and confirmed that characterization and reactivity testing are performed on all shipments of the Martin Marietta MgO (Moody 2009c). The procedure outlined by Nemer (2008) determines the reactive mole percents of periclase and lime by first hydrating a sample of MgO in deionized water at approximately 245°C to form brucite and portlandite $[\text{Ca}(\text{OH})_2(\text{s})]$. The hydrated MgO sample is then dehydrated and the mass of dehydrated MgO and the mass of water are measured. The mass of water lost during dehydration and the mass of MgO, when converted to moles, provide the mole percents of periclase and lime available to react in the Martin Marietta MgO sample. The procedure provided by Nemer (2008) is adequate for testing the moles of periclase plus lime

that would rapidly react with brine in the repository. The procedure provided by Moody (2009c) did not include the spreadsheet attachment outlining the calculation; this spreadsheet will be examined during EPA's next annual inspection.

Nemer (2009) performed a study to demonstrate that the current MgO acceptance test (Nemer 2008) would reliably detect MgO shipments with insufficient reactive periclase plus lime. In this investigation, the MgO acceptance test was performed on six samples composed of different ratios of high-purity MgO and non-reactive $\text{Al}_2\text{O}_3(\text{s})$. The results established that the MgO acceptance test reliably determined known concentrations of reactive MgO with maximum errors of approximately 1%. These results demonstrated that the MgO acceptance test would detect MgO shipments with a percentage of reactive MgO less than the specified 96 ± 2 mole % reactive periclase plus lime.

DOE provided the results of testing of 127 samples from 105 MgO shipments (Moody 2009c). These tests were performed by an outside laboratory or by Sandia National Laboratories (SNL). The results indicated that the minimum measured reactivity of the Martin Marietta MgO was 96.2 mole %. The mean and standard deviation (1σ) calculated using all reported results were 97.9 ± 0.7 mole %, which exceeds the specified 96 ± 2 mole % reactive periclase plus lime. Based on the results of MgO acceptance testing reported by Moody (2009c), the Martin Marietta MgO backfill material will have sufficient reactivity to control chemical conditions in the WIPP repository.

EPA noted DOE's statement in Appendix MgO-2009, Section 4.2.2, that hydromagnesite will completely convert to magnesite during the 10,000-year WIPP regulatory time period (Cotsworth 2009a, Comment 1-C-18). EPA observed that a recent evaluation of the likely conversion rate for hydromagnesite to magnesite cited data from Vance et al. (1992) showing hydromagnesite may persist under some conditions for up to 6,200 years (SC&A 2008a). DOE's arguments supporting the formation of magnesite for the majority of the WIPP regulatory period in Appendix MgO-2009, Section 4.4.2, were considered in detail by SC&A (2008a) and found to be inadequate for establishing that hydromagnesite would rapidly convert to magnesite during the WIPP regulatory period. EPA pointed out that relatively slow CPR degradation rates could result in the formation of hydromagnesite throughout the 10,000-year regulatory period (Cotsworth 2009a). Consequently, even if hydromagnesite converts to magnesite in the repository within hundreds to thousands of years, hydromagnesite formed relatively late in the regulatory period by CPR degradation may be available to influence repository chemical conditions.

DOE responded that it is unclear whether hydromagnesite will persist or convert to magnesite during the 10,000-year WIPP regulatory period (Moody 2009a). This statement is consistent with the calculation of the EEF by Vugrin et al. (2007), who randomly sampled the uncertainty in the moles of CO_2 consumed per mole of MgO reacted (see Section 4.4). Because of the uncertainty in whether hydromagnesite or magnesite formation will control CO_2 fugacity, EPA has specified that the CO_2 fugacity used to calculate actinide solubilities should be established by the brucite-hydromagnesite buffer [reaction (13)], which should provide an upper bound on actinide solubilities (see Section 6.0). DOE stated that information clarifying the uncertainties associated with the rate of conversion of hydromagnesite to magnesite would be attached as an erratum to CRA-2009, Appendix MgO (Moody 2009a).

EPA also observed that the CRA-2009 discussion of MgO uncertainties (Appendix MgO-2009, Section 6.2.4.4) did not include the uncertainties associated with the chemical composition of the CPR in the WIPP inventory (Cotsworth 2009a, Comment 1-C-20). DOE responded that although Vugrin et al. (2006) did not address uncertainties associated with the chemical composition of CPR materials in the WIPP inventory, DOE acknowledges that such uncertainties exist (Moody 2009a). Consequently, DOE will include a statement adding chemical composition uncertainties to the errata attached to Appendix MgO (DOE 2009).

4.6 BACKFILL EFFICACY CONCLUSIONS

Evaluation of the available data indicates that the MgO backfill will continue to control CO₂ fugacities under inundated conditions and maintain chemical conditions in WIPP brines that limit actinide solubilities. There are no data available regarding the carbonation rate of MgO under humid conditions in the WIPP repository, but maintenance of low CO₂ partial pressures is not important for these conditions. The current emplacement plan ensures adequate amounts of MgO, because the quantities of CPR and MgO are monitored in each room of the repository during emplacement, and additional MgO is emplaced if necessary to maintain the MgO EF of 1.2.

Because of uncertainties in the rate at which hydromagnesite will convert to magnesite in the repository environment, it is assumed for PA that the brucite-hydromagnesite reaction will buffer CO₂ fugacity at levels consistent with relatively low actinide solubilities under inundated conditions. EPA requested additional documentation from DOE regarding the characterization of the Martin Marietta MgO currently used as WIPP backfill and the acceptance testing that is currently carried out for this material. The MgO reactivity testing procedure and test results provided by DOE (Moody 2009c) demonstrate that the current backfill material contains a sufficient percentage of reactive periclase plus lime to control chemical conditions in the repository, and that the testing procedure now in use would detect any MgO shipments with inadequate percentages of reactive periclase plus lime.

5.0 ACTINIDE OXIDATION STATES

The actinide oxidation states assumed in the CRA-2009 PA have remained unchanged since the CCA (DOE 2009, Appendix SOTERM-3.9). The assumptions regarding the oxidation states were peer reviewed and approved for the CCA as part of the Dissolved Actinide Source Term and Chemical Conditions conceptual models (Wilson et al. 1996a, 1996b, 1997a, 1997b).

As part of the Chemical Conditions conceptual model, equilibrium is not assumed for redox reactions among the actinides. Actinide oxidation states were determined based on the assumption that reducing conditions would be established relatively quickly in the WIPP repository, combined with the results of a literature review and experimental investigations. The actinide oxidation states that were predicted to persist in the WIPP repository environment over the long term were (DOE 1996, Appendix SOTERM):

- Americium(III), curium(III) and thorium(IV)
- Plutonium(III) and plutonium(IV)
- Neptunium(IV) and neptunium(V)
- Uranium(IV) and uranium(VI)

Actinide solubilities are calculated for WIPP PA using the Fracture-Matrix Transport code (FMT). FMT does not include the calculation of redox states. Because it is assumed for PA that plutonium, neptunium and uranium may be present in either of two oxidation states, an oxidation-state parameter (GLOBAL:OXSTAT) is sampled from a uniform distribution (DOE 2009, Appendix SOTERM-5.2; Fox 2008). Calculated solubilities for the plutonium(III), neptunium(IV) and uranium(IV) oxidation states are assumed for half of the PA realizations, and calculated solubilities for the plutonium(IV), neptunium(V) and uranium(VI) oxidation states are assumed for the other half of the PA realizations.

The actinide oxidation states assumed for the PA calculations are important because of the effects of redox state on solubility. Reduced actinides [plutonium(III), plutonium(IV), neptunium(IV), and uranium(IV)] form solids that have lower solubilities than actinides in higher oxidation states [plutonium(V), plutonium(VI), neptunium(V), and uranium(VI)]. However, plutonium(III) is generally more soluble than plutonium(IV).

5.1 ACTINIDE OXIDATION STATE INFORMATION DEVELOPED BEFORE THE PABC04

EPA (1998d) reviewed and agreed with the expected oxidation states used in the CCA PA and PAVT. At the time of the CCA, most stakeholder questions about actinide oxidation states concerned the possible persistence of plutonium(VI) in the WIPP repository. EPA (1998d) considered a number of experimental studies indicating that reductants, including soluble iron, metallic iron, humics and other organic ligands, would reduce plutonium to the (III) and (IV) oxidation states under equilibrium conditions in the repository (Weiner 1996; Felmy et al. 1989; Rai and Ryan 1985; Choppin 1991).

EPA (2006c) reviewed information regarding likely actinide oxidation states in WIPP brines that became available after the CCA. Grambow et al. (1996) evaluated the sorption and reduction of

uranium(VI) from brine solutions on iron corrosion products, including hydrous iron(II)-magnesium oxides and magnetite [Fe₃O₄], under anoxic conditions. Addition of uranium(VI) to experiments with brine and iron corrosion products produced a rapid decrease in aqueous uranium concentrations. Most of the uranium associated with the solid phases appeared to be uranium(VI), rather than uranium(IV), so sorption of uranium(VI) appeared to be the dominant process for removing uranium from solution. In the solution phase, reduction of uranium(VI) to uranium(IV) was observed, but to a lesser extent than predicted by thermodynamic calculations.

A series of experiments conducted with WIPP brines in contact with actual TRU waste were included in the STTP (Villareal et al. 2001). The experiments were designed to simulate anticipated repository conditions based on the conceptualization of the WIPP repository at the time the experiments began. The presence of plutonium(V) and plutonium(VI) was detected in samples from a few STTP experiments (DOE 2004, Appendix PA, Attachment SOTERM, Section 4.8). EPA reviewed the STTP results and concluded that the STTP results do not appear to be reliable indicators of plutonium oxidation states or actinide solubilities in the WIPP repository environment because the experimental conditions, including high CO₂ fugacities and low pH, were not representative of WIPP repository conditions (MFG 2000; TEA 2001, TEA 2002).

Haschke et al. (2000) reported that PuO_{2+x}(s), (in which x is less than or equal to 0.27) is the stable binary plutonium oxide phase in air. This phase contains a significant amount of plutonium(VI) in addition to plutonium(IV) in its structure. Previous investigations indicated that PuO₂(s), which contains only plutonium(IV), is the most stable plutonium oxide. Because plutonium(IV) solids are relatively insoluble, plutonium is generally considered to be relatively immobile under most environmental conditions. Based on the Haschke et al. (2000) article, Madic (2000) stated that the presence of plutonium(VI) in PuO_{2+x}(s), which could increase plutonium mobility in the environment, should be considered in safety evaluations of long-term plutonium storage. EPA considered the possible formation of PuO_{2+x}(s) in the WIPP repository and concluded that no experimental evidence of its formation was available in brines or under the reducing conditions anticipated in the repository (MFG 2000, TEA 2002). On the other hand, the Agency observed that experimental studies (Grambow et al. 1996; Slater et al. 1997), in addition to the studies previously considered for the CCA have shown that iron metal and iron corrosion products reduce actinide oxidation states and actinide solution concentrations in brines (MFG 2000; TEA 2001).

Xia et al. (2001) investigated the distribution of plutonium, neptunium and uranium oxidation states in synthetic ERDA-6 WIPP brine in the presence of powdered metallic iron. These experiments were carried out under an inert (argon) atmosphere over a pH range from approximately 8 to 12. The results of these experiments indicated that the effects of adding iron powder on the plutonium(VI) concentrations in solution (initially 2.5×10^{-4} M) depended on pcH.⁶ At pcH values less than 9, iron addition resulted in decreased Eh values, and plutonium(VI) decreased to concentrations ranging from 10^{-5} to 10^{-8} M. However, at pcH values from 9 to 12, iron addition produced only small decreases in Eh values and plutonium(VI)

⁶ pH is the -log of the hydrogen ion activity, whereas pcH is the -log of the hydrogen ion concentration; the hydrogen ion activity and hydrogen ion concentration are nearly equal in dilute aqueous solutions, but may significantly diverge in high-ionic-strength solutions.

concentrations. Xia et al. (2001) attributed this limited effect at higher pcH to the formation of coatings that limited the availability of the iron metal to the brine. To confirm the formation of coatings as the cause of the limited effects of the powdered iron, a second addition of iron powder was carried out in the higher-pcH experiments. This second iron addition reduced measured Eh and plutonium concentrations in the brine solution at pcH values of approximately 9 and 12, although the effects at pcH 10 were small. Spectroscopic examination of the brines indicated that 8% to 90% of the plutonium remaining in solution was present in the +V oxidation state. Xia et al. (2001) interpreted these results to mean that more iron was required to maintain reducing conditions in higher-pcH brine solutions. Absorption spectroscopy was used to determine that plutonium(VI) disappeared in brine solutions with added iron powder. Xia et al. (2001) suggested that the plutonium in solution could be plutonium(V) in equilibrium with $\text{PuO}_2 \cdot x\text{H}_2\text{O}(\text{s})$, although the concentration of plutonium(V) in the monitored solution was below the detection limit for spectrophotometric determination.

In experiments carried out by Xia et al. (2001) with neptunium(V) in synthetic ERDA-6 brine, iron addition decreased neptunium solution concentrations and appears likely to have reduced neptunium(V) to neptunium(IV). In experiments with uranium(VI) in ERDA-6 brine, iron addition did not result in the reduction of uranium(VI) to uranium(IV), probably because of the effects of the brine on the reducing capacity of iron powder (Xia et al. 2001).

Reed et al. (1997) reported experimental results related to the effects of oxalic acid, citric acid and EDTA on the stability of neptunium(VI) and plutonium(VI) in brine solutions. These complexing agents are important, because they have been reported in the WIPP inventory and may affect actinide solubilities (Section 6.0). A mixture of EDTA, citrate, and oxalate was added to ERDA-6 brine at pH values of 8 and 10 with 10^{-4} M carbonate, to ERDA-6 brine at pH 10 without carbonate, and to G-Seep brine at pH 5 and 7 without carbonate. In the G-Seep brine, the plutonium(VI) was rapidly reduced to form plutonium(V) and plutonium(IV) organic complexes. The presence of carbonate in the ERDA-6 brine at pH 8 slowed the reduction rate of plutonium(VI) to plutonium(IV) and plutonium(V) species. At pH 10 in the presence of carbonate, no reduction was observed and the plutonium(VI)-carbonate complex predominated in solution. In the absence of carbonate at pH 10 in ERDA-6 brine, slow reduction of plutonium(VI) was observed. Based on these results, it appears that hydrolytic and carbonate species stabilize plutonium(VI) with respect to reduction by the organic ligands. The addition of iron coupons to these experiments caused the reduction of plutonium(VI) to plutonium(IV) and a consequent decrease in plutonium solution concentrations (ANL 1997).

In experiments with citrate, oxalate, and EDTA at pH 5 and 7 in G-Seep brine, neptunium(VI) was rapidly reduced to neptunium(V) (Reed et al. 1997). There was no evidence of further reduction of neptunium(V) to neptunium(IV) after 2 months duration. The presence of carbonate complexes at pH values of 8 and 10 in ERDA-6 brine slowed the rate of neptunium(VI) reduction. In the absence of carbonate at pH 10, neptunium(VI) was rapidly removed from solution to form neptunium(IV) and (V) organic complexes and precipitates.

Humic acids are likely to form in the WIPP repository as a product of microbial degradation of CPR (DOE 2004, Appendix PA, Attachment SOTERM-2.2.2). The reduction of plutonium(V) by humic acids was investigated in 5 m NaCl in the presence and absence of divalent cations (calcium and magnesium) at pcH values of 5.7 and 8 (André and Choppin 2000). Increasing

concentrations of divalent cations and humic acid increased the rates and percentages of plutonium(V) reduced by the humic acid.

EPA (2006c) reviewed the information that had been developed since the CCA regarding potential actinide oxidation states under WIPP repository conditions, and concluded that the available evidence continued to support the actinide oxidation state assumptions used for the WIPP PA calculations.

5.2 ACTINIDE OXIDATION STATE INFORMATION DEVELOPED AFTER THE PABC04

CRA-2009 (DOE 2009, Appendix SOTERM-2009) addressed processes that may influence actinide oxidation states in the WIPP repository environment, including iron corrosion, microbial processes, radiolysis and interactions with organic ligands. Microbial degradation of CPR may produce significant quantities of H₂S, generating solid reaction products such as FeS(s) or PbS(s) and increasing H₂S fugacity. Sulfide solids and H₂S would likely reduce actinide oxidation states.

CRA-2009 Appendix SOTERM-2009, Section SOTERM-2.3.4 (DOE 2009) stated that reduced iron species, both zero-valent iron in steel and aqueous reduced iron (Fe²⁺), will reduce higher-valence-state actinides in WIPP brines, leading to lower actinide solubilities. Telander and Westerman (1997) identified the corrosion products of low-carbon steel in anoxic WIPP brines as Fe, Mg(OH)₂ and as mackinawite (FeS) in the presence of H₂S. Another anoxic corrosion study carried out with mild steel in WIPP brines identified the corrosion product as a green-rust-like compound using Mössbauer spectroscopy (Wang et al. 2001); green rusts are a metastable corrosion product consisting of Fe(II)/Fe(III) hydroxide compounds containing non-hydroxyl anions. The presence of zero-valent iron, iron hydroxides, and iron sulfides will influence the redox states of the actinides in WIPP repository brines. Detailed discussions of the expected effects of iron in the WIPP repository on redox states of uranium, neptunium, and plutonium were provided in Appendix SOTERM-2009 Section SOTERM-3.3.1.1, Section SOTERM-3.4.1, and Section SOTERM-3.5.1.1, respectively.

The effects of microbial processes on actinide valence states under the anaerobic, reducing conditions in the long-term WIPP repository were addressed in Appendix SOTERM-2009 Section SOTERM-2.4.1.2. The effects of actinide bioreduction are considered as part of the assumed actinide oxidation states. Although limited WIPP-specific data are available, literature data indicate that bioreduction of actinides may occur in the WIPP repository.

5.2.1 Uranium

DOE (2009, Appendix SOTERM-2009, Section SOTERM-3.3.1.1) addressed the anticipated effects of iron on the valence state of uranium in WIPP repository brines. The use of zero-valent iron barriers for the removal of uranyl ions [UO₂²⁺] from groundwater is well-known, and both reduction with precipitation and sorption by iron corrosion products have been cited as mechanisms whereby uranyl ion is removed from solution (e.g., Grambow et al. 1996, Gu et al. 1998). Green rusts, such as those produced by iron corrosion in WIPP brines (Wang et al. 2001), have been shown to reduce uranium(VI) to uranium(IV) (Dodge et al. 2002, O'Loughlin et al.

2003). However, other studies have shown that under anoxic conditions, uranium(VI) may be slowly and incompletely reduced to uranium(IV) (Fiedor et al. 1998, Xia et al. 2001).

Because of the role of sulfides in the formation of uranium roll-front deposits, a relatively large amount of data is available demonstrating that uranium(VI) is reduced to uranium(IV) by sulfide solids, such as pyrite [FeS₂] and by H₂S. Uranium reduction from uranium(VI) to uranium(IV) by reaction with H₂S is used in the restoration of groundwater affected by uranium in situ recovery operations. However, this reaction may be inhibited by carbonate in solution (e.g., total carbonate of 2 × 10⁻³ M at pH 9), because the reduction reaction involves the uranyl hydroxide species, rather than uranyl carbonate species (Hua et al. 2006).

Numerous studies of bioreduction of uranium have been carried out, although most studies have not been performed under conditions directly applicable to WIPP. Bioreduction of uranium(VI) to uranium(IV) under anaerobic conditions has been demonstrated (e.g., Lovley and Phillips 1992, Frederickson et al. 2000, Suzuki et al. 2003). However, uranium solution speciation may inhibit bioreduction (Brooks et al. 2003, Neiss et al. 2007) and organic ligands such as citrate may maintain uranium(IV) in solution after uranium bioreduction has occurred (Francis and Dodge 2008).

Francis et al. (2000) examined the biotransformation of uranyl nitrate, uranyl citrate, uranyl-EDTA and uranyl carbonate by a denitrifying halophilic bacterium isolated from the WIPP repository. This bacterium, *Halomonas* sp. (WIPP1A), does not reduce iron or uranium. This study demonstrated that an increase in microbial activity could enhance uranium solubility through the formation of the soluble uranyl carbonate species. However, the presence of the WIPP MgO backfill will control CO₂ fugacities at relatively low levels, limiting high uranium concentrations caused by carbonate complexation.

5.2.2 Neptunium

DOE (2009) discussed the expected neptunium valence states in WIPP brines in Appendix SOTERM-2009, Section SOTERM-3.4.1, and concluded that the +IV oxidation state is the most likely under the anoxic conditions predicted for the repository. Rai and Ryan (1985) tested the ability of several reducing agents to maintain the neptunium(IV) redox state in solution; their results indicated that powdered metallic iron maintains neptunium in the +IV oxidation state. Similarly, Xia et al. (2001) determined that metallic iron powder reduced neptunium(V) to neptunium(IV), and caused the precipitation of NpO₂·xH₂O(am) in experiments with dilute NaCl and ERDA-6 brine.

Banaszak et al. (1999) evaluated the reduction of neptunium(V) to neptunium(IV) in the presence of an anaerobic microbial consortium isolated from lake-bottom sediments. Their results indicated that microbially produced iron(II) or manganese(II/III) may serve as the electron donors for neptunium(V) reduction. Rittmann et al. (2002)⁷ determined that an anaerobic sulfate-reducing consortium reduced neptunium(V) to neptunium(IV) with precipitation of an insoluble neptunium(IV) solid; however, the presence of ligands produced by

⁷ This study was incorrectly referenced as Banaszak et al. (1998) in DOE (2009, Appendix SOTERM Section 3.4.1).

fermentation was found to limit immobilization by precipitation under some circumstances. Icopini et al. (2007) found that reduction of neptunium(V) to neptunium(IV) was enhanced in the presence of citrate, but citrate caused the reduced neptunium(IV) to remain soluble.

5.2.3 Plutonium

The redox reactions expected for plutonium in WIPP brines were addressed in Appendix SOTERM-2009, Section SOTERM-3.5 (DOE 2009). The plutonium oxidation states used in PA are plutonium(III) and plutonium(IV); plutonium(III) is generally more soluble than plutonium(IV). In their discussion of plutonium(III) and plutonium(IV) oxidation states, DOE (2009, Appendix-2009, Section SOTERM-3.5) stated that use of plutonium(III) in half of the PA realization is a conservatism, based on the higher solubility of plutonium(III) relative to plutonium(IV).

Rai et al. (2002) evaluated the reductive dissolution of amorphous $\text{PuO}_2(\text{s})$ by aqueous Fe^{2+} . In these experiments, conducted in low-ionic-strength solutions, reductive dissolution was observed with the presence of plutonium(III) in solution, confirmed by spectroscopic, solvent extraction and thermodynamic analysis of the data. Ding et al. (2006) investigated the speciation of plutonium solids heterogeneously precipitated by iron and aluminum metal in water, NaCl solutions and ERDA-6 brine. Their results indicated that reductive precipitation of plutonium(VI) in the initial solution produced materials identical to the $\text{PuO}_{2+x-y}(\text{OH})_{2y} \cdot z\text{H}_2\text{O}$ produced by other methods, such as hydrolysis of plutonium(IV).

Reed et al. (2006) found that addition of iron coupons and aqueous Fe^{2+} to WIPP brines containing plutonium(VI) with and without carbonate at pH values from 5 to 10 resulted in reduction to plutonium(IV) and rapid decreases in aqueous plutonium concentrations. Reed et al. (2006) determined using x-ray absorption near-edge spectroscopy (XANES) and extended x-ray absorption fine structure analysis (EXAFS) that the plutonium precipitated as a solid and on the surfaces of the iron coupons was predominantly if not exclusively present as plutonium(IV). The oxidation state of the plutonium remaining in the aqueous phase was not directly determined, but was believed to be plutonium(IV) or possibly plutonium(III), based on the low solubility. Reed et al. (2006) noted that the preponderance of plutonium(IV) in the system was not consistent with the thermodynamic data, which would predict the existence of plutonium(III) under anoxic conditions in the presence of iron. It was suggested that the presence of plutonium(IV) may have been caused by buildup of radiolytically produced oxychlorides over the 2-year experiments. Aqueous Fe^{2+} addition under anoxic conditions caused significant decreases in dissolved plutonium in the brine at all pH values except in the Salado brine at pH of 5. Absorption spectroscopy measurements in this sample indicated that plutonium was present in solution as plutonium(V).

Neck et al. (2007)⁸ evaluated thermodynamic and solubility data for plutonium hydroxides and hydrous oxides under different redox conditions. Their evaluation showed that $\text{Pu}(\text{OH})_3(\text{s})$ is unstable under reducing conditions within the stability field of water, converting to $\text{PuO}_2(\text{hyd})$,

⁸ DOE (2009, Appendix SOTERM-2009, Section SOTERM-3.8.1) incorrectly referenced this paper as Neck et al. (2003).

with the solubility of this phase determined by the equilibrium concentrations of aqueous plutonium(III) and plutonium(IV) species.

Altmaier et al. (2009) investigated the solubility of plutonium(IV) hydrous oxide in 0.25 M and 3.5 M MgCl₂ solutions at approximately pH 9 in the presence of metallic iron powder. The solutions were pre-equilibrated with brucite for 0.25 M MgCl₂ experiments or korshunovskite [Mg₂Cl(OH)₃•4H₂O(cr)]⁹ for 3.5 M MgCl₂ experiments. In these experiments, plutonium(III) was the dominant oxidation state in solution. Altmaier et al. (2009) also investigated plutonium(IV) hydrous oxide solubility in alkaline (pH 11 to 12) 3.5 to 4.0 M CaCl₂ solutions in contact with metallic iron; these pH values are higher than those anticipated in WIPP brines. At these pH values, plutonium(IV) was the dominant oxidation state in solution and the formation of calcium-plutonium-hydroxyl complexes was observed. In experiments without iron powder, the plutonium oxidation state was predominantly plutonium(V), with significant amounts of plutonium(IV) complexes at pH values greater than 10.

DOE (2009, Appendix SOTERM-2009, Section SOTERM-3.5.2) cited experiments by Reed et al. (2009) carried out to confirm the reduction of higher-valent plutonium by reduced iron in brine and to establish the reactivity of plutonium with iron oxides. The document Reed et al. (2009) was requested by EPA (Cotsworth 2009a, Comment 1-23-2c) and the final document (Reed et al. 2010) was received in March 2010. Reed et al. (2010) summarized the existing literature data on redox reactions of higher-valent plutonium under reducing conditions, including results reported by Xia et al. (2001) discussed in Section 5.1 above and Reed et al. (2006) that are reviewed above. Reed et al. (2010) also described previously unreported results of experiments to evaluate the reduction of plutonium(VI) in brine by iron. The goals of these experiments were to resolve apparent discrepancies in the literature (e.g., between the results of Xia et al. 2001 and Reed et al. 2006), confirm the results of Reed et al. (2006) and extend this work to include the effects of iron(II) and iron(III) oxide phases on plutonium oxidation states.

Experiments were carried out for 4 weeks at room temperature under anoxic conditions in ERDA-6 brine in the presence of iron powder without carbonate at pH 8 and 10 to reproduce the results of Xia et al. (2001). An additional experiment was carried out in GWB brine at pH 7 to extend the results to the different brine composition. Other experiments were carried out in ERDA-6 brine with carbonate ion in the presence of an iron coupon at pH 8 and 10 to reproduce the results of Reed et al. (2006). An additional experiment was carried out in GWB brine at pH 7 without carbonate ion in the presence of an iron coupon to extend the results to the different brine composition. In the experiments at pH 7 (GWB) and 8 (ERDA 6), plutonium concentrations decreased rapidly in the brines when either iron powder or an iron coupon was present. At pH 10, the plutonium concentration decreased more slowly, and the concentration was still decreasing at the time of the report.

Reed et al. (2010) also reported the results of experiments in ERDA-6 brine to evaluate the effects of iron oxidation state on plutonium(VI) reduction. These experiments were carried out with carbonate ion at pH 9, with the addition of an iron coupon, iron powder, colloidal iron(II), colloidal iron(III), iron(III) oxide or magnetite, which is an iron(II/III) oxide. The results of these experiments showed that addition of the iron powder, iron coupon or magnetite rapidly

⁹ DOE has referred to this material as “phase 3.”

reduced plutonium concentrations in solution. XANES analysis showed that the aqueous plutonium(VI) was reduced to form solid plutonium(IV) phases by the zero-valent iron and iron(II). A smaller decrease in the aqueous plutonium concentration was observed in the iron(III) oxide experiment. Because no reductant was available in these experiments, the decreased plutonium concentration was believed to be caused by sorption.

Reed et al. (2010) concluded that zero-valent iron and iron(II) minerals reduced plutonium(V) and plutonium(VI) to form relatively insoluble plutonium(IV) solid phases. The presence of iron(III) mineral phases did not result in plutonium reduction, but did result in a decrease in plutonium concentrations through sorption. In the most recent plutonium reduction experiments in ERDA-6 brine at pH 8 and 10 by Reed et al. (2010), significant plutonium(VI) reduction by iron powder was observed, unlike the limited reduction observed by Xia et al. (2001). Reed et al. (2010) suggested that the divergent results may have been caused by differences in the oxygen content of the experiments, the chemistry or condition of the iron powder, or differences in the relative activities of the plutonium used in the experiments.

In the caption for Figure SOTERM-11 (DOE 2009, Appendix SOTERM-2009), DOE stated that the Eh-pH diagram demonstrated that plutonium(IV) species will be stable at near-neutral pH. EPA requested additional explanation from DOE regarding this assertion, observing that at the reducing conditions expected in the repository, near the lower stability limit for water, plutonium(III) species appear to be the most stable, i.e., PuCO_3^+ and $\text{Pu}(\text{CO}_3)_2^-$ (Cotsworth 2009a, Comment 1-C-12). Moody (2009c) responded that for the PABC09, there had been no change in the conceptual model assumption of a 0.5 probability that plutonium would be present in the plutonium(III) oxidation state and a 0.5 probability that plutonium would be present in the plutonium(IV) oxidation state. The intent of Appendix SOTERM-2009, Figure SOTERM-11 was to support the existence of lower plutonium oxidation states (III and IV) instead of higher plutonium oxidation states (V and VI) under the reducing conditions in the WIPP repository and not to differentiate between the stability of plutonium(III) and plutonium(IV) under WIPP conditions.

DOE (2009, Appendix SOTERM-2009, Section SOTERM-3.5.1.2) addressed plutonium bioreduction, stating that there are relatively few studies of the bioreduction of plutonium and no studies have been conducted using halophiles that will exist in the WIPP repository. Reed et al. (2007) found that *Shewanella alga* reduced plutonium(V) to less-soluble plutonium(III) or plutonium(IV). Boukhalfa et al. (2007)¹⁰ conducted plutonium(IV) reduction experiments with metal-reducing bacteria, freshly precipitated plutonium(IV) solids and EDTA; in this study, it was established that addition of the EDTA chelating agent enhanced reduction of the plutonium(IV) to plutonium(III), and that the plutonium(III)-EDTA aqueous species remained in solution. Ohnuki et al. (2007) evaluated the reduction of plutonium(VI) by *Bacillus subtilis* with and without the presence of bentonite clay; the results of this study suggest that plutonium(IV) is preferably sorbed to bacterial cells in the mixture, and that plutonium(VI) is reduced to plutonium(V) and plutonium(IV). Icopini et al. (2009) determined that the metal-reducing bacteria *Geobacter metallireducens* GS-15 and *Shewanella oneidensis* MR-1 reduced plutonium(V) and plutonium(VI) to plutonium(IV); no plutonium(III) production was observed

¹⁰ This study was incorrectly referenced as Icopini et al. (2007) in Appendix SOTERM-2009, Section SOTERM-3.5.1.2 (DOE 2009).

in the experiments. The reduced plutonium(IV) formed a nanoparticulate solid on the surface of or within the cell walls of the bacteria.

5.3 RADIOLYSIS

Both the Chemical Conditions and Dissolved Actinide Source Term conceptual models include assumptions regarding the effects of radiolytic processes on actinide oxidation states (SC&A 2008b, Appendix A):

- *Brine radiolysis could produce reactive species, such as hydrogen peroxide [H_2O_2]. Any oxidized species such as hydrogen peroxide are expected to react quickly with iron metal and dissolved iron(II) species in solution. Consequently, radiolysis is not expected to affect the oxidation-reduction conditions in the repository*
- *Metastable phases observed in laboratory experiments will become more stable with time, and solubilities observed in these experiments provide an upper concentration limit. The effects of radiolysis will not cause actinide solids to become more soluble over time.*

These assumptions were peer reviewed and accepted at the time of the CCA (Wilson et al. 1996a, 1996b, 1997a, 1997b).

DOE (2009, Appendix SOTERM-2009, Section SOTERM-2.4.2.1) stated that the likely products of WIPP brine radiolysis will include oxychloride and chloride species (ClO^- , $HOCl$, Cl_2 and Cl_3^-) and hypobromite ion (OBr^-). However, DOE (2009, Appendix SOTERM-2009, Section SOTERM-2.4.2.1) concluded that the effects of brine radiolysis will take place mainly at the solid-liquid interface and any radiolytic effects, such as oxidizing aqueous species or higher-valence-state actinides, are expected to be quickly mitigated by the bulk brine chemistry and the reaction of reducing agents with the oxidizing radiolysis products. WIPP-specific investigations cited to support this assumption include Reed et al. (2006), Reed et al. (2009), and Lucchini et al. (2009). Reed et al. (2009) and Lucchini et al. (2009) were not provided with the CRA-2009, and EPA requested these documents for review (Cotsworth 2009a, Comment 1-23-2b,c). Review of Lucchini et al. (2009) indicated that the correct reference in this context was Lucchini et al. (2005). Lucchini et al. (2005) examined the stability of hypochlorite (OCl^-) and hydrogen peroxide in WIPP brines and the effects of these species on uranium(VI) in solution. Hypochlorite and hydrogen peroxide were found to be unstable in WIPP brine, so that significant build up of these radiolytic species is unlikely, even in the absence of metallic iron. Preliminary experiments that involved addition of hypochlorite or hydrogen peroxide to brine containing uranium(VI) resulted in precipitation of uranium-bearing phases.

The available information regarding brine radiolysis and reduction reactions caused by iron in the repository continues to support the conceptual model assumptions regarding the lack of significant effects of radiolysis on oxidation-reduction conditions and actinide oxidation states in the repository.

5.4 VALIDITY OF ACTINIDE OXIDATION STATE ASSUMPTIONS FOR THE PABC09

For the PABC09, it was assumed that uranium may exist in either the +IV or +VI oxidation state. This assumption remains valid, based on the available data. Uranium(IV) is likely to be the most stable oxidation state under the reducing conditions in the WIPP repository. However, uranium(VI) may persist because of the effects of aqueous speciation on uranium reduction. It is assumed that neptunium will be present in the WIPP repository in either the +IV or +V oxidation state. The available evidence indicates that neptunium will most likely be present in the +IV oxidation state. The assumption that neptunium may be present in the +V oxidation state in the WIPP repository brines is conservative, because of the greater solubility of neptunium(V) solid phases. However, because of the relatively small neptunium inventory, the assumption of higher neptunium solubility in half of the PA realizations is unlikely to affect PA results. The assumption that plutonium will be present in the less-soluble +III and +IV oxidation states, rather than the more-soluble +V and +VI oxidation states, continues to be supported by the available data. The relatively more soluble plutonium(III) oxidation state may be stable or may metastably persist under anticipated WIPP repository conditions. Radiolytic effects on actinide oxidation states have been assumed to be mitigated by the effects of reducing materials, mainly iron metal, in the WIPP repository and the available data continue to support this assumption.

6.0 DISSOLVED ACTINIDE SOURCE TERM

Actinides in the WIPP waste inventory may dissolve in brines that enter the repository, either as brine that flows into the repository from the DRZ in the Salado Formation, or brine that flows up a borehole that intersects both the repository and a pressurized brine region in the underlying Castile Formation. The actinide solubilities calculated for PA include americium, curium, neptunium, plutonium, thorium and uranium. Actinide solubilities are calculated using thermodynamic modeling that depends on a number of assumptions related to chemical conditions in the repository and to the chemical behavior of the actinides in solution. Consequently, both the Chemical Conditions and Dissolved Actinide Source Term conceptual models are important for the calculation of dissolved actinide concentrations used in PA. These conceptual models are described in detail by SC&A (2008b, Appendix A).

The Chemical Conditions conceptual model includes assumptions related to the mineralogy of the Salado Formation in contact with WIPP brines, the compositions of the Salado and Castile brines that may enter the repository and contact waste, organic ligand concentrations and the reactions that may control important chemical parameters, such as pH, redox and CO₂ fugacities. The Chemical Conditions conceptual model also includes assumptions regarding the redox states of actinides and metals in solution. The Dissolved Actinide Source Term conceptual model includes a number of assumptions, including assumptions about the oxidation states of the actinides, equilibrium of the brine with respect to precipitation-dissolution reactions, the existence of reducing conditions in the repository, the important inorganic and organic constituents for determining actinide speciation in brines and use of the Pitzer activity coefficient model.

The FMT code is used to calculate actinide solubilities for WIPP PA. The FMT calculations of aqueous concentrations in WIPP brines are based on calculations of aqueous speciation and solubility equilibria performed using the Pitzer activity coefficient model. The FMT code does not include reactions representative of redox processes, so the oxidation state of each actinide must be assumed for the calculations (Section 5.0).

6.1 CCA AND PAVT DISSOLVED ACTINIDE SOURCE TERM

The Dissolved Source Term and Chemical Conditions conceptual model assumptions were peer reviewed and approved for the CCA PA (Wilson et al. 1996a, 1996b, 1997a, 1997b). DOE performed FMT modeling calculations to determine the solubilities of americium(III), thorium(IV) and neptunium(V) in end-member Salado (Brine A) and Castile (ERDA-6) brine. It was assumed that actinide solubilities in brine mixtures would be adequately represented by calculations with the end-member brines. For these solubility calculations, it was assumed that the brines would be in equilibrium with the Salado minerals anhydrite, halite and magnesite, as well as brucite and magnesite that would form from hydration and carbonation, respectively, of the MgO backfill. The minerals glauberite [Na₂Ca(SO₄)₂] and korshunovskite were allowed to precipitate from the brines.

6.1.1 FMT Code and Database

The CCA actinide solubility calculations were performed with FMT Version 2.0. EPA (1998d) identified the database used for the CCA calculations as FMT_HMW_345_960501FANG.CHEMDAT, but noted that it was not clear which database had been used. Based on the date indicated in the file name, EPA (1998d) believed the database was representative of the database used for the CCA PA actinide solubility calculations. Novak and Moore (1996), however, stated that HMW_3456_960318.CHEMDAT and HMW_3456_960325.CHEMDAT were used for the FMT calculations, and that the data in these two files that were used in the solubility calculations were identical.

6.1.2 Oxidation-State Analogy

The oxidation-state analogy was used to extend the calculated americium(III), thorium(IV) and neptunium(V) solubilities to the other actinides and oxidation states important to WIPP PA. The oxidation-state analogy, part of the Dissolved Actinide Source Term conceptual model, is the assumption that all actinides in the same oxidation state will form the same aqueous species and isostructural compounds. Consequently, plutonium(III) and curium(III) solubilities in WIPP brines are assumed to be equal to calculated americium(III) solubilities, and uranium(IV), plutonium(IV) and neptunium(IV) solubilities are assumed to be equal to calculated thorium(IV) solubilities. Calculated neptunium(V) solubilities are used only for neptunium, because it is the only actinide predicted to be present in WIPP brines in the +V oxidation state.

6.1.3 Uranium(VI) Solubility

Because DOE could not develop an adequate thermodynamic model for uranium(VI), fixed concentrations of 8.7×10^{-6} M (Salado brine) and 8.8×10^{-6} M (Castile brine) were used for PA. EPA (1998d) reviewed DOE's predictions of uranium(VI) solubilities, including the information in the CCA and supporting documents (Hobart and Moore 1996, Novak and Moore 1996), and additional information that became available after the CCA. EPA (1998d) noted two assumptions that DOE relied on in selecting this uranium(VI) concentration for PA. One of DOE's assumptions was that carbonate would be completely absent from repository brines, when in fact the brucite-hydromagnesite reaction will control carbonate concentrations at relatively low but non-zero levels. Another assumption made by DOE was that a model for uranium(VI) could not be developed because of uncertainties regarding uranium(VI) hydrolysis species; EPA (1998d) noted that the dominant species in the pH range relevant to the WIPP repository are likely to be carbonate complexes, such as UO_2CO_3^0 , $\text{UO}_2(\text{CO}_3)_2^{2-}$ and $\text{UO}_2(\text{CO}_3)_3^{4-}$. Therefore, precise knowledge of the stabilities of the hydrolysis species may not be necessary to model uranium(VI) solubility under the expected repository conditions, because only a small fraction of the total dissolved uranium(VI) exists as hydrolysis species. However, EPA (1998d) accepted the use of a single uranium(VI) concentration in PA because it was consistent with the available data presented in Reed and Wygmans (1997) and Hobart and Moore (1996) and uncertainties associated with this estimated concentration were believed to be adequately accounted for by the sampled uncertainty distribution.

6.1.4 CCA PA and PAVT Actinide Solubility Uncertainties

The actinide solubilities used in WIPP PA are constants; uncertainties in these values are accounted for by sampling a cumulative distribution function representing uncertainty and multiplying the solubilities by the antilog of the sampled value to determine the actinide concentrations used in PA for each realization. The determination of the actinide solubility uncertainty distribution used in the CCA PA and PAVT was reviewed in detail by EPA (1998d). To obtain this distribution, DOE compared experimentally measured solubility data used to develop the solubility models in FMT to the concentrations predicted by curve-fitting with the code NONLIN (Babb 1996). DOE also compared solubilities reported in the literature with concentrations predicted using FMT for the conditions of the experiments. The population of errors from these comparisons was accumulated and used to generate a cumulative distribution. DOE excluded data for the +IV and +VI actinides from the evaluation, because they believed these datasets to be inconsistent or technically deficient. The remaining data consisted of +III actinide solubility measurements (139 values) and +V actinide solubility measurements (11 values). These data were combined to generate a single distribution, which ranged on a log scale from -2.0 to 1.4, with a median value of -0.09 (DOE 2004, Appendix PA, Attachment SOTERM). This distribution was used to represent the uncertainties associated with the solubilities for all four actinide oxidation states.

6.1.5 Effects of Organic Ligands on Actinide Solubilities

Acetate, citrate, EDTA and oxalate were identified as organic ligands that could potentially affect actinide solubilities, because these ligands are water soluble and present in significant quantities in the WIPP inventory (DOE 1996). Possible concentrations of these ligands were estimated by DOE (1996) using the inventory amounts and a brine volume of 29,841 m³, which was the smallest quantity of brine required to be in the repository that will support transport away from the repository (Larson 1996). The organic ligand concentrations calculated by DOE (1996) are listed in Table 6-1. DOE (1996, Appendix SOTERM, Section 5) determined that actinide solubilities would not be significantly affected by the presence of organic ligands because other constituents, including transition metals in the waste and magnesium from the MgO backfill, would compete with the actinides for binding sites on the organic ligands. EPA (1998d) reviewed literature data related to actinide complexation by organic ligands and information presented by DOE (1996, Appendix SOTERM, Section 5). EPA (1998d) also performed solubility modeling at low ionic strength to estimate the effect of EDTA on thorium(IV) solubility in brine. The results of these calculations indicated that the effect of EDTA is likely to be negligible at the EDTA concentrations predicted for the repository. EPA (1998d) concluded that the available evidence supported the assumption by DOE (1996) that organic ligands would not significantly affect actinide solubilities.

Table 6-1. Ligand Concentrations Calculated for the CCA PAVT, PABC04 and PABC09

Ligand	CCA PAVT (m) (DOE 1996)	PABC04 (M) (Brush 2005)	PABC09 (M) (Brush and Xiong 2009)
Brine Volume (m ³)	29,841	10,011	17,400
Acetate ^a	1.1×10^{-3}	1.06×10^{-2}	1.94×10^{-2}
Citrate ^b	7.4×10^{-3}	8.06×10^{-4}	2.38×10^{-3}
EDTA ^c	4.2×10^{-6}	8.14×10^{-6}	6.47×10^{-5}
Oxalate ^d	4.7×10^{-4}	4.55×10^{-2}	1.73×10^{-2}

a – Sum of acetic acid (CH₃COOH) and sodium acetate (NaCH₃COO)

b – Sum of citric acid (C₆H₈O₇) and sodium citrate (NaC₆H₇O₇)

c – Assumed monosodium EDTA

d – Sum of oxalic acid (H₂C₂O₄) and sodium oxalate (NaHC₂O₄)

6.1.6 Actinide Solubility Calculations for the CCA PAVT

After review of the conceptual model and CCA PA results, EPA (1997a, 1997b, 1998a, 1998d) directed DOE to use the assumption that reaction of brucite to form metastable hydromagnesite would control CO₂ fugacities in the WIPP repository, rather than the brucite-magnesite reaction. DOE also incorporated more realistic thermodynamic data for thorium(IV) and neptunium(V) in the FMT database, based on information that had become available since the CCA PA (EPA 1998d). The results of these actinide solubility calculations, carried out for the CCA PAVT, are summarized in Table 6-2.

The FMT code version used for the CCA PAVT actinide solubility calculations was Version 2.2. EPA (1998d) identified the FMT database version for the CCA PAVT actinide solubility calculations as HMW_970407_HMAG5424.CHEMDAT; however, Brush and Xiong (2003b) identified the database version for the CCA PAVT slightly differently, as FMT_970407.CHEMDAT. Based on the description in EPA (1998d), the two names appear to refer to the same database version.

6.2 CRA-2004 PA DISSOLVED ACTINIDE SOURCE TERM

The assumptions used to calculate actinide solubilities for the CRA-2004 PA were revised by DOE (2004, Appendix PA, Attachment SOTERM). DOE's revisions to the conceptual model for these calculations included a change in the Salado brine composition from Brine A to GWB, and the assumption that the mineral assemblage that buffers CO₂ fugacity in the absence of significant microbial activity would be brucite-calcite instead of brucite-hydromagnesite. DOE (2004, Appendix PA, Attachment SOTERM) also updated the FMT database and incorporated calculations of the effects of organic ligands (acetate, citrate, EDTA and oxalate), using newly developed data for actinide-organic ligand complex formation and the formation of magnesium-organic ligand complexes. Consequently, the potential effects of organic ligands on actinide solubilities were included in the calculations, instead of being assumed to be negligible.

Table 6-2. Actinide Solubility Calculations for the CCA PAVT, the PABC04 and the PABC09

Property or Actinide Oxidation State	CCA PAVT No Organic Ligands		PABC04 With Organic Ligands		PABC09 With Organic Ligands	
	Salado (Brine A)	Castile (ERDA-6)	Salado (GWB)	Castile (ERDA-6)	Salado (GWB)	Castile (ERDA-6)
Brine						
pH	8.69	9.24	8.69	8.94	8.69	8.98
pcH	--	--	9.39	9.64	9.40	9.68
Log CO ₂ fugacity	-5.50	-5.50	-5.50	-5.50	-5.50	-5.50
Total Carbon (M)	--	--	2.16×10^{-5}	5.18×10^{-5}	3.50×10^{-4}	4.48×10^{-4}
III (M)	1.2×10^{-7}	1.3×10^{-8}	3.87×10^{-7}	2.88×10^{-7}	1.66×10^{-6}	1.51×10^{-6}
IV (M)	1.3×10^{-8}	4.1×10^{-8}	5.64×10^{-8}	6.79×10^{-8}	5.63×10^{-8}	6.98×10^{-8}
V (M)	2.4×10^{-7}	4.8×10^{-7}	3.55×10^{-7}	8.24×10^{-7}	3.90×10^{-7}	8.75×10^{-7}
VI (M) ^a	8.7×10^{-6}	8.8×10^{-6}	10^{-3}	10^{-3}	10^{-3}	10^{-3}
Equilibrium Nonradionuclide Solid Phases	Anhydrite, halite, brucite, hydromagnesite, korshunovskite	Anhydrite, halite, brucite, glauberite, hydromagnesite	Anhydrite, halite, brucite, hydromagnesite, whewellite, korshunovskite	Anhydrite, halite, brucite, hydromagnesite, whewellite, glauberite	Anhydrite, halite, brucite, hydromagnesite, whewellite, korshunovskite	Anhydrite, halite, brucite, hydromagnesite, whewellite, glauberite
Equilibrium Radionuclide Solid Phases	AmOHCO ₃ (cr), ThO ₂ (am), KNpO ₂ CO ₃ (s)		Am(OH) ₃ (s), ThO ₂ (am), KNpO ₂ CO ₃ (s),		Am(OH) ₃ (s), ThO ₂ (am), KNpO ₂ CO ₃ (s),	
FMT Database	FMT_970407.CHEMDAT		FMT_050405.CHEMDAT		FMT_050405.CHEMDAT	
FMT output filename	--	--	FMT_CRA1BC_GWB_HMAG_ORGS_007	FMT_CRA1BC_ER6_HMAG_ORGS_007	FMT_PABC09_GWB_HMAG_ORGS_005.OUT	FMT_PABC09_E6_HMAG_ORGS_013.OUT

a – DOE did not develop a solubility model for the +VI actinides. Therefore, for all PAs, a fixed concentration was assumed for uranium(VI), which is the only +VI actinide predicted to be present in the WIPP repository in significant concentrations.

6.2.1 FMT Code and Database

FMT Version 2.4 was used for the CRA-2004 PA actinide solubility calculations; the database was FMT_021120.CHEMDAT (Brush and Xiong 2003a; DOE 2004, Appendix PA, Attachment SOTERM-3.3). Changes to the FMT database between the CCA PAVT and CRA-2004 PA are documented in Giambalvo (2002a, 2002b, 2002c, 2002d, 2002e, 2003) and were reviewed by EPA (2006c). Changes to the database since the CCA PAVT included revisions to the thermodynamic data for americium(III) aqueous species and americium solids, and minor revisions to the thermodynamic data for some thorium(IV) aqueous species and Pitzer interaction parameters. A more significant change was incorporation of thermodynamic data for the protonation of organic ligands and complexation of organic ligands with actinides and with magnesium, based on data from Choppin et al. (2001).

EPA (2006c) reviewed the revised FMT database and compared the changes from the previous version to the corresponding references. EPA (2006c) found that the changes to both aqueous and organic species were minor, and all changes were well supported by the referenced documents. Based on their review of the data and process used to update the thermodynamic data in the FMT database since the CCA PAVT, EPA (2006c) found that the revised database (FMT_021120.CHEMDAT) was an acceptable update of the previous version (FMT_970407.CHEMDAT).

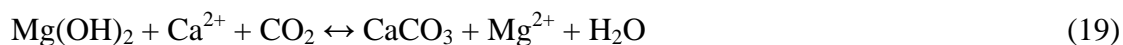
6.2.2 Salado Brine Formulation

For the CCA PAVT actinide solubility calculations, the brine formulation referred to as Brine A was used to simulate intergranular Salado brines. However, the new GWB Salado brine formulation was used in the CRA-2004 PA actinide solubility calculations. Brush and Xiong (2003a) discussed the use of both GWB and Brine A in the CRA-2004 PA to simulate intergranular Salado brines, and provided the compositions of these brines. A detailed discussion of GWB brine and a comparison of this brine to Brine A was provided by Snider (2003b).

EPA (2006c) reviewed the documentation supporting replacement of the Brine A formulation with the GWB formulation for calculating actinide solubilities in Salado brine. This evaluation included a comparison of actinide solubilities calculated using the two Salado brine formulations. EPA (2006c) found that use of the GWB brine formulation instead of the Brine A formulation was appropriate and adequately documented.

6.2.3 Carbon Dioxide Buffering in the Absence of Significant Microbial Activity

DOE (2004, Appendix PA, Attachment SOTERM, Section 2.2.2 and Appendix BARRIERS, Section 2.3.2.4) addressed the different reactions likely to buffer CO₂ fugacity. DOE stated that calcite is stable under WIPP conditions, and has been observed to form readily at low temperatures in GWB and ERDA-6 brines because of the rapid carbonation of lime or portlandite. In PA realizations with significant microbial production of CO₂, DOE stated that the amount of calcium ion available is likely to be overwhelmed by the amount of CO₂, so the brucite-calcite reaction:



was suppressed to allow the brucite-hydromagnesite reaction to control CO₂ fugacities. However, in the absence of significant microbial CO₂ production, DOE stated that sufficient calcium ions would be available to allow control of CO₂ fugacities by the brucite-calcite reaction.

EPA (2006c) reviewed the documentation and FMT modeling calculations provided by DOE related to the assumption that brucite-calcite would control CO₂ fugacities in PA realizations without significant microbial activity. EPA (2006c) concluded that DOE had not provided adequate information to support the assumption that brucite-calcite reaction would control the CO₂ fugacity in the absence of significant microbial consumption of CPR. EPA (2006c) found that DOE had not adequately defined “the absence of significant microbial activity in the WIPP” (DOE 2004, Appendix PA, Attachment SOTERM, Section 2.2.2), and DOE had not performed a mass-balance calculation to indicate how much or how little degradation would be required to produce amounts of CO₂ sufficient to essentially remove all calcium in the brines and result in buffering by brucite-hydromagnesite (reaction 12). EPA (2006c) noted that because microbial degradation probability would be increased for subsequent PA calculations, essentially including some microbial degradation in all realizations (Section 3.3.1.1), the assumption that brucite-calcite will buffer CO₂ fugacities in some realizations would not be included in the PABC04 calculations, so further consideration of this assumption was no longer warranted.

6.2.4 Uranium(VI) Solubility

For the CRA-2004 PA, DOE used the same estimated uranium (VI) concentration as for the CCA PA and PAVT. EPA (2006c) noted that DOE had not conducted a review of new data regarding the solubility of the +VI actinides since the CCA, and carried out a review of uranium(VI) solubility data in NaCl brines to determine whether the assumed uranium(VI) concentration used in the CRA-2004 PA was still justified.

The uranium(VI) solubility data for WIPP-relevant pH and ionic strengths reviewed by EPA (2006c) are summarized in Table 6-3. EPA (2006c) concluded that a sodium uranate phase, such as clarkeite [NaUO₂O(OH)•H₂O(c)], is the most likely uranium(VI) solubility-controlling solid at WIPP repository conditions. The dominant uranium(VI) aqueous species at repository pH conditions and carbonate ion concentrations is likely to be the triscarbonate complex [UO₂(CO₃)₃⁴⁻], according to information presented by Lin et al. (1998) and Millero (1999). Low-ionic-strength speciation data presented by Wall and Wall (2004) in their evaluation of uranium(VI) complexation by organic ligands also indicated that the triscarbonate complex will be the dominant uranium(VI) aqueous species. EPA (2006c) further observed that calculations of uranium(VI) speciation performed with these data at anticipated WIPP repository carbonate ion concentrations showed that over 99% of uranium(VI) in solution could be either the triscarbonate complex or UO₂(CO₃)₂²⁻. Based on their evaluation of the available data, EPA (2006c) concluded that the presence of free carbonate ion at the concentration calculated in GWB brine for the CRA-2004 PA (2.16 × 10⁻⁵ M, run 18) would increase uranium(VI) concentrations by a factor of about 250, relative to the concentration without carbonate.

EPA (2006c) noted that a solubility of 3×10^{-5} M was reported by Díaz Arocas and Grambow (1998) for sodium uranate in 5 M NaCl brine at pH 8.9 in the absence of carbonate. This concentration is probably a reasonable upper limit for the solubility of an alkali or alkaline-earth uranate solid in NaCl brines in the absence of carbonate. This upper limit was increased by approximately two orders of magnitude to be consistent with the carbonate concentrations expected in the WIPP repository, based on the speciation calculations mentioned above carried out with low-ionic-strength data. Thus, EPA (2006c) determined that a reasonable upper limit for uranium(VI) solubility in WIPP brines would be approximately 10^{-3} M. This concentration is approximately two orders of magnitude higher than the mid-range value used in the CCA PA, PAVT, and CRA-2004 PA, and exceeds the upper limit of the solubility uncertainty range used in these assessments. However, it is reasonable that the upper limit should be considerably higher than the Hobart and Moore (1996) estimate because their value was for systems without carbonate and was a mid-range rather than an upper-limit estimate. The selected upper-limit value is also reasonably consistent with the 0.50 fractile estimate (2×10^{-3} M) developed by an expert panel for moderate-pH systems in the presence of carbonate (Hobart et al. 1996). Based on this review of the uranium(VI) solubility data, EPA directed DOE to use the revised, higher uranium(VI) of 10^{-3} M for the PABC04 (Cotsworth 2005).

6.2.5 Actinide Solubility Uncertainties Used in PA

The uncertainty distribution previously determined for the CCA PA and PAVT was used to represent the actinide solubility uncertainties for the CRA-2004 PA (DOE 2004, Appendix PA, Attachment SOTERM, Section 3.6). Because the available solubility data and the FMT database had changed since the CCA PA and PAVT, EPA requested that DOE re-evaluate the uncertainties associated with the actinide solubilities, using the currently available actinide solubility data (Cotsworth 2004a, Comment C-23-16).

DOE re-evaluated the uncertainties associated with actinide solubilities (Triay 2005, Xiong et al. 2004). The database used for this evaluation was FMT_040628.CHEMDAT. This database was modified from the version used for the CRA-2004 PA (FMT_021120.CHEMDAT) by correcting the molecular weight of oxalate and adding solid calcium oxalate (whewellite, $\text{CaC}_2\text{O}_4 \cdot \text{H}_2\text{O}$) to the database (Xiong 2004). Because none of the calculations used in the uncertainty evaluation involved oxalate or other ligands, using either database would have yielded the same results (Xiong et al. 2004).

Separate evaluations of the solubility uncertainty distribution were carried out for the +III, +IV and +V actinide oxidation states. Solubility data used to develop the FMT database as well as literature data were evaluated. For each data point, the predicted solubility was calculated for the relevant experimental conditions using FMT. The difference value (D) was calculated by subtracting the logarithm of the predicted solubility from the logarithm of the measured solubility. These difference values were used to develop histograms and cumulative distribution functions. The +III evaluation was based on 243 measured and calculated solubilities, the +IV evaluation included 159 solubilities, and the +V evaluation included 136 solubilities (Xiong et al. 2004).

Table 6-3. High Ionic Strength Uranium Solubility Data Evaluated by EPA (2006c)

Uranium(VI) concentration	pH	Carbon Dioxide	Solution	Solid	Reference
3×10^{-5} M	8.9	Absent	5 m NaCl	$\text{Na}_{0.68}\text{UO}_{3.34} \cdot 2.15\text{H}_2\text{O}(\text{s})$	Díaz Arocas and Grambow (1998)
9×10^{-5} M	7.6	Absent	5 m NaCl	$\text{Na}_{0.45}\text{UO}_{3.23} \cdot 4.5\text{H}_2\text{O}(\text{s})$	Díaz Arocas and Grambow (1998)
$\sim 5 \times 10^{-3}$ m	not specified ^a	10^{-5} [CO_3^{2-}]	5 M NaCl	$\text{UO}_2\text{CO}_3(\text{s})$	Lin et al. (1998)
4.5×10^{-7} and 2×10^{-6} M ^b	7	10^{-4} M Carbonate	G-Seep brine	Not determined	Reed and Wygmans (1997)
5.0×10^{-7} and 2×10^{-6} M ^b	7	Absent	G-Seep brine	Not determined	Reed and Wygmans (1997)
1.1×10^{-8} M	8	10^{-4} M Carbonate	ERDA-6 brine	Not determined	Reed and Wygmans (1997)
5.5×10^{-7} M	10	Absent	ERDA-6 brine	Not determined	Reed and Wygmans (1997)
$> 1 \times 10^{-4}$ M	10	10^{-4} M Carbonate	ERDA-6 brine	None formed	Reed and Wygmans (1997)
2.8×10^{-6} m	9.8	Absent	5.2 m WIPP brine	$\text{UO}_2\text{OH}_2^{\text{c}}$	Palmer (1996) ^d
1.82×10^{-3} M	8.4 (pcH)	$10^{-3.5}$ atm	Brine A	Schoepite (oversaturation)	Yamazaki et al. (1992)
1.81×10^{-3} M	8.4 (pcH)	$10^{-3.5}$ atm	Brine A	Schoepite (oversaturation)	Yamazaki et al. (1992)
1.4×10^{-3} M	8.4 (pcH)	$10^{-3.5}$ atm	Brine A	Schoepite (undersaturation)	Yamazaki et al. (1992)
1.8×10^{-3} M	8.4 (pcH)	$10^{-3.5}$ atm	Brine A	Schoepite (undersaturation)	Yamazaki et al. (1992)
3.8×10^{-7} M	10.4 (pcH)	Low	Brine A	$\text{K}_2\text{U}_2\text{O}_7$ (oversaturation)	Yamazaki et al. (1992)
3.1×10^{-7} M	10.4 (pcH)	Low	Brine A	$\text{K}_2\text{U}_2\text{O}_7$ (oversaturation)	Yamazaki et al. (1992)
1.8×10^{-7} M	10.4 (pcH)	Low	Brine A	$\text{K}_2\text{U}_2\text{O}_7$ (undersaturation)	Yamazaki et al. (1992)
1.7×10^{-7} M	10.4 (pcH)	Low	Brine A	$\text{K}_2\text{U}_2\text{O}_7$ (undersaturation)	Yamazaki et al. (1992)

a – Probably less than 7

b – The lower concentration was reported on page 4 of the text, but a higher concentration was illustrated in Figure 1A

c – Solid should probably have been identified as $\text{UO}_2(\text{OH})_2(\text{s})$, uranium(VI) concentration as cited by Hobart and Moore (1996)

d – Hobart and Moore (1996) table cites Palmer et al. (1996), but reference list cites Palmer (1996) personal communication

The sources of the data used in the evaluation are listed in Table 1 of Xiong et al. (2004). Comparison of these data with the data in FMT_040628.CHEMDAT and the discussion of these data in Giambalvo (2002a, 2002c, 2002d) indicate that not all of the data used to develop the database were included in the uncertainty analysis. For example, solubility data for $\text{AmOHCO}_3(\text{s})$ (Felmy et al. 1990; Fanghänel et al. 1999) were included in the FMT database, but were not included in the uncertainty analysis (Xiong et al. 2004). The reasons these and other data were omitted were not provided by DOE. However, data for the solubility-controlling

solids under WIPP repository conditions, as determined by FMT modeling, were included in the uncertainty analysis.

For the +III actinides, the difference values ranged from -2.85 to +2.85 (Xiong et al. 2004). The median value was slightly less than 0, indicating that the FMT calculations predicted a higher concentration than the measured solubility slightly more often than the calculations predicted concentrations lower than the measured solubility. The data used to generate the uncertainty distribution were primarily for neodymium phases, but included some solubility data for americium phases. This uncertainty range was broader than the range used for the CCA PA, CCA PAVT and CRA-2004 PA. Because the revised uncertainty distribution included only data for +III actinides and neodymium, which are expected to exhibit analogous solubility behavior, EPA (2006c) determined that it is likely to be a more reasonable representation of uncertainty associated with the modeled +III actinide solubilities.

The difference values for the +IV actinides ranged from -2.85¹¹ to +3.3, with a median value between 0.6 and 0.75 (Xiong et al. 2004). This positive median value indicated that in the majority of comparisons, the measured solubility was higher than the concentration predicted by the FMT calculations. DOE carried out an additional evaluation of the +IV actinide solubility model to determine the cause of the under-prediction of the experimental data (Nowak 2005, Xiong et al. 2005). Nowak (2005) re-evaluated the thorium(IV) data in the FMT database and recommended a revision to the μ^0/RT value for Th(OH)₄(aq). This revision to the aqueous speciation data (database FMT_050405.CHEMDAT) was found by Xiong et al. (2005) to result in a significant improvement in the ability of the +IV actinide solubility model to predict the available solubility data at high ionic strength.

The difference values for the +V actinide solubilities ranged from -1.8 to +1.95, with a median value slightly less than 0 (Xiong et al. 2004). Brush et al. (2005) stated that the uncertainty distribution for the +V actinides would not be used for PA, because neptunium is the only actinide expected to be present in the +V oxidation state in the equilibrium WIPP repository (see Section 5.0). Neptunium solubility will not be considered in future PA calculations, because the neptunium inventory is insufficient to affect the long-term performance of the repository, regardless of its solubility (Brush et al. 2005, EPA 2006d).

Xiong et al. (2005) combined the +III, +IV and +V datasets to form a single distribution. This distribution ranged from -3.0 to + 3.3, with a median value slightly above 0. The slightly positive median value indicated that for a small majority of cases, the FMT-calculated solubilities were slightly less than the measured solubilities.

DOE proposed to use the combined uncertainty distribution calculated with the +III, +IV, and +V solubility data in combination with the estimated uranium(VI) concentration from Hobart and Moore (1996) for PA (Brush et al. 2005). However, based on the evaluation of the available data regarding uranium(VI) solubility under long-term repository conditions (Section 6.2.4) and the lack of a technical justification for using the combined uncertainty distribution for the +VI actinide concentration uncertainty, it was determined that a single value representing the upper end of the solubility range that could be anticipated under repository conditions would be more

¹¹ Figure 3 and Table 2 of Xiong et al. (2004) indicate that one value of -4.95 was observed; however, the text noted that this value was in error and should have been 0.65.

defensible for use in PA. The evaluation of this upper limit value for uranium(VI), carried out before the PABC04, is described in Section 6.2.4.

EPA (2006c) noted that the uncertainty distributions developed by DOE for use with the +III and +IV actinide solubilities have some potentially significant limitations. For example, none of the solubilities were measured in experiments with ligands (Xiong et al. 2004), and DOE did not appear to include all data used to develop the FMT database in the uncertainty analysis. In addition, no data related to +VI actinides were evaluated because of the lack of a thermodynamic model for this oxidation state. However, EPA (2006c) observed that the revised uncertainty ranges for the +III and +IV actinides are greater than the single range used in the CCA PA and PAVT, are based on larger datasets than were previously used and only data relevant to the specific oxidation state were used to generate the distributions. Consequently, EPA (2006c) determined that these uncertainty ranges were adequate and the revised uncertainty distributions for the +III, +IV and +V actinides were used for the PABC04 (see Section 6.3.5).

6.2.6 Temperature Effects on Actinide Solubilities

EPA (2006c) addressed the potential effects of temperature on actinide solubilities in the WIPP repository. Temperature effects on actinide solubilities were assumed to be negligible for the CRA-2004 PA, based on calculations performed at the time of the CCA (DOE 2004, Appendix PA, Attachment SOTERM, Section 2.2.4). DOE has not subsequently revised these calculations to account for the potential effects of inventory changes since the CCA and for the effects of non-uniform waste loading, e.g., the high proportion of pipe overpack waste in Panel 1. Although DOE has not quantitatively assessed the possible effects of these changes, EPA (2006c) concluded that it is reasonable to assume that repository temperature will not be significantly affected by these changes, and that it remains reasonable to assume that the effects of temperature on actinide solubilities will be negligible. However, in the event that heat-source plutonium or wastes containing significant heat-generating fission products are placed in WIPP in excess of the amounts assumed during the CCA, the validity of the CCA calculations that were used to estimate temperature increases may require re-evaluation (EPA 2006c).

6.2.7 Effects of Organic Ligands on Actinide Solubilities

DOE used inventory estimates available at the time of the CCA to identify acetate, citrate, EDTA and oxalate as organic ligands that could affect actinide solubilities (DOE 2004, Appendix PA, Attachment SOTERM, Section 5.0). EPA (2006c) noted that DOE (2004) did not address whether new inventory information, such as new waste streams included since the CCA, might affect identification of complexing agents that should be addressed in the calculations. Reported inventories of the four ligands evaluated for the CRA-2004 changed between the CCA and the CRA-2004, including increased concentrations of acetate, changes in oxalate and citrate inventories that appear to have been caused by transposing the data during the CCA, and a decrease in the estimated inventory of EDTA (DOE 2004, Appendix PA, Attachment SOTERM, Table SOTERM-4).

DOE (2004, Appendix PA, Attachment SOTERM, Sections 3.5 and 5.0) included the effects of acetate, citrate, EDTA and oxalate on the calculated solubilities of the +III, +IV and +V actinides used in the CRA-2004 PA. Brush and Xiong (2003c) calculated the organic ligand

concentrations used in the actinide solubility calculations by dividing the total reported ligand inventory by 29,841 m³ of brine, which was the smallest volume of brine reported to be required in the repository for transport away from the repository (Larson 1996, DOE 1996). After the solubility calculations had been used in the CRA-2004 PA, it was discovered that the organic ligand inventories were slightly in error (DOE 2004, Brush and Xiong 2003d). However, because the corrected organic ligand inventories and concentrations were smaller than those used in the CRA-2004 PA solubility calculations, it was determined that using the incorrect organic ligand concentrations would conservatively overestimate actinide solubilities (DOE 2004).

DOE (2004, Appendix PA, SOTERM, Section 5.0) stated that organic ligands would not significantly affect the +III and +IV actinide solubilities. EPA (2006c) evaluated the likely effects of organic ligands on actinide solubilities by comparing results contained in the FMT output files for calculations performed with and without organic ligands (Brush and Xiong 2003a, 2003c). This comparison indicated that the +IV actinide solubilities were not significantly affected by organic ligands at the concentrations assumed for these calculations, but that higher +III actinide solubilities were observed in FMT calculations with organic ligands than in calculations without organic ligands. These higher concentrations occurred because AmEDTA⁻ constituted approximately one-quarter to one-half of the aqueous americium(III) species in FMT calculations with organic ligands. The comparisons by EPA (2006c) also indicated that oxalate complexation significantly increased neptunium(V) solubilities.

DOE (2004, Appendix TRU WASTE, Section 3.8) stated that no upper or lower limit is required for the quantities of organic ligands in the repository, because organic ligand concentrations have an insignificant impact on actinide solubility. EPA requested that DOE conduct a sensitivity analysis to determine the likely effects of variations in the organic ligand concentrations (Cotsworth 2004a, Comment C-23-15). Experimental investigation of microbial degradation of CPR for the WIPP program has indicated that ligands including acetate, lactate and oxalate can be produced by the degradation reactions (Gillow and Francis 2003). Therefore, EPA also requested that DOE assess whether the production of organic ligands during microbial degradation of CPR could have significant effects on actinide solubilities (Cotsworth 2004a, Comment G-13).

Thermodynamic data for acetate, citrate, EDTA, lactate, and oxalate complex formation with the +III, +IV, +V and +VI actinides were included in the FMT database used for the CRA-2004 PA actinide solubility calculations (Section 6.2.1). Data were also included for complexation of these ligands with Mg²⁺ to assess the effects of competition of Mg²⁺ and Ca²⁺ (by analogy to Mg²⁺) on actinide complexation by these ligands. Consequently, the necessary data were available to carry out sensitivity calculations with FMT for the +III, +IV and +V actinides, and thereby investigate whether variations in the quantities of ligands and the potential presence of lactate from microbial degradation could affect actinide solubilities (Triay 2005). Details of these calculations were provided by Brush and Xiong (2004).

FMT solubility calculations were carried out for both GWB and ERDA-6 brines, and for microbial and nonmicrobial realizations. DOE carried out these calculations assuming four potential concentrations for organic ligands:

- No organic ligands

- Organic ligand concentrations equal to those used in the CRA-2004 PA FMT calculations
- Organic ligand concentrations equal to those used in the CRA-2004 PA FMT calculations, plus added lactate and acetate equal to the mean concentrations produced by microbial degradation of cellulose in the Gillow and Francis (2003) experiments
- Organic ligand concentrations an order of magnitude greater than the CRA-2004 PA FMT concentrations, plus additional lactate and acetate

EPA (2006c) examined the FMT results for the microbial vector calculations, in which brucite-hydromagnesite buffered CO₂ fugacity. Based on the results of DOE's sensitivity analysis calculations, EPA (2006c) found that the solubilities of the +III actinides appear to be sensitive to the assumed concentration of EDTA, but not to acetate, citrate, lactate, or oxalate at the evaluated concentrations. The results of the FMT calculations indicated that the varying concentrations of organic ligands did not change the +IV actinide concentrations. The +V actinide solubilities appear to be strongly affected by organic ligand complexation. Concentrations of +V actinides in the FMT calculations with CRA-2004 PA concentrations of organic ligands increased by factors of 4.32 and 9.44 for GWB and ERDA-6, respectively, compared to calculations with no organic ligands. These increased concentrations were observed because of the complexation of neptunium(V) by oxalate at lower organic ligand concentrations, and by both oxalate and acetate at the highest organic ligand concentrations.

EPA requested that DOE assess the potential effects of ligand complexation on the +VI actinides, which would only include uranium under long-term WIPP repository conditions (Cotsworth 2004a, Comment C-23-13). Thermodynamic data for complexation of uranium(VI) by acetate, citrate, EDTA, lactate and oxalate in brines have been determined (Choppin et al. 2001). However, DOE has not developed a model for uranium(VI) aqueous speciation and solubility in brines, so the effects of organic ligands on uranium(VI) solubility could not be assessed using FMT calculations.

Although a high-ionic-strength uranium(VI) model has not been developed, Wall and Wall (2004) performed calculations using low-ionic-strength thermodynamic data to demonstrate that the effects of organic ligands on uranium(VI) solubility would likely be small. These calculations were reviewed and extended by EPA (2006c). EPA (2006c) concluded that, based on the low-ionic-strength data, organic ligand complexes of uranium(VI) are likely to constitute a very small fraction of total uranium(VI) in solution. EPA (2006c) also assessed the likely relative proportions of UO₂²⁺-ligand species and hydrolysis species using high-ionic-strength stability data from Choppin et al. (2001) for the uranium(VI)-organic ligand species, and from Bronikowski et al. (1999) for the hydrolysis species. The results of these calculations indicated that UO₂EDTA²⁻, which had the highest calculated fraction among the organic ligand species, would be present at a concentration equal to approximately 10% of the total uranium(VI) hydrolysis and ligand species. Because uranium(VI)-carbonate species are expected to be present in much greater concentrations than the hydrolysis species, UO₂EDTA²⁻ will constitute an even smaller percentage of the total dissolved uranium species under WIPP conditions. Accordingly, EPA (2006c) concluded that organic ligands are unlikely to complex uranium(VI) to an extent that will significantly affect uranium(VI) solubilities in the WIPP repository environment.

In summary, EPA (2006c) concluded in its review of CRA-2004 that the concentrations of the +III and +V actinides could be affected by the concentrations of EDTA or oxalate and acetate in the repository, respectively. The available evidence showed that the +IV actinides were relatively insensitive to organic ligands over the range of evaluated organic ligand concentrations, and that microbially produced lactate is unlikely to significantly affect actinide solubilities at the concentrations expected, based on the microbial degradation experiments carried out for the WIPP program. The effects of EDTA concentrations on the modeled +III actinide concentrations indicate that the assumed concentrations, and hence the inventory, of organic ligands are potentially important for PA. However, the potential effects of oxalate and acetate on the solubility of the +V actinides are less important for PA, because neptunium is the only actinide assumed to be present in the equilibrium WIPP repository in the +V oxidation state, and the neptunium inventory is too low to significantly contribute to radionuclide releases (EPA 2006d). Evaluation of the available data regarding the complexation of uranium(VI) under anticipated WIPP repository conditions indicated that organic ligands are unlikely to significantly affect uranium(VI) solubilities in WIPP brines, because of the formation of relatively stable uranium(VI)-carbonate species.

6.3 PABC04 DISSOLVED ACTINIDE SOURCE TERM

At the direction of EPA (Cotsworth 2005), DOE incorporated a number of changes in the prediction of actinide solubilities for the PABC04 relative to the CRA-2004 PA. These changes included use of the updated FMT thermodynamic database, revised estimated concentrations of organic ligands, revised actinide solubility uncertainties and a revised uranium(VI) concentration.

6.3.1 FMT Code and Database

FMT Version 2.4 was used for both the CRA-2004 PA and the PABC04 actinide solubility calculations (Brush and Xiong 2003b; Brush and Xiong 2005a). The FMT database used in the CRA-2004 PA actinide solubility calculations (FMT_021120.CHEMDAT) was revised several times, ultimately resulting in the version used in the PABC04 actinide solubility calculations (FMT_050405.CHEMDAT). The database changes since the CRA-2004 PA actinide solubility calculations included a revision of the thermodynamic data for one thorium aqueous species (Section 6.2.5), correction of the molecular weight of oxalate, and addition of a calcium-oxalate solid phase (whewellite). These changes were reviewed and accepted by EPA (2006b).

DOE (2009, Appendix MgO-2009, Section SOTERM-5.1) stated that the actinide solubilities in WIPP brines calculated for the CRA-2004 PA and PABC04 differed because of changes in the thermodynamic database for the +III, +IV and +V models. However, EPA noted that changes to the calculated actinide solubilities were the result of changes to the standard chemical potential (μ^0/RT) for $\text{Th}(\text{OH})_4(\text{aq})$, and changes in organic ligand concentrations (Cotsworth 2009a, Comment 1-C-19). DOE agreed that the original statement was incorrect, and included the observation that addition of solubility data for the calcium-oxalate solid whewellite in the FMT database also affected the calculated solubility of the +V actinides (Moody 2009a). This information will be included as errata attached to Appendix SOTERM-2009 (DOE 2009).

6.3.2 Salado Brine Formulation

Two Salado Brine formulations, Brine A and GWB, have been used in PA actinide solubility calculations. Brine A was used in the CCA PA and PAVT calculations. However, GWB is believed by DOE to more closely resemble the average composition of intergranular Salado brines at the repository horizon (Brush and Xiong 2005a). Therefore, DOE used the GWB composition for calculating actinide solubilities in Salado brine for the CRA-2004 PA (DOE 2004, Appendix PA, Attachment SOTERM) and PABC04 (Brush 2005, Brush and Xiong 2005a). EPA (2006b, 2006c) concluded that the GWB formulation is more representative of intergranular Salado brine, and the use of the GWB brine composition in the CRA-2004 PA and PABC04 actinide solubility calculations was appropriate (see Section 6.2.2).

6.3.3 Carbon Dioxide Buffering Reactions

The MgO hydration and carbonation phases assumed to be present in solubility calculations with Salado (GWB) brine were brucite, korshunovskite and hydromagnesite. For actinide solubility calculations with Castile (ERDA-6) brine, brucite and hydromagnesite were assumed to be present. These MgO hydration and carbonation phases were the same as those assumed to control pH and CO₂ fugacity for the CRA-2004 PA calculations that included significant microbial activity (DOE 2004, EPA 2006c). EPA (2006c) reviewed the results of MgO hydration and carbonation experiments carried out by DOE and agreed that these phases are the most likely to control pH and CO₂ fugacities in the WIPP repository brines during the 10,000-year regulatory period. For CRA-2004 PA realizations without significant microbial activity, DOE had assumed that the brucite-calcite reaction would control CO₂ fugacity (DOE 2004, Appendix PA, Attachment SOTERM). EPA (2006c) determined that DOE had not adequately supported the assumption that the brucite-calcite reaction would control CO₂ fugacities in the absence of significant microbial activity. However, because the microbial degradation probability was changed for the PABC04 so all realizations included microbial activity (Section 3.3.3.3), it was appropriate to use the brucite-hydromagnesite reaction to buffer CO₂ fugacity in all actinide solubility calculations for the PABC04 (Brush 2005, Brush and Xiong 2005a).

6.3.4 Uranium(VI) Solubility

Because DOE did not address potential new information related to the solubility of uranium(VI) that had become available since the CCA PAVT, EPA (2006c) reviewed the available literature to determine whether the assumed +VI actinide solubility should be revised. This review took into consideration the presence of low, but significant, carbonate ion concentrations in the presence of the brucite-hydromagnesite buffer, as well as the uranium(VI) aqueous species and solid phases likely to form under WIPP repository conditions (see Section 6.2.4). Based on the results of this review, EPA specified the use of a fixed upper-limit value of 10⁻³ M for the uranium(VI) concentration in the PABC04 (Cotsworth 2005).

6.3.5 Actinide Solubility Uncertainties Used in PA

The uncertainty distribution assigned to the actinide solubilities and sampled in the CRA-2004 PA calculations was the same as the distribution developed for and used in the CCA PA and PAVT calculations (DOE 2004). However, because the available solubility data and the FMT

database had changed since the CCA PA and PAVT, EPA requested that DOE re-evaluate the uncertainties associated with the actinide solubilities for the PABC04, using the currently available information (Cotsworth 2004a, Comment C-23-16).

Xiong et al. (2004) evaluated the uncertainties associated with the calculated actinide solubilities by comparing solubilities modeled with the FMT database FMT_040628.CHEMDAT and measured solubilities from published literature studies. Because of consistent differences between measured and predicted solubilities for the +IV actinides, DOE revised the FMT thermodynamic database to version FMT_050405.CHEMDAT and updated the +IV actinide solubility uncertainty analysis (Nowak 2005, Xiong et al. 2005; Section 6.2.5).

The revised approach taken by Xiong et al. (2004, 2005) included the development of separate uncertainty distributions for the +III, +IV and +V actinide solubilities (Table 6-4). This approach was reviewed by EPA (2006b, 2006c) (Section 6.2.5). EPA (2006b) concluded that the overall approach used in the PABC04 for estimating the uncertainties associated with the actinide solubilities was a substantial improvement over the approach used for the CCA PA and PAVT. The use of a larger dataset and the determination of separate uncertainty distributions for the +III, +IV and +V actinide solubilities for the PABC04 were more likely to provide reasonable estimates of the uncertainties than the approach taken for the CCA PA, PAVT and CRA-2004 PA. However, the approach of Xiong et al. (2004, 2005) for selecting the data for the evaluation may not have included all available experimental data. In addition, EPA (2006b) noted that a number of inconsistencies appear to have occurred because of the inclusion of data used to develop the FMT database in some cases and its exclusion in others. Comparison of the separate PABC04 uncertainty distributions developed for the three modeled actinide oxidation states with the single uncertainty distribution used in the CCA PA, PAVT, and CRA-2004 PA showed that the revised ranges were generally wider, particularly on the upper end of the distributions. Therefore, EPA (2006b) concluded that it is likely that the revised actinide solubility uncertainty distributions would result in the more frequent use of higher actinide solubilities in PA. EPA (2006b) also observed that the larger amount of experimental data used to develop the distributions, the development of uncertainty distributions for each of the modeled actinide oxidation states and the large ranges developed for the uncertainties indicate that these uncertainty distributions were reasonable and acceptable for use in the PABC04.

Table 6-4. Cumulative Density Function Ranges Established by the PABC04 Actinide Solubility Uncertainty Analysis

Actinide Oxidation State	Cumulative Density Function Range ^a
III	-3.00 to 2.85
IV	-1.80 to 2.40
V	-1.95 to 1.95

a – At the lower end of the range, there is a zero probability that a difference value is less than or equal to this number; at the upper end of the range, the probability is equal to one because all difference values were less than or equal to this number (Brush et al. 2005).

Source: Xiong et al. 2005

6.3.6 Organic Ligand Concentrations

The concentrations of organic ligands were re-evaluated for the PABC04 actinide solubility calculations based on a revised estimate of the minimum amount of brine that could lead to a release from the repository. Stein (2005) re-evaluated the minimum amount of brine that could lead to a brine release from the WIPP repository for the PABC04. The minimum brine volume required for a release was calculated to be 10,011 m³. EPA (2006b) noted that this volume was calculated assuming the brine release occurred from the entire repository. EPA (2006b) observed that it is likely that waste panels will respond individually to a drilling intrusion, because of the robust panel seals that will be in place. Consequently, EPA (2006b) stated that a potentially more realistic approach would be to calculate the minimum brine volume based on releases from a single panel. EPA (2006b) noted that the individual PA realizations would be influenced if modeling was carried out on a panel-by-panel basis, but the effects on the mean concentrations released would probably be small. EPA (2006b) ultimately concluded that the use of the minimum amount of brine that could be released from the entire repository, and assuming that all ligands are dissolved in this amount of brine, is likely to be a reasonable approximation for calculating ligand concentrations and the resulting actinide solubilities.

The masses of organic ligands used to calculate concentrations for the CRA-2004 PA were later found to be overestimates of the amounts likely to be in the repository (Brush and Xiong 2003d). However, because these higher concentrations would overestimate releases from the repository, the actinide solubilities calculated using these higher organic ligand masses were used in the CRA-2004 PA (DOE 2004). For the PABC04, the corrected masses of organic ligands reported by Crawford and Leigh (2003) were used to calculate ligand concentrations (Brush and Xiong 2005b). Leigh (2005) found that none of the revisions to the WIPP inventory for the PABC04 had resulted in changes to the total masses of organic ligands expected in the WIPP inventory; therefore, Leigh (2005) recommended the use of the ligand inventories listed in Leigh (2003), which are the same as those listed in Crawford and Leigh (2003). These masses were converted to moles and divided by 10,011 m³ to yield the organic ligand concentrations used in the actinide solubility calculations. The resulting organic ligand concentrations used for the PABC04 solubility calculations are compared to the PAVT organic ligands concentrations in Table 6-1.

6.3.7 Results of the PABC04 Actinide Solubility Calculations

Changes and improvements incorporated into the calculation of actinide solubilities for the PABC04 implemented after the CCA PAVT included:

- Incorporation of organic ligand complexation data into the FMT database, so the effects of organic ligands on +III, +IV, and +V actinide solubilities could be calculated directly
- Refinement of the FMT database using new +III, +IV and +V actinide data
- Use of GWB instead of Brine A as the Salado Brine formulation for actinide solubility calculations
- Correction of the minimum brine volume necessary for DBR
- Revision of the estimated uranium(VI) solubility to account for new data

- Recalculation of actinide solubility uncertainties based on a much larger number of solubility measurements, with separate distributions developed for the +III, +IV and +V actinide solubilities, instead of the single distribution used for the CCA PAVT

As a result of these changes and improvements, the calculated +III, +IV and +V actinide solubilities for the PABC04 were slightly higher than the solubilities calculated for the CCA PAVT (Table 6-2). The uncertainties associated with these solubilities were also greater than the single uncertainty distribution used in the CCA PAVT. The results of the calculations also indicated that organic ligands could significantly affect actinide solubilities, particularly EDTA complexation of the +III actinides. As a consequence of the higher calculated solubilities and associated uncertainties, the importance of DBR to total releases was increased in the PABC04, compared to the CRA-2004 PA and the CCA PAVT. However, cuttings and cavings releases continued to dominate total radionuclide releases, except at low probabilities (Leigh et al. 2005a).

EPA (2006b) concluded that although the actinide solubility calculations carried out for the PABC04 were significantly improved over the calculations for the CCA PAVT, some areas of uncertainty remain. The uranium(VI) solubility specified for use in the PABC04 was a relatively high, fixed value, because of the limited solubility data available for WIPP-relevant conditions, and because DOE had not developed a solubility model for the +VI actinides. EPA (2006b) recommended that DOE obtain additional data related to the likely solubility of uranium(VI) in WIPP brines and use these data to develop a thermodynamic solubility model. The relatively large uncertainty associated with +IV actinide solubilities, even though the uncertainty was determined using data used in the development of the FMT database, indicates that the +IV actinide solubility model could be improved for future PA calculations. Finally, EPA (2006b) also recommended that a more thorough and systematic approach should be implemented for identifying and selecting data for development of the actinide solubility uncertainty distributions for future WIPP PAs.

6.4 CRA-2009 PA DISSOLVED ACTINIDE SOURCE TERM

The actinide solubilities calculated for the PABC04 were also used for the CRA-2009 PA dissolved actinide source term. Use of the PABC04 actinide solubilities for the CRA-2009 PA did not take into account the most recent inventory data. The potential consequences of using this earlier inventory are reviewed in this section, along with recent changes to the minimum brine volume used to calculate organic ligand concentrations for actinide solubility calculations. Information provided by CRA-2009 Appendix SOTERM-2009 (DOE 2009, Appendix SOTERM-2009, Sections SOTERM-3.0 and SOTERM-4.0) regarding the dissolved actinide source term and relevant aqueous solubility and speciation data for actinides in WIPP brines that have become available since the PABC04 are also reviewed.

The actinide solubilities used in the CRA-2009 PA are listed in Table PA-10 (DOE 2009 Appendix PA-2009).¹² EPA noted that this table lacked units, which should be moles/liter (Cotsworth 2009a, Comment 1-C-21). DOE agreed that the units for this table are moles/liter,

¹² Appendix PA-2009, Table PA-10 cites the source of these concentrations as Appendix SOTERM-2009, Table SOTERM-16. However, the appropriate citation is Appendix SOTERM-2009, Table SOTERM-17.

and that this information would be included with the errata attached to Appendix PA-2009 (Moody 2009a).

6.4.1 Waste Inventory

The components in the WIPP waste inventory and emplacement materials are relevant to calculating actinide solubilities, because some of these components may affect the WIPP repository chemistry and actinide source term. The information needed for PA that may influence repository chemistry includes the amounts of iron-based metals/alloys, aluminum-based metals/alloys, other metals/alloys (including lead), CPR, oxyanions (nitrate, sulfate and phosphate), complexing agents (organic ligands) and cement.

It is currently assumed in WIPP PA that sufficient iron-based metals and alloys are present in the repository to maintain reducing conditions and the actinide oxidation states that are assumed for PA; this assumption is supported by the large quantities of iron-based metals and alloys in the inventory and waste packaging materials (Section 5.0). It is also assumed in WIPP PA that anoxic corrosion of iron-based metals and alloys will be a significant source of gas generation in the repository, but that anoxic corrosion of other metals, such as aluminum and lead, will not contribute significantly to gas generation rates; this assumption is consistent with the current inventories of these metals (Section 3.2).

The quantities of CPR from waste, waste packaging and waste emplacement materials are important because microbial gas generation produces CO₂, and high CO₂ fugacity could affect actinide solubility and speciation. However, the MgO backfill will control CO₂ fugacity at relatively low values, so the effects of CO₂ on actinide speciation and solubility are predicted to be relatively small (Section 4.0). Sulfate, nitrate, and phosphate are potentially important, because sulfate and nitrate are possible electron acceptors during microbial degradation of CPR (Section 3.3) and phosphate is a nutrient for microbial growth.

Complexation by EDTA, oxalate and acetate have been shown to increase the solubilities of the +III and +V actinides (Section 6.2.7), so the quantities of organic ligands in the WIPP inventory are important to PA. The presence of large quantities of cementitious waste could result in high pH values (Section 4.0 and Section 6.4.3.2). The total curies of each isotope in the repository are important for calculating releases and are also important for PA because some radionuclides, such as curium, may be present in quantities that are too low to achieve the calculated solubility when the total inventory is dissolved in the minimum brine volume.

The WIPP waste inventory used for the PABC04 was described by Appendix TRU WASTE in the CRA-2004 (DOE 2004) and by Leigh et al. (2005b). The waste inventory used for the CRA-2009 PA was the same inventory used for the PABC04, except for the addition of waste emplacement materials that had been inadvertently omitted from the PABC04 (DOE 2009, Section 24.6.2). The PABC04 inventory was based on data received by September 30, 2002, from the waste-generator sites, with updates identified by EPA during their review of the CRA-2004 (Leigh et al. 2005b). The actinide solubilities calculated for the PABC04 using these inventory data were also used for the CRA-2009 PA (Table 6-2).

The most recent available inventory information for the CRA-2009 PA was developed using data received from the TRU waste sites as of December 31, 2007 (Crawford et al. 2009). Comparison of the most recent inventory data for organic ligands (Crawford et al. 2009) with the quantities used to calculate actinide solubilities for the PABC04 shows that organic ligand quantities have increased for acetic acid, citric acid, sodium citrate, and sodium EDTA (Table 6-5). Because of the potential effects of organic ligands on actinide solubilities, EPA instructed DOE to include the revised inventory of organic ligands in the PABC09 actinide solubility calculations (Cotsworth 2009a, Comments 1-23-1 and 1-23-4). In addition, EPA requested that DOE include the updated inventory of organic ligands in their identification of ligands most likely to influence actinide solubilities in the repository, and in their discussion of the extent to which ligands are likely to affect actinide solubilities (Cotsworth 2009a, Comments 1-C-6 and 1-C-14). Moody (2009a) responded that DOE would perform the PABC09, which would include updated EDTA, acetate, citrate and oxalate concentrations, based on the information provided in Crawford et al. (2009) and provide documentation of this PA to EPA.

Table 6-5. Changes in Reported Ligand Inventories between the PABC04 and PABC09

Compound	PABC04 Inventory [kg] (Leigh 2005)	PABC09 Inventory [kg] (Crawford et al. 2009)
Acetic acid	142	13,200
Sodium acetate	8,510	9,700
Citric acid	1190.5	5,680
Sodium citrate	400	2,550
Sodium EDTA	25.6	354
Oxalic acid	13,796	26,600
Sodium oxalate	33,940	646

Curium has been shown using previous inventory data to be present in quantities that are below its predicted solubility, when dissolved in the minimum brine volume. Neptunium-237 is also present in relatively low quantities. The inventories of these actinides, decayed through repository closure at 2033, are provided in Table 6-6. Dissolution of these quantities of curium and neptunium in the minimum brine volume of 17,400 m³ (Clayton 2008) results in a curium concentration less than the +III actinide solubilities calculated for the PABC09, but the inventory-based neptunium-237 concentration exceeds the +V actinide solubilities calculated for the PABC09 (Table 6-6). These results are consistent with previous evaluations of the inventories of curium and neptunium, which have concluded that curium will be present at concentrations below its calculated solubility, and neptunium will be of little significance to repository performance because of its low total curies (EPA 2006d).

Table 6-6. Curium and Neptunium Inventory and Calculated Solubilities

	Nuclide	Inventory Activity (Ci) ^a	Inventory Mass (g)	Concentration (M)	PABC09 Actinide Solubility (M) ^b
Curium	Cm-244	3,046	37.1	8.78×10^{-8}	1.66×10^{-6} (GWB) 1.51×10^{-6} (ERDA-6)
	Cm-245	0.669	3.93		
	Cm-246	6.56	21.2		
	Cm-247	0.027	282		
	Cm-248	0.131	30.6		
Neptunium	Np-237	39.0	54,915	1.34×10^{-5}	3.90×10^{-7} (GWB) 8.75×10^{-7} (ERDA-6)

a – Crawford et al. 2009, Table A-1, inventory decayed to 2033

b – FMT output files FMT_PABC09_GWB_HMAG_ORGS_005.OUT and FMT_PABC09_E6_HMAG_ORGS_013.OUT

6.4.2 Minimum Brine Volume

The minimum brine volume necessary for a brine release is used with the inventory data to calculate organic ligand concentrations for the actinide solubility calculations. The minimum brine volume used for these calculations was originally 29,841 m³ (Larson 1996), but was changed to 10,011 m³ based on an evaluation by Stein (2005) for the PABC04 and the CRA-2009 PA dissolved actinide source term calculations (Section 6.3.6). Clayton (2008) recalculated the minimum brine volume and obtained a value of 17,400 m³. Increasing the minimum brine volume would decrease the organic ligand concentrations calculated for the actinide solubility calculations. However, increasing the minimum brine volume from 10,011 m³ to 17,400 m³ does not completely offset the increase in reported organic ligand inventories (Table 6-5).

EPA requested additional information regarding the minimum brine volume calculations (Cotsworth 2009b, Comment 2-23-7). EPA questioned whether the minimum brine volume was realistic or conservative. EPA observed that the porosity surface used to develop room void volumes might overstate the void volumes, leading to higher required brine volumes for DBR and lower organic ligand concentrations for the actinide solubility calculations. In response, Moody (2009c) demonstrated that the assumed minimum brine volume of 17,400 m³ is a bounding lower limit for DBR by comparing the overall repository-scale brine volume to the DBR volumes for the CRA-2009 PA, replicate R1. This comparison showed that non-zero DBR volumes were not observed unless the repository-scale brine volume was significantly in excess of 20,000 m³. DOE also calculated that the DBR volume-weighted average of the overall repository-scale brine volume was 64,300 m³. Consequently, use of the 17,400 m³ minimum brine volume to calculate organic ligand concentrations appears to be conservative and acceptable.

6.4.3 Repository Chemical Conditions

DOE (2009, Appendix SOTERM-2009, Section SOTERM-2.2) summarized repository conditions that could potentially affect actinide solubilities. Assumptions regarding many of

these conditions are addressed in the Chemical Conditions conceptual model, which is summarized by SC&A (2008b, Appendix A.2).

6.4.3.1 Conceptual Model Assumptions

DOE (2009, Appendix SOTERM-2009, Table SOTERM-1) provided a summary of current WIPP chemistry model assumptions. EPA noted that this list of assumptions is incomplete with respect to the Gas Generation, Chemical Conditions and Dissolved Actinide Source Term conceptual models (Cotsworth 2009a, Comment 1-C-7). DOE indicated in their response that this list was intended to address only chemical conditions assumptions and not assumptions related to actinide solubility (Moody 2009b). One assumption included in Table SOTERM-1 (DOE 2009) was that pH is controlled by MgO, borate and carbonate. However, the Chemical Conditions and Dissolved Actinide Source Term conceptual models do not include an assumption that pH would be influenced by borate. Instead, brine pH is assumed in the current conceptual models to be controlled by brucite dissolution (SC&A 2008b, Appendices A.2 and A.3). Although DOE (2009, Appendix SOTERM-2009, Section SOTERM-2.3.2) noted that the presence of borate in both ERDA-6 and GWB brines and the boric acid pK_a (negative log of the acid dissociation constant) of 9.0 would help maintain the pH of the brines in the range of 8 to 10, evidence is not presented to show that the limited borate concentrations in the brines would be significant. Any questions related to the role of borate in buffering brine pH are of relatively minor importance, because the anticipated pH in WIPP repository brines would not be significantly affected.

DOE (2009, Appendix SOTERM-2009, Sections SOTERM-2.2.1 and SOTERM-2.2.2) reviewed information about repository pressure and temperature. The information presented is consistent with the Chemical Conditions conceptual model assumption that pressure will not significantly affect actinide solubilities, and that temperature is not expected to significantly depart from ambient conditions. Consequently, these assumptions continue to be appropriate for PA.

6.4.3.2 WIPP Brines

WIPP brine formulations used for the CRA-2004 PA, PABC04, and CRA-2009 PA have been GWB for Salado brine and ERDA-6 for Castile brine. DOE (2009, Appendix SOTERM-2009, Table SOTERM-2) provided the compositions of GWB and ERDA-6 brines before and after equilibration. Table SOTERM-2 referenced Brush et al. (2006) and stated that equilibration took place with MgO. Although these data were reproduced in Brush et al. (2006), the data were originally obtained from the PABC04 FMT modeling output files (Brush 2005). It should also be noted that the solid phases in equilibrium with brine in these modeling calculations included the MgO reaction products brucite and hydromagnesite, rather than MgO, the Salado minerals halite and anhydrite, the oxalate solid whewellite, and in the case of GWB, the solid phase korshunovskite that formed from brine interaction with the initial brucite reactant phase.

DOE (2009, Appendix SOTERM-2009, Section SOTERM-2.3.2) addressed pH buffering in repository brines. The Chemical Conditions conceptual model includes the assumption that MgO backfill will hydrate to form brucite; the brucite dissolution reaction (10) will maintain moderately alkaline pH values, and the carbonation of brucite to form hydromagnesite [reaction (13)] will maintain relatively low CO₂ fugacity (Section 4.1.1). The discussion presented by

DOE (2009, Appendix SOTERM-2009, Section SOTERM-2.3.2) is consistent with the assumptions regarding pH in the Chemical Conditions and Dissolved Actinide Source Term conceptual models, except for the relatively minor assumption that borate contributes to pH buffering (Section 6.4.3.1). DOE (2009, Section 2.3.2) also discussed the expected pH when little or no carbonate is present. However, the current Gas Generation conceptual model includes the assumption that microbial degradation of cellulose and CO₂ production occurs in all PA realizations, so this discussion is of limited relevance to PA. EPA noted that the pH for ERDA-6 brine was slightly misstated as 9.02 after equilibration with Salado minerals and MgO reaction products, but the ERDA-6 brine pH calculated for the PABC04 was in fact 8.94 (Table 6-2) (Cotsworth 2009a, Comment 1-C-8). DOE acknowledged and corrected this slight misstatement (Moody 2009c).

Two studies that investigated the pH buffering capacity of Mg-rich brines were reviewed by DOE (2009, Appendix SOTERM-2009, Section SOTERM-2.3.2). Schuessler et al. (2001) was an EQ3/6 modeling study of the interaction of MgCl₂-saturated brine with cementitious waste forms and MgO/CaO buffer materials. In the first simulation, the effects of cement corrosion on pH and brine chemistry were investigated, and it was determined that the pH was controlled by the ratio of cement to water in the reactant mixture. In a second simulation for a single cement:water ratio, the brine pH varied as a function of the amount of MgO added to the system. The brine pH was predicted to vary between approximately 7.6 and 8.4, with the lower pH range associated with greater amounts of MgO. Schuessler et al. (2001) concluded that the cement:water ratio is the parameter that most effectively controls pH.

Altmaier et al. (2003) determined the solubility of Mg(OH)₂(cr) in MgCl₂ and NaCl solutions, as well as in MgCl₂-NaCl mixtures. In experiments with MgCl₂ concentrations above 2 m, Mg(OH)₂ was observed to convert to korshunovskite. This phase has been predicted to precipitate from GWB brine during FMT modeling calculations, although GWB has a lower initial magnesium concentration of 1 M. In MgCl₂ solutions from 0.01 to 1.0 m, pmH values measured in solution ranged from approximately 9 to 9.7, which is consistent with the PABC09 pmH values predicted for GWB and ERDA-6 of 9.34 and 9.63, respectively.

Brush et al. (2006) performed geochemical reaction-path modeling calculations to simulate microbial degradation of CPR; in some cases, the reaction-path modeling resulted in relatively high pH values and evolution of the WIPP brine composition away from a sodium-chloride ± magnesium composition toward a magnesium-sulfide composition. Such high pH, magnesium-sulfide brine compositions differ from the brine compositions assumed in the Dissolved Actinide Source Term conceptual model (SC&A 2008b), and might result in actinide solubilities that are significantly different from those calculated using current PA assumptions. SC&A (2008b) reviewed the reaction-path modeling to simulate CPR degradation that was performed by Brush et al. (2006), Wolery and Sassani (2007) and Lichtner (2007). The results of that review indicated that most of these simulations were inconsistent with the Chemical Conditions conceptual model, because the brines did not remain in equilibrium with anhydrite. SC&A (2008b) performed additional reaction-path calculations using assumptions more consistent with the Gas Generation and Chemical Conditions conceptual models. The possible diffusive transport of sulfate for microbial degradation of CPR was also evaluated to determine the likelihood that repository brines would remain in equilibrium with this Salado Formation solid phase. The results of the evaluation indicated that adequate sulfate will be available to maintain

relatively moderate pH values under conditions with sufficient water to sustain a DBR, an assumption that is included in the Chemical Conditions conceptual model.

DOE (2009, Appendix SOTERM-2009, Section SOTERM-2.3.2) cited Brush et al. (2006) as supporting documentation for the PABC04. However, EPA observed that this document was prepared after approval of the PABC04, and the appropriate reference is Brush (2005) (Cotsworth 2009a, Comment 1-C-17); this error was corrected by Moody (2009b).

6.4.3.3 Cement Inventory

DOE (2009, Appendix SOTERM-2009, Section SOTERM-2.3.3) did not directly address the influence of the cementitious waste inventory on brine pH in the WIPP repository. The potential effects of cementitious materials in the repository are addressed within the Chemical Conditions conceptual model, where it is acknowledged that portlandite in cementitious materials could react with CO₂ to form calcite. This reaction could buffer pH at relatively high values, compared to the brucite dissolution reaction. Evaluation of the effects of portlandite on brine pH at the time of the CCA showed that the effects of cementitious waste on pH are expected to be minimal because of calcite precipitation and reaction of the portlandite with MgCl₂ in the brine to form CaCl₂ (SC&A 2008b, Appendix A.2; DOE 1996, Appendix SOTERM, Section 2.2.2):



At the time of the CCA, it was believed that 2×10^9 moles of MgO would be added to the repository, and 8×10^6 moles of portlandite would be present as cementitious material in the waste (DOE 1996, Appendix SOTERM-2009, Section SOTERM-2.2.2). DOE used these fixed quantities of MgO and portlandite to calculate the pH and CO₂ fugacity as a function of the amount of CO₂ produced by microbial reaction, the volume of brine in the repository, and the type of brine (DOE 1996, Appendix SOTERM, Section 2.2.2). The mass of cement reported for the CCA was 8.54×10^6 kg (Storz 1996), whereas the mass of cement reported by Crawford et al. (2009) based on the most recent inventory information has increased to 1.23×10^7 kg. EPA noted this increase in the reported cement inventory, and also noted the decreased quantities of MgO likely to be placed in the repository because of the decrease in the MgO EF from 1.95 to 1.2 (Section 4.4) (Cotsworth 2009b, Comment 2-C-24). Accordingly, EPA requested additional information from DOE regarding the possible consequences of the changed amounts of MgO and cement on pH buffering in WIPP brines and potential impacts on actinide solubilities.

DOE responded that the MgO excess factor has been demonstrated as sufficient to prevent acidification of the repository (Moody 2009c). However, the effect of portlandite in cement would be to raise, not lower, brine pH. DOE stated portlandite will react with CO₂ first, before the reaction of MgO, and that degradation of 11.5% of cellulosic materials is sufficient to react with all the portlandite reported in the PABC09 inventory. This explanation is not completely consistent with previous evaluations of the effects of portlandite, which indicated that portlandite would dissolve in brine, react with MgCl₂ in solution via reaction (20), and precipitate brucite. Consequently, portlandite dissolution would result in lower magnesium concentrations. If excessive quantities of portlandite dissolve, the available magnesium in solution could be completely consumed, resulting in relatively high pH values such as those predicted by DOE

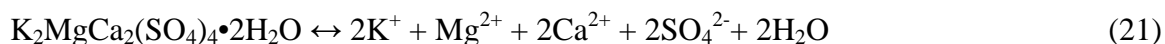
(1996) and Schuessler et al. (2001) for systems with high proportions of Ca(OH)₂ relative to Mg(OH)₂.

The potential effects of cement in the current waste inventory in the presence of the predicted amount of MgO backfill was evaluated using mass balance calculations to determine if the amount of portlandite in the cement could exceed the amount of magnesium in the brine and in polyhalite in the Salado Formation. The amount of portlandite in the cement was estimated assuming that the cement contains 5%, 7.5%, or 10% by weight Ca(OH)₂ (Storz 1996), resulting in repository-wide estimates of 8.30×10^6 moles, 1.25×10^7 moles, and 1.66×10^7 moles of Ca(OH)₂, respectively. The repository brine volume was assumed equal to 17,400 m³, the minimum volume necessary for DBR. The amounts of Salado polyhalite in the system were calculated assuming a DRZ volume of 1.58×10^6 m³, a rock density of 1,180 kg/m³ (Brush et al. 2006), and the assumption that Salado Formation contains 1.7% polyhalite by weight (Brush 1990). The moles of portlandite from cement dissolution, polyhalite from the Salado Formation and magnesium in the brine were calculated on the basis of 1 kg of H₂O for both GWB and ERDA-6 (Table 6-7).

Table 6-7. Mass Balance Calculations Comparing Moles of Portlandite in Cement to Moles of Magnesium Available from Brine and Polyhalite, Minimum Brine Volume of 17,400 m³

Brine	Portlandite in Cement (%)	Portlandite (moles/kg H ₂ O)	Magnesium in Brine (moles/kg H ₂ O)	Magnesium in Polyhalite (moles/kg H ₂ O)	Magnesium in Brine and Polyhalite (moles/kg H ₂ O)
GWB	0	0.000	1.217	6.662	7.879
GWB	5	0.569	1.217	6.662	7.879
GWB	7.5	0.854	1.217	6.662	7.879
GWB	10	1.138	1.217	6.662	7.879
ERDA-6	0	0.000	0.021	6.150	6.171
ERDA-6	5	0.525	0.021	6.150	6.171
ERDA-6	7.5	0.788	0.021	6.150	6.171
ERDA-6	10	1.051	0.021	6.150	6.171

Addition of portlandite would be expected to result in the precipitation of brucite according to reaction (20), maintaining the moderately alkaline pH predicted for the WIPP brine in the presence of the MgO backfill, provided sufficient magnesium is available in the brine or in polyhalite, which can dissolve and release additional magnesium:



For GWB brine, which has a relatively high magnesium concentration, the moles of magnesium in the brine alone are greater than the moles of portlandite in cement (Table 6-7), so sufficient magnesium would be present to maintain moderately alkaline conditions. ERDA-6 has a much lower magnesium concentration than GWB, and the amount of magnesium initially present in the brine may not be sufficient to maintain the pH. However, magnesium released by polyhalite dissolution would be available to react with hydroxyl ion released by portlandite dissolution, precipitating brucite according to reaction (20). The increased potassium, calcium and sulfate

from polyhalite dissolution would be expected to result in precipitation of anhydrite [$\text{CaSO}_4(\text{s})$] and syngenite [$\text{K}_2\text{Ca}(\text{SO}_4)_2 \cdot \text{H}_2\text{O}(\text{s})$]. Because the moles of magnesium in polyhalite significantly exceed the moles of portlandite in these calculations, it appears that increases in the cement inventory may cause more dissolution of polyhalite, but would be unlikely to cause high brine pH.

6.4.3.4 Iron and Lead Corrosion

Iron corrosion and its effects on repository chemistry were addressed by DOE (2009, Appendix SOTERM-2009, Section SOTERM-2.3.4). The WIPP inventory contains a large excess of iron in both the waste and steel packaging materials (Crawford et al. 2009). DOE (2009, Appendix SOTERM-2009, Section SOTERM-2.3.4) indicated that magnetite and siderite are likely reaction products of iron corrosion in the WIPP brines. However, formation of siderite to sequester CO_2 is not included in the Gas Generation conceptual model. As discussed in Section 3.1, SC&A (2008b) previously considered information regarding the formation of these solid phases during iron corrosion, and concluded that the available data indicated that the iron corrosion products in the WIPP repository would be $\text{Fe}(\text{OH})_2 \cdot x\text{H}_2\text{O}(\text{s})$ and $\text{FeS}(\text{s})$, which are incorporated in the Gas Generation conceptual model. Because of the potential formation of significant quantities of H_2S during CPR degradation by sulfate reduction, the stability of $\text{FeS}(\text{s})$ may preclude consumption of significant amounts of CO_2 through siderite precipitation, as indicated by low-ionic-strength calculations carried out by Wall and Enos (2006).

Lead is present in both WIPP waste and as packaging material for RH waste (Crawford et al. 2009), so reactions involving lead could affect WIPP brine chemistry. DOE (2009, Appendix SOTERM-2009, Section SOTERM-2.3.5) discussed potential mitigation of lead reactivity by formation of a protective oxide, carbonate, chloride or sulfate protective layer. The effects of lead corrosion are not currently included in the Gas Generation conceptual model or the Chemical Conditions conceptual model. Although carbonate might be removed from WIPP brines by precipitation of lead carbonate solid phases, it is also possible that interaction with H_2S formed during CPR degradation by sulfate reduction would result in precipitation of lead sulfide, based on the results of low-ionic-strength calculations (Wall and Enos 2006). Because of the uncertainty associated with the formation of lead carbonate phases, the removal of CO_2 from repository brines by lead is not included in calculations of the quantities of MgO required to maintain low CO_2 fugacity (Section 4.0).

6.4.3.5 Organic Ligands

Because the actinide solubilities used in the CRA-2009 PA were based on calculations performed for the PABC04, the most recent inventory was not accounted for in the actinide solubilities (Section 6.4.1). The most recent inventory data show that the masses of organic ligands have increased significantly since the PABC04 (Table 6-5). Brush and Xiong (2009) calculated the organic ligand concentrations used for the PABC09 (Table 6-1) from the masses of organic ligands in the most recent inventory (Crawford et al. 2009) and the 17,400 m^3 minimum brine volume required for a release (Clayton 2008). EPA requested additional information from DOE regarding the sensitivity of normalized releases to the increased organic ligands inventory (Cotsworth 2009a, Comment 1-23-4). Moody (2009a) responded to this request by providing a sensitivity analysis performed by Brush et al. (2008).

Brush et al. (2008) used the brine compositions, assumptions and FMT code and database used to calculate actinide solubilities for the PABC04 to calculate actinide solubilities with an assumed EDTA concentration of 10 times and 100 times the concentrations calculated by Brush and Xiong (2005b) for the PABC04. Brush et al. (2008) considered the likely effects on PA of higher +III, +IV and +V actinide solubilities caused by increased EDTA concentrations. The potential effects of increased EDTA concentrations on uranium(VI) concentrations were not assessed by Brush et al. (2008), because a thermodynamic speciation and solubility model has not been developed for uranium(VI). Brush and Xiong (2005b) calculated an EDTA concentration of 8.14×10^{-6} M, so EDTA concentrations of 8.14×10^{-5} M and 8.14×10^{-4} M were used by Brush et al. (2008) to calculate actinide solubilities for comparison with the solubilities calculated for the PABC04 (Table 6-8). The effects of the revised actinide solubilities on PA were determined using the PA codes ALGEBRACDB, PANEL, SUMMARIZE and CCDFGF to establish mean CCDFs for DBRs and total releases for the actinide solubilities at each of the EDTA concentrations.

Table 6-8. PABC09 Organic Ligand Concentrations and Concentrations Used in the Sensitivity Calculations by Brush and Xiong (2004) and Brush et al. (2008)

Organic Ligand	PABC09 (Brush and Xiong 2009) (moles/L)	Brush and Xiong (2004) (moles/L)	Brush et al. (2008) (moles/L)
Acetate	1.94×10^{-2}	5.05×10^{-3} to 7.89×10^{-2}	1.06×10^{-2}
Citrate	2.38×10^{-2}	2.71×10^{-4} to 3.83×10^{-3}	8.06×10^{-4}
EDTA	6.47×10^{-5}	2.73×10^{-6} to 3.87×10^{-5}	8.14×10^{-6} to 8.14×10^{-4}
Oxalate	1.73×10^{-2}	2.16×10^{-2} to 2.16×10^{-1}	4.55×10^{-2}

Brush et al. (2008) examined the effects of increased EDTA concentrations on the americium(III), thorium(IV) and neptunium(V) solubilities calculated using FMT. The results indicated that the increased EDTA concentrations affected only the predicted americium(III) solubilities in both GWB and ERDA-6 brine, because of increased formation of the AmEDTA⁻ aqueous species. Because the solubility of plutonium in the +III oxidation state is predicted by analogy to americium(III), the results of these calculations indicate that increased EDTA concentrations would be expected to increase americium solubility in all PA realizations and plutonium solubility in the 50% of realizations that have an assumed +III oxidation state for plutonium. The +III actinide solubilities calculated by Brush et al. (2008) at the highest EDTA concentration were 1.77×10^{-5} M (GWB) and 1.87×10^{-5} M (ERDA-6). The speciation calculations in FMT do not include the potential effects of competition with the +III actinides for organic ligands by metals, such as iron and nickel from steel corrosion or sodium present in the brines. Consequently, the FMT calculations presented by Brush et al. (2008) are expected to provide upper-bound estimates of the effects of EDTA on dissolved actinide concentrations in WIPP brines.

Brush et al. (2008) compared the mean CCDFs for DBR and total releases calculated for EDTA concentrations equal to the concentrations used for the PABC04 solubility calculations and for EDTA concentrations 10 times and 100 times the PABC04 concentrations. Mean DBR and total releases are increased by increasing EDTA concentrations, with effects on mean total releases most evident at probabilities of 0.1 or less. The results of these calculations showed that

although increasing EDTA concentrations may increase mean total releases at relatively low probabilities, the mean total releases still remain well below release limits.

DOE (2009, Appendix SOTERM-2009, Section SOTERM-2.3.6) addressed the potential effects of competition from transition metals, such as Fe^{2+} and Ni^{2+} , on actinide complexation by organic ligands. The possibility that the transition metals can effectively compete with actinides for organic ligands has been discussed since the CCA (DOE 1996, Appendix SOTERM, Section SOTERM-5). DOE (2004, Appendix TRU WASTE, Section 2.4.1.3) cited these low-ionic-strength calculations carried out to evaluate the competition of transition metals, including iron and nickel, with actinides for EDTA. EPA (1998d) reviewed these calculations at the time of the CCA and questioned their applicability because of the high nickel concentration assumed in the solution and because DOE had not supported its assertion that both nickel and iron would have high solubilities in high-ionic-strength solutions relative to low-ionic strength conditions. EPA (1998d) instead assessed the relative importance of ligands on actinide solubilities by evaluating the effects of EDTA on the solubility of $\text{ThO}_2(\text{am})$ at lower ionic strength. The results of these calculations indicated that thorium(IV) was not significantly complexed by EDTA in the pH range expected in the WIPP repository, and EDTA was primarily present as Ca^{2+} and Mg^{2+} complexes. Because DOE has now included thermodynamic data for organic ligand complexation of actinides in the FMT database, the results obtained using the low-ionic-strength calculations performed by EPA (1998d) were confirmed by the PABC04 actinide solubility calculations for the +IV actinides at high ionic strength. However, it appears that the +III and +V actinide solubilities are affected by EDTA and oxalate complexation, respectively. DOE responded to the request for additional information regarding iron and nickel complexation with organic ligands at high ionic strength, acknowledging that these calculations were superseded by the PABC04 calculations with organic ligands (Detwiler 2004b). DOE (2009) has not presented new data or performed FMT calculations at high ionic strength that include competition of transition metals for organic ligands. Although transition metals are likely to be complexed by EDTA, the presence of H_2S in the repository from CPR degradation by sulfate reduction may limit the aqueous concentrations of these metals because of the low solubilities of transition-metal sulfides, such as FeS and NiS . Consequently, DOE's assertion that transition metals can effectively compete with actinides for organic ligands in WIPP brines remains plausible but unsubstantiated.

DOE (2009, Appendix SOTERM-2009, Section SOTERM-2.3.6) seemed to indicate that actinide competition with Ca^{2+} and Mg^{2+} was not included in WIPP PA. However, both Mg^{2+} and Ca^{2+} (by analogy with Mg^{2+}) complexation constants with organic ligands are included in the current FMT database, and formation of organic ligand complexes with Ca^{2+} and Mg^{2+} are included in the actinide solubility calculations used in PA.

DOE (2009, Appendix SOTERM-2009, Section SOTERM-2.4.1.1) cited the potential degradation of organic ligands, which could lead to lower actinide solubilities. However, EPA noted that production of organic ligands had been observed by Gillow and Francis (2003) in WIPP-specific microbial degradation experiments (Cotsworth 2009a, Comment 1-C-16). DOE acknowledged that both production and consumption of many organic acids can occur in microbially active systems (Moody 2009c). However, for WIPP PA, it is assumed that production and consumption of organic ligands does not occur. Because of uncertainties associated with potential microbial consumption or production of organic ligands, actinide

solubility calculations have been carried out using bounding organic ligand concentrations based on the total inventory and minimum brine volume. Sensitivity studies of the effects of organic ligand concentrations on repository releases (Brush and Xiong 2004, Brush et al. 2008) have shown that although actinide solubilities are affected by organic ligand concentrations, predicted releases from the repository are less than release limits, even when organic ligand concentrations were significantly increased over inventory-estimated values for the PABC04. The organic ligand concentrations used in the organic ligand sensitivity analyses by Brush and Xiong (2004) and Brush et al. (2008) are summarized in Table 6-8 and compared to the PABC09 organic ligand concentrations. The highest concentrations of acetate, EDTA and oxalate used in the sensitivity analyses exceeded the PABC09 concentrations. The highest citrate concentrations used in the sensitivity analyses are less than the PABC09 concentration.

DOE (2009, Appendix SOTERM-2009, Section SOTERM-3.7) stated that only citrate and EDTA are expected to influence actinide speciation and potentially actinide solubilities in WIPP. EPA requested that DOE evaluate the potential role of citrate complexation of actinides in the WIPP repository based on previous sensitivity calculations, any newly available data (e.g., Felmy et al. 2006), and changes in the organic ligand inventory (Cotsworth 2009a, Comment 1-C-6). DOE clarified this statement (Moody 2009c), indicating that these statements pertained to the magnitude of the formation constants for citrate and EDTA complexes with the +III and +IV actinides and the fact that only EDTA and citrate have the potential to significantly affect actinide solubilities. The actual effects of organic ligands are included in the actinide solubility calculations based on their estimated inventories.

DOE (2009, Appendix SOTERM-2009, Section SOTERM-4.6) stated that organic ligands do not significantly affect actinide solubilities, despite data presented in Table SOTERM-19 showing that ligands increased the calculated +III actinide solubilities by factors of 1.71 (GWB) and 3.32 (ERDA-6), and +V actinide solubilities by factors of 1.50 (GWB) and 1.53 (ERDA-6). EPA requested that DOE re-evaluate this statement, given the large increases in the organic ligands inventory since the PABC04 (Cotsworth 2009a, Comment 1-C-14). Moody (2009c) responded that the increased ligands inventory would be included in actinide solubility calculations for the PABC09.

6.4.3.6 *Changes in WIPP Repository Chemical Conditions After the PABC04*

There have been no significant changes to assumptions in the Chemical Conditions conceptual model since the PABC04. It has been assumed since the time of the CCA that CPR degradation and iron corrosion would establish and maintain reducing conditions. It has also been assumed that radiolysis will not lead to oxidizing conditions and actinides in higher oxidation states, such as plutonium(V) or plutonium(VI). Although DOE (2009, Appendix SOTERM-2009, Section SOTERM-2.5) correctly pointed out that the WIPP TRU inventory was updated, the inventory changes were not accounted for in the CRA-2009 PA calculations of actinide solubilities. These changes were incorporated into the PABC09 calculations.

6.4.4 Actinide Aqueous Speciation and Solubility Data

DOE (2009, Appendix PA-2009, Sections PA-3.0 and PA-4.0) provided summaries of the chemistry of thorium, uranium, neptunium, plutonium, americium and curium under WIPP-

relevant conditions. These data and additional literature data were reviewed to determine if the aqueous speciation and solubility data in the FMT database used for the CRA-2009 PA and PABC09 remain adequate for PA calculations.

The CRA-2009 includes speciation diagrams for americium(III) (Appendix SOTERM-2009, Figure SOTERM-16), thorium(IV) (Figure SOTERM-17) and neptunium(V) (Figure SOTERM-18) based on calculations by Richmann (2008). Because the Richmann (2008) reference was not provided with the CRA-2009, EPA requested a copy for review (Cotsworth 2009a, Comment 1-23-2d). Moody (2009b) provided this reference to EPA. The speciation diagrams in Figures SOTERM-16 through SOTERM-18 are discussed in the appropriate subsections below.

6.4.4.1 Thorium

Figure SOTERM-17 (DOE 2009, Appendix SOTERM-2009) is an Eh-pH diagram prepared for thorium assuming a GWB brine composition in the presence of organic ligands after equilibration with anhydrite, halite, brucite, korshunovskite, hydromagnesite and whewellite (Brush et al. 2005, output file FMT_CRA1BC_007_GWB_HMAG_ORGS.OUT) (Richmann 2008). The total thorium concentration included in the calculations was based on the results reported for the PABC04 for GWB brine without organic ligands (Brush et al. 2005, output file FMT_CRA1BC_008_GWB_HMAG_NOORGS.OUT). At the time Richmann (2008) performed these calculations, these results were representative of the predicted conditions for GWB brine in the repository. The diagram illustrates that the dominant thorium aqueous species at the pH conditions expected in the repository brines would be $\text{Th}(\text{OH})_4^0$, with smaller contributions from $\text{Th}(\text{OH})_3\text{CO}_3^-$.

The thorium solubility and aqueous speciation data included in the FMT database are important to PA, because the solubilities calculated for thorium(IV) are also used to predict the solubilities of uranium(IV), neptunium(IV) and plutonium(IV) (Section 6.1.2). Solubility data reported by Felmy et al. (1991) were used to derive the μ^0/RT value for $\text{ThO}_2(\text{am})$ in the FMT database FMT_050405.CHEMDAT (Giambalvo 2002c). $\text{Th}(\text{OH})_4^0$ is the only hydrolysis species included in the FMT database, and the hydrolysis constant reported by Neck et al. (2002) was used to calculate the μ^0/RT value for this species (Nowak 2005, Xiong et al. 2005). EPA (2006b) assessed the reliability of the thorium data for predicting the solubility of thorium(IV) in part by examining the results of the PABC04 solubility uncertainty analysis for +IV actinides (Xiong et al. 2005) (Section 6.3.5). The +IV actinide solubility uncertainty distribution was determined by comparing solubility data for amorphous and microcrystalline $\text{Th}(\text{OH})_4(\text{s})$ from solubility studies carried out at ionic strengths equal to 3 M (Felmy et al. 1991), to the FMT-calculated solubilities at the experimental conditions using the FMT_050405.CHEMDAT database. Because the median of the differences between the measured and calculated thorium solubilities was close to zero, the results indicated that the current database provided reasonably realistic predictions of thorium (IV) solubilities (EPA 2006b). The data used to determine the +IV actinide solubility uncertainty distribution were obtained only from the same study used to determine the $\text{ThO}_2(\text{am})$ solubility data in the FMT database. Solubility data obtained in solutions with ionic strengths less than 3 M (Östholms et al. 1994, Baston et al. 1996, Neck et al. 2002, Felmy et al. 1991 results obtained at $I = 0.6 \text{ M}$ and 1.2 M) were not included in the uncertainty distribution evaluation because the FMT calculations consistently predicted

thorium(IV) concentrations that were higher than the measured data at lower ionic strengths (Xiong et al. 2005).

The thorium stability constants listed in Table SOTERM-9 (DOE 2009, Appendix SOTERM-2009) differ in some respects from the stability constant data used to derive the thorium μ^0/RT data in the FMT database. Data for ThOH^{3+} , $\text{Th}(\text{OH})_2^{2+}$ and $\text{Th}(\text{OH})_3^+$ are not included in the FMT database because these hydrolysis species are expected to be unimportant under the pH conditions in the repository brines. The stability constant for $\text{Th}(\text{OH})_4^0$ in Table SOTERM-9 was used by Nowak (2005) to derive the μ^0/RT value in the FMT database. The $\log K_{\text{sp}}^0$ (\log_{10} solubility product at zero ionic strength) of -47.8 for $\text{Th}(\text{OH})_4(\text{am})$ in this table was reported by Neck et al. (2002) and Altmaier et al. (2004) and is lower than the $\log K_{\text{sp}}^0$ of -45.5 used to calculate the μ^0/RT value for $\text{ThO}_2(\text{am})$ in the current FMT database. The higher $\log K_{\text{sp}}^0$ data used to derive the μ^0/RT for $\text{ThO}_2(\text{am})$ in the FMT database along with the stability constant for $\text{Th}(\text{OH})_4^0$ in the database would be expected to result in higher predicted dissolved thorium(IV) concentrations.

Neck et al. (2002) determined the solubility of amorphous thorium hydroxide in 0.5 M NaCl using titration with laser-induced breakdown detection (LIBD) of colloid formation. Using this approach at pH 3 to 5, the H^+ and thorium concentrations at the onset of colloid formation provided the solubility of $\text{Th}(\text{OH})_4(\text{am})$ without any influence from colloidal thorium species. Neck et al. (2002) used LIBD to establish that the presence of intrinsic colloids caused the higher $\log K_{\text{sp}}^0$ values reported by other studies, including Felmy et al. (1991) and Rai et al. (1997). Rothe et al. (2002) used x-ray absorption fine structure (XAFS) spectroscopy to evaluate the aqueous speciation under chemical conditions comparable to these studies and also identified thorium intrinsic colloids as the cause of the higher thorium solution concentrations. Altmaier et al. (2004) evaluated the solubility of amorphous hydrated thorium hydroxide in dilute to concentrated NaCl and MgCl_2 solutions equilibrated with brucite or korshunovskite and demonstrated that stable intrinsic thorium colloids were also present in 5 M NaCl solutions. In concentrated MgCl_2 solutions, pseudocolloids were observed to form through thorium adsorption onto magnesium hydroxychloride colloids.

Altmaier et al. (2004) stated that, based on the experimental data from Neck et al. (2002) for the solubility of $\text{Th}(\text{OH})_4(\text{am})$ and the stability constant for the $\text{Th}(\text{OH})_4^0$ aqueous species derived by Ekberg et al. (2000), the aqueous concentration of thorium determined by the reaction,



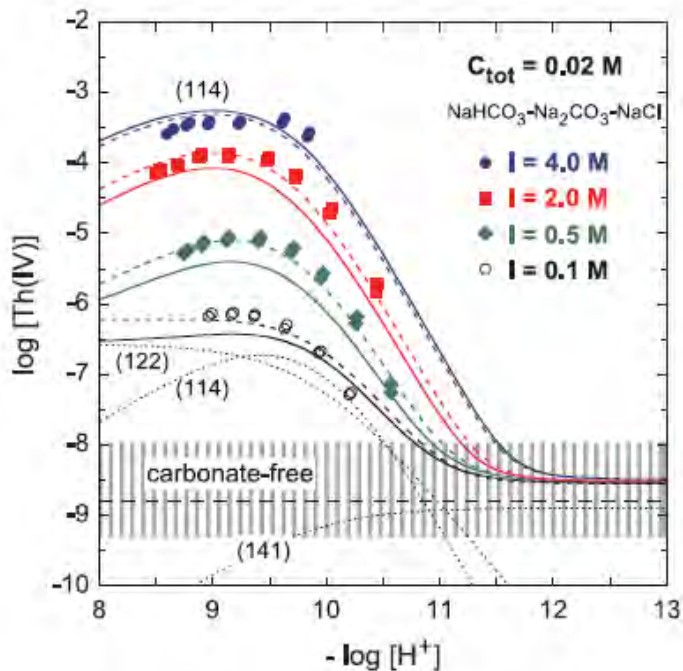
would be $\log [\text{Th}(\text{OH})_4^0] = -8.8 \pm 0.6$. This is the same concentration used by Giambalvo (2002c) based on data from Ryan and Rai (1987) to develop the +IV actinide data in the CRA-2004 PA FMT database (FMT_021120.CHEMDAT). The FMT database was revised prior to the PABC04, CRA-2009 PA and PABC09 to include a different stability constant for $\text{Th}(\text{OH})_4^0$ that yields $\log [\text{Th}(\text{OH})_4^0] = -7.0$ in equilibrium with amorphous thorium hydroxide (Nowak 2005). The available data from Neck et al. (2002) and Altmaier et al. (2004) indicate that the higher dissolved thorium concentrations calculated with the current FMT database (FMT_050405.CHEMDAT) likely include not only dissolved thorium, but also a significant contribution from intrinsic thorium colloids. The potential effects on PA of the formation of intrinsic thorium colloids are considered in Sections 7.0 and 8.0.

The thorium-carbonate aqueous species included in FMT_050405.CHEMDAT are $\text{Th}(\text{CO}_3)_5^{6-}$ and $\text{Th}(\text{OH})_3\text{CO}_3^-$. Giambalvo (2002c) stated that these species were included in the database based on an evaluation by Novak (1996) of solubility data in the presence and absence of carbonate from Felmy et al. (1991, 1997). DOE (2009, Appendix SOTERM-2009, Section SOTERM-3.2.1) observed that use of $\text{Th}(\text{CO}_3)_5^{6-}$ for the +IV actinide speciation in WIPP PA is a conservative assumption that overpredicts the solubility of the +IV oxidation state at pH greater than 10. However, at the total carbonate concentrations and pcH values predicted for the PABC09 (9.40 for GWB and 9.68 for ERDA-6), significant concentrations of $\text{Th}(\text{CO}_3)_5^{6-}$ are not present in the brines. Consequently, inclusion of the $\text{Th}(\text{CO}_3)_5^{6-}$ aqueous species in the FMT database does not appear to cause overprediction of the +IV actinide solubilities under WIPP conditions.

Altmaier et al. (2005) performed $\text{ThO}_2 \cdot x\text{H}_2\text{O}(\text{am})$ solubility experiments in 0.5 M NaCl from pcH 4.5 to 13.5, and determined that in solutions with total carbonate equal to 0.015, 0.04 and 0.1 M, the aqueous speciation of thorium was dominated by $\text{Th}(\text{OH})_4^0$ and the thorium-hydroxide-carbonate species $\text{ThOH}(\text{CO}_3)_4^{5-}$ and $\text{Th}(\text{OH})_2(\text{CO}_3)_2^{2-}$, with additional minor contributions from $\text{Th}(\text{OH})_2\text{CO}_3^0$, and $\text{Th}(\text{OH})_3\text{CO}_3^-$. At pH greater than 11, $\text{Th}(\text{OH})_4\text{CO}_3^{2-}$ also became important. Although $\text{Th}(\text{CO}_3)_5^{6-}$ is known to form at high bicarbonate and carbonate concentrations, significant concentrations of this species did not form at total carbonate concentrations less than or equal to 0.1 M.

Altmaier et al. (2006) experimentally determined the solubility of $\text{ThO}_2 \cdot x\text{H}_2\text{O}(\text{am})$ in 0 to 4 M NaCl solutions containing carbonate and bicarbonate. Total carbonate concentrations in these experiments were 0.02 M and 0.1 M and pcH was varied from 8 to 11. Their results from experiments with a total carbonate concentration of 0.02 M are reproduced in Figure 6-1. These results were obtained at a higher total carbonate concentration than predicted for GWB (3.5×10^{-4} M) and ERDA-6 (4.5×10^{-4} M) for the PABC09. However, this figure shows that increasing ionic strength from 0.1 to 4 M significantly increased $\text{ThO}_2 \cdot x\text{H}_2\text{O}(\text{am})$ solubility at the pcH values from 9.4 to 9.7 expected in repository brines. The effects of higher ionic strength in WIPP repository brines (6.8 to 7.6 M) would be expected to be partially if not completely offset by the low total carbon concentrations in WIPP brines compared to 0.02 M in the experiments included in Figure 6-1. However, because the repository brines have ionic strengths higher than the maximum ionic strength in Figure 6-1, the possibility that carbonate may affect total thorium concentrations under repository conditions cannot be ruled out.

In response to Comment 1-23-3 (Cotsworth 2009a), Borkowski and Richmann (2009) compared the thorium data provided in the recent literature with the data in the FMT database (FMT_050405.CHEMDAT) and evaluated the difference in the $\text{Th}(\text{CO}_3)_5^{6-}$ stability constant. Although the stability constant in the FMT database is four orders of magnitude less than the $\text{Th}(\text{CO}_3)_5^{6-}$ stability constant selected by a recent critical review of thorium solubility and aqueous speciation data (Rand et al. 2008), this difference is unlikely to affect total thorium concentrations under repository conditions. Borkowski and Richmann (2009) noted that the FMT database included the hydroxycarbonate species $\text{Th}(\text{OH})_3\text{CO}_3^-$, but did not include stability constants for the other hydroxycarbonate species such as $\text{ThOH}(\text{CO}_3)_4^{5-}$ and $\text{Th}(\text{OH})_2(\text{CO}_3)_2^{2-}$. Borkowski and Richmann (2009) stated that the presence of these other hydroxycarbonate species in the FMT database “could improve the accuracy but not the conservatism” of the current thorium model, but did not provide the basis for this conclusion.



The experimental data are compared with model predictions (solid lines) based on the equilibrium constants and SIT coefficients from Altmaier et al. (2005); the speciation (dotted lines) shown is for 0.1 M NaCl. The dashed lines represent best fits to the data at the different ionic strengths.

Figure 6-1. Solubility of $\text{ThO}_2 \cdot x\text{H}_2\text{O}(\text{am})$ in 0.1 M to 4 M NaCl with a Total Carbonate Concentration of 0.02 M

(Source: Altmaier et al. 2006, Figure 2)

EPA noted the additional literature data regarding thorium-carbonate speciation and suggested that this information may necessitate an update to the thorium speciation data in the FMT database (Kelly 2010, Comment 4-C-35). EPA also observed, however, that it was uncertain whether revising the thorium data in the FMT database would significantly affect calculated total thorium concentrations under repository conditions. EPA requested that DOE compare thorium concentrations in solubility experiments that included carbonate (Östhols et al. 1994, Rai et al. 1995, Felmy et al. 1997, Altmaier et al. 2005, Altmaier et al. 2006) to FMT-calculated thorium concentrations under the same conditions (Kelly 2010). Comparison of the FMT calculation results to the experimentally measured concentrations would allow for an evaluation of whether the FMT results were reasonably consistent with these data, or consistently over- or underpredicted thorium concentrations in carbonate solutions. EPA also recommended that DOE evaluate the available data in an effort to derive Pitzer parameters for the thorium-hydroxycarbonate species not currently in the FMT database and to update the thorium aqueous speciation data in the FMT database for future PAs.

Xiong et al. (2010b) presented the results of FMT modeling calculations carried out to predict thorium concentrations at the conditions reported for the experiments carried out by Rai et al. (1995), Altmaier et al. (2005) and Altmaier et al. (2006). The data used by Felmy et al. (1997)

were previously reported by Rai et al. (1995). The results reported by Östholms et al. (1994) were from experiments carried out in 0.5 M NaClO₄ solutions. These results were not compared to FMT-calculated thorium(IV) concentrations because a previous evaluation had shown that the current FMT database does not provide accurate predicted thorium concentrations in solutions with ionic strength less than 3 M (Xiong et al. 2005).

Xiong et al. (2010b) compared FMT-calculated thorium solubilities for 26 measurements from Rai et al. (1995), which were carried out at high Na₂CO₃ concentrations (0.98, 1.0 and 1.48 M) and high pcH (11.57 to 13.14). The calculated and measured thorium(IV) concentrations were in reasonable agreement and the calculated solubilities were not consistently greater or less than the measured concentrations. This result is as expected, because data reported by Rai et al. (1995) and reiterated by Felmy et al. (1997) were used to derive the μ^0/RT data in the FMT database for Th(CO₃)₅⁶⁻ and Th(OH)₃CO₃⁻ (Giambalvo 2002c).

Xiong et al. (2010b) also compared FMT-calculated thorium solubilities with measured solubilities reported by Altmaier et al. (2005) and Altmaier et al. (2006). Xiong et al. (2010b) stated that Altmaier et al. (2005) provided results for four experiments in which the ionic strength equaled or exceeded 3 M. These experiments had pcH values ranging from 12.44 to 12.52 and Na₂CO₃ concentrations from 1.35 to 1.82 M. The FMT-calculated results exceeded the measured thorium(IV) concentrations in these experiments by a factor of 1.7 to 10. Altmaier et al. (2006) performed solubility experiments with amorphous thorium(IV) hydrous oxide in carbonate solutions at ionic strengths up to 4 M (Figure 6-1). Xiong et al. (2010b) compared FMT-calculated solubilities to the measured solubilities in the 4 M NaCl experiments and found that the FMT calculations were consistently less than the measured solubilities by an order of magnitude or more. This consistent under-prediction is of particular significance, because these experiments were conducted at pcH values that span those expected in WIPP repository brines rather than the high pcH values of the data from Rai et al. (1995) and Altmaier et al. (2005); on the other hand, the total carbonate concentrations were significantly greater than those predicted in WIPP brines. These results indicate that the thorium-carbonate speciation data in the current FMT database are not completely consistent with the available experimental data. Xiong et al. (2010b) correctly noted that the total carbonate concentrations in WIPP brines are much lower than the concentrations used in the Altmaier et al. (2006), but neglected the enhanced stability of the ThOH(CO₃)₄⁵⁻ aqueous species with increasing ionic strength. However, the effects of much lower carbonate concentrations are likely to outweigh the effects of higher ionic strength in WIPP repository brines. Consequently, carbonate complexation of thorium(IV) is likely to have relatively small effects on total thorium concentrations under WIPP repository conditions and will not have significant effects on WIPP PA results. However, DOE should update the thorium-carbonate aqueous speciation data in the FMT database for the CRA-2014 PA to be consistent with currently available data and to minimize uncertainty associated with this issue.

Borkowski and Richmann (2009) compared the aqueous speciation data for the thorium-sulfate species in the FMT database, Th(SO₄)₂⁰ and Th(SO₄)₃²⁻ to the data in the recent critical review (Rand 2008). Rand et al. (2008) included the aqueous thorium-sulfate species ThSO₄²⁺ that is not included in the FMT database. The stability constant data for the other aqueous thorium-sulfate species in the Rand et al. (2008) review were about two orders of magnitude lower than the stability constants in the FMT database. Because of the relatively low sulfate concentrations in the WIPP brines and the importance of thorium hydrolysis and carbonate species formation,

the differences in the thorium-sulfate aqueous speciation data between the FMT database and the Rand et al. (2008) critical review are not expected to significantly affect predicted thorium concentrations in WIPP repository brines.

Information presented by DOE (2009, Appendix SOTERM-2009) indicated that borate complexation of +III (Section SOTERM-3.6.2) and +VI actinides (Section SOTERM-3.3.2) may affect aqueous speciation and solubility. EPA requested that DOE address the possibility that the +IV actinides could be similarly affected by borate complexation (Cotsworth 2009a, Comment 1-23-6b). DOE reported that the potential effects of borate complexation on the solubility of +IV actinides are being addressed by ongoing WIPP-specific experiments (Moody 2009c). Although only preliminary data are available from these experiments, DOE explained that for the +IV actinides, it is unlikely that borate complexation will significantly affect solubilities under WIPP conditions because the strong hydrolysis of the +IV actinides would predominate over borate complexation.

DOE (2009, Appendix SOTERM-2009, Section SOTERM-4.4) stated that the chemical potential for the solubility of $\text{Th}(\text{OH})_4(\text{s})$ was changed during development of the current FMT database (FMT_050405.CHEMDAT). However, EPA observed that only the chemical potential for $\text{Th}(\text{OH})_4(\text{aq})$ changed in this database version, and requested that DOE correct this statement (Cotsworth 2009a, Comment 1-C-10). DOE acknowledged that this was a typographical error (Moody 2009b).

Brendebach et al. (2007) identified the formation of calcium-thorium-hydroxide complexes that resulted in high solubilities of thorium(IV) hydrous oxides in alkaline CaCl_2 solutions. Under the investigated conditions, pH 11 to 12 and CaCl_2 concentrations greater than 0.5 M, the dominant aqueous thorium species was identified as $\text{Ca}_4[\text{Th}(\text{OH})_8]^{4+}$. Altmaier et al. (2009) reported the analogous plutonium(IV) aqueous species $\text{Ca}_4[\text{Pu}(\text{OH})_8]^{4+}$ in 3.5 M CaCl_2 solutions at pH 11 to 12. Although formation of the $\text{Ca}_4[\text{Th}(\text{OH})_8]^{4+}$ or $\text{Ca}_4[\text{Pu}(\text{OH})_8]^{4+}$ species could result in relatively high thorium or plutonium concentrations under pH and calcium concentrations controlled by the interaction of cementitious waste forms with brine, these high pH and high calcium concentration conditions are not predicted to occur in the WIPP repository environment.

6.4.4.2 Uranium

Uranium is assumed to be present in WIPP brines as uranium(IV) in 50% of the PA realizations, and as uranium(VI) in 50% of the PA realizations (see Section 5.0). The solubility of uranium(IV) is assumed equal to the thorium(IV) solubility (Section 6.1.2). Because DOE has not developed a model for calculating the solubility of uranium(VI), a fixed bounding concentration of 10^{-3} M is assumed for PA (Section 6.3.4).

DOE (2009, Appendix SOTERM-2009) addressed the solubility and speciation of uranium(VI) (Section 3.3.1.3), and provided WIPP-specific experimental results from Lucchini et al. (2009) that have become available since the PABC04. Because this report was not provided with the CRA-2009, EPA requested a copy from DOE for review (Cotsworth 2009a, Comment 1-23-2b). This report was received from DOE (Moody 2009b), but the correct citation is Lucchini et al. (2010).

Lucchini et al. (2010) investigated the solubility of uranium(VI) solid phases in brine, using sequential addition of uranium(VI) stock solution to the brines to establish oversaturation with respect to potential uranium(VI) phases. Experiments were carried out in simulated GWB from approximately pcH 6 to 9 and in simulated ERDA-6 from approximately pcH 8 to 12. All experiments were carried out in a nitrogen atmosphere and CO₂ was excluded from the experiments. The concentrations of uranium(VI) in the carbonate-free GWB and ERDA-6 brines were approximately 10 to 100 times lower than previously reported for carbonate-free 5 M NaCl brines by Díaz Arocas and Grambow (1998). At moderately alkaline pcH values, the solubility of uranium was about one order of magnitude higher in GWB than in ERDA-6 brine (Figure 6-2).

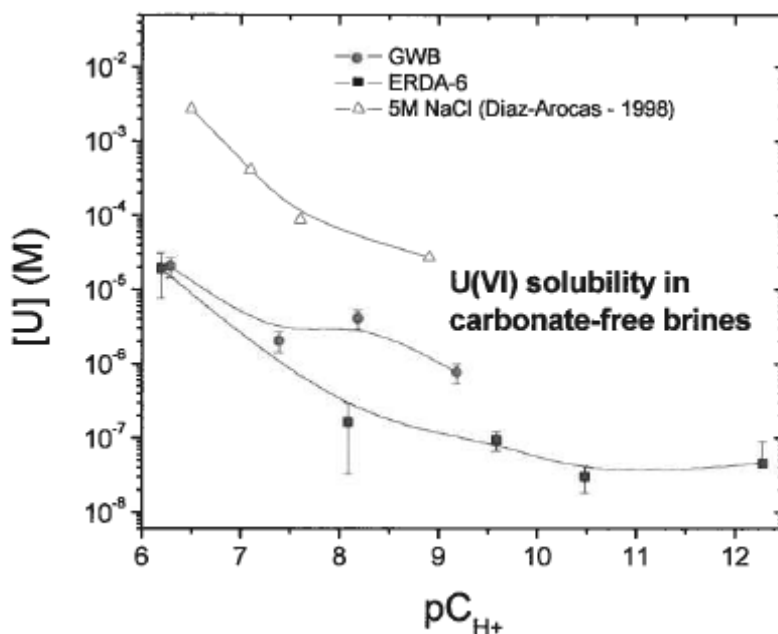


Figure 6-2. Uranium(VI) Solubility Measured in Carbonate-Free Brine as a Function of pcH

(Source: Lucchini et al. 2010, Figure 4-9)

DOE (2009, Appendix SOTERM-2009, Section SOTERM-3.3.1.3) noted the higher solubility in GWB brine compared to ERDA-6 brine, and attributed the higher solubility to complexation by higher borate and sulfate ion concentrations in GWB. In a letter sent to DOE (Cotsworth 2009a, Comment 1-23-6c), EPA observed that higher concentrations in these experiments and in neodymium solubility experiments (Section 6.4.4.5) attributable to borate complexation do not appear to be consistent with the current Dissolved Actinide Source Term conceptual model assumption that states (SC&A 2008b, Appendix A.3):

The important ions in WIPP brines are H⁺, Na⁺, K⁺, Mg²⁺, OH⁻, Cl⁻, CO₃²⁻, SO₄²⁻, and Ca²⁺. Other ions such as PO₄³⁻, F⁻, Al³⁺, Fe²⁺, and Fe³⁺ may be important, but their effects are included only in a qualitative understanding of the chemical environment.

However, borate complexation of uranium(VI), if it occurs to a significant extent, would not substantially change the current understanding of likely uranium(VI) solubility in WIPP brines because it is expected that uranyl carbonate species are likely to dominate aqueous speciation under WIPP repository conditions. DOE clarified that the potential effects of borate complexation on actinide solubilities were still under investigation, and that different solubilities predicted in GWB and ERDA-6 brine were likely caused by the many differences between the two brines and not solely by different borate concentrations (Moody 2010a).

During a discussion of the uranium(VI) solubility results in Figure SOTERM-10, DOE (2009, Appendix SOTERM-2009, Section SOTERM-3.3.2) stated that the pcH in WIPP brines would be approximately 8.7. EPA noted that the correct pcH range in WIPP brines is 9.39 to 9.64, based on FMT modeling carried out for the PABC04 (Table 6-2) (Cotsworth 2009a, Comment 1-23-5). Accordingly, EPA requested that DOE correct the cited pcH values and reinterpret the solubility data in light of the corrected values. DOE agreed that the cited pcH values were incorrect and included changes to statements in SOTERM-3.3.2 (Moody 2009c). DOE further stated that these inconsistencies “do not change or significantly impact the conclusions regarding actinide solubilities.”

Because of the probable importance of carbonate complexation on uranium(VI) concentrations in brine under repository conditions, the experiments reported by Lucchini et al. (2010) cannot be used to revise the upper limit of 10^{-3} M established for uranium(VI) at the time of the PABC04 (Section 6.3.4). However, these experiments provide a baseline for experiments planned by DOE for uranium solids solubility in WIPP brines with carbonate.

6.4.4.3 Neptunium

Neptunium is assumed to be present in the +IV oxidation state in 50% of the PA realizations and in the +V oxidation state in the other 50% of the PA realizations. Neptunium(IV) solubility is assumed equal to the solubility of thorium(IV) (see Section 6.1.2). Neptunium is the only actinide expected to be present in the +V oxidation state in the WIPP repository. Accordingly, a model was developed for calculating neptunium(V) solubilities under repository conditions. The neptunium aqueous species in the FMT database include inorganic hydrolysis and carbonate species, as well as complexes formed with the organic ligands acetate, citrate, EDTA, lactate and oxalate. The results of the PABC04 actinide solubility calculations indicated that the predominant aqueous neptunium(V) species under WIPP repository conditions would be NpO_2^+ , $\text{NpO}_2\text{CO}_3^-$, $\text{NpO}_2\text{Acetate}(\text{aq})$, and $\text{NpO}_2\text{Oxalate}^-$. Figure SOTERM-18 (DOE 2009, Appendix SOTERM-2009) was prepared assuming a GWB brine composition in the presence of organic ligands after equilibration with anhydrite, halite, brucite, korshunovskite, hydromagnesite and whewellite (Brush et al. 2005, output file FMT_CRA1BC_007_GWB_HMAG_ORGS.OUT) (Richmann 2008). The total neptunium concentration included in the calculations was based on the results reported for the PABC04 for GWB brine without organic ligands (Brush et al. 2005, output file FMT_CRA1BC_008_GWB_HMAG_NOORGS.OUT). At the time Richmann (2008) performed these calculations, the brine composition represented the expected conditions for GWB brine in the repository. In the absence of organic ligands, the results of the PABC04 and PABC09 FMT modeling calculations with database FMT_050405.CHEMDAT indicated that the dominant neptunium species under WIPP repository conditions would be NpO_2^+ and $\text{NpO}_2\text{CO}_3^-$,

which is consistent with the Eh-pH diagram presented in Figure SOTERM-18 of the CRA-2009 (DOE 2009, Appendix SOTERM-2009).

The uncertainty analysis carried out by Xiong et al. (2004, 2005) for the PABC04 provided some information regarding the reliability of the thermodynamic data for neptunium(V) in the current FMT database (FMT_050405.CHEMDAT). The neptunium(V) data in the database and the data sources are described by Giambalvo (2002d). Xiong et al. (2004, 2005) used this database to perform FMT calculations of the expected solubilities of neptunium solids at the experimental conditions of solubility studies carried out by Al Mahamid et al. (1998), Novak et al. (1996), Novak et al. (1997) and Runde and Kim (1995). The differences between the reported and calculated solubilities were used to develop an uncertainty distribution for the solubility of neptunium(V). The median value of the distribution was slightly positive, indicating that the solubility model tended to predict neptunium(V) solubilities that were slightly lower than the measured solubilities.

Although a solubility model has been developed for neptunium(V), the inventory of neptunium-237 in the repository is relatively small and does not significantly affect repository performance (EPA 2006d, Section 3.2.1). Neptunium-237 is included in calculations of radionuclide releases through DBR, but not for cuttings, cavings or spallings or for calculations of releases by transport through the Salado or Culebra (DOE 2004, Appendix PA, Figure PA-21).

6.4.4.4 *Plutonium*

Plutonium isotopes represent a large fraction of the activity in WIPP CH and RH waste (DOE 2009, Appendix SOTERM-2009, Section 3.5). It is assumed for PA that plutonium will be present in the +III oxidation state in 50% of the PA realizations and in the +IV oxidation state in 50% of the PA realizations (see Section 5.0). The solubility of plutonium(III) in WIPP brines is assumed equal to the FMT-modeled concentration of americium(III), and the solubility of plutonium(IV) is assumed equal to the FMT-modeled solubility of thorium(IV) (Section 6.1.2).

6.4.4.5 *Americium and Curium*

Americium, along with plutonium, constitutes a significant fraction of the total activity in the WIPP inventory (DOE 2009, Appendix SOTERM-2009, Section SOTERM-3.6). As a result, the solubility of americium solids in WIPP brines is important for calculating potential releases from the repository. The solubility of americium solids in WIPP brines is also used to predict the concentrations of plutonium(III) and curium(III) using the oxidation-state analogy (Section 6.1.2). Curium isotopes are present in the WIPP inventory in relatively small amounts. If the entire inventory of curium isotopes is dissolved in the minimum quantity of brine, the resulting concentration is below the predicted solubility (Table 6-6). Plutonium and americium isotopes are included in calculations of all release mechanisms, whereas curium isotopes are included in calculated releases by cuttings and cavings, spallings and by DBR, but not in releases by transport through the Salado or Culebra (DOE 2009, Appendix PA, Figure PA-21).

The aqueous speciation and solid-phase solubility data for americium(III) included in the current database (FMT_05405.CHEMDAT) are described by Giambalvo (2002a), and were reviewed and accepted by EPA (2006c) for the PABC04. These data are primarily derived from studies

involving americium and curium, although the K_{sp}^0 for one solid phase $[\text{NaAm}(\text{CO}_3)_2 \cdot 6\text{H}_2\text{O}(\text{cr})]$ was obtained from an investigation with a neodymium analogue. Giambalvo (2002a) compared americium(III) concentrations calculated with FMT to $\text{Am}(\text{OH})_3(\text{s})$ solubility results in 5 M NaCl (Runde and Kim 1995) and found that the calculated solubilities were consistent with the measured solubilities. The results of both the PABC04 and PABC09 actinide solubility calculations indicated that the principal aqueous americium species under WIPP repository conditions are likely to be AmEDTA^- and $\text{Am}(\text{OH})_2^+$. Actinide solubility calculations in the absence of organic ligands for both the PABC04 and PABC09 indicated that the dominant aqueous americium species in the absence of organic ligands in WIPP brines would be $\text{Am}(\text{OH})_2^+$. The stable americium solid under WIPP repository conditions is $\text{Am}(\text{OH})_3(\text{s})$ based on the results of FMT calculations for both the PABC04 and PABC09.

Figure SOTERM-16 (DOE 2009, Appendix SOTERM-2009) illustrated the principal americium species as a function of pH and Eh in the absence of organic ligands. EPA noted a minor typographical error in the formula for $\text{Am}(\text{OH})_3(\text{s})$, and requested information regarding the carbonate concentration, total americium concentration and assumed ionic strength used in the generation of the figure (Cotsworth 2009a, Comment 1-C-13). This information was provided by Richmann (2008). Figure SOTERM-16 was constructed assuming the GWB brine composition in the presence of organic ligands after equilibration with anhydrite, halite, brucite, korshunovskite, hydromagnesite and whewellite (Brush et al. 2005, output file FMT_CRA1BC_007_GWB_HMAG_ORGS.OUT). The total americium concentration included in the calculations were based on the results reported for the PABC04 for GWB brine without organic ligands (Brush et al. 2005, output file FMT_CRA1BC_008_GWB_HMAG_NOORGS.OUT). At the time Richmann (2008) performed these calculations, these results represented the expected conditions for GWB brine in the repository.

Neck et al. (2009) performed solubility experiments with $\text{Nd}(\text{OH})_3(\text{s})$ in NaCl, MgCl_2 and CaCl_2 solutions of varying ionic strengths. These data were combined with existing solubility and hydrolysis data for americium(III) and curium(III) to develop an aqueous speciation and solubility model covering a wide pH range in dilute to concentrated solutions. Ternary complexes of the +III actinides have been identified with calcium and hydroxide ion that were assumed to be $\text{Ca}[\text{Cm}(\text{OH})_3]^{2+}$, $\text{Ca}_2[\text{Cm}(\text{OH})_4]^{3+}$ and $\text{Ca}_3[\text{Cm}(\text{OH})_6]^{3+}$ (Neck et al. 2009, Rabung et al. 2008). These ternary species are unlikely to be important under WIPP repository conditions because they affect the solubility of the +III actinides only at pH greater than about 11 and at relatively high calcium concentrations, which are not anticipated in the WIPP repository environment. Neck et al. (2009) provided an internally consistent thermodynamic model including Pitzer parameters, and there appear to be some differences between the data compiled by Neck et al. (2009) and the data included in the FMT database. For example, the $\log K_{sp}^0$ used to derive the μ^0/RT value for $\text{Am}(\text{OH})_3(\text{s})$ in the FMT database is -27.5 (Giambalvo 2002a), whereas the values selected by Neck et al. (2009) for $\text{Am}(\text{OH})_3(\text{cr,aged})$ equals -26.4 and for $\text{Am}(\text{OH})_3(\text{am})$ equals -25.1, indicating slightly higher solubilities than the current FMT database. Neck et al. (2009) was not available for evaluation by DOE prior to the PABC09, but information in this reference should be considered with respect to possible revisions to the FMT database for the CRA-2014.

DOE (2009, Appendix SOTERM-2009, Section SOTERM-3.6.2) provided a summary of the results of a WIPP-specific solubility investigation, carried out using neodymium(III) as an analogue for americium(III), and by analogy plutonium(III) and curium(III). DOE (2009) stated that the solubility data for neodymium(III) in WIPP brines support the current WIPP PA calculations of the solubilities of +III actinides because the calculated solubilities remain conservative. DOE (2009) observed that neodymium(III) solubility in WIPP brine was not strongly influenced by carbonate concentrations as high as 0.01 M in the experiments because borate complexation masked the effects of carbonate. DOE also stated that borate is the predominant +III actinide complexing agent in brine in the WIPP-relevant pH range from 7.5 to 10. In the CRA-2009, DOE cited Borkowski et al. (2008) for the results of the experiments. Because this reference was not provided with the CRA-2009, EPA requested a copy for review (Cotsworth 2009a, Comment 1-23-2a). EPA received this report from DOE (Moody 2009b), but the correct citation is Borkowski et al. (2009).

Based on a review of Appendix SOTERM-2009, Section SOTERM-3.6.2 and the supporting Borkowski et al. (2009) report, EPA requested additional information from DOE in two completeness letters (Cotsworth 2009a, Comments 1-23-6a and 1-C-9; Kelly 2010, Comments 4-C-26 through 4-C-34) and in an email requesting additional information (Peake 2010, Questions 1 through 9). A few of these questions and comments were of relatively minor importance to the results of WIPP PA. In Comment 4-C-28 (Kelly 2010, Moody 2010c), EPA noted that Figure 3-4 was attributed to Kim et al. (1984), but the correct reference appeared to be Bernkopf and Kim (1984). EPA also noted that Borkowski et al. (2009) stated that neodymium solubility was studied in 5 M NaCl solutions with 0.01 M carbonate, but this carbonate concentration was not listed in the test matrices in the report (Kelly 2010, Comment 4-C-33). DOE explained that the test matrices represented initial conditions planned for the experiments, but that additional experiments were later included in the investigation (Moody 2010c).

The information requested by EPA of greater potential significance to WIPP PA can be grouped into a few general areas of inquiry:

- Selection and characterization of the solid starting materials in the experiments (Comment 4-C-32, Question 1), which may have caused initial increases in neodymium concentrations in undersaturation experiments followed by decreasing concentrations as the experiments approached steady state (Comment 4-C-29) and higher neodymium(III) concentrations in carbonate-free undersaturation experiments than in oversaturation experiments at pH values of approximately 7.3 and 8.0 (Question 6)
- The effects of carbonate on measured neodymium(III) concentrations in the experiments, including the carbonate concentrations in the experiments and whether DOE is recommending revision of the americium-carbonate species included in the FMT database (Comments 1-C-9, 4-C-27, 4-C-30, 4-C-34, Question 9)
- Additional information supporting the proposed importance of neodymium(III) complexation by borate (Comments 4-C-26, 4-C-31, Questions 2, 3, 7)
- Whether the measured neodymium(III) solubilities in WIPP brine are consistent with the FMT-modeled concentrations of +III actinide solubility (Comment 1-23-6a, Questions 4, 5, 8)

Selection and Characterization of Solid Starting Materials and Effects on Experimental Results

The crystallinity and chemical composition of solids used in the undersaturation experiments are important to the interpretation of the results. The potential effects of the crystallinity of a solid phase on solubility is demonstrated by the $\log K_{sp}^0$ of -26.4 for $\text{Am}(\text{OH})_3(\text{cr, aged})$ and $\log K_{sp}^0$ of -25.1 for $\text{Am}(\text{OH})_3(\text{am})$ provided by Neck et al. (2009), which show that the crystallinity of $\text{Am}(\text{OH})_3(\text{s})$ can affect americium solubilities by more than an order of magnitude. Solution concentrations in the undersaturation experiments could increase and then decrease over the course of the experiments if the initial solid material was poorly crystalline or if it was unstable relative to another solid that formed during the experiments.

The solid phase used in the carbonate-free undersaturation experiments was $\text{Nd}(\text{OH})_3(\text{cr})$. This material was obtained commercially and characterized by XRD (Borkowski et al. 2009). Borkowski et al. (2009) used $\text{NdOHCO}_3(\text{cr})$ in the undersaturation experiments that included carbonate, stating that “a mixed hydroxycarbonate phase was expected to be the predominant phase in WIPP brine when carbonate was present at high pH.” However, this statement is inconsistent with FMT modeling results for the PABC04 and PABC09, which showed that $\text{Am}(\text{OH})_3(\text{s})$ would control +III actinide solubilities in the presence of the relatively low carbonate concentrations in WIPP brines. Only indirect evidence is available regarding the final composition and crystallinity of the solid phases used in the experiments because the quantities of solids produced by the oversaturation experiments were too small to be characterized. In response to a request for additional information regarding the solubility-controlling solid phase in the neodymium(III) solubility experiments with carbonate (Peake 2010, Question 1), DOE stated that the results of long-term solubility experiments would be expected to be independent of the initial phase present (Moody 2010a). DOE stated that agreement of the neodymium solubilities in experiments conducted with $\text{Nd}(\text{OH})_3(\text{s})$ and $\text{NdOHCO}_3(\text{s})$ initially present in GWB indicated that the stable phase in the neodymium experiments at WIPP-relevant carbon dioxide fugacities was $\text{Nd}(\text{OH})_3(\text{s})$. This result would be in agreement with the FMT actinide solubility modeling results for the PABC04 and PABC09 that indicated $\text{Am}(\text{OH})_3(\text{s})$ would be the stable phase under repository conditions (EPA 2006b, Brush et al. 2009).

However, the FMT modeling results carried out to simulate experimental conditions (Xiong et al. 2010b) showed that $\text{Nd}(\text{OH})_3(\text{s})$ may not have been the stable solid phase in all neodymium(III) solubility experiments in the presence of carbonate. These results indicate that $\text{Nd}(\text{OH})_3(\text{s})$ was predicted to be stable only under higher-pcH conditions in the presence of carbonate (Table 6-9). In all 5 M NaCl experiments with 0.001 M or 0.01 M total carbonate, all ERDA-6 experiments with 0.01 M total carbonate and all GWB experiments with 1.0×10^{-4} to 0.01 M total carbonate, $\text{Am}(\text{OH})_3(\text{s})$ was not predicted to be stable at the final experimental conditions. For two examples cited by Moody (2010a, Table 1), experiments in GWB brine at pcH 8.4 and 0.001 M total carbonate¹³ or 10^{-4} M total carbonate,¹⁴ FMT calculations indicated that the stable phase would be $\text{NdOHCO}_3(\text{cr})$.

¹³ Xiong et al. (2010b) output files FMT_LANL09_GWB_1E-4_C_PCH_009, FMT_LANL09_GWB_1E-4_C_PCH_010 and FMT_LANL09_GWB_1E-4_C_PCH_011

¹⁴ Xiong et al. (2010b) output file FMT_LANL09_GWB_1E-3_C_PCH_012

Table 6-9. Solid Americium Phases Predicted by FMT Modeling Calculations

(Xiong et al. 2010b)

Brine	Total Carbonate Concentration (M)	Final pH	Predicted Solid Phases
5 M NaCl	1.00×10^{-5}	8.14 to 8.35	AmOHCO ₃ (cr)
		8.42 to 8.94	AmOHCO ₃ (cr) and Am(OH) ₃ (s)
		9.22 to 10.8	Am(OH) ₃ (s)
	1.00×10^{-4}	8.34 to 9.14	AmOHCO ₃ (cr)
		9.27 to 9.39	AmOHCO ₃ (cr) and Am(OH) ₃ (s)
	0.001	8.69 to 9.26	AmOHCO ₃ (cr)
	0.01	8.54 to 9.36	AmOHCO ₃ (cr) and NaAm(CO ₃) ₂ •6H ₂ O(cr)
		9.48 to 10.30	AmOHCO ₃ (cr)
11.91 to 13.17		Am(OH) ₃ (s)	
ERDA-6	1.00×10^{-5}	8.05 to 8.12	AmOHCO ₃ (cr)
		8.96 to 10.05	AmOHCO ₃ (cr) and Am(OH) ₃ (s)
	1.00×10^{-4}	7.97 to 9.03	AmOHCO ₃ (cr)
		9.66 to 10.13	AmOHCO ₃ (cr) and Am(OH) ₃ (s)
	4.71×10^{-4}	9.73	Am(OH) ₃ (s) ¹⁵
	0.001	8.06 to 9.61	AmOHCO ₃ (cr)
		9.85 to 9.90	AmOHCO ₃ (cr) and Am(OH) ₃ (s)
	0.01	8.20 to 9.00	AmOHCO ₃ (cr) and NaAm(CO ₃) ₂ •6H ₂ O(cr)
9.31 to 10.30		AmOHCO ₃ (cr)	
GWB	1.00×10^{-5}	6.64 to 7.89	AmOHCO ₃ (cr)
		8.30 to 8.39	AmOHCO ₃ (cr) and Am(OH) ₃ (s)
	1.00×10^{-4}	6.63 to 8.37	AmOHCO ₃ (cr)
	3.50×10^{-4}	9.40	Am(OH) ₃ (s) ¹⁶
	0.001	6.58 to 8.39	AmOHCO ₃ (cr)
	0.01	6.54 to 8.64	AmOHCO ₃ (cr)

The NdOHCO₃(cr) starting material was analyzed by XRD, and Borkowski et al. (2009) reported that “Analysis of the characteristic lines confirmed the predominance of a neodymium mixed-hydroxy-carbonate phase.” Based on this statement, EPA requested additional information, asking whether XRD data for this material may have indicated that a mixture of phases was present in this material; EPA also requested that DOE address the potential impact on the solubility results if such a mixture was present (Kelly 2010, Comment 4-C-32). Additional information provided by DOE indicated that the XRD pattern obtained with the synthesized NdOHCO₃(s) phase matched the reference pattern for this phase (Moody 2010c). DOE noted in their response that the presence of small amounts (on the order of 5%) of the hydroxide and carbonate phases used to synthesize this material could not be completely ruled out based on the XRD analysis. However, the presence of small amounts of these other phases would not affect the overall conclusions of the study.

¹⁵ PABC09 actinide solubility modeling calculations without organics, output file FMT_PABC09_E6_HMAG_ORGS_014.OUT

¹⁶ PABC09 actinide solubility modeling calculations without organics, output file FMT_PABC09_GWB_HMAG_ORGS_006.OUT

Use of solid phases in undersaturation experiments that are not stable under the conditions of the experiments or use of poorly crystalline solids that might dissolve and reprecipitate as a more crystalline, stable solid could result in initial increases in solution concentrations followed by decreasing solution concentrations over time. Borkowski et al. (2009, Figure 4-7) showed that in the GWB undersaturation experiments with carbonate, such initial increases followed by decreasing concentrations were observed. EPA asked whether this effect was also observed in the undersaturation experiments with carbonate carried out with 5 M NaCl and ERDA-6 brine (Kelly 2010, Comment 4-C-29). Moody (2010c) provided additional data indicating that this effect was observed in the experiments with ERDA-6, but that samples were not obtained from the 5 M NaCl experiments that would indicate whether this effect occurred. Based on the results reported by Borkowski et al. (2009, Figure 4-7) and Moody (2010c), it appears that use of an unstable or poorly crystalline solid starting material resulted in steady-state conditions being approached from oversaturation in all neodymium(III) solubility experiments with carbonate in GWB and ERDA-6 brine.

The carbonate-free undersaturation experiments in GWB used solid $\text{Nd}(\text{OH})_3(\text{cr})$ as the solid starting material, and this phase is expected to be stable under the conditions of the experiments. However, in carbonate-free solubility experiments at pcH values of approximately 7.3 and 8.0, the neodymium(III) concentrations measured from undersaturation were reported to be significantly higher than the concentrations measured from oversaturation (Borkowski et al. 2009). EPA requested additional information regarding the potential cause of the concentration differences (Peake 2010, Question 6). DOE responded that higher concentrations observed in the undersaturation experiments were caused by initial disequilibrium in the experiments because of the addition of an unstable phase to the experiment and the relative rate of dissolution of this phase and precipitation of the more-stable solubility-controlling phase (Moody 2010a). DOE noted that over time, the concentrations in the undersaturation and oversaturation experiments would be expected to approach the same final concentration. Additional data provided in their response showed that the concentrations in the undersaturation experiments had continued to decline, as expected if the initial phase was unstable because of small grain size or poor crystallinity.

Borkowski et al. (2009) measured the neodymium(III) solubility of $\text{Nd}(\text{OH})_3(\text{s})$ or $\text{Nd}_2(\text{CO}_3)_3(\text{s})$ in GWB brine with an initial carbonate concentration of 0.01 M at pcH values of approximately 6.9, 7.7 and 8.6. After 117 days, the final concentrations in both sets of experiments were similar as a function of pcH regardless of the solid phase that was added. Borkowski et al. (2009) stated that these results indicated that the final solid phase controlling neodymium(III) concentrations in all experiments was $\text{Nd}(\text{OH})_3(\text{cr})$, including undersaturation experiments carried out with $\text{NdOHCO}_3(\text{cr})$ or $\text{Nd}_2(\text{CO}_3)_3(\text{s})$. However, according to the FMT modeling calculations performed by Xiong et al. (2010b), the stable solid phase in GWB at these pcH values with 0.01 M total carbonate should be $\text{NdOHCO}_3(\text{s})$ (Table 6-9).

Because the solid phases in contact with the solutions at the end of the experiments were not characterized and the FMT calculations indicate that different solids, including $\text{NdOHCO}_3(\text{cr})$, $\text{NaNd}(\text{CO}_3)_2 \cdot 6\text{H}_2\text{O}(\text{cr})$ and $\text{Nd}(\text{OH})_3(\text{s})$ were stable at the various experimental conditions, the identities of the solid phases present at the end of the experiments is uncertain. The available data indicate that solid-phase dissolution and reprecipitation occurred during the undersaturation experiments. Consequently, steady-state concentrations were generally approached from

oversaturation and under such conditions, the results of the neodymium(III) solubility experiments provide an upper limit on neodymium concentrations that may be observed in WIPP brines.

Effects of Carbonate Concentrations on Measured Neodymium(III) Concentrations

DOE (2009, Appendix SOTERM-2009, Section SOTERM-3.6.2) stated that there was “(e)xcellent agreement with comparable literature values for Nd(III) solubility in carbonate-free, simplified 5 M NaCl brine.” This agreement was illustrated by Figure 4-4 of Borkowski et al. (2009), which compared the experimental results with Runde and Kim (1995) solubility data reviewed by Giambalvo (2002a) and used to develop the americium data in the FMT database (Figure 6-3). The Borkowski et al. (2009) data in carbonate-free 5 M NaCl experiments and the solubility data used to develop the FMT database appear to be in reasonably good agreement up to a pcH of 10, which is the expected upper limit for brine pcH in the WIPP environment. At pcH values greater than 10, the neodymium concentrations in the Borkowski et al. (2009) experiments were higher than the Runde and Kim (1995) solubility data, possibly because the concentrations were close to the analytical detection limit of approximately 4×10^{-9} M reported by Borkowski et al. (2009).

Comparison of the experimental results in 5 M NaCl without carbonate (Figure 6-3) and with carbonate (Figure 6-4, Borkowski et al. 2009, Figure 4-5 and DOE 2009, Appendix SOTERM-2009, Figure SOTERM-15) indicates that carbonate had a noticeable effect on neodymium solubilities at pcH values greater than about 9. However, the carbonate concentrations were not reported by DOE (2009) for the data in Figure SOTERM-15. EPA requested information regarding the concentrations of carbonate used in the 5 M NaCl experiments that appear to decline at pcH values greater than 10 (Cotsworth 2009a, Comment 1-C-9). DOE (Moody 2009c) reported that the Figure SOTERM-15 data (DOE 2009, Appendix SOTERM-2009) included data collected without carbonate and with total carbonate concentrations ranging from 0.0001 M to 0.01 M. Moody (2010c) provided additional documentation of the experimental data (Borkowski 2010) in response to another request for information on these experiments (Kelly 2010, Comment 4-C-34). Examination of the data tables indicated that the experiments reported above pcH 10 in 5 M NaCl were carried out in carbonate-free brine and 0.01 M total carbonate brine.

Because WIPP brines are predicted to have pcH values between 9 and 10, the potential formation of americium-carbonate complexes that might be demonstrated by Figure 6-4 could affect predicted actinide solubilities in the repository. Data provided by Borkowski (2010) from pcH 9 to 10 in 5 M NaCl were plotted in Figure 6-5 as a function of initial carbonate concentration. Examination of the data in Figure 6-5 shows that the increased neodymium concentrations observed in this pcH region are mostly observed in the 0.01 M total carbonate brines, whereas lower total carbonate concentrations do not generally appear to affect neodymium(III) concentrations. Because WIPP brines are predicted to have much lower total carbonate concentrations than 0.01 M, the results in 5 M NaCl do not indicate that americium complexation by carbonate will have significant effects on total americium concentrations in WIPP brines. This conclusion is consistent with the FMT modeling carried out for the PABC09, which showed that at the total carbonate concentrations established by the reaction of brucite to form hydromagnesite (approximately 0.0004 M), significant quantities of americium-carbonate

complexes will not be present in solution. FMT modeling calculations carried out simulating the conditions of the experiments by Xiong et al. (2010b) indicated that complexation of neodymium by carbonate was only significant in 5 M NaCl with 0.01 M total carbonate, in ERDA-6 with 0.01 M total carbonate and in GWB in 0.01 M and 0.001 M total carbonate. Because lower total carbonate concentrations will be maintained by the reaction of brucite to form hydromagnesite in the repository, significant complexation of +III actinides by carbonate is not expected to occur.

Borkowski et al. (2009) established initial carbonate concentrations in their experiments by adding a known quantity of carbonate to the solution, as an alternative to maintaining equilibrium between the solutions and a gas with a fixed CO₂ concentration. Borkowski et al. (2009) did not report measurements of the total carbonate concentration in the solutions sampled at the end of the experiments. EPA requested additional information regarding whether any loss of carbonate could have occurred during the experiments (Peake 2010, Question 9), or whether dissolution of the initial NdOHCO₃(s) could have significantly increased carbonate concentrations (Kelly 2010, Comment 4-C-27; Peake 2010, Question 9). Carbonate concentrations were measured in the experiments after 3 years (Moody 2010a). The measured concentrations were typically 80% or more of the initial carbonate concentrations. Only small amounts of the neodymium-carbonate solid were added to the carbonate-bearing experiments with brine to minimize potential effects of the solid on brine chemistry (Moody 2010c). Complete dissolution of this quantity of solid in the brine would result in an increase in the carbonate concentration of 2.5×10^{-4} M. Such an increase would have a minimal impact on the higher-concentration experiments (0.001 M and 0.01 M carbonate), but could have significantly increased the carbonate concentration in the lower concentration experiments (1×10^{-4} M and 1×10^{-5} M carbonate). DOE stated that visual inspection indicated that less than 10% of the initial neodymium-hydroxycarbonate phase was converted to the hydroxide phase, although no explanation was provided of the changes in appearance observed during conversion from the hydroxycarbonate to the hydroxide phase (Moody 2010c). Because carbonate concentrations less than 0.001 M do not appear to affect neodymium solubilities in the brines investigated by Borkowski et al. (2009), even complete dissolution of the neodymium hydroxycarbonate phase would not be expected to significantly affect neodymium solubilities.

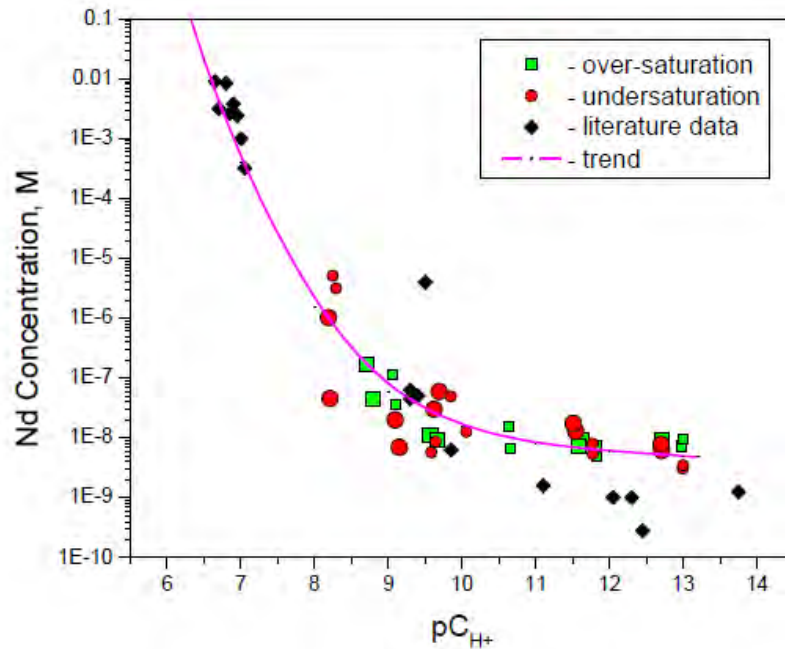


Figure 6-3. Neodymium(III) Solubility in Carbonate-Free 5 M NaCl

Literature Data are from Runde and Kim (1995)
 (Source: Borkowski et al. 2009, Figure 4-4)

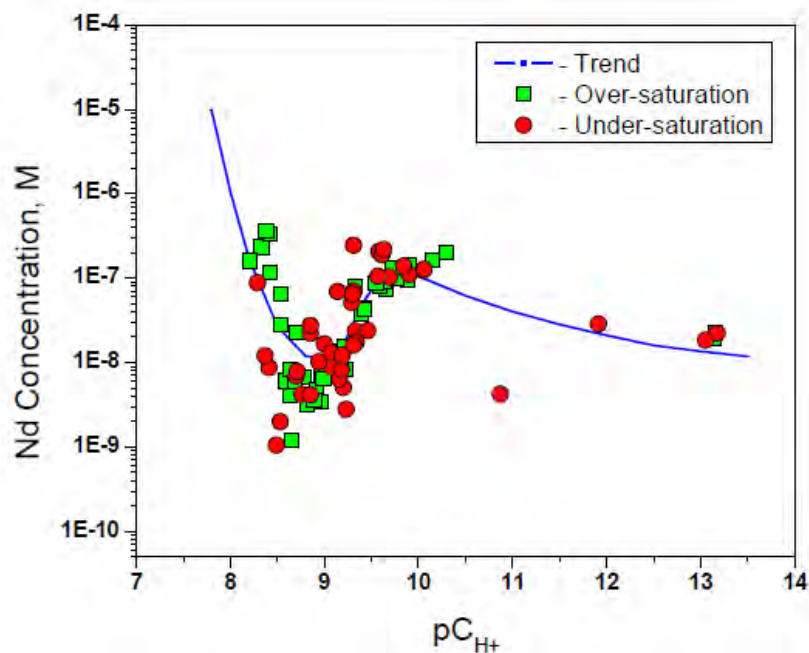


Figure 6-4. Neodymium(III) Solubility in 5 M NaCl in the Presence of Carbonate from 0.00001 M to 0.01 M

(Source: Borkowski et al. 2009, Figure 4-5)

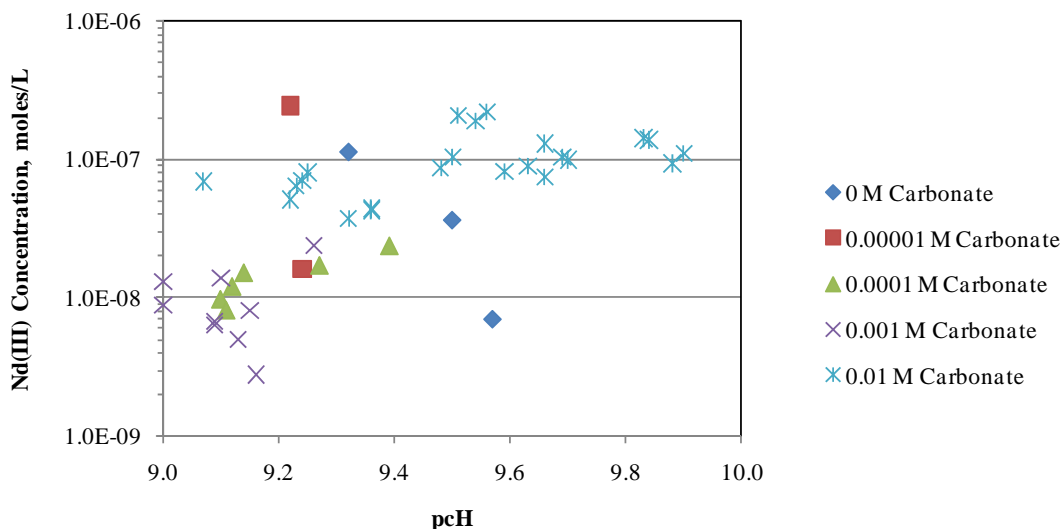


Figure 6-5. Neodymium(III) Solubility in 5 M NaCl at WIPP-Relevant pcH Values from 9 to 10 as a Function of Total Carbonate Concentration

Borkowski et al. (2009) stated that the addition of carbonate to solutions modeled with Geochemists Workbench led to a slight increase in the neodymium concentration because of the formation of the $\text{Nd}_2(\text{CO}_3)_2^{2+}$ aqueous species. This species is not included in the FMT database, so EPA asked DOE whether this species should be added to the database (Kelly 2010, Comment 4-C-30). DOE's response indicated that this species would not be important in WIPP repository brines, so it need not be added to the database (Moody 2010c).

Neodymium Complexation by Borate

In the GWB experiments at pcH values between about 6 and 8, neodymium concentrations decreased as a function of increasing pcH (Figure 6-6). However, above pcH 8, neodymium(III) concentrations in GWB increased up to the maximum pcH investigated of 8.6. Experiments were not performed in higher-pcH GWB brine because magnesium solids precipitated when GWB was adjusted to higher pcH values.

In ERDA-6 brine, neodymium(III) concentrations initially increased as pcH increased above 6.5, reached a maximum at approximately pcH 9.5, then decreased at pcH 10.5 to approximately 10^{-8} M (Figure 6-7). Borkowski et al. (2009) attributed the increasing neodymium(III) concentrations in GWB and ERDA-6 brines as a function of increasing pcH to borate complexation. In the pcH range from approximately 7.5 to 10.5, Borkowski et al. (2009) stated that neodymium complexation with borate or tetraborate predominates over neodymium complexation with carbonate. When the pcH was increased above 10, Borkowski et al. (2009) stated that neodymium hydrolysis becomes dominant.

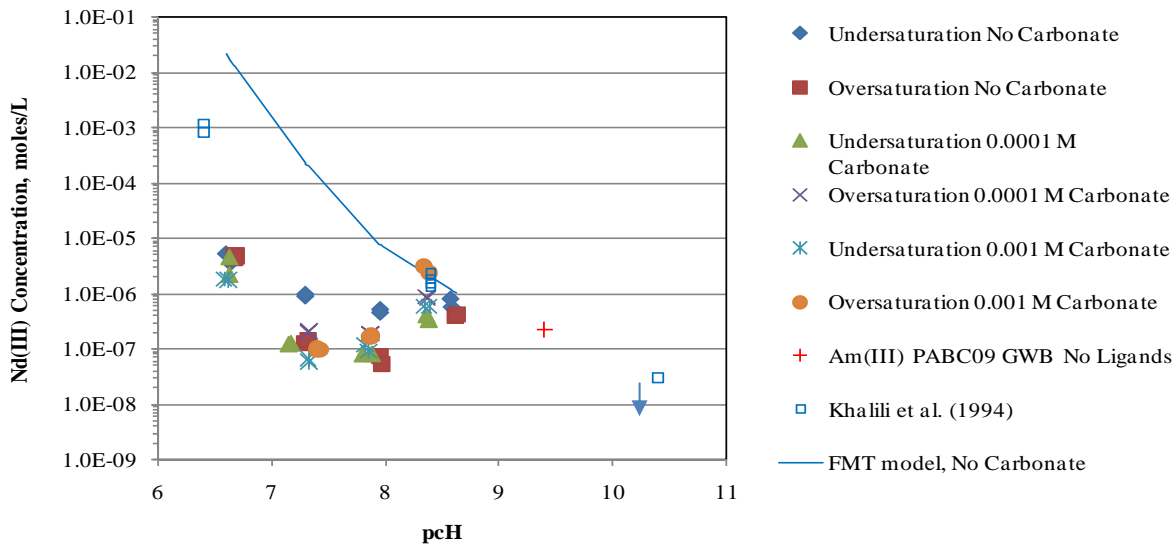


Figure 6-6. Neodymium Solubility Experiment Results in GWB without Carbonate and Carbonate Concentrations Bracketing Repository Conditions Compared to PABC09 Modeled Value without Organic Ligands, Khalili et al. (1994) Results and FMT-Predicted Concentrations¹⁷

(Sources: Borkowski et al. 2009, Borkowski 2010, Brush et al. 2009, Xiong et al. 2010b)

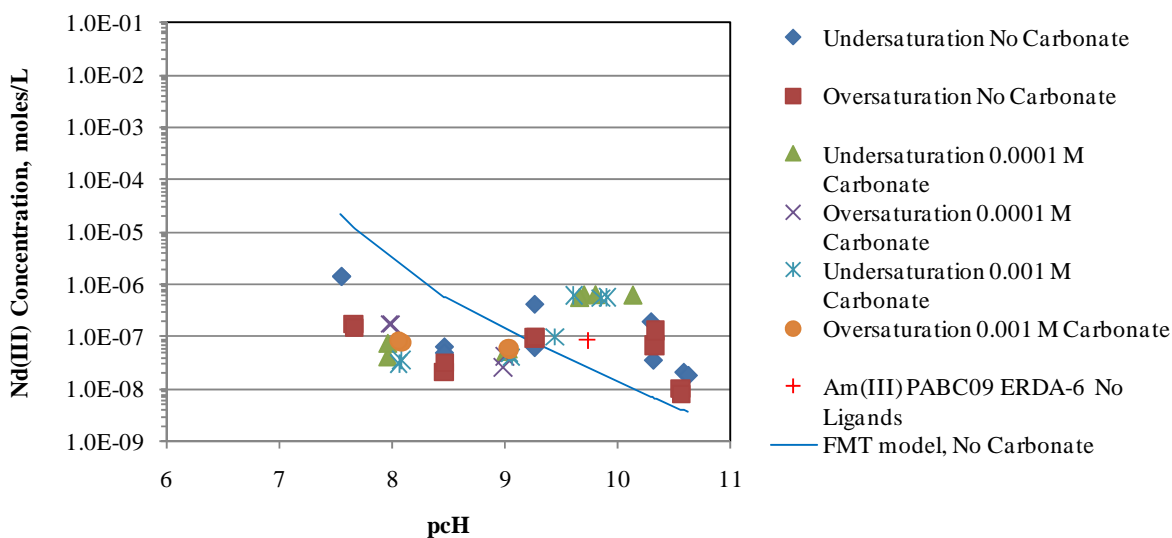


Figure 6-7. Neodymium Solubility Experiment Results in ERDA-6 without Carbonate and Carbonate Concentrations Bracketing Repository Conditions Compared to the PABC09 Modeled Concentration without Organic Ligands and FMT-Predicted Concentrations

(Sources: Borkowski et al. 2009, Borkowski 2010, Brush et al. 2009, Xiong et al. 2010b)

¹⁷ The neodymium concentration observed by Khalili et al. (1994) at pcH 10.4 was less than $3 (\pm 3) \times 10^{-8}$ M.

Borkowski et al. (2009) stated that boric acid was the only brine component with a pKa in this pH region. The identity of the proposed actinide(III)-borate aqueous complex was stated in equation 2-5 of Borkowski et al. (2009) as $\text{AmB}(\text{OH})_4^{2+}$, but aqueous species in equations 4-9 and 4-10 of Borkowski et al. (2009) were tetraborate complexes of the form NdB_4O_7^+ and $\text{Nd}(\text{B}_4\text{O}_7)_2^-$.

EPA requested additional information regarding the proposed complexation of neodymium(III) by borate or tetraborate. EPA noted that Borkowski et al. (2009) had identified both borate and tetraborate aqueous species and asked DOE to address whether there was a basis for assuming the identity of the species that would form and the anticipated effects of the formation of such species on neodymium(III) solubility in GWB and ERDA-6 brines (Kelly 2010, Comment 4-C-26). DOE explained that the ambiguity in the borate speciation occurred because the chemistry of borate is complex and the speciation of borate at high pH is not clearly addressed by the scientific literature (Moody 2010c). DOE carried out XRD analysis, showing that the tetraborate species is retained in WIPP brines after borate is added to the brines as the tetraborate species. DOE is also performing EXAFS measurements to confirm the structure of the neodymium-borate complexes. DOE has proposed the following speciation of the neodymium-tetraborate species:



EPA noted that the formation of significant actinide(III)-borate aqueous species appeared to be previously unreported. EPA asked DOE to identify whether there was scientific literature that either supported or contradicted the formation of such species (Kelly 2010, Comment 4-C-31). No literature reports related to complexation of actinides by borate have been identified. However, some data are available regarding complexation of aluminum(III) and iron(III) by borate. Moody (2010c) provided supporting information in the form of two references; Bousher (1995) and Byrne and Thompson (1997). An additional reference related to borate complexation of metals is Öhman and Sjöberg (1985). Bousher (1995) calculated a stability constant for $\text{AlB}(\text{OH})_4^{2+}$ from the solubility data of Shchigol and Burchinskaya (1961). However, the Shchigol and Burchinskaya (1961) solubility data have been questioned because of experimental procedure problems (Bassett 1980, Öhman and Sjöberg 1985). Öhman and Sjöberg (1985) performed additional experiments showing that either aluminum-borate complexes did not form or were very weak. The experimental results of Byrne and Thompson (1997) indicate that iron(III) is weakly complexed by borate ion. In summary, the available literature data lend little support to the complexation of the +III actinides by borate, because aluminum(III) and iron(III) complexation by borate appears to be weak and it is difficult to extrapolate data from these metals to the actinides. However, literature data do not appear to be available that would rule out complexation of the +III actinides by borate.

EPA requested additional information regarding the observed differences in neodymium concentrations at similar pH in GWB and ERDA-6 brine, which were attributed by Borkowski et al. (2009) to borate complexation (Peake 2010, Question 2). EPA noted that GWB has approximately 2.5 times the borate concentration of ERDA-6. In experiments without carbonate, EPA observed that the neodymium concentrations measured at pH 8.7 in ERDA-6 brine

(without carbonate) was approximately 5×10^{-8} M (Figure 6-5). In GWB brine at pcH 8.7 is approximately 5×10^{-7} M (Figure 6-4). EPA asked DOE to explain the neodymium-borate speciation that would account for a ten-fold increase in neodymium concentrations with a 2.5-fold increase in borate concentration. Moody (2010a) stated that even without the potential effects of borate complexation, the current +III actinide solubility modeling with FMT predicted different solubilities in GWB and ERDA-6. DOE pointed out in their response that different +III actinide solubilities in the two brines are likely caused by a number of differences between the brines, such as ionic strength and different cation concentrations, and should not be attributed only to borate complexation. The comments by Borkowski et al. (2009) were characterized as “preliminary in nature and not yet the accepted position of the WIPP project.”

EPA also noted that the neodymium(III) concentrations observed in ERDA-6 and in 5 M NaCl (Figure 6-8) were virtually the same at pcH 10.5 (Peake 2010, Question 3). If borate complexation was the cause of the observed maximum concentration at about pcH 10 in ERDA-6, it was unclear what would cause borate complexation to cease at higher pcH. If hydrolysis becomes more important at higher pcH, then higher concentrations of species such as $\text{Nd}(\text{OH})_3^0$ would be present in addition to the neodymium-borate species and would not replace them. DOE stated in their response that the solution concentration of neodymium-borate complexes become unimportant with increasing pcH because of decreasing neodymium solubility (Moody 2010a).

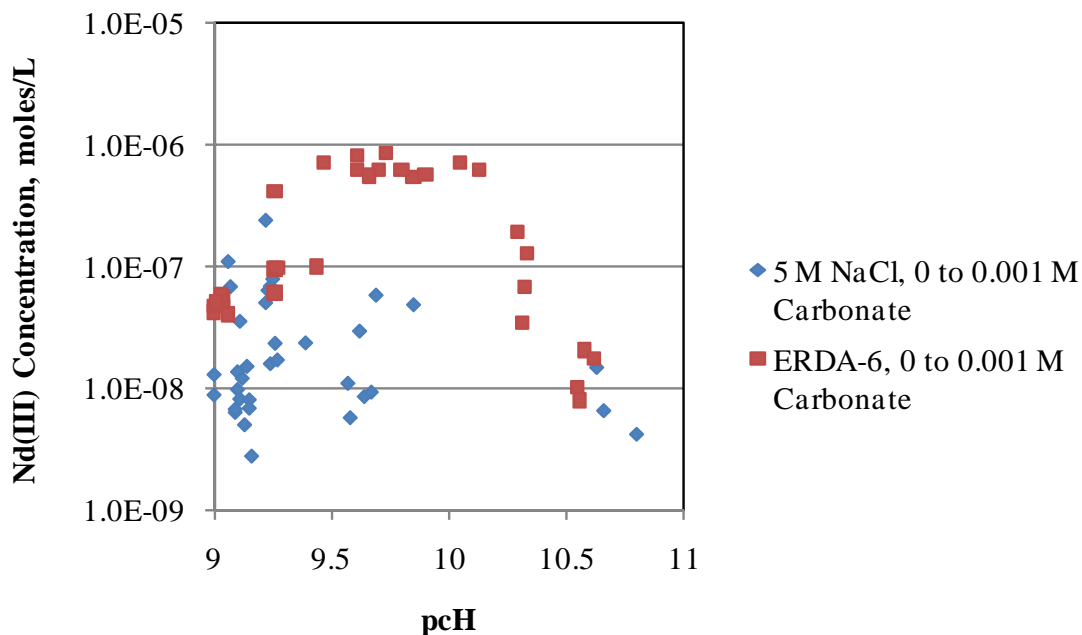


Figure 6-8. Neodymium Solubility Experiment Results in 5 M NaCl and ERDA-6 with Carbonate Concentrations from 0 to 0.001 M, Undersaturation and Oversaturation Experiments

(Source: Borkowski 2010)

The current actinide solubility conceptual model does not include the assumption that complexation by borate has significant effects on actinide solubilities (Cotsworth 2009a, Comment 1-23-6c). Consequently, EPA asked DOE to address whether the current FMT database is adequate for predicting actinide solubilities for PA when it does not include borate species for the +III actinides. In their response, DOE stated that for the +III actinides, complexation by borate effectively substitutes for the calculated effect of carbonate presently in the WIPP model. This response is inconsistent with the predicted lack of effect of carbonate on total americium concentrations in FMT modeling results for WIPP repository conditions (Peake 2010, Question 7). In addition, because an excess of $\text{Am}(\text{OH})_3(\text{s})$ is assumed to be available to repository brines, competition between borate and carbonate for limited amounts of americium would not occur and americium-borate aqueous species would form in addition to americium-carbonate complexes. DOE clarified in their response that the effects of borate on neodymium solubility have not yet been fully evaluated, and that the point of the statement in the previous response had been to note that borate and carbonate complexation behave similarly in the brine systems investigated (Moody 2010a).

Agreement of Experimental Results with FMT-Predicted Solubilities

DOE (2009, Appendix SOTERM-2009, Section SOTERM-3.6.2) cited agreement of the experimentally measured neodymium(III) concentrations with the actinide solubilities calculated at a pcH of approximately 8.5 for the CRA-2004 PA (DOE 2004, Appendix PA, Attachment SOTERM). EPA noted that the correct pcH range from PABC04 calculations is 9.39 to 9.64 (Table 6-2) (Cotsworth 2009a Comment 1-23-5). EPA requested that DOE revise the cited pcH and reinterpret the solubility data with respect to the higher pcH expected in WIPP brines. DOE agreed that the cited pcH values were incorrect and included changes to statements in SOTERM-3.6.2 (Moody 2009c). DOE further stated that these inconsistencies “do not change or significantly impact the conclusions regarding actinide solubilities.”

The GWB and ERDA-6 experimental results without carbonate and with total carbonate concentrations (0.001 and 0.0001 M) bracketing those predicted for the WIPP repository brines are shown in Figures 6-6 and 6-7. Figures 6-6 and 6-7 also include the results of the PABC09 americium(III) calculations for GWB and ERDA-6 under repository conditions without organic ligands and predicted +III concentrations based on FMT modeling calculations carried out at the conditions of the Borkowski et al. (2009) experiments. The neodymium(III) solubility experiment results in GWB were only obtained at pcH values up to 8.64; under repository conditions GWB is predicted to have a pcH of 9.4 (Figure 6-6). Khalili et al. (1994) carried out neodymium(III) solubility experiments at pcH values of 6.4, 8.4 and 10.4 in a synthetic brine similar to GWB (Figure 6-6). Experimental results were obtained by Borkowski et al. (2009) over a pcH range in ERDA-6 brine that included the predicted repository pcH of 9.7 (Figure 6-7).

The experimentally measured neodymium(III) concentrations in ERDA-6 brine at pcH values of approximately 9.7 exceed the FMT-calculated concentration by nearly an order of magnitude (Figure 6-7). The highest-pcH results reported for GWB were obtained at pcH 8.6, and range from about 3.9×10^{-7} M to about 8.5×10^{-7} M. At pcH 8.6 in ERDA-6, the neodymium(III) solubility was approximately 5×10^{-7} M, and increased sharply as a function of pcH up to 10.1. Extending the results in GWB (Figure 6-7) by paralleling the “shoulder” in the ERDA-6 results

(Figure 6-6) could result in neodymium concentrations that significantly exceed the FMT-predicted concentration for americium(III) under WIPP conditions at pcH 9.40 in GWB. EPA accordingly requested information from DOE regarding the potential effects on PA of such significantly higher +III actinide solubilities (Cotsworth 2009a, Comment 1-23-6a).

DOE responded that it was not technically correct to extrapolate the GWB data from lower pcH to the pcH 9.4 conditions expected in the repository without “consideration of the complexation chemistry and known pH dependencies” (Moody 2009c). DOE pointed out that the pcH range for the GWB brine experiments were limited by the cloud point, which represented precipitation of brucite and reduction of the magnesium concentration in the GWB. Consequently, the higher-pcH GWB would become more like ERDA-6 brine as pcH was increased. DOE’s evaluation of the trends led to an estimated neodymium concentration of 5×10^{-7} M with an uncertainty of 3×10^{-7} M in the pcH range from 9 to 9.5 in GWB (Moody 2009c). This estimated range overlaps the +III actinide concentration of 2.3×10^{-7} M calculated for the PABC09 for GWB brine without organic ligands.

EPA noted in a follow-up question that the predicted magnesium concentration in GWB brine at repository conditions was 0.55 M, which is 29 times the magnesium concentration in ERDA-6 (Peake 2010, Question 4). DOE responded that the chemistry of the WIPP brines was complex and that these complexities are not properly captured by linear extrapolation (Moody 2010a). DOE used the uranium(VI) solubility data collected in GWB by Lucchini et al. (2010) to illustrate that under some circumstances, increasing pcH could result in solubility trends that first increase, then decrease (Figure 6-2). It is not clear that neodymium concentrations in GWB at the repository pcH of 9.4 will decline and approach the concentrations in ERDA-6 at the same pcH. For example, uranium(VI) in GWB brine at the moderately alkaline pcH values expected in the repository has a measured concentration approximately an order of magnitude higher than the concentration measured in ERDA-6 brine (Figure 6-2). Consequently, the results of the neodymium(III) experiments in GWB have introduced some uncertainty regarding the expected concentration of americium(III) in GWB brine at pcH 9.4.

The extent of the differences between the neodymium(III) concentrations measured in WIPP brines and 5 M NaCl and the concentrations calculated with FMT was difficult to determine based on the information presented by Borkowski et al. (2009). Consequently, EPA requested that DOE perform FMT calculations to predict the concentrations of neodymium(III) under the conditions of the solubility experiments in 5 M NaCl, GWB and ERDA-6 brines (Peake 2010, Question 8). The results of FMT modeling carried out to simulate the experimental conditions for the neodymium(III) solubility experiments were provided by Xiong et al. (2010b).

In all modeled experiments that did not contain carbonate (5 M NaCl, ERDA-6 and GWB), the stable solid phase was predicted to be $\text{Nd}(\text{OH})_3(\text{s})$. $\text{NdOHCO}_3(\text{cr})$ was predicted to be the stable solid phase in the 5 M NaCl solutions at lower pcH with 10^{-5} M to 0.001 M total carbonate, with $\text{Nd}(\text{OH})_3(\text{s})$ formation predicted at higher pcH and lower total carbonate concentrations (Table 6-9). In the 5 M NaCl experiments with 0.01 M total carbonate, the stable solids were predicted to be both $\text{NdOHCO}_3(\text{cr})$ and $\text{NaNd}(\text{CO}_3)_2 \cdot 6\text{H}_2\text{O}(\text{cr})$ up to pcH 9.36, $\text{NdOHCO}_3(\text{cr})$ from pcH 9.48 to 10.30 and $\text{Nd}(\text{OH})_3(\text{s})$ above pcH 11.91. For 5 M NaCl experiments carried out without carbonate, FMT-predicted concentrations in the 5 M NaCl experiments were in

reasonable agreement with measured concentrations (Xiong et al. 2010b, Figure 1). A few measured concentrations from pcH 8.2 to 9.2 were significantly lower than the predicted concentrations. Because the lowest neodymium concentrations at pcH values of 8.21, 8.29, 9.09 and 9.15 were carried out from undersaturation, the $\text{Nd}(\text{OH})_3(\text{cr})$ in the experiments may not have fully equilibrated with the solution at the time the samples were collected. At pcH values greater than 11, measured neodymium(III) concentrations were slightly higher than the predicted concentrations, possibly because of the proximity of the measured concentrations to the analytical detection limit of approximately 4×10^{-9} M. In the 5M NaCl experiments with 10^{-5} M to 10^{-4} M total carbonate, the measured neodymium(III) concentrations were less than the predicted concentrations; at pcH values of approximately 8.5 in these experiments, measured neodymium(III) concentrations were about 2 orders of magnitude less than predicted concentrations (Xiong et al. 2010b, Figures 2 and 3). In the 5 M NaCl experiments with 0.001 M to 0.01 M total carbonate, measured concentrations were slightly less than the predicted concentrations at pcH values ranging from 8.54 to 10.39 (Xiong et al. 2010b, Figures 4 and 5). At pcH values ranging from 11.91 to 13.17 in 0.01 M carbonate solutions, the measured concentrations exceeded predicted concentrations by more than an order of magnitude.

FMT modeling calculations simulating experiments carried out in ERDA-6 brine with 10^{-5} M to 0.001 M carbonate indicated that $\text{NdOHCO}_3(\text{cr})$ was stable at lower pcH values and $\text{Nd}(\text{OH})_3(\text{s})$ plus $\text{NdOHCO}_3(\text{cr})$ were the stable phases at higher pcH (Table 6-9). In ERDA-6 brine with 0.01 M carbonate, the stable solid phases were predicted to be $\text{NdOHCO}_3(\text{cr})$ and $\text{NaNd}(\text{CO}_3)_2 \cdot 6\text{H}_2\text{O}(\text{cr})$ up to pcH 9 and $\text{NdOHCO}_3(\text{cr})$ at higher pcH (Table 6-9). In ERDA-6 brine with total carbonate less than or equal to 0.001 M, measured neodymium(III) concentrations were consistently less than the FMT-predicted concentrations at pcH values ranging from 7.55 to 8.46 (Figure 6-7); the differences between the measured and predicted concentrations in this pcH range were approximately an order of magnitude or more. Predicted and measured concentrations were similar at pcH values ranging from 9.04 to 9.44, but at pcH values ranging from 9.61 to 10.13, measured concentrations consistently exceeded FMT-predicted concentrations by approximately an order of magnitude (Figure 6-7). At the highest pcH values of approximately 10.6 investigated in carbonate-free ERDA-6 experiments, the FMT-predicted concentrations were similar to the measured concentrations.

For GWB experiments with 10^{-5} M carbonate, FMT modeling calculations indicated that $\text{NdOHCO}_3(\text{cr})$ was the stable phase up to pcH 7.89 and $\text{Nd}(\text{OH})_3(\text{s})$ and $\text{NdOHCO}_3(\text{cr})$ were the stable phases at higher pcH (Table 6-9). In GWB brine experiments with 10^{-4} M to 0.01 M carbonate, the stable solid phase was predicted to be $\text{NdOHCO}_3(\text{cr})$. In GWB experiments with 0.001 M carbonate or less, relatively good agreement was observed between measured and FMT-predicted concentrations at the highest pcH investigated of approximately 8.6. However, significant disagreement was observed between measured and predicted neodymium(III) concentrations at lower pcH values ranging from 6.60 to 7.97, with predicted concentrations at pcH 6.60 that were more than 3 orders of magnitude greater than the measured concentrations (Figure 6-6). Khalili et al. (1994) measured neodymium solubilities in a brine similar to GWB. Characterization of the solid phases indicated that $\text{Nd}(\text{OH})_3 \cdot n\text{H}_2\text{O}(\text{am})$ formed at pcH 6.4 and 8.4 and the $\text{Nd}_2(\text{CO}_3)_3 \cdot 8\text{H}_2\text{O}$ formed at pcH 10.4 (Figure 6-6). The solubility results of Khalili et al. (1994) at pcH 6.4 are more than 2 orders of magnitude greater than the results of Borkowski et al. (2009) at pcH 6.63, but are still significantly less than the FMT-predicted

concentration at this pcH. DOE did not provide an explanation for these significant differences between the measured and predicted neodymium(III) concentrations at lower pcH. However, the results illustrated in Figure 6-6 show that the current FMT model does not provide a good representation of measured +III actinide solubilities in GWB at pcH values of 8 or less.

The experimental results most relevant to the WIPP repository are the ERDA-6 and GWB experiments from 10^{-4} M to 0.001 M total carbonate and at the moderately alkaline pcH values of approximately 9.4 to 9.7 expected in the repository because of the presence of the MgO backfill. Experiments were not conducted in GWB at repository-relevant pcH conditions, so no conclusions can be reached regarding the solubility results for the neodymium analogue in this brine. However, experiments conducted in ERDA-6 brine at WIPP-relevant total carbonate and pcH indicate that the measured concentrations exceeded FMT-predicted concentrations by slightly more than an order of magnitude. This difference has been attributed to the complexation of the +III actinides by borate, which is not currently included in the actinide solubility conceptual model or in the FMT database.

Conclusions

The aqueous speciation and solid-phase solubility data for americium(III) in the FMT database used for the CRA-2009 PA and PABC09 actinide solubility calculations has remained unchanged since the PABC04. Additional information, including data summarized by Neck et al. (2009) and the results of experiments reported by Borkowski et al. (2009), has recently become available, but was not available in time to revise the FMT database before the CRA-2009 or PABC09 calculations were carried out. This information and any other new data that become available should be considered with respect to FMT database revisions for the CRA-2014 PA.

Review of the information provided by DOE on the aqueous solubilities and solubility-controlling solids in neodymium(III) solubility experiments (Borkowski et al. 2009, Borkowski 2010, Xiong et al. 2010b) yielded the following observations:

- Only indirect evidence is available regarding the final composition and crystallinity of the solid phases in the experiments, because the solid phases were present in quantities that were too small to be characterized. FMT calculation results for the experiments conducted by Borkowski et al. (2009) predicted that not only $\text{Nd}(\text{OH})_3(\text{s})$ would form, but also $\text{NdOHCO}_3(\text{s})$ and $\text{NaNd}(\text{CO}_3)_2 \cdot 6\text{H}_2\text{O}(\text{cr})$ in some carbonate-bearing solutions. Consequently, the identities of the solid phases present at the end of the carbonate-bearing experiments is uncertain.
- The results of the neodymium(III) experiments and FMT modeling carried out by Xiong et al. (2010b) confirm that carbonate complexation of the +III actinides is unlikely to be significant at WIPP-relevant pcH (9 to 10) and total carbonate concentrations (1.0×10^{-4} to 0.001 M).
- Experimental results in ERDA-6 brine at WIPP-relevant pcH values and carbonate concentrations were approximately one order of magnitude higher than FMT-predicted concentrations under these conditions. This discrepancy was attributed to complexation

of the +III actinides by borate. Experimental results in GWB brine were not obtained at WIPP-relevant pcH values, so the effects of borate complexation in GWB brine under WIPP-relevant conditions remain undetermined.

- Significant disagreement between measured and predicted concentrations at low pcH values (6.60 to 7.97) in carbonate-free GWB indicates that the FMT model is not well parameterized under these conditions. The cause of this disagreement between the measured and predicted solubilities is not known.

Higher organic ligand concentrations are assumed for the PABC09 than for previous WIPP PA calculations. As a result of the increased EDTA concentration assumed for WIPP brines, it is possible that higher solubilities observed in the neodymium(III) solubility experiments in ERDA-6 brines at WIPP-relevant pcH and total carbonate conditions may be of relatively minor importance to PA. The predicted +III actinide solubilities for the PABC09 are 1.7×10^{-6} M in GWB brine and 1.5×10^{-6} M in ERDA-6. The predicted concentration in ERDA-6 brine in the presence of organic ligands is slightly higher than the concentrations measured by Borkowski et al. (2009) at pcH 9.7. Brush et al. (2008) assessed the effects of higher EDTA concentrations and consequent higher +III actinide solubilities on WIPP repository performance. The highest EDTA concentration used in the calculations resulted in predicted +III actinide solubilities of 1.8×10^{-5} M in GWB and 1.9×10^{-5} M in ERDA-6 brine. These concentrations are approximately an order of magnitude greater than the concentrations predicted for the PABC09 and the ERDA-6 concentration exceeds the concentrations measured by Borkowski et al. (2009) at WIPP-relevant pcH values. Although Brush et al. (2008) found that higher +III actinide solubilities increased DBR and total repository releases, the effects were most evident at low probabilities and WIPP performance complied with EPA containment requirements. Because the possible effects of borate complexation of the +III actinides indicated by the Borkowski et al. (2009) experimental results are likely to be less than those considered by Brush et al. (2008), borate complexation of the +III actinides is likely to have little effect on overall repository performance.

6.4.4.6 Actinide Solubility Uncertainty Distribution

Implementation of the dissolved actinide source term calculations has remained the same since the PABC04. The calculated solubilities for the +III, +IV and +V actinides are constant values, with associated uncertainty distributions. The uncertainty distributions for each oxidation state were sampled for each realization from the distributions developed for the PABC04 (Xiong et al. 2004, 2005) (Section 6.3.5). The +III, +IV and +V actinide solubilities used in each PA realization are the products of the antilog of the sampled uncertainties multiplied by the calculated solubilities. The uranium(VI) solubility used in PA remains equal to the fixed value of 10^{-3} M (Section 6.3.4).

During EPA's completeness review of the CRA-2009 (DOE 2009), EPA noted that additional data related to the solubilities of actinides had become available since the PABC04 (Cotsworth 2009a, Comment 1-23-3). EPA requested that DOE evaluate the possible effects of these additional data on the solubility uncertainty distributions developed for the PABC04. DOE prepared updated uncertainty distributions for the +III and +IV actinides that were sampled for the PABC09 (Xiong et al. 2009a). These updated uncertainty distributions are addressed in Section 6.5.5.

6.4.4.7 Other Thermodynamic Data

In addition to μ^0/RT data for actinide solids and aqueous species, the FMT database includes data for the aqueous speciation of the major elements and mineral solubilities. DOE (2009, Appendix SOTERM-2009, Section SOTERM-4.4) included the statement that the “effects of hydromagnesite and calcite precipitation were added” to this version of the database. EPA requested additional explanation of this statement, because data for hydromagnesite and calcite have been included in the FMT database since the CCA PAVT (Cotsworth 2009a, Comment 1-C-11). DOE corrected this statement to show that the μ^0/RT value for whewellite [$\text{CaC}_2\text{O}_4 \cdot \text{H}_2\text{O}(\text{s})$] was added to database version FMT_050405.CHEMDAT.

6.5 PABC09 DISSOLVED ACTINIDE SOURCE TERM

Actinide aqueous speciation and solubility calculations for the PABC09 were summarized by Brush et al. (2009). Aqueous speciation and solubility calculations were carried out for the +III, +IV and +V actinides. DOE has not developed an aqueous speciation and solubility model for actinides in the +VI oxidation state. In the WIPP repository environment, only uranium is predicted to be present in the +VI oxidation state. Because DOE has not developed a model for the +VI oxidation state, the uranium(VI) concentration of 10^{-3} M established by a review of the available literature (EPA 2006c) was used in the PABC09.

To facilitate technical review of the actinide solubility calculations for the PABC09, EPA requested that DOE provide copies of all FMT input and output files used to update the actinide solubility uncertainty analysis, evaluations of the effects of organic ligand inventory changes on actinide solubilities, or any other solubility calculations performed for the PABC09 (Cotsworth 2009a, Comment 1-C-23). EPA requested a copy of the revised database and documentation of all changes, if the FMT database was to be modified from the version used for the PABC04.

6.5.1 FMT Code and Database

FMT version 2.4 was used to perform the actinide speciation and solubility calculations for the PABC09 (Brush et al. 2009b), which is the same version used for the PABC04. The FMT database used for the PABC09 (FMT_050405.CHEMDAT) was also the same version used for the PABC04 (Brush et al. 2009b, Moody 2009a). DOE (2009, Appendix SOTERM-2009) reviewed aqueous speciation and solubility data that have become available since the development of FMT_050405.CHEMDAT, but did not revise the FMT database. Although some differences between the chemical models in the FMT database and the published literature were noted (Section 6.4), FMT calculations carried out with this database provided reasonable estimates of actinide solubilities in WIPP repository brines. Based on the available data relevant to actinide solubilities and speciation in brines, and comparison of FMT-calculated solubilities to measured solubilities, a review and update of this database should be carried out prior to the CRA-2014. This review and database update should include consideration of:

- Information summarized by Neck et al. (2009) for the +III actinides
- Results of WIPP-specific neodymium(III) experiments (Borkowski et al. 2009, Borkowski 2010) for the +III actinides

- Results for thorium(IV) hydroxide solubility and carbonate speciation provided by Neck et al. (2002), Rothe et al. (2002) and Altmaier et al. (2004, 2005, 2006)
- Results from continuing WIPP-specific experiments regarding the speciation and solubility of uranium(VI) (Lucchini et al. 2010) if available
- Other literature data that become available in time for inclusion in the FMT database review before the CRA-2014 PA

6.5.2 Chemical Conditions Assumptions

The aqueous speciation and solubility calculations were carried out using the GWB formulation of Salado brine, which was previously reviewed and accepted for use in PA (EPA 2006c). For simulations of aqueous speciation and solubility in Castile brine, calculations were performed using the ERDA-6 brine formulation, which has been used since the CCA PA. Equilibrium with the Salado minerals halite and anhydrite and the MgO backfill hydration and carbonation reaction products brucite, korshunovskite and hydromagnesite was assumed in FMT calculations used for the PABC09 dissolved actinide source term.

6.5.3 Organic Ligand Concentrations

DOE used the most recent inventory data (Table 6-5) and the most recent estimate of the minimum brine volume necessary for DBR (Clayton 2008) to calculate organic ligand concentrations for the PABC09 (Table 6-1, Brush and Xiong 2009). Because the most recent inventory data for organic ligands were incorporated in the actinide solubility calculations, the effects of the updated inventory on the dissolved actinide source term were included in the PABC09 calculations (Cotsworth 2009a, Comment 1-23-4). Because of changes in the predicted organic ligand inventory and minimum brine volume, organic ligand concentrations used in the WIPP PA dissolved actinide source term calculations have changed since the CCA PAVT and PABC04 (Table 6-1). Acetate and EDTA concentrations have increased by approximately an order of magnitude since the CCA PAVT. Citrate concentrations have decreased slightly since the CCA PAVT and oxalate concentrations have increased by more than an order of magnitude.

The aqueous speciation and solubility calculations were carried out both with and without the predicted organic ligand concentrations. The results obtained with organic ligands were used to determine dissolved actinide source term concentrations for the PABC09. Results of the calculations without organic ligands provide an indication of the effects of organic ligands on actinide solubilities in WIPP brines and are also useful for comparisons to literature solubility and speciation data obtained without organic ligands.

6.5.4 Results of Actinide Solubility Calculations

The results of the actinide solubility calculations for GWB and ERDA-6 brine for the PABC09 are summarized in Table 6-10. Comparison of the results with and without organic ligands shows that the only effect of organic ligands on the major elements in the brines was a slightly higher magnesium concentration. The presence of organic ligands had a significant effect on the total predicted +III actinide solubilities, increasing the predicted americium(III) solubility by a factor of 7 in GWB and by a factor of 17 in ERDA-6. Examination of the reported aqueous

speciation of the +III actinides indicated americium(III)-EDTA complexation caused the higher predicted +III actinide solubility in both GWB and ERDA-6 (Table 6-11).

The presence of organic ligands had essentially no effect on predicted +IV actinide solubilities in GWB or ERDA-6 brine (Table 6-10). The principal thorium aqueous species were predicted to be $\text{Th}(\text{OH})_4^0$ and $\text{Th}(\text{OH})_3\text{CO}_3^-$ both with and without organic ligands (Table 6-11). Organic ligands increased the predicted +V actinide solubility by approximately a factor of two (Table 6-11). Enhanced solubility of neptunium(V) in the presence of organic ligands was caused by the complexation of NpO_2^+ by acetate and oxalate (Table 6-11).

The calculated actinide solubilities used in the PABC04 and PABC09 are higher than the solubilities used in the CCA PAVT. The increased concentrations of the +III actinides were primarily caused by increased inventories of organic ligands. Smaller increases in the +IV actinide solubilities resulted from changes in the thorium(IV) data in the FMT database since the CCA PA. Thorium(IV) and neptunium(V) concentrations are predicted to be controlled by the solubilities of $\text{ThO}_2(\text{am})$ and $\text{KNpO}_2\text{CO}_3(\text{s})$, respectively, which has remained unchanged since the CCA PAVT. For the CCA PAVT, $\text{AmOHCO}_3(\text{cr})$ was predicted to be the solubility-controlling solid for the +III actinides. As a result of revisions to the FMT database between the CCA PAVT and the PABC04, $\text{Am}(\text{OH})_3(\text{s})$ was predicted to be the solubility-controlling solid phase for the PABC04 and PABC09.

Brush et al. (2009) performed FMT calculations in addition to the calculations summarized in Table 6-10. These calculations included changes in the assumed reaction that controlled carbonate concentrations:

- Brucite-magnesite (reaction 12), which would result in total carbonate concentrations lower than predicted for the brucite-hydromagnesite reaction
- Brucite-nesquehonite (reaction 15), which would result in total carbonate concentrations higher than predicted for the brucite-hydromagnesite reaction
- Brucite-calcite (reaction 19), which would result in total carbonate concentrations slightly higher in GWB and slightly lower in ERDA-6 than predicted for the brucite-hydromagnesite reaction

These calculations were performed to better understand the sensitivity of the actinide solubilities to total carbonate concentrations. The results of these calculations were not used in the PABC09 dissolved actinide solubility source term.

Experimental investigations of MgO hydration have shown that a magnesium-hydroxychloride solid phase forms in addition to brucite in GWB brine (Snider 2002, Deng et al. 2009). The phase korshunovskite [$\text{Mg}_2(\text{OH})_3\text{Cl}\cdot 4\text{H}_2\text{O}(\text{s})$] is included in the FMT database used for the PABC09 (FMT_050405.CHEMDAT), but experimental investigations with GWB brine and Martin Marietta MgO have detected the formation of phase 5 [$\text{Mg}_3(\text{OH})_5\text{Cl}\cdot 4\text{H}_2\text{O}(\text{s})$] rather than korshunovskite (Deng et al. 2009). Brush et al. (2009) used an FMT database that included both magnesium-hydroxychloride phases (FMT_090720.CHEMDAT, Xiong 2009) to calculate which phase would be stable under repository conditions and the potential effects of phase 5 formation

on actinide solubilities. The results indicated that phase 5 is the stable magnesium-hydroxychloride phase, as observed in the MgO hydration experiments in GWB. Predicted formation of this phase in place of korshunovskite had only minor effects on calculated actinide solubilities. These FMT calculations were not used in the PABC09 dissolved actinide source term. Use of the revised database FMT_090720.CHEMDAT in dissolved actinide source term calculations for a future PA would require a review of the supporting documentation (Xiong 2009, Xiong et al. 2009b, Xiong et al. 2010a), which has not yet been carried out.

Table 6-10. PABC09 Actinide Solubility Modeling Results With and Without Organic Ligands

Brine	GWB		ERDA-6	
	With Ligands ^a	Without Ligands	With Ligands ^a	Without Ligands
pH (standard units)	8.69	8.69	8.98	9.02
pcH	9.40	9.40	9.68	9.73
Ionic Strength	7.64	7.59	6.77	6.72
Carbon dioxide fugacity (atm)	3.135×10^{-6}	3.135×10^{-6}	3.135×10^{-6}	3.135×10^{-6}
Sodium (M)	4.308	4.331	5.284	5.325
Potassium (M)	0.5209	0.5208	0.09607	0.09615
Magnesium (M)	0.5842	0.5590	0.1362	0.1060
Calcium (M)	9.798×10^{-3}	0.01039	0.01123	0.01129
Chloride (M)	5.399	5.440	5.232	5.255
Sulfate (M)	0.2097	0.1922	0.1760	0.1679
Total Carbon (M)	3.499×10^{-4}	3.502×10^{-4}	4.476×10^{-4}	4.709×10^{-4}
Boron (M)	0.1762	0.1762	0.06240	0.06245
Bromine	0.02967	0.02966	0.01089	0.01090
Oxalate (M)	1.246×10^{-3}	0.00	2.438×10^{-4}	0.00
Acetate (M)	0.02164	0.00	0.01921	0.00
EDTA (M)	7.217×10^{-5}	0.00	6.408×10^{-5}	0.00
Citrate (M)	2.655×10^{-3}	0.00	2.357×10^{-3}	0.00
Americium(III) (M)	1.656×10^{-6}	2.252×10^{-7}	1.514×10^{-6}	8.667×10^{-8}
Thorium(IV) (M)	5.626×10^{-8}	5.642×10^{-8}	6.982×10^{-8}	7.196×10^{-8}
Neptunium(V) (M)	3.905×10^{-7}	2.209×10^{-7}	8.746×10^{-7}	5.379×10^{-7}
Uranium(VI) (M) ^b	0.001	0.001	0.001	0.001
Solid Phases	Anhydrite, halite, brucite, korshunovskite, ThO ₂ (am), KNpO ₂ CO ₃ (s), Am(OH) ₃ (s), hydromagnesite, whewellite	Anhydrite, halite, brucite, korshunovskite, ThO ₂ (am), KNpO ₂ CO ₃ (s), Am(OH) ₃ (s), hydromagnesite	Anhydrite, halite, brucite, ThO ₂ (am), KNpO ₂ CO ₃ (s), Am(OH) ₃ (s), hydromagnesite, whewellite, glauberite	Anhydrite, halite, brucite, ThO ₂ (am), KNpO ₂ CO ₃ (s), Am(OH) ₃ (s), hydromagnesite
Output File Name	FMT_PABC09_GWB_H MAG_ORGS_005.OUT	FMT_PABC09_GWB_H MAG_NOORGS_006.OU T	FMT_PABC09_E6_HMA G_ORGS_013.OUT	FMT_PABC09_E6_HMA G_NOORGS_014.OUT

a – Results used for CRA-2009 dissolved actinide source term

b – DOE did not develop a solubility model for the +VI actinides. Consequently, a fixed concentration was assumed for uranium(VI), which is the only +VI actinide predicted to be present in the WIPP repository in significant concentrations.

Table 6-11. Aqueous Actinide Speciation, PABC-2009 FMT Calculations With and Without Organic Ligands*

Aqueous species that constitute more than 2% of the total are indicated in bold.

Brine	GWB		ERDA-6	
	With Ligands	Without Ligands	With Ligands	Without Ligands
Total Americium(III) (M)	1.656×10^{-6}	2.252×10^{-7}	1.514×10^{-6}	8.667×10^{-8}
Am ³⁺	1.240×10^{-11}	1.350×10^{-11}	2.274×10^{-12}	1.792×10^{-12}
AmOH ²⁺	2.414×10^{-9}	2.379×10^{-9}	5.851×10^{-10}	4.851×10^{-10}
Am(OH) ₂ ⁺	2.114×10^{-7}	2.215×10^{-7}	9.025×10^{-8}	8.487×10^{-8}
Am(OH) ₃ ⁰	6.033×10^{-10}	6.188×10^{-10}	6.930×10^{-10}	7.121×10^{-10}
AmCO ₃ ⁺	3.734×10^{-10}	3.716×10^{-10}	1.864×10^{-10}	1.696×10^{-10}
Am(CO ₃) ₂ ⁻	1.331×10^{-10}	1.338×10^{-10}	3.023×10^{-10}	3.329×10^{-10}
Am(CO ₃) ₃ ³⁻	3.386×10^{-11}	3.322×10^{-11}	7.746×10^{-11}	9.415×10^{-11}
Am(CO ₃) ₄ ⁵⁻	1.049×10^{-11}	9.230×10^{-12}	7.823×10^{-13}	8.654×10^{-13}
AmAc ²⁺	2.116×10^{-9}	--	2.975×10^{-10}	--
AmCit ⁰	1.403×10^{-9}	--	5.792×10^{-10}	--
AmEDTA ⁻	1.437×10^{-6}	--	1.421×10^{-6}	--
AmOx ⁺	2.327×10^{-11}	--	3.246×10^{-12}	--
Total Thorium(IV) (M)	5.626×10^{-8}	5.642×10^{-8}	6.982×10^{-8}	7.196×10^{-8}
Th(OH) ₄ ⁰	4.515×10^{-8}	4.528×10^{-8}	4.762×10^{-8}	4.774×10^{-8}
Th(OH) ₃ CO ₃ ⁻	1.111×10^{-8}	1.113×10^{-8}	2.220×10^{-8}	2.421×10^{-8}
Th(CO ₃) ₅ ⁶⁻	4.019×10^{-16}	2.742×10^{-16}	1.925×10^{-17}	1.796×10^{-17}
ThAc ₂ ²⁺	2.631×10^{-20}	--	7.384×10^{-21}	--
ThCit ⁺	1.679×10^{-19}	--	9.825×10^{-20}	--
ThEDTA ⁰	6.169×10^{-17}	--	2.834×10^{-17}	--
ThOx ²⁺	1.161×10^{-22}	--	0.00	--
Total Neptunium(V) (M)	3.905×10^{-7}	2.209×10^{-7}	8.746×10^{-7}	5.379×10^{-7}
NpO ₂ ⁺	1.168×10^{-7}	1.156×10^{-7}	1.437×10^{-7}	1.190×10^{-7}
NpO ₂ OH ⁰	4.081×10^{-9}	4.160×10^{-9}	9.411×10^{-9}	8.687×10^{-9}
NpO ₂ (OH) ₂ ⁻	5.974×10^{-12}	6.114×10^{-12}	2.602×10^{-11}	2.622×10^{-11}
NpO ₂ CO ₃ ⁻	9.843×10^{-8}	1.000×10^{-7}	3.994×10^{-7}	3.988×10^{-7}
NpO ₂ (CO ₃) ₂ ³⁻	1.126×10^{-9}	1.141×10^{-9}	9.811×10^{-9}	1.129×10^{-8}
NpO ₂ (CO ₃) ₃ ⁵⁻	1.339×10^{-11}	1.293×10^{-11}	7.788×10^{-11}	9.517×10^{-11}
NpO ₂ Ac ⁰	1.324×10^{-7}	--	2.593×10^{-7}	--
NpO ₂ Cit ²⁻	4.302×10^{-10}	--	2.006×10^{-9}	--
NpO ₂ EDTA ³⁻	3.470×10^{-12}	--	3.805×10^{-12}	--
NpO ₂ Ox ⁻	3.719×10^{-8}	--	5.087×10^{-8}	--
Output File Name	FMT_PABC09_ GWB_HMAG_ ORGS_005.OUT	FMT_PABC09_ GWB_HMAG_ NOORGS_006. OUT	FMT_PABC09_ E6_HMAG_ ORGS_013.OUT	FMT_PABC09_ E6_HMAG_ NOORGS_014. OUT

* All americium-sulfate and americium-chloride aqueous complexes [AmCl²⁺, AmCl₂⁺, AmSO₄⁺, Am(SO₄)⁻] and all thorium-sulfate aqueous complexes [Th(SO₄)₂⁰, Th(SO₄)₃²⁻] were present at negligible concentrations. Only the highest-concentration actinide-organic ligand aqueous species are listed.

6.5.5 Actinide Solubility Uncertainties

Xiong et al. (2009a) described the development of uncertainty distributions for the +III and +IV actinide solubilities sampled for the PABC09 calculations. Xiong et al. (2009a) did not develop an uncertainty distribution for the +V actinides because an actinide solubility uncertainty distribution for the +V actinides is not sampled in PA. Neptunium is the only actinide expected to be present in WIPP repository brines in the +V oxidation state and neptunium does not have a significant effect on PA (Section 9.0).

The approach used to develop the +III and +IV actinide solubility uncertainty distributions was the same approach used for the PABC04 (Xiong et al. 2004, 2005). Solubility data for the +III and +IV actinides were selected from the literature based on a set of criteria. The current FMT code (Version 2.4) and database (FMT_050405.CHEMDAT) were used to calculate the predicted solubility at the conditions of each experiment. Difference values between the predicted (S_p) and measured (S_m) solubilities were calculated using the equation:

$$D = \log_{10}S_m - \log_{10}S_p \quad (25)$$

Using this equation, the difference value is negative if the FMT-calculated solubility is greater than the measured solubility, positive if the FMT-calculated solubility is less than the measured solubility and zero if the FMT calculated solubility and the measured solubility are equal. The difference values calculated for the +III and +IV oxidation states were accumulated into separate probability distributions. These two distributions were sampled during the PABC09 and used with the FMT-calculated solubilities in GWB and ERDA-6 under repository conditions (Table 6-10) to calculate the concentrations of the +III and +IV actinides used for each brine in each PA realization. Using this approach, if a negative difference value is sampled from the distribution, the actinide solubility used in the PA realization is less than the solubility value in Table 6-10 and if a positive difference value is sampled, the actinide solubility used in the PA realization is greater than the solubility value in Table 6-10.

The process used by Xiong et al. (2009a) to develop the uncertainty distributions included use of a set of criteria to select solubility data from the literature. The criteria specified for selecting the literature data included:

G1: Experimental studies published from January 1, 1990 through December 31, 2008

G2: Experimental studies from peer-reviewed journals and unpublished reports such as officially released reports from government laboratories

G3: Solubility studies

G4: Studies in which water was the solvent

G5: Studies obtained at temperatures and pressures close to WIPP conditions, i.e., temperatures from 20°C to 30°C and atmospheric pressure, and with phase-separation methods similar to those employed for the data used to parameterize the thorium(IV) and americium(III) models included in the FMT database

G6: Results from experimental investigations of thorium(IV), neodymium(III), americium(III) and curium(III) were included because these elements were used to parameterize the thorium(IV) and americium(III) solubility models; other actinide oxidation states such as plutonium(IV) were excluded because of potential systematic differences between their solubilities and possible experimental difficulties maintaining oxidation states

G7: Studies with characterized solubility-controlling solids that are included in the FMT database, and in which the solubility controlling solid did not completely dissolve

G8: Studies with aqueous solutions of known composition

G9: Studies with dissolved elements or species for which data were not included in the FMT database were excluded from development of the uncertainty distributions

G10: Results from studies for which the investigators provided a complete description of the experiments and the original solubility data

S1: Results from thorium(IV) solubility experiments carried out with solutions with ionic strength of 3 M or greater, based on the evaluation by Xiong et al. (2005)

During an EPA/DOE technical exchange meeting in February 2010, SNL staff stated that another requirement for the evaluation was that solubility data used to parameterize the FMT database were not included in the development of the uncertainty distributions.

6.5.5.1 +IV Actinide Solubility Uncertainty Distribution

Comparison of the maximum and minimum values for the PABC04 and PABC09 +IV actinide solubility uncertainty distributions shows that the updated distribution has a higher maximum and lower minimum value (Table 6-12). The mean and median for the PABC09 +IV actinide solubility distribution are negative, indicating that FMT calculations tended to predict higher concentrations than the experimentally measured solubility data. Such a tendency toward overprediction of +IV actinide solubilities would not have a conservative effect on PA, because sampling of these negative difference values in the uncertainty distribution reduces the actinide solubilities used in PA.

The +IV actinide uncertainty distribution for the PABC04 was developed using 45 thorium(IV) solubility measurements reported by Felmy et al. (1991) in 3 M NaCl (Xiong et al. 2005). For the PABC09 +IV actinide solubility uncertainty evaluation, Xiong et al. (2009a) included 3 M NaCl solubility data from Felmy et al. (1991) (45 measurements); 4 m NaCl, 6 m NaCl, 1.6 m MgCl₂, and 3 m MgCl₂ solubility data from Rai et al. (1997) (89 measurements); and 6 measurements from Altmaier et al. (2004) in 5 M NaCl, 2.5 M MgCl₂ and 4.5 M MgCl₂. Because data from the investigation by Felmy et al. (1991) were used to derive the ThO₂(am) solubility data in the FMT database (Giambalvo 2002c), inclusion of these data is inconsistent with the statement by SNL staff that data from studies used to parameterize the database were excluded. The mean and median difference values calculated with the 45 solubilities measured by Felmy et al. (1991) in 3 M NaCl and pH greater than 3.6 were slightly positive (Table 6-13), indicating that the FMT-calculated concentrations tended to be slightly less than the

experimentally measured concentrations. The range of difference values calculated for the Felmy et al. (1991) data is slightly less than the total range of difference values calculated for the PABC09 (Table 6-13).

Table 6-12. Comparison of the Thorium(IV) and Americium(III) Solubility Uncertainty Distribution Statistics for the PABC04 and the PABC09

(Xiong et al. 2009a)

Actinide Oxidation State	Thorium(IV)		Americium(III)	
	PABC04	PABC09 ^a	PABC04	PABC09 ^b
Performance Assessment				
Mean	0.108	-0.346	0.035	-0.142
Median	0.075	-0.520	-0.031	0.072
Standard Deviation	0.837	0.995	0.900	1.17
Maximum	2.40	3.30	2.85	2.70
Minimum	-1.80	-2.25	-3.00	-4.20

a – The PABC09 thorium(IV) statistics listed in Xiong et al. (2009a) differed slightly from the summary statistics in the spreadsheet (PABC09 Th(IV) Uncertainty Analysis 091124.xls) provided to EPA: mean = -0.349, median = -0.517, standard deviation = 0.992, maximum = 3.19 and minimum = -2.21.

b – The PABC09 americium(III) statistics listed in Xiong et al. (2009a) differed slightly from the summary statistics in the spreadsheet (PABC09 Am(III) Uncertainty Analysis 091124.xls) provided to EPA: mean = -0.145, median = 0.090, standard deviation = 1.17, maximum = 2.68 and minimum = -4.16.

Table 6-13. Comparison of Difference Values Calculated for the PABC09 and for Individual Investigations

Data	Mean	Median	Standard Deviation	Maximum	Minimum	Number
PABC09 ^a	-0.346	-0.520	0.995	3.30	-2.25	140
Felmy et al. (1991)	0.109	0.0577	0.844	2.39	-1.75	45
Rai et al. (1997)	-0.728	-0.793	0.745	1.37	-2.21	89
Altmaier et al. (2004)	1.82	1.40	1.09	3.19	0.778	6
Östhols et al. (1994)	0.791	0.808	0.145	1.03	0.517	19
Rai et al. (1995)	0.0299	0.0772	0.447	0.778	-1.22	26
Altmaier et al. (2005)	-0.674	-0.733	0.381	-0.228	-1.00	4
Altmaier et al. (2006)	1.18	1.05	0.231	1.59	0.959	12
High-ionic-strength carbonate ^b	0.292	0.226	0.716	1.59	-1.22	42
PABC09 uncertainty data without uncentrifuged data and with high-ionic-strength carbonate data ^c	-0.271	-0.290	0.893	2.39	-2.21	176

a – Felmy et al. (1991), Rai et al. (1997), Altmaier et al. (2004)

b – Rai et al. (1995), Altmaier et al. (2005), Altmaier et al. (2006)

c – Felmy et al. (1991), Rai et al. (1997), Rai et al. (1995), Altmaier et al. (2005), Altmaier et al. (2006)

Pitzer parameters describing the ternary interaction of Th⁴⁺, Na⁺ and Cl⁻ selected for inclusion in the FMT database were derived by Rai et al. (1997) (Giambalvo et al. 2002c). Consequently, use of these data in the uncertainty evaluation is inconsistent with the statement by SNL staff that data from studies used to parameterize the database were excluded. The difference values calculated for the experiments conducted by Rai et al. (1997) in concentrated NaCl and MgCl₂ solutions (Table 6-13) show that the solubilities calculated using FMT tended to be higher than the measured solubilities. Inclusion of these data in the uncertainty evaluation resulted in the lower mean and median values for the +IV actinide solubility uncertainty distribution for the

PABC09 than for the PABC04 (Table 6-12), reducing the mean and median +IV actinide concentrations used in the PABC09.

Xiong et al. (2009a) excluded most of the experimental solubility data from Altmaier et al. (2004) from the calculation of the +IV actinide solubility uncertainty distribution and included only six results from samples that were uncentrifuged and unfiltered. Because no phase separation was carried out with these samples, these samples included both dissolved thorium and thorium colloids. Inclusion of these uncentrifuged, unfiltered results in the uncertainty distribution evaluation is inconsistent with criterion G5, because filtration was used to remove colloids from solutions for the thorium solubility data used to parameterize the FMT database (Felmy et al. 1991). Inclusion of the unfiltered, uncentrifuged samples from Altmaier et al. (2004) increased the number of samples with positive difference values. In fact, the highest difference values for the +IV actinide solubility uncertainty evaluation were obtained from the 4.5 M MgCl₂ solubility experiments from Altmaier et al. (2004), which included thorium pseudocolloids (Section 6.4.4.1). Although including these data in the evaluation was inconsistent with the stated criteria, it increased the frequency of positive difference values in the uncertainty distribution and the mean dissolved +IV actinide concentration used in the PABC09.

The decision to exclude the Altmaier et al. (2004) ultracentrifuged results was made on the basis of criterion G5, because phase separation was carried out by ultracentrifuging the samples instead of filtration. The consequence of excluding these data may have been fewer negative difference values, so ultimately this exclusion may have increased the mean thorium(IV) concentration used in the PABC09. Xiong et al. (2009a) rationalized that the current FMT model is still adequate for PA, because the dissolved plus colloidal thorium(IV) predicted under these conditions are higher than they would be based on the ultracentrifuged results of Altmaier et al. (2004). However, intrinsic thorium colloids are not included in the colloidal actinide source term model (Section 7.0) and Xiong et al. (2009a) did not present calculations of the total mobilized thorium concentration to support this statement. Calculations considering the effects of intrinsic thorium colloids on total mobilized thorium are addressed in Section 8.0.

Experimental data in carbonate-bearing solutions with ionic strengths greater than 3 M reported by Altmaier et al. (2005), Altmaier et al. (2006) and Rai et al. (1995) were not included in the uncertainty evaluation. Xiong et al. (2009a) used criterion G9 to exclude these data, based on the thorium-carbonate speciation schemes used to interpret the data. This use of criterion G9 is questionable, because although different species are used in the FMT model to describe thorium complexation by carbonate and hydroxycarbonate species than in the excluded studies, this speciation should either be adequate for calculating thorium concentrations in the presence of carbonate or should be revised. In the absence of such an FMT database update, including these data in the uncertainty evaluation provides an indication of the ability of the current thorium-carbonate speciation scheme to predict measured solubilities. The exclusion of the Rai et al. (1995) data is particularly questionable because these data were considered by Felmy et al. (1997), and this study was in turn used to calculate the μ^0/RT values for Th(CO₃)₅⁶⁻ and Th(OH)₃CO₃⁻ in the FMT database (Giambalvo 2002c). EPA requested that DOE compare FMT-calculated thorium solubilities to the measured solubilities in experimental studies that included carbonate by Östhols et al. (1994), Rai et al. (1995), Felmy et al. (1997), Altmaier et al. (2005) and Altmaier et al. (2006) (Kelly 2010, Comment 4-C-35).

Xiong et al. (2010b) examined the results reported by Östholms et al. (1994), Rai et al. (1995), Felmy et al. (1997), Altmaier et al. (2005) and Altmaier et al. (2006) as requested by EPA. Xiong et al. (2010b) did not further consider the results included in Felmy et al. (1997), because these data were a summary of data obtained by Östholms et al. (1994) and Rai et al. (1995). Xiong et al. (2010b) eliminated the results reported by Östholms et al. (1994) from consideration based on criterion S1. However, examination of the difference values previously reported by DOE (Xiong et al. 2005) for the results by Östholms et al. (1994) showed that the FMT-predicted solubilities were consistently less than the measured values, resulting in positive difference values (Table 6-13). Consequently, it appears that FMT calculations overpredict thorium(IV) solubilities measured in the low-ionic-strength solutions reported by Felmy et al. (1991), but underpredict the solubilities measured by Östholms et al. (1994) under conditions where thorium-carbonate species are dominant. Inclusion of the Östholms et al. (1994) data in the uncertainty evaluation would be expected to increase the mean and median difference values in the uncertainty distribution sampled for PA. Because the maximum difference value of 1.03 calculated for the Östholms et al. (1994) results was less than the maximum difference value of 3.30 sampled for the PABC09, the range of difference values would not be affected by inclusion of the Östholms et al. (1994) results. However, because the actinide solubility model does not appear to be well parameterized for solutions that have less than 3 M ionic strength, these data should continue to be excluded from the determination of the +IV actinide solubility uncertainty distribution.

Xiong et al. (2010b) evaluated 26 thorium(IV) solubility results reported by Rai et al. (1995) in solutions with an ionic strengths greater than or equal to 3 M. The mean and median difference values were slightly positive (Table 6-13), indicating that the FMT-predicted solution concentrations tended to be less than the experimentally measured values. Inclusion of these results in the uncertainty distribution would increase the mean and median of the distribution. The range of difference values fell within the range of the distribution sampled for the PABC09, so inclusion of these data would not have altered the sampled range.

For the four results of the Altmaier et al. (2005) evaluation for which difference values were calculated, all FMT-predicted concentrations were higher than the measured concentrations (Table 6-13), resulting in negative difference values. On the other hand, FMT-predicted concentrations were consistently an order of magnitude less than the 12 measured concentrations reported by Altmaier et al. (2006). Combining the thorium solubility results carried out with carbonate in high-ionic-strength solutions showed that the mean and median difference values for these investigations were positive, indicating that FMT tended to underpredict thorium solubilities in the presence of carbonate (Table 6-13). However, these mean and median values are relatively small, and these investigations were conducted at higher carbonate concentrations than anticipated in the WIPP repository. Consequently, carbonate speciation is likely to have only small effects on thorium concentrations under WIPP repository conditions. To minimize these uncertainties associated with the effects of carbonate on thorium(IV) solubilities, DOE should include an evaluation of thorium-carbonate speciation in their review and update of the FMT database prior to the CRA-2014 PA.

Removing the uncentrifuged solubility data (Altmaier et al. 2004) and including the high-ionic-strength thorium solubility data obtained in carbonate solutions in the uncertainty distribution increased the mean and median to some extent, decreased the maximum difference value in the

distribution and had no effect on the minimum value (Table 6-13). The frequency distribution diagram for the recalculated +IV actinide solubility uncertainty (Figure 6-9) shows that the recalculated distribution is reasonably symmetric, having nearly equal numbers of negative and positive difference values. Although the increased mean difference value would increase mean calculated releases relative to the mean releases calculated for the PABC09, these changes would be relatively small, would be likely to occur only at low probabilities where DBR is important and would not significantly affect repository compliance.

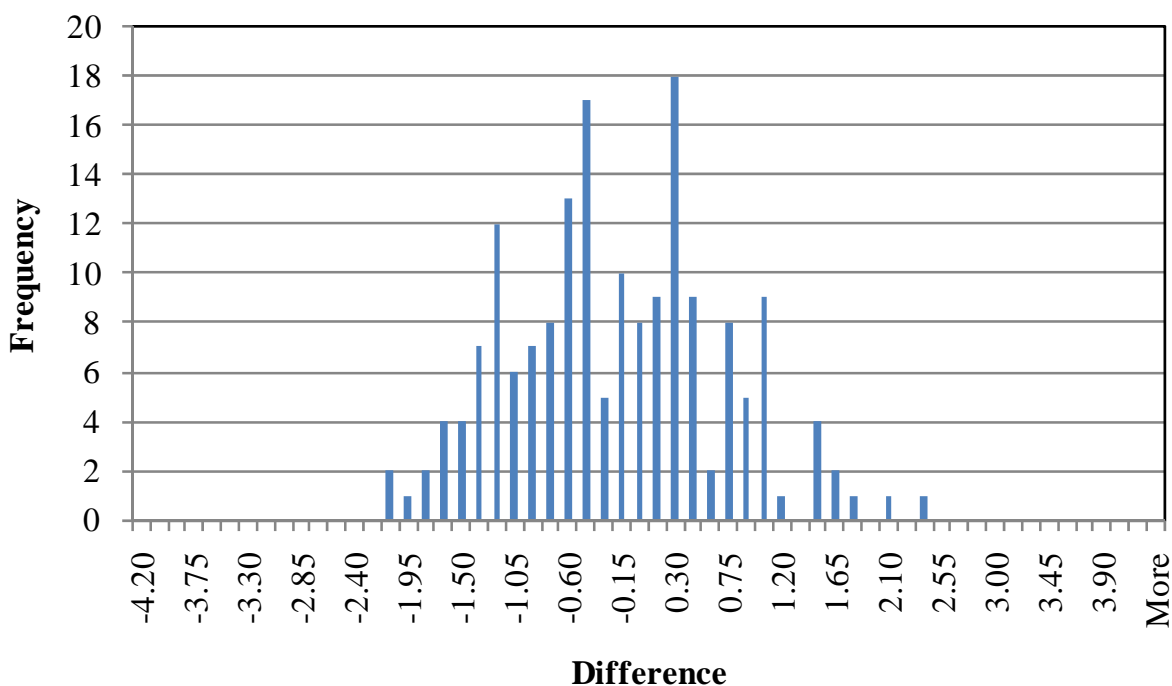


Figure 6-9. Recalculated Uncertainty Distribution for +IV Actinide Solubilities

6.5.5.2 +III Actinide Solubility Uncertainty Distribution

The median of the +III actinide solubility uncertainty distribution developed for the PABC09 was slightly positive, indicating that FMT calculations more frequently resulted in +III actinide concentrations less than the measured concentrations (Table 6-12). The mean of the +III actinide solubility uncertainty distribution used in the PABC09 was negative, indicating that the amount by which the FMT model predicted +III actinide solubilities higher than the measured values tended to be greater than the amount by which the FMT model underpredicted +III actinide solubilities. Compared to the uncertainty distribution used in the PABC04, the uncertainty distribution used for the PABC09 had a lower mean and a slightly higher median value. The maximum in the uncertainty distribution was slightly lower, but the minimum decreased by more than an order of magnitude.

Xiong et al. (2005) used a total of 243 neodymium(III) and americium(III) solubility measurements (Khalili et al. 1994, Rao et al. 1999, Runde and Kim 1995, Silva 1982) to develop

the PABC04 uncertainty distribution for the +III actinide solubility. Xiong et al. (2009a) used 346 solubility measurements for americium(III) and neodymium(III) from Borkowski et al. (2009), Khalili et al. (1994), Meinrath and Kim (1991), Meinrath and Takeishi (1993), Rao et al. (1996a, 1996b), Rao et al. (1999) and Runde and Kim (1995) to develop the solubility uncertainty distribution for the +III actinides. Xiong et al. (2009a) stated that no curium(III) solubility data were included in the evaluation because none of the studies met all of their stated criteria. The +III actinide solubility model in the FMT database was parameterized based on the solubility of curium(III) (e.g., Könnecke et al. 1997), but these data were excluded because it was assumed that using these data would bias the uncertainty distribution. This criterion might be a reasonable basis for excluding the data from Könnecke et al. (1997) and any other data used to parameterize the +III actinide model, but this exclusion is inconsistent with the approach used to develop the +IV actinide solubility uncertainty distribution, which included data from Felmy et al. (1991) and Rai et al. (1997) even though these data were used to develop the thorium(IV) solubility and Pitzer parameter data in the FMT database (Section 6.5.5.1).

Solubility results reported by Silva (1982) were included in the determination of the +III actinide solubility uncertainty distribution for the PABC04, but were excluded from the PABC09 evaluation. Xiong et al. (2009a) stated that these data were excluded because the publication date was prior to January 1, 1990. Although limiting the dates of the literature search carried out to identify new data was a practical approach, using an arbitrary date to remove previously identified solubility data from the uncertainty distribution evaluation is unjustified. No other reason for excluding the Silva (1982) data was presented, such as technical limitations in the study. Elimination of the Silva (1982) data is particularly questionable because the difference values were almost all positive, indicating that FMT calculations consistently underpredicted the solubilities (Table 6-14). The FMT calculations underpredicted the measured values by a substantial amount, in most cases by an order of magnitude and in a number of cases by 2.3 to 2.8 orders of magnitude. The effect of omitting these data from the evaluation was to decrease the number of positive difference values and decrease the mean +III actinide concentrations used in the PABC09 calculations.

Table 6-14. Americium(III) PABC09 Uncertainty Distribution and Range of Difference Values Calculated for Excluded Data

	Mean	Median	Standard Deviation	Maximum	Minimum	Number
PABC09 ^a	-0.142	0.072	1.17	2.70	-4.20	346
Clayton (2010) ^b	-0.250	-0.225	not reported	2.70	-3.75	536
Silva (1982)	1.33	1.28	0.681	2.79	-1.35	38
Khalili et al. (1994) pcH 6.4 and 8.4	-0.297	-0.218	0.505	0.442	-1.47	29
Khalili et al. (1994) pcH 8.4	-0.085	0.098	0.185	0.442	-0.218	24
Khalili et al. (1994) pcH 6.4	-1.32	-1.34	0.104	-1.22	-1.47	5
Rao et al. (1999) all data	-0.244	-0.144	0.716	1.34	-2.93	105
Rao et al. (1999) pcH > 7.4 (G Seep), pcH > 8.1 (ERDA-6)	-0.645	-0.677	0.662	0.657	-1.778	28
Rao et al. (1999) pcH < 7.4 (G Seep), pcH < 8.1 (ERDA-6)	-0.0984	-0.0291	0.682	1.34	-2.93	77

Table 6-14. Americium(III) PABC09 Uncertainty Distribution and Range of Difference Values Calculated for Excluded Data

	Mean	Median	Standard Deviation	Maximum	Minimum	Number
Rao et al. (1999) pcH < 7.4 (G Seep)	-0.717	-0.704	0.427	-0.174	-1.31	7
Borkowski et al. (2009) 5 M NaCl	-0.563	-0.695	0.957	1.64	-3.12	120
Borkowski et al. (2009) ERDA-6, pcH ≤ 8.1	-0.691	-0.540	0.818	0.360	-1.91	14
Borkowski et al. (2009) GWB, pcH ≤ 7.4	-1.51	-1.37	1.33	1.01	-3.67	28
Recalculated ^c	0.181	0.134	0.862	2.79	-2.93	354

- a – Borkowski et al. (2009, 5 M NaCl, GWB 6.6 ≤ pcH ≤ 7.4, ERDA-6 7.9 ≤ pcH ≤ 8.1), Khalili et al. (1994, pcH 6.4), Meinrath and Kim (1991), Meinrath and Takeishi (1993), Rao et al. (1996a), Rao et al. (1996b), Rao et al. (1999, excluded G Seep brine pcH > 7.4, ERDA-6 pcH > 8.1), Runde and Kim (1995)
- b– Borkowski et al. (2009), Khalili et al. (1994, pcH 6.4), Meinrath and Kim (1991), Meinrath and Takeishi (1993), Rao et al. (1996a), Rao et al. (1996b), Rao et al. (1999, excluded G Seep brine pcH > 7.4, ERDA-6 pcH > 8.1), Runde and Kim (1995)
- c– Silva (1982), Khalili et al. (1994, pcH 6.4 and 8.4), Meinrath and Kim (1991), Meinrath and Takeishi (1993), Rao et al. (1996a), Rao et al. (1996b), Rao et al. (1999), Runde and Kim (1995)

Xiong et al. (2009a) excluded solubility data from investigations in WIPP brines (Khalili et al. 1994, Rao et al. 1999, Borkowski et al. 2009) obtained at pcH greater than 7.4 in Salado Brines (GWB and G-Seep) and at pcH greater than 8.1 in ERDA-6. The rationale for excluding these data was that complexation of +III actinides by borate probably increased solubilities above these pcH values (Borkowski et al. 2009), and there are no americium(III)-borate aqueous species data in the FMT database. Thus, criterion G9 was used to exclude these data at higher pcH. Excluding these data may have literally complied with criterion G9, but exclusion of solubility data obtained in WIPP brines at moderately alkaline pcH values could be interpreted as implying that the current FMT database is not adequate for calculating +III actinide solubilities at the pcH values predicted in the WIPP repository, pcH 9.4 for GWB and pcH 9.7 for ERDA-6. Because the lack of americium-borate aqueous species in the FMT database would be expected to result in the underprediction of total americium concentrations in WIPP brine at higher pcH, including these data would be expected to result in a larger number of positive difference values in the PABC09 uncertainty distribution.

Clayton (2010) evaluated the effects of including the higher-pcH data obtained in GWB and ERDA-6 from Borkowski (2010) in the calculation of the uncertainty distribution. For the evaluation, Clayton began with the difference values used to calculate the +III actinide solubility uncertainty distribution [file PABC09 Am(III) Uncertainty Analysis 091124.xls] and replaced the difference values associated with the Borkowski et al. (2009) results in that file with difference values calculated from the experimentally measured concentrations and FMT-calculated concentrations from Xiong et al. (2010b). Clayton (2010) then regenerated the uncertainty distribution for the +III actinides using these data (Table 6-14, file UPDATEDSOLUBILITYUNCERTAINTIES.xls). Comparison of the difference values for the Borkowski et al. (2009) data in these two files indicates that the two evaluations used different data sets. For example, the minimum difference value in file PABC09 Am(III) Uncertainty

Analysis 091124.xls for the Borkowski et al. (2009) data is -4.16, whereas in file UPDATEDSOLUBILITYUNCERTAINTIES.xls the minimum difference value for the Borkowski et al. (2009) data is -3.67. Clayton (2010) found that replacing the Borkowski et al. (2009) solubility data in the distribution decreased the mean and median and increased the minimum difference value.

Inclusion of any data from the Borkowski et al. (2009) investigation during development of the +III actinide solubility uncertainty distribution is inconsistent with criterion G7, because only indirect means were used to characterize the solid phases. In many experiments, the stable solid phases predicted by FMT calculations were not $\text{Nd}(\text{OH})_3(\text{s})$ (Table 6-9) as concluded by Borkowski et al. (2009) through indirect means. Because of uncertainty associated with the solid phase or phases that formed in the Borkowski et al. (2009) experiments (Section 6.4.4.5), these results should not have been included in the PABC09 uncertainty evaluation. The results from the Borkowski et al. (2009) neodymium(III) experiments that were included in the +III actinide solubility uncertainty distribution evaluation resulted in difference values that were predominantly negative (Table 6-14), and would have decreased the mean concentration of the +III actinides used in the PABC09.

Solubility data from Khalili et al. (1994) at pcH 6.4 were included in the development of the +III actinide uncertainty distribution, but pcH 8.4 data were excluded (Xiong et al. 2009a). The difference values calculated for the excluded pcH 8.4 data varied over a small range, and had an average near zero (Table 6-14). Because the difference values for the pcH 8.4 data were all relatively close to zero, the FMT-calculated solubilities were in reasonably good agreement with the measured solubilities at moderately alkaline pcH, despite the presence of borate in the solutions. Difference values calculated using the pcH 6.4 data, on the other hand, were significantly negative (Table 6-14), because the FMT-calculated concentrations at pcH 6.4 exceeded the measured solubilities by more than an order of magnitude. These relatively high predicted americium(III) concentrations at pcH 6.4 compared to measured concentrations in Salado brine were also observed for the Borkowski et al. (2009) neodymium(III) solubility results at pcH values from 6.60 to 7.97 in GWB brine (Section 6.4.4.5, Figure 6-6). Inclusion of the lower-pcH data and exclusion of the higher-pcH data from Khalili et al. (1994) consequently shifted the uncertainty distribution toward lower difference values and tended to reduce the +III actinide solubilities used in the PABC09.

Rao et al. (1999) carried out solubility experiments in G-Seep brine (similar to GWB brine) at 1 atm P_{CO_2} and atmospheric P_{CO_2} conditions. All experiments conducted at atmospheric P_{CO_2} except for one were excluded from the uncertainty distribution evaluation because of pcH greater than 7.4 (pcH 7.51 to 7.82). The excluded data had a relatively small range of difference values with a slightly positive mean value (Table 6-14). This relatively small range in difference values indicates that the FMT-predicted solubilities were in relatively good agreement with the experimentally measured concentrations in this pcH range, even though the FMT database did not include americium(III)-borate species. The difference values included in the PABC09 uncertainty distribution from G-Seep experiments at pcH less than 7.4 (pcH 5.63 to 7.67) had difference values that were uniformly negative (Table 6-14) and that generally decreased with decreasing pcH. These negative difference values indicated that at lower pcH in G-Seep brine, the FMT calculations consistently overpredicted the measured solubilities, as was observed for

the results of Borkowski et al. (2009) and Khalili et al. (1994). Inclusion of the lower-pcH data and exclusion of the higher-pcH data from the Rao et al. (1999) G-Seep brine experiments shifted the uncertainty distribution toward lower difference values and decreased the dissolved +III actinide concentrations used in the PABC09.

Rao et al. (1999) carried out solubility experiments in ERDA-6 at 1 atm P_{CO_2} and at atmospheric P_{CO_2} conditions. The experimental results excluded because pcH was greater than 8.1 had difference values that were negative. Consequently, in higher-pcH ERDA-6 brine (pcH from 8.15 to 9.98), the FMT-calculated solubilities were consistently higher than the measured solubilities, even though the FMT database did not include americium(III)-borate aqueous species. The lower-pcH ERDA-6 experiments (pcH 6.39 to 8.0) included in the uncertainty distribution had difference values that ranged from -2.93 to 0.970, with an average of -0.296. For ERDA-6 brine, the exclusion of the Rao et al. (1999) experiments at higher pcH reduced the number of negative difference values in the uncertainty distribution.

The effect of excluding the higher-pcH data in GWB (greater than 7.4) and ERDA-6 brine (greater than 8.1) is likely to have reduced the number of difference values close to zero (based on the Khalili et al. 1994 data and Rao et al. 1999 G-Seep data) and possibly the number of positive difference values (based on the Borkowski et al. 2009 data). However, the ERDA-6 higher-pcH data of Rao et al. (1999) had negative difference values, so excluding these data slightly lowered the number of negative difference values in the distribution. The majority of the difference values at lower pcH calculated from experiments carried out in WIPP brines were significantly negative (Table 6-14), indicating that the FMT calculations consistently overpredicted the measured solubilities. In some cases (e.g., GWB brine experiments reported by Borkowski et al. 2009) these differences were quite large, up to nearly four orders of magnitude.

The +III actinide solubility uncertainty distribution was recalculated to determine the effects of excluding the Borkowski et al. (2009) data and including data from Silva (1982), Khalili et al. (1994) at pcH 6.4 and 8.4, Meinrath and Kim (1991), Meinrath and Takeishi (1993), Runde and Kim (1995), Rao et al. (1996a, 1996b) and all data from Rao et al. (1999). The difference values used in the calculation were obtained from the file provided by Moody (2010d, UPDATEDSOLUBLITYUNCERTAINTIES.xls). The recalculated +III actinide solubility distribution has a slightly higher mean, median and maximum than the uncertainty distribution used in the PABC09, and a significantly higher minimum (Table 6-14). A positive mean difference value is consistent with the observation of higher concentrations of neodymium(III) in WIPP brines at WIPP-relevant pcH values than predicted by FMT. The frequency distribution diagram for the recalculated +III actinide solubility uncertainty (Figure 6-10) shows that the recalculated distribution is reasonably symmetric, having nearly equal numbers of negative and positive difference values.

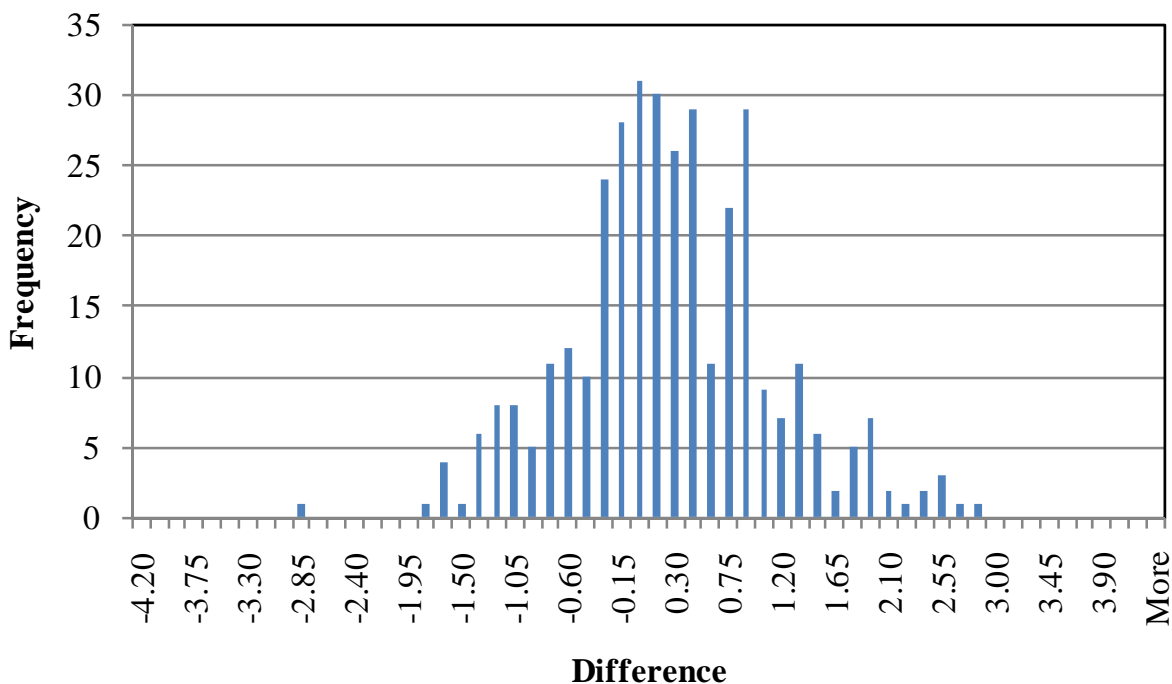


Figure 6-10. Recalculated Uncertainty Distribution for +III Actinide Solubilities

The negative difference values calculated for most WIPP brine experiments at lower pcH (Table 6-14) indicates that the FMT database is not well-parameterized for the +III actinides under these conditions. However, the pcH in WIPP brines will be higher than these pcH values because of the MgO backfill. Including negative difference values calculated from low-pcH data that are not relevant to WIPP conditions in the +III actinide solubility uncertainty distribution appears to have inappropriately decreased the actinide solubilities used in some PABC09 realizations. However, because the mean of the recalculated uncertainty distribution is only slightly higher than the mean of the distribution sampled for the PABC09, the effects on mean repository releases are likely to have been small.

6.5.5.3 Adequacy of the PABC09 Uncertainty Distribution Evaluation

The PABC09 actinide solubility uncertainty distribution is improved in some respects over the PABC04 distribution. An extensive literature search was carried out to identify actinide solubility data to include in the evaluation and the data selection process included clearly stated data-selection criteria. However, some issues were identified in the application of these criteria, and some of these issues had non-conservative effects or effects that could not be determined using the available information. These issues included exclusion of the Silva (1982) americium(III) solubility data because of an arbitrarily selected date range for data inclusion, exclusion of thorium(IV) solubility data because of ultracentrifugation to separate the dissolved species from the aqueous species, exclusion of thorium(IV) solubility data from several studies because of different thorium-carbonate species assumed by the studies' authors, inclusion of a large amount of data from Borkowski et al. (2009) despite uncertainty regarding the solubility-controlling phases and exclusion of solubility data measured in WIPP brines at WIPP-relevant

pH conditions because of concerns about borate complexation of the +III actinides at higher pH.

The +IV and +III actinide solubility uncertainty distributions were recalculated to address these issues. Removing the uncentrifuged solubility data (Altmaier et al. 2004) and including high-ionic-strength thorium-carbonate data in the +IV actinide solubility uncertainty distribution increased the mean and median difference values. Recalculation of the +III actinide solubility uncertainty distribution only slightly increased the mean and median difference values. Although the increased mean difference values for the +III and +IV actinide solubility uncertainty distributions would increase mean releases relative to the mean releases calculated for the PABC09, these changes would be relatively small, would likely occur only at low probabilities where DBR is important and would not significantly affect repository compliance. Consequently, the actinide solubility uncertainty distributions sampled for the PABC09 were adequate.

7.0 COLLOIDAL ACTINIDE SOURCE TERM

The Colloidal Actinide Source Term conceptual model was peer reviewed prior to the CCA PA and PAVT and found to be adequate, if somewhat conservative (Wilson et al. 1996a). This conceptual model and its implementation were the same in the CCA PAVT, PABC04, CRA-2009 PA and PABC09.

It has been assumed that four types of colloids can form in the WIPP repository and influence the Actinide Source Term:

- Microbial colloids
- Humic colloids
- Intrinsic colloids
- Mineral fragment colloids

These four types of colloids are described by DOE (1996, Appendix SOTERM, Section 6.1.2). Microbial colloids may act as substrates for actinide sorption, or they may intracellularly bioaccumulate actinides. Humic substances are relatively small (less than 100,000 atomic mass units) and are often powerful substrates for uptake of metal cations. Intrinsic colloids are hydrophilic actinide macromolecules that may in some cases mature into hydrophobic mineral fragment colloids. Mineral fragment colloids are hydrophobic, hard-sphere amorphous, or crystalline solids. Mineral fragment colloids may act as substrates for actinide sorption, or may consist of precipitated or coprecipitated actinide solids.

The concentrations of actinide intrinsic colloids and mineral fragment colloids used in PA are constant values (Table 7-1). The concentrations of intrinsic plutonium(IV) colloids were determined based on the results of experimental investigations carried out with plutonium(IV) (DOE 1996 Appendix SOTERM Section 6.3.2.3, Papenguth and Behl 1996). A literature review did not provide evidence of the formation of other actinide intrinsic colloids, so the concentrations of thorium, uranium, neptunium, plutonium(III) and americium intrinsic colloids were set equal to zero (DOE 1996, Appendix SOTERM, Section 6.3.2.4).

More recent investigations, however, have identified the formation of intrinsic thorium colloids in dilute solution and in brines. Neck et al. (2002) found that intrinsic thorium colloids were present at low ionic strength based on ultracentrifugation of sampled solutions. Neck et al. (2002) determined that previous investigations of amorphous thorium hydrous oxide solubility had established higher log K_{sp0} values because of incomplete separation of these colloids from solution. Based on the results reported by Neck et al. (2002), it is likely that intrinsic thorium colloids affected the results from Felmy et al. (1991) that were used to determine the solubility data for ThO₂(am) in the current FMT database (FMT_050405.CHEMDAT). Bitea et al. (2003) investigated the formation and stability of thorium(IV) colloids in 0.5 M NaCl and found that these colloids remained stable over the course of 400 days without exhibiting agglomeration or precipitation. Results reported by Altmaier et al. (2004) indicated that intrinsic thorium colloids can form and remain stable at high ionic strength, with total mobilized thorium concentrations (dissolved plus intrinsic colloids) of approximately $10^{-6.3}$ M. EPA observed that this mobilized thorium concentration exceeds the dissolved thorium concentrations calculated for the PABC09 by nearly an order of magnitude and that formation of intrinsic thorium colloids was not

accounted for in PA (Kelly 2010, Comment 4-C-36). EPA requested that DOE address whether significant thorium intrinsic colloids could form in the WIPP repository and stated that, unless the formation of these colloids could be ruled out by the available data, DOE should also address the possible effects of the formation of intrinsic thorium colloids on repository performance.

Table 7-1. Actinide Concentrations Associated with Mineral Fragment and Intrinsic Colloids

	Mineral Fragment Colloids (M)	Intrinsic Colloids (M)
Thorium(IV)	2.6×10^{-8}	0.0
Uranium(IV)	2.6×10^{-8}	0.0
Uranium(VI)	2.6×10^{-8}	0.0
Neptunium(IV)	2.6×10^{-8}	0.0
Neptunium(V)	2.6×10^{-8}	0.0
Plutonium(III)	2.6×10^{-8}	0.0
Plutonium(IV)	2.6×10^{-8}	1.0×10^{-9}
Americium(III)	2.6×10^{-8}	0.0

Source: DOE 1996, Appendix SOTERM, Table SOTERM-14

DOE (Moody 2010d) stated that thorium colloids observed by Altmaier et al. (2004) are not expected to form in the WIPP repository environment. Additional information on this topic was provided by Xiong et al. (2010b). Xiong et al. (2010b) argued that the Altmaier et al. (2004) results did not demonstrate that thorium(IV) colloids would form in WIPP brines, because the Altmaier et al. (2004) investigation was carried out using pure NaCl or MgCl₂ solutions and not more complex WIPP brines. Xiong et al. (2010b) also stated that “the WIPP colloidal actinide source term program, carried out to support the WIPP CCA, did not identify intrinsic or mineral-fragment colloids,” citing the CCA as support for this statement (DOE 1996, Appendix SOTERM, Section 6.0). This statement is inaccurate, because mineral fragment colloids for thorium, uranium, neptunium, plutonium and americium are included in the colloidal actinide source term model based on experimental results obtained with hematite [Fe₂O₃(cr)], goethite [FeO(OH)(cr)] and bentonite (Papenguth 1996). Intrinsic plutonium(IV) colloids were measured in NaCl brines at pH values of approximately 4 and 7, but at pH values of approximately 8 and higher, intrinsic plutonium(IV) colloid concentrations in the experiments were at or below the analytical detection limit of 10⁻⁹ M (DOE 1996, Appendix SOTERM Section 6.3.2.3). Because the expected pH of the repository was approximately 9.3, the concentration of intrinsic plutonium(IV) colloids used in PA was set equal to the analytical detection limit (Table 7-1).

Appendix SOTERM Section 6.3.2.2 (DOE 1996) addressed the potential formation of intrinsic colloids of actinides other than plutonium. In this discussion, it was acknowledged that formation of thorium polymers has been identified in the scientific literature, but these polymers were of relatively low molecular weight and “would behave no differently than dissolved monomeric species.” No WIPP-specific experimental data were discussed that would identify or exclude the possible formation of thorium colloids in WIPP brines. More recently, however, Neck et al. (2002), Bitea et al. (2003) and Altmaier et al. (2004) have identified the formation of intrinsic thorium(IV) colloids in dilute solutions and in brines. Bitea et al. (2003) used ultrafiltration (1.2 nm) to determine the concentrations of thorium(IV) colloids in their solutions, and also used LIBD results to approximately determine colloid size. LIBD measurements indicated that colloid particle size was about 2 to 10 nm in three of the experiments, with a

higher particle size of approximately 250 nm in a fourth experiment. Because colloids are defined as particles that range in size from 1 nm to 1,000 nm (DOE 1996, Appendix SOTERM, Section 6.3.2.2), the thorium(IV) colloids identified by Bitea et al. (2003) appear to fall into a size range consistent with the transport properties of colloids rather than dissolved species.

As noted by Xiong et al. (2010b), the results reported by Neck et al. (2002), Bitea et al. (2003) and Altmaier et al. (2004) were not carried out in WIPP brines. However, this argument is unpersuasive, given that the experiments used to establish the concentration of plutonium(IV) intrinsic colloids for WIPP PA were carried out in 0.001 to 5.0 M NaCl rather than in WIPP brines (DOE 1996, Appendix SOTERM, Figure SOTERM-8). Because Altmaier et al. (2004) identified intrinsic thorium colloids in concentrated NaCl and MgCl₂ brines, which are the major constituents in WIPP brines (Table 2-1), there appears to be credible evidence that intrinsic thorium colloids might form and remain stable in WIPP brines. DOE did not assess the potential effects of intrinsic thorium colloid formation on PA because they concluded these colloids would not form in the WIPP repository environment (Moody 2010d, Xiong et al. 2010b). Because the possible formation of intrinsic thorium colloids cannot be ruled out on the basis of the available information, the potential effects of intrinsic thorium colloid formation are assessed in Section 8.0.

In a public comment, Citizens Against Radioactive Dumping (CARD) asked whether DOE included reports of plutonium nano-colloids (Soderholm et al. 2008) in the WIPP radionuclide release scenarios. DOE (2010) noted that Soderholm et al. (2008) provided information about the structure of plutonium intrinsic colloids, but did not address the stability of these colloids, their relevance to groundwater/brine systems and transport properties. DOE (2010) observed that plutonium nano-colloids of the size reported by Soderholm et al. (2010) are included in WIPP PA as part of the dissolved concentration fraction. Colloidal plutonium(IV) is also included in WIPP PA as a fixed concentration equal to the analytical detection limit in experiments with WIPP brines (Papenguth and Behl 1996). Because the combined dissolved and colloidal plutonium concentrations address the potential effects of plutonium nano-colloids on total mobilized plutonium, DOE has adequately accounted for the potential formation of plutonium nano-colloids in the PABC09.

The concentrations of actinides associated with mineral fragment colloids, also called pseudocolloids, were determined from experiments that measured their kinetic stability in WIPP-relevant brines and estimates of adsorption site densities. These experiments were carried out using a variety of minerals or materials (Papenguth 1996). These actinide concentrations from mineral fragment colloids have been used in all WIPP PAs (Table 7-1). At the time the experiments were designed, MgO backfill was not included in the repository design, so formation of mineral fragment colloids from MgO and its reaction products was not investigated. A triangular distribution spanning one order of magnitude about the geometric mean was developed for mineral fragment colloid concentrations, but this distribution was not sampled for PA. Instead, the maximum parameter values were used (DOE 1996, Appendix SOTERM, Section 6.3.1.2).

Recent experimental data have indicated that mineral fragment colloids formed in MgCl₂ solutions with an ionic strength from 2.5 to 4.5 M may mobilize thorium in brines (Altmaier et al. 2004). EPA requested that DOE address whether such mineral fragment colloids may form

in WIPP and whether these colloids could significantly affect repository performance (Kelly 2010, Comment 4-C-36). DOE stated in their response that the thorium pseudocolloids observed by Altmaier et al. (2004) are not expected to form in the WIPP repository environment (Moody 2010d, Xiong et al. 2010b). DOE based this assessment on (1) the instability of korshunovskite relative to phase 5 in WIPP brine, (2) low calculated magnesium concentrations in WIPP brines and (3) the high solids-to-solution ratio in the repository.

Xiong et al. (2010b) reiterated the argument by Altmaier et al. (2004) that higher MgO solid-to-solution ratios in the repository would result in sorption of thorium on the immobile phases in the repository. However, although sorption of radionuclides onto immobile phases in the repository may occur, this process is not included in the current conceptual models used for PA.

Calculations performed using the current version of the FMT database (FMT_050405.CHEMDAT) indicate that korshunovskite will form in GWB brine. However, experimental investigations of the hydration of the Martin Marietta MgO currently used in the WIPP backfill indicate that phase 5 forms instead of korshunovskite (Deng et al. 2009). Phase 5 formation was also observed in Premier MgO hydration experiments (Snider 2002, Snider 2003a). Xiong et al. (2010b) report that FMT calculations carried out with a database revised to include solubility data for phase 5 (FMT_090720.CHEMDAT) indicated that phase 5 was stable relative to phase 3. Although this database and these calculations have not yet been reviewed by EPA, the results of the calculations are consistent with the experimental data obtained with GWB brine. Xiong et al. (2010a) experimentally investigated the solubility of phase 5 and established that phase 5 is stable relative to korshunovskite under the pH and magnesium concentrations expected in WIPP brines. Because there is no experimental evidence that korshunovskite will form in the repository, colloids associated with this solid phase reported by Altmaier et al. (2004) would not be expected to affect actinide transport.

Although the colloids reported by Altmaier et al. (2004) are unlikely to form in the repository, examination of the data used to develop the colloidal actinide source term model has shown that the potential formation of mineral fragment colloids by MgO and its hydration and carbonation products under WIPP-relevant conditions has not been evaluated. Because colloids capable of transporting actinides have been demonstrated to form under some conditions, this omission introduces some uncertainty into the colloidal actinide source term model.

Actinide concentrations associated with humic substances are based on proportionality constants (Table 7-2). Proportionality constants determined for thorium(IV) were extended to uranium(IV), neptunium(IV), and plutonium(IV), and proportionality constants developed for americium(III) were extended to plutonium(III). Proportionality constants for neptunium(V) and uranium(VI) were based on data for these oxidation states (DOE 1996, Appendix SOTERM, Table SOTERM-12). The proportionality constants were calculated from experimentally determined humic substance solubilities in brines at various concentrations of Ca^{2+} and Mg^{2+} ; data on site-binding capacities measured for the WIPP research program and literature values; actinide complexation factors for americium(III), thorium(IV), neptunium(V) and uranium(VI) binding on humic substances; and stability constants for Ca^{2+} and Mg^{2+} binding to humic substances. The maximum value used in PA (CAPHUM, Table 7-2) represents the theoretical maximum concentration of actinides that can be bound by a humic substance, assuming a solubility limit of 2 mg/liter, the highest site-binding capacity for fulvic acids of 5.56 meq OH/g

and the limiting case of a monovalent actinide species (DOE 1996, Appendix SOTERM, Section 6.3.3.2).

Actinide concentrations associated with microbial colloids are also based on proportionality constants (Table 7-2). For microbes, the proportionality constant is related to the actinide element, rather than the oxidation state. Experimental data on the mobile concentrations of microbes and bioaccumulation and toxicity experiments were used to develop the proportionality constants. Upper limits for the concentrations of actinides for microbial colloids were established based on the concentration at which no growth was observed (Table 7-2). Because of the high radiation levels of americium, no maximum concentration value was determined for americium. Because of limited data, distributions were not developed for the proportionality constants or the maximum concentrations for microbial colloids, and single values were used in PA (DOE 1996, Appendix SOTERM, Section 6.3.4.2).

Table 7-2. Proportionality Constants and Maximum Concentrations for Humic and Microbial Colloids

	Proportionality Constant Humic Colloids in Salado Brine ^a	Proportionality Constant Humic Colloids in Castile Brine ^b	Maximum Sorbed on Humics (M)	Proportionality Constant Microbes ^a	Maximum Sorbed by Microbes ^c
Parameter	PHUMSIM	PHUMCIM	CAPHUM	PROPMIC	CAPMIC
Thorium(IV)	6.3	6.3	1.1×10^{-5}	3.1	0.0019
Uranium(IV)	6.3	6.3	1.1×10^{-5}	0.0021	0.0021
Uranium(VI)	0.12	0.51	1.1×10^{-5}	0.0021	0.0023
Neptunium(IV)	6.3	6.3	1.1×10^{-5}	12.0	0.0027
Neptunium(V)	9.1×10^{-4}	7.4×10^{-3}	1.1×10^{-5}	12.0	0.0027
Plutonium(III)	0.19 ^d	1.37 ^d	1.1×10^{-5}	0.3	6.8×10^{-5}
Plutonium(IV)	6.3	6.3	1.1×10^{-5}	0.3	6.8×10^{-5}
Americium(III)	0.19 ^d	1.1 ^d	1.1×10^{-5}	3.6	NA ^e

a – Units of moles colloidal actinide per mole dissolved actinide

b – Units of moles colloidal actinide per mole dissolved actinide

c – Units of moles total mobile actinide per liter

d – For Salado brine, the maximum value in the distribution is used for PA; for Castile brine, a cumulative distribution from 0.065 to 1.60 with a mean value of 1.1 and a median of 1.37 is sampled for PA

e – Not applicable

Source: DOE 1996, Appendix SOTERM, Table SOTERM-14

The parameter values for the colloidal actinides in Tables 7-1 and 7-2 have been used in all WIPP PA calculations since the CCA PA. Using the actinide solubilities calculated for the CCA PA, the largest contribution to the mobile actinide source term was actinides associated with humic substances and microbes (DOE 1996, Appendix SOTERM, Section 6.4).

DOE (2009, Appendix SOTERM-2009, Section SOTERM-3.8) provided a discussion of additional information relevant to colloids in WIPP brines that has become available since the CCA. Wall and Mathews (2005) evaluated the solubility of humic acids in GWB and ERDA-6 brines and the effects of MgO on the quantities of humic acids in WIPP brines. Wall and Mathews (2005) found that GWB and ERDA-6 brine promoted coagulation of the humic acid, although complete humic acid removal was not observed. Humic acids were completely

removed from the brines in the presence of either reagent-grade MgO or Premier MgO, which was the backfill material being emplaced in WIPP at the time of the experiments (Section 4.3).

EPA requested clarification of the parameter descriptions in Table SOTERM-21 (DOE 2009, Appendix SOTERM-2009), indicating that PHUMCIM and PHUMSIM, the proportionality constants for humic colloids in Castile and Salado brine, respectively, were calculated assuming equilibrium with brucite and magnesite, and that complexes with organic ligands were not included in the solubility calculations (Cotsworth 2009a, Comment 1-C-15). This clarification was necessary because the actinide solubility calculations carried out for the PABC04 and used for the CRA-2009 PA included the assumption of equilibrium with brucite and hydromagnesite, and included organic ligand complexation of actinides. In their response, DOE acknowledged that the PHUMCIM and PHUMSIM descriptions should have stated that actinide solubility calculations included organic ligands, and that the solubilities were calculated assuming equilibrium with the magnesium-bearing minerals brucite and hydromagnesite (Moody 2009a). DOE will include these changes as errata attached to Appendix SOTERM-2009 (DOE 2009).

No changes have been made to the Colloidal Actinide Source Term conceptual model or its implementation since the CCA PAVT. Some data developed since the CCA PAVT, most notably the evidence from Wall and Mathews (2005), indicate that the current model is likely to conservatively overestimate actinides associated with humic colloids in the source term. However, evidence that thorium intrinsic and mineral-fragment colloids may form in brines and increase thorium mobilization has also been presented. The formation of intrinsic thorium colloids cannot be ruled out based on the available evidence. Consequently, the potential effects of intrinsic thorium colloids on total mobilized thorium are considered in the following section. The available data do not conclusively demonstrate that mineral-fragment colloids will form in the repository from MgO hydration or carbonation products. However, the lack of data regarding the potential formation of mineral fragment colloids from MgO and its hydration and carbonation products in the repository should be evaluated.

8.0 TOTAL MOBILIZED ACTINIDE CALCULATIONS FOR PA

The information required to calculate the dissolved and colloidal actinide concentrations for each PA realization includes:

- Whether the scenario uses the Salado or Castile end-member brine composition (DOE 2009, Appendix SOTERM-2009, Table SOTERM-24)
- The dissolved concentrations of +III, +IV, +V, and +VI actinides in the brine (Table 6-10; Section 6.5)
- Sampled uncertainty values for the +III and +IV actinide solubilities (Section 6.5.5)¹⁸
- Whether actinides with multiple possible oxidation states are present in their relatively reduced [uranium(IV), neptunium(IV) and plutonium(III)] or relatively oxidized [uranium(VI), neptunium(V) and plutonium(IV)] oxidation states
- The constant concentrations of intrinsic and mineral-fragment colloids (Table 7-1)
- The proportionality constants and maximum concentrations of humic and microbial colloid actinides (Table 7-2); of these parameters, only the proportionality constant for the +III actinide humic colloids in ERDA-6 brine is sampled for PA; all other proportionality constants are fixed values
- The total inventory of the actinide

DOE (2009, Appendix SOTERM-2009, Section SOTERM-5.0) provided a discussion of the PA calculations of the actinide source term and example calculations of actinide solubility and colloidal actinides. Table SOTERM-25 (DOE 2009, Appendix SOTERM-2009) provided dissolved and colloidal actinide concentrations calculated using median parameter values for the CCA PAVT and the PABC04. Dissolved and colloidal actinide concentrations calculated using FMT-calculated dissolved concentrations, the mean uncertainty parameters and the colloidal actinide parameters for the PABC09 are summarized in Table 8-1.

Because the constant concentrations of mineral fragment colloids and intrinsic colloids are relatively low, contributions of these types of colloids to the total mobile actinides are low for all actinide oxidation states for the mean PABC09 case (Table 8-1). In GWB brine, the majority of the total mobilized actinides are colloidal, except for plutonium(III) and uranium(VI). For ERDA-6 brine, only uranium(VI) is dominated by the dissolved fraction of the total mobilized concentration. This calculation demonstrates that the Colloidal Actinide Source Term conceptual model and its implementation significantly influence predicted total mobilized actinide concentrations.

¹⁸ Although Xiong et al. (2004, 2005) developed an uncertainty distribution for the solubility of the +V actinide oxidation state, this uncertainty was not used in the CRA-2004 PABC (Garner and Leigh 2005; DOE 2009, Appendix SOTERM-2009, Section SOTERM-5.1.3). Neptunium, which is the only actinide predicted to be present in repository brines in the +V state, does not have a significant effect on PA because of its low concentration in the inventory (see Section 9.0).

Table 8-1. PABC09 Mean Dissolved and Colloidal Actinides

Radionuclide and Oxidation State	Brine	FMT-Calculated Dissolved Concentration (M)	Mean SOLVAR (Xiong et al. 2009a)	Mean Solubility (M)	Mineral Fragment Colloids (M)	Intrinsic Colloids (M)	Humic Colloids (M)	Microbial Colloids (M)	Total Colloidal (M)	Total Mobilized (M)	Dissolved (%)	Colloidal (%)
Americium(III)	GWB	1.66×10^{-6}	-0.142	1.20×10^{-6}	2.60×10^{-8}	0.00	2.27×10^{-7}	4.31×10^{-6}	4.56×10^{-6}	5.76×10^{-6}	21	79
Plutonium(III)	GWB	1.66×10^{-6}	-0.142	1.20×10^{-6}	2.60×10^{-8}	0.00	2.27×10^{-7}	3.59×10^{-7}	6.13×10^{-7}	1.81×10^{-6}	66	34
Thorium(IV)	GWB	5.63×10^{-8}	-0.346	2.54×10^{-8}	2.60×10^{-8}	0.00	1.60×10^{-7}	7.87×10^{-8}	2.65×10^{-7}	2.90×10^{-7}	9	91
Uranium(IV)	GWB	5.63×10^{-8}	-0.346	2.54×10^{-8}	2.60×10^{-8}	0.00	1.60×10^{-7}	5.33×10^{-11}	1.86×10^{-7}	2.11×10^{-7}	12	88
Neptunium(IV)	GWB	5.63×10^{-8}	-0.346	2.54×10^{-8}	2.60×10^{-8}	0.00	1.60×10^{-7}	3.05×10^{-7}	4.90×10^{-7}	5.16×10^{-7}	5	95
Plutonium(IV)	GWB	5.63×10^{-8}	-0.346	2.54×10^{-8}	2.60×10^{-8}	1.00×10^{-9}	1.60×10^{-7}	7.61×10^{-9}	1.95×10^{-7}	2.20×10^{-7}	12	88
Neptunium(V)	GWB	3.90×10^{-7}	-- ^a	3.90×10^{-7}	2.60×10^{-8}	0.00	3.55×10^{-10}	4.68×10^{-6}	4.71×10^{-6}	5.10×10^{-6}	8	92
Uranium(VI)	GWB	1.00×10^{-3}	-- ^a	1.00×10^{-3}	2.60×10^{-8}	0.00	1.10×10^{-5}	2.10×10^{-6}	1.31×10^{-5}	1.01×10^{-3}	99	1
Americium(III)	ERDA-6	1.51×10^{-6}	-0.142	1.09×10^{-6}	2.60×10^{-8}	0.00	1.20×10^{-6}	3.92×10^{-6}	5.14×10^{-6}	6.23×10^{-6}	17	83
Plutonium(III)	ERDA-6	1.51×10^{-6}	-0.142	1.09×10^{-6}	2.60×10^{-8}	0.00	1.20×10^{-6}	3.27×10^{-7}	1.55×10^{-6}	2.64×10^{-6}	41	59
Thorium(IV)	ERDA-6	6.98×10^{-8}	-0.346	3.15×10^{-8}	2.60×10^{-8}	0.00	1.98×10^{-7}	9.75×10^{-8}	3.22×10^{-7}	3.53×10^{-7}	9	91
Uranium(IV)	ERDA-6	6.98×10^{-8}	-0.346	3.15×10^{-8}	2.60×10^{-8}	0.00	1.98×10^{-7}	6.61×10^{-11}	2.24×10^{-7}	2.56×10^{-7}	12	88
Neptunium(IV)	ERDA-6	6.98×10^{-8}	-0.346	3.15×10^{-8}	2.60×10^{-8}	0.00	1.98×10^{-7}	3.78×10^{-7}	6.02×10^{-7}	6.33×10^{-7}	5	95
Plutonium(IV)	ERDA-6	6.98×10^{-8}	-0.346	3.15×10^{-8}	2.60×10^{-8}	1.00×10^{-9}	1.98×10^{-7}	9.44×10^{-9}	2.35×10^{-7}	2.66×10^{-7}	12	88
Neptunium(V)	ERDA-6	8.75×10^{-7}	-- ^a	8.75×10^{-7}	2.60×10^{-8}	0.00	6.48×10^{-9}	1.05×10^{-5}	1.05×10^{-5}	1.14×10^{-5}	8	92
Uranium(VI)	ERDA-6	1.00×10^{-3}	-- ^a	1.00×10^{-3}	2.60×10^{-8}	0.00	1.10×10^{-5}	2.10×10^{-6}	1.31×10^{-5}	1.01×10^{-3}	99	1

a – Neptunium(V) and uranium (VI) solubility uncertainty parameters are not sampled for PA

Evaluation of recent data regarding the formation and stability of intrinsic thorium colloids (Section 7.0) indicates that such colloids may form and remain stable in brines. The incomplete separation of intrinsic thorium colloids from solution has apparently resulted in higher reported $\log K_{sp}^0$ values for $\text{ThO}_2(\text{am})$ in some investigations compared to the value reported by Altmaier et al. (2004), because the latter study used ultracentrifugation to completely remove intrinsic thorium colloids from solution. DOE (1996, Appendix SOTERM Section 6.3.2.2) noted that thorium colloids had been reported in the literature, but these colloids were of small size and likely to be transported as dissolved species. However, the total thorium concentration composed of dissolved and intrinsic thorium colloids reported by Altmaier et al. (2004) was 5.01×10^{-7} M, approximately an order of magnitude greater than the mean dissolved concentrations of thorium in GWB or ERDA-6 used in the PABC09 (Table 8-1).

In EPA's review, the dissolved thorium concentration of 1.58×10^{-9} M and intrinsic thorium colloid concentration of 5.01×10^{-7} M reported by Altmaier et al. (2004) were used to calculate the total mobilized thorium(IV) concentrations in GWB and ERDA-6. In this evaluation of the concentrations of mobilized actinides, the mean values of the recalculated uncertainty distributions for the +III and +IV actinides were also used (Section 6.5.5, Tables 6-13 and 6-14) to consider the effects of the combined changes. For both brines, mobilized concentrations of each actinide increased by approximately a factor of two for the +III actinides and by less than a factor of two for the +IV actinides as shown in the final column of Table 8-2. This factor was obtained by dividing the total mobilized actinides recalculated in Table 8-2 by the total mobilized actinides used in the PABC09 from Table 8-1.

The effects of the increased total mobilized thorium concentration on PA will be relatively small because the WIPP inventory is dominated by isotopes of americium and plutonium, rather than thorium (Fox and Clayton 2010). This assessment is supported by DOE's investigation of the sensitivity of PABC09 total releases to sampled parameters (Kirchner 2010). The only sampled parameter associated with actinide concentrations that strongly affected total releases was found to be the uncertainty associated with the solubility of the +III actinides (SOLMOD3:SOLVAR). The total mobilized thorium concentration will also have no effect on cuttings and cavings releases from the repository, which dominate total releases at high probabilities.

The higher recalculated plutonium(III) and americium(III) total mobilized concentrations are related to the higher mean for the recalculated uncertainty distribution for the +III actinide solubilities. The mean concentrations used in PA obtained by multiplying the FMT-calculated dissolved concentration by the antilog of the mean SOLMOD3:SOLVAR are 2.52×10^{-6} M in GWB and 2.29×10^{-6} M in ERDA-6. Brush et al. (2008) assessed the effects of higher +III actinide solubilities on WIPP repository performance; up to 1.8×10^{-5} M in GWB and 1.9×10^{-5} M in ERDA-6 brine, almost an order of magnitude higher than the recalculated solubilities. Brush et al. (2008) determined that these higher +III actinide solubilities affected repository releases only at low probabilities, and that mean total releases remained well within repository release limits.

Table 8-2. Recalculated Mean Dissolved and Colloidal Actinides Using Thorium Dissolved and Intrinsic Colloid Data of Altmaier et al. (2004) and Recalculated Mean Uncertainty Distribution Values

Radionuclide and Oxidation State	Brine	FMT-Calculated Dissolved Concentration (M)	Mean SOLVAR (recalculated)	Mean Solubility (M)	Mineral Fragment Colloids (M)	Intrinsic Colloids (M)	Humic Colloids (M)	Microbial Colloids (M)	Total Colloidal (M)	Total Mobilized	Dissolved (%)	Colloidal (%)	Factor Increase In Total Mobilized Concentration
Americium(III)	GWB	1.66×10^{-6}	0.181	2.52×10^{-6}	2.60×10^{-8}	0.00	4.78×10^{-7}	9.07×10^{-6}	9.57×10^{-6}	1.21×10^{-5}	21	79	2.10
Plutonium(III)	GWB	1.66×10^{-6}	0.181	2.52×10^{-6}	2.60×10^{-8}	0.00	4.78×10^{-7}	7.55×10^{-7}	1.26×10^{-6}	3.78×10^{-6}	67	33	2.09
Thorium(IV)	GWB	1.58×10^{-9}	-0.271	8.49×10^{-10}	2.60×10^{-8}	5.01×10^{-7}	5.35×10^{-9}	2.63×10^{-9}	5.35×10^{-7}	5.36×10^{-7}	0.2	99.8	1.85
Uranium(IV)	GWB	5.63×10^{-8}	-0.271	3.02×10^{-8}	2.60×10^{-8}	0.00	1.90×10^{-7}	6.33×10^{-11}	2.16×10^{-7}	2.46×10^{-7}	12	88	1.17
Neptunium(IV)	GWB	5.63×10^{-8}	-0.271	3.02×10^{-8}	2.60×10^{-8}	0.00	1.90×10^{-7}	3.62×10^{-7}	5.78×10^{-7}	6.08×10^{-7}	5	95	1.18
Plutonium(IV)	GWB	5.63×10^{-8}	-0.271	3.02×10^{-8}	2.60×10^{-8}	1.00×10^{-9}	1.90×10^{-7}	9.05×10^{-9}	2.26×10^{-7}	2.56×10^{-7}	12	88	1.17
Neptunium(V)	GWB	3.90×10^{-7}	--	3.90×10^{-7}	2.60×10^{-8}	0.00	3.55×10^{-10}	4.68×10^{-6}	4.71×10^{-6}	5.10×10^{-6}	8	92	1.00
Uranium(VI)	GWB	1.00×10^{-3}	--	1.00×10^{-3}	2.60×10^{-8}	0.00	1.10×10^{-5}	2.10×10^{-6}	1.31×10^{-5}	1.01×10^{-3}	99	1	1.00
Americium(III)	ERDA-6	1.51×10^{-6}	0.181	2.29×10^{-6}	2.60×10^{-8}	0.00	2.52×10^{-6}	8.25×10^{-6}	1.08×10^{-5}	1.31×10^{-5}	18	82	2.10
Plutonium(III)	ERDA-6	1.51×10^{-6}	0.181	2.29×10^{-6}	2.60×10^{-8}	0.00	2.52×10^{-6}	6.87×10^{-7}	3.23×10^{-6}	5.52×10^{-6}	41	59	2.09
Thorium(IV)	ERDA-6	1.58×10^{-9}	-0.271	8.49×10^{-10}	2.60×10^{-8}	5.01×10^{-7}	5.35×10^{-9}	2.63×10^{-9}	5.35×10^{-7}	5.36×10^{-7}	0.2	99.8	1.52
Uranium(IV)	ERDA-6	6.98×10^{-8}	-0.271	3.74×10^{-8}	2.60×10^{-8}	0.00	2.36×10^{-7}	7.85×10^{-11}	2.62×10^{-7}	2.99×10^{-7}	13	87	1.17
Neptunium(IV)	ERDA-6	6.98×10^{-8}	-0.271	3.74×10^{-8}	2.60×10^{-8}	0.00	2.36×10^{-7}	4.49×10^{-7}	7.10×10^{-7}	7.48×10^{-7}	5	95	1.18
Plutonium(IV)	ERDA-6	6.98×10^{-8}	-0.271	3.74×10^{-8}	2.60×10^{-8}	1.00×10^{-9}	2.36×10^{-7}	1.12×10^{-8}	2.74×10^{-7}	3.11×10^{-7}	12	88	1.17
Neptunium(V)	ERDA-6	6.98×10^{-8}	--	8.75×10^{-7}	2.60×10^{-8}	0.00	6.48×10^{-9}	1.05×10^{-5}	1.05×10^{-5}	1.14×10^{-5}	8	92	1.00
Uranium(VI)	ERDA-6	8.75×10^{-7}	--	1.00×10^{-3}	2.60×10^{-8}	0.00	1.10×10^{-5}	2.10×10^{-6}	1.31×10^{-5}	1.01×10^{-3}	99	1	1.00

9.0 ACTINIDES INCLUDED IN PERFORMANCE ASSESSMENT CALCULATIONS

Mobilized actinide are important only in calculating direct brine releases and releases by transport through the Culebra to the WIPP boundary. The primary release mechanism—cuttings and caving—is independent of extent of actinide mobilization. Although actinide solubilities and colloidal actinide concentrations are calculated for thorium, uranium, neptunium, plutonium, americium and curium, not all elements and isotopes contribute significantly to releases. Inclusion of all radionuclides in the WIPP inventory in the PA calculations would be both computationally complex and prohibitively time consuming. Consequently, the number of radionuclides directly included in PA was reduced using an algorithm developed for the CCA (DOE 2009, Appendix PA-2009, Section PA-4.3.3 and Figure PA-21). Calculations of releases through DBR included isotopes of plutonium, americium, uranium, thorium, neptunium and curium. A smaller number of plutonium, americium, uranium and thorium isotopes were used to calculate releases by transport through the Culebra and Salado. Within these suites of actinides, the primary contributors to the initial activity in the repository are Am-241, Pu-238, Pu-239 and Pu-240. Due to radioactive decay, at times greater than about 2,000 years, the main contributor to total normalized activity is Pu-239, with a small contribution from Pu-240 (Fox and Clayton 2010). Isotopes of thorium, uranium, and neptunium do not contribute significantly to total normalized activity at any time.

DOE stated that radionuclide releases are dominated by plutonium and americium (DOE 2004, Appendix TRU WASTE). As an independent verification of this assertion, EPA (2006d) evaluated the potential importance of neptunium-237 on PA because of the potential for higher neptunium solubilities in the presence of organic ligands (see Section 6.2.7). The results of these calculations indicated that neptunium-237 would not contribute significantly to potential releases, and that its omission from the CRA-2004 PA and any subsequent PA was acceptable. Curium isotopes also make up a relatively small fraction of the radionuclide inventory and will not contribute significantly to radionuclide releases, compared to americium and plutonium (EPA 2006d).

10.0 CULEBRA DOLOMITE DISTRIBUTION COEFFICIENTS

Radionuclides may reach the Culebra member of the Rustler Formation via brine flow through a borehole that intersects the repository (DOE 2004, Section 6.4.6.2.1; DOE 2009, Appendix PA, Section 6.8.3). Radionuclides introduced into the Culebra may be transported through natural groundwater flow to the accessible environment (DOE 2004, Section 6.4.6.2). Predictions of transport and release of radionuclides through the Culebra are affected by sorption onto minerals along this potential pathway. Accordingly, DOE developed distribution coefficients (K_{ds}) to express a linear relationship between sorbed and aqueous concentrations of the radionuclides (DOE 2004, Section 6.4.6.2.1).

10.1 DISTRIBUTION COEFFICIENTS USED IN THE CCA PA AND PAVT

The distribution coefficients used in the CCA PA and PAVT were developed using data from experiments carried out at Los Alamos National Laboratory (LANL) and SNL:

- Sorption studies carried out with ‘dolomite-rich Culebra rock’ by Triay and coworkers
- Sorption studies performed using pure dolomite from Norway and synthetic NaCl solutions by Brady and coworkers
- Transport studies using intact core samples of Culebra rock by Lucero and coworkers

Sorption data from these sources were compiled and evaluated by Brush (1996), and the selected K_d values were used in the CCA PA and CCA PAVT (Table 10-1). These values were subsequently updated by Brush and Storz (1996) because of slight errors in the calculated K_d values.

The differences between the K_d values reported by Brush (1996) and by Brush and Storz (1996) resulted from corrections of errors in the mass of dolomite used to calculate K_d values in the sorption studies by Brady and coworkers and corrections of errors in the density of brine used to calculate K_d values in the experiments by Triay and coworkers (Brush and Storz 1996). The revised values from Brush and Storz (1996) were not available in time for inclusion in the CCA PA or PAVT; however, Brush and Storz (1996) stated that the relatively small changes in the K_d values were unlikely to significantly impact PA results.

Brush (1996) and Brush and Storz (1996) provided K_d values for actinide elements for both deep (Castile and Salado) brines and Culebra brines. For conservatism, only the ranges of K_{ds} for the brine having the smaller mean value were used in PA. A uniform distribution was used for all K_d ranges in the CCA PA (Brush 1996; Brush and Storz 1996). Sorption experiments were conducted in the presence of organic ligands, but DOE did not revise the ranges of K_{ds} to include the potential effects of organic ligands because they assumed that metals present in the waste (such as iron and nickel) would compete with actinides for the organic ligands and would limit the effects of ligands on actinide sorption (Brush 1996, Brush and Storz 1996).

Table 10-1. Comparison of Matrix K_d Values for the CCA PA and PAVT With Matrix K_d Values for the CRA-2004 PA, PABC04, CRA-2009 PA and PABC09

K_d Range [m ³ /kg]	CCA PA and PAVT (Brush 1996)	CRA-2004 PA, PABC04 and CRA-2009 PA (Brush and Storz 1996)	High Concentration Organics (Brush and Storz 1996) ^a	PABC09 (Clayton 2009) ^b
Americium(III)	0.02–0.5	0.02–0.4	0.00505–0.00740	0.005–0.4
Plutonium(III)	0.02–0.5	0.02–0.4	--	0.005–0.4
Thorium(IV)	0.9–20	0.7–10	0.000467–0.00469	0.0005–10
Uranium(IV)	0.9–20	0.7–10	--	0.0005–10
Neptunium(IV)	0.9–20	0.7–10	--	0.0005–10
Plutonium(IV)	0.9–20	0.7–10	--	0.0005–10
Neptunium(V)	0.001–0.2	0.001–0.2	0.00–0.00249	0.00003–0.2
Uranium(VI)	0.00003–0.03	0.00003–0.02	0.00–0.0101	0.00003–0.02

a – SPC brine (Salado) with 0.0489 M acetate, 0.003417 M citrate, 1.1×10^{-5} M EDTA, and 0.00288 M lactate; H-17 brine (Culebra) and ERDA-6 brine (Castile) with 0.0195 M acetate, 0.00340 M citrate, 1.46×10^{-5} M EDTA, and 0.00076 M lactate

b – Log-uniform distribution

EPA (1998c) evaluated the ranges and distributions of K_d values used in the CCA PA. EPA accepted the ranges used in the CCA, but disagreed with the uniform distribution for these ranges. EPA instead specified a log-uniform distribution for the K_d ranges for use in the PAVT.

10.2 DISTRIBUTION COEFFICIENTS USED IN THE PABC04 AND CRA-2009 PA

Hansen and Leigh (2003) provided a reconciliation of parameter values between the CCA (PAVT) and the CRA-2004 PA. Hansen and Leigh (2003) documented that there were no changes in the ranges of K_d values for uranium(VI), uranium(IV), plutonium(III), plutonium(IV), thorium(IV), and americium(III) between the CCA PA and the PAVT. Hansen and Leigh (2003) noted the two errors in the procedures used to calculate the matrix K_d s that were identified by Brush and Storz (1996), and reiterated the conclusion of Brush and Storz (1996) that these errors would have minimal effects on PA.

During the review of the CRA-2004 PA and PABC04, EPA (2006c) examined the parameter data sheets and the references therein in Appendix PA, Attachment PAR (DOE 2004). These parameters are the matrix K_d values used in PA for uranium(VI), uranium(IV), plutonium(III), plutonium(IV), thorium(IV), and americium(III). In addition to the K_d ranges and log-uniform distribution of the data, each parameter data sheet included references to the relevant site-specific experimental data and discussion of the technical basis (laboratory results) for data selection. The key references EPA (2006c) used in their evaluation of the matrix K_d values were Brush (1996), Brush and Storz (1996), Wall (2001) and Hansen and Leigh (2003).

In discussing the parameter baseline, including K_d s, Wall (2001) appeared to use the EPA (1998d) conclusions to address key technical issues, such as the use of brines with lower pH than expected in the repository and the effect of organic ligands. Regarding the latter, EPA (1998d) agreed that the effect of organic ligands on actinide sorption could be ruled out because sufficient concentrations of non-actinide cations would be available to complex with these ligands. However, aqueous speciation data and modeling calculations available from the CRA-

2004 (EPA 2006c, Section 8.0) indicated that solubilities of the +III and +V actinides could be affected by organic ligands. Consequently, EPA (2006c) re-examined the K_d values measured in brines with organic ligands (Brush and Storz 1996).

The reported values for low and intermediate organic ligand concentrations were judged to be the most applicable to WIPP repository conditions. The ranges of K_d values reported for americium(III) and uranium(VI) in the presence of organic ligands were found to be consistent with the ranges of K_d values used in the CRA-2004 PA and PABC04. However, values on the order of approximately 4 ml/g were observed for thorium(IV) in the presence of organic ligands, whereas the range of values used in the CRA-2004 PA and PABC04 was 700 to 10,000 ml/g. This lower K_d for thorium(IV) appeared to be inconsistent with the results of geochemical modeling because thorium(IV) does not appear to be significantly complexed by organic ligands (EPA 2006c, Section 8.5). EPA (2006c) concluded that this inconsistency may have been the result of higher CO_2 fugacities and lower pH in the experiments than are expected in the WIPP repository.

The data regarding the potential effects of organic ligands on actinide sorption were previously considered by EPA (1998b). At that time, EPA concluded that the results of the speciation calculations, K_d values reported in the literature and expected increased adsorption under alkaline conditions indicated that the K_d ranges exclusive of the organic ligands were sufficiently representative of actinide solid/liquid partitioning for modeling actinide transport in the Culebra.

No additional sorption experiments have been carried out since the CCA PA and PAVT. The CRA-2009 PA used the same ranges of K_d values and distributions as the CRA-2004 PA and PABC04 (DOE 2009, Appendix PA-2009, Section PA-2.1.4.7). This was confirmed by examining the parameter data sheets for the actinide K_d values (Parameters 29 through 34) (Fox 2008). Comparison of the K_d ranges used in the CCA PA and PAVT with the ranges used in the CRA-2004 PA, PABC04 and CRA-2009 PA, indicated that the differences were small (Table 10-1). Furthermore, the revised K_d ranges are more conservative because the lower K_d values should result in less sorption. EPA (2006c) determined that the revised K_d ranges used in the CRA-2004 PA and PABC04 were acceptable, because no new experimental sorption data were available, the changes to the K_d ranges were minor and conservative and these changes had been previously reviewed and found acceptable by EPA (1998b).

Higher ligand concentrations have been predicted for the PABC09 than for previous PAs (Table 6-1). The current predicted acetate and citrate concentrations are similar to concentrations in the high-ligand-concentration experiments reported by Brush and Storz (1996), and the current predicted EDTA concentration exceeds the concentrations reported for the high-ligand-concentration experiments.

The range of K_d values measured for neptunium(V) in the presence of high concentrations of organic ligands is compared to the range of K_d values established by Brush and Storz (1996) in Table 10-1. Although the measured K_d values for neptunium(V) in the presence of high concentrations of organic ligands falls at the lower end of the K_d range used in PA, the effects on PA of lower K_d values for neptunium(V) are likely to be insignificant because of the relatively small amount of neptunium in the WIPP inventory. The range of K_d values measured for uranium(VI) with high concentrations of organic ligands is reasonably similar to the range

selected for PA by Brush and Storz (1996). Consequently, the effects of organic ligands on the transport of neptunium(V) or uranium(VI) through the Culebra are not likely to be significant for PA.

For both americium(III) and thorium(IV), however, the K_d ranges measured in experiments with high concentrations of organic ligands are significantly lower than the K_d ranges used in PA. Because of the importance of americium(III), plutonium(III) and plutonium(IV) to total releases from the repository, smaller K_d values for the +III and +IV oxidation state have the potential to significantly affect PA results. For that reason, EPA requested additional information from DOE regarding the possible effects of increased ligand concentrations and lower K_d values on +III and +IV actinide releases by transport through the Culebra (Comment 3-C-25, Cotsworth 2009c).

10.3 DISTRIBUTION COEFFICIENTS USED IN THE PABC09

DOE re-evaluated the range of K_d values used to assess retardation of actinides during transport through the Culebra (Moody 2010b). There was no evidence that the upper bound should be changed. Consequently, the upper bounds for the K_d ranges were maintained, but the lower bounds were reduced to account for the possibility of higher organic ligand concentrations.

Clayton (2009) provided details regarding the changes in the K_d ranges. The lower limit for the uranium(VI) K_d range was not modified, because this value was already effectively equal to zero. Although neptunium is not currently included in the Culebra transport calculations, DOE updated its K_d range to maintain consistency. Because the K_d ranges sampled for PA are assumed to have a log-uniform distribution, assumption of a lower K_d limit of zero is not valid. Consequently, the lower limit of the uranium(VI) K_d was also assumed for the lower limit for the neptunium(V) K_d (Table 10-1). The K_d ranges used in the PABC09 are summarized in Table 10-1. The revised lower-bound values for the K_d s used in the PABC09 are consistent with the lower limits of the ranges observed in the experiments with high concentrations of organic ligands. Consequently, the K_d ranges were appropriately conservative for use in the PABC09.

11.0 EFFECTS OF HETEROGENEOUS WASTE LOADING

In all solubility calculations carried out for WIPP PA, it has been assumed that waste would be homogeneously loaded in the repository. At the time of the CCA, no information was available regarding the potential patterns of waste loading that might occur, and this assumption was appropriate. However, EPA noted during their review of the CRA-2004 PA that Panel 1 waste loading information indicated that the assumption of homogeneity was incorrect. Because shipments of waste placed in Panel 1 included an intensive campaign of waste shipments from the Rocky Flats site, 54% of the waste in Panel 1 was from that site (Leigh 2003). In addition to the Panel 1 waste loading information, inclusion of the Option D panel closure makes it less likely that brine in contact with waste in one panel of the repository will contact brine in another panel.

EPA (2006c) evaluated the potential effects of waste heterogeneity on the results of PA. This evaluation included the potential effects on actinide solubility calculations and the MgO EF calculations. As described in Section 4.3.3 of this document, DOE has accounted for the potential effects of heterogeneous waste loading on the MgO EF by implementing an approved emplacement plan that ensures the required EF is maintained on a room-by-room basis (Detwiler 2004a).

The Environmental Evaluation Group (EEG) questioned whether the assumption of homogeneous chemical conditions in the repository is appropriate (Oversby 2000). As an alternative to the approach used by DOE, EEG recommended calculating releases that would occur if a small number of waste drums containing relatively high concentrations of actinides and organic ligands are intersected by a borehole. This waste could be leached by drilling fluid, and if this borehole then reached an underlying brine pocket, EEG maintained that an unacceptable release of actinides could result. EEG recommended that DOE assess repository performance by calculating the range of actinide concentrations that could be released under this scenario, and multiplying by the probability of the scenario. This approach was considered on several occasions (EPA 1998a, TEA 2000, TEA 2001). EPA observed that WIPP PAs are based on a probabilistic approach, rather than the calculation of solubilities associated with a worst-case scenario as suggested by EEG, and this probabilistic approach had been peer-reviewed and found to be acceptable. EPA also found that the effects of waste heterogeneity on PA were adequately addressed by the uncertainties assigned to the actinide solubilities (EPA 1998a, TEA 2000, TEA 2001).

During review of the CRA-2004 PA, EPA requested additional information from DOE regarding the potential effects of heterogeneous waste loading on the assumption of homogeneous chemical conditions throughout the entire repository (Cotsworth 2004a, Comment G-12). DOE responded with an assessment of the potential effects of higher amounts of plutonium in Panel 1 than would be expected, based on homogeneous emplacement throughout a 10-panel repository (Detwiler 2004c). DOE stated that the only likely effect of this higher-than-expected loading of plutonium in Panel 1 would be increased radiolysis that could cause plutonium to speciate as plutonium(V) or plutonium(VI), instead of the reduced oxidation states predicted for the repository (see Section 5.0). However, because of microbial consumption of CPR and the amounts of metallic iron in the repository, including the large amounts of stainless steel in the

pipe overpacks in Panel 1, DOE stated that reducing conditions and lower plutonium oxidation states would still be maintained in Panel 1.

Heterogeneous waste loading is unlikely to affect actinide solubilities if a relatively high proportion of the actinide inventory is present in a single panel, because of the assumption of chemical equilibrium with respect to the solubilities of actinide solid phases. However, the placement of waste with a high proportion of the organic ligand inventory in a panel could affect actinide solubilities. DOE has accounted for this possibility in the actinide solubility calculations by assuming that the entire organic ligand inventory is dissolved in the minimum amount of brine necessary for a release from the repository (DOE 2009, Appendix SOTERM-2009, Section SOTERM-2.3.6). This approach ensures that the effects of heterogeneous waste placement are adequately accounted for in the actinide solubility calculations, provided that the inventory of organic ligands is bounded.

12.0 EFFECTS OF CHEMICAL PROCESSES ON REPOSITORY WATER BALANCE

Chemical processes that may affect the quantity of water in the repository include microbial degradation of CPR, anoxic corrosion, MgO hydration to form brucite or hydromagnesite, dehydration of hydromagnesite to form magnesite and anoxic corrosion of iron-based metal. The effects of potential water production by CPR degradation have not been included in PA, because of uncertainties associated with microbial degradation. The assumption that this portion of the water balance can be omitted has been part of the Gas Generation conceptual model since the CCA PA (SC&A 2008b). Consumption of water by reaction with MgO to form brucite or hydromagnesite is not accounted for in PA, even though these phases may persist throughout all, or a significant fraction of the 10,000-year regulatory period. Although the effects of CPR degradation and hydration of MgO on the water balance are not accounted for in PA, consumption of water by anoxic corrosion of iron in the waste and waste containers is included in calculations of brine saturation in PA. However, the effects of formation of FeS instead of $\text{Fe}(\text{OH})_2 \cdot x\text{H}_2\text{O}$ during iron corrosion on the quantity of water consumed have not been included in PA. Geochemical modeling of CPR degradation using EQ3/6 by Wolery and Sassani (2007) indicated that CPR degradation could result in significant increases in the amount of brine in the WIPP repository. SC&A (2008b) performed a qualitative evaluation of the possible effects of various chemical processes on brine generation and consumption, and concluded that the potential importance of CPR degradation, MgO hydration and carbonation and FeS precipitation on the water balance in the repository warranted additional evaluation.

EPA observed during their review of the CRA-2009 (DOE 2009) that the potential effects of processes other than anoxic corrosion on the repository water balance had not been addressed (Cotsworth 2009a, Comment 1-C-5). Consequently, EPA requested additional information from DOE regarding whether production of water by CPR degradation and consumption of water by brucite hydration and hydromagnesite persistence might significantly affect predicted repository performance.

The potential for water consumption or production by reactions involving magnesium-based minerals and microbial degradation of CPR was acknowledged by DOE in their response (Moody 2009a). DOE noted that when small amounts of brine enter the repository, it will be consumed by reaction with MgO, and repository performance is unlikely to be affected by microbial reactions. DOE further stated that if a large amount of brine enters the repository, the MgO backfill would be hydrated, microbial degradation of CPR would be assumed to occur and the amount of water produced could under some circumstances affect repository performance. DOE concluded that although it would be appropriate to include all water balance considerations in future PA calculations, the uncertainties associated with water balance changes caused by brucite hydration, hydromagnesite persistence in the repository and production of water by CPR degradation preclude their inclusion in the repository water balance at this time.

DOE's assessment that microbial production of water during CPR degradation, and consumption of water by MgO hydration and hydromagnesite persistence are likely to be important only when relatively large quantities of brine enter the repository is reasonable. It is also true that a relatively large amount of uncertainty is associated with whether plastics and rubber will degrade during the repository performance period. Because plastics and rubber constitute approximately

two-thirds of the CPR carbon in the repository, this uncertainty increases uncertainties associated with water production by CPR degradation. Consequently, DOE's assessment that implementation of a more detailed repository water balance is not practical at this time is reasonable. DOE has stated that their analysis of the repository water balance will continue, which is appropriate, because of the importance of the water balance to repository chemical processes, such as anoxic corrosion, MgO hydration and microbial degradation of CPR.

13.0 SUMMARY AND CONCLUSIONS

The conceptual model and implementation of gas generation from anoxic corrosion used for the PABC09 continue to be supported by the available data. The microbial gas generation rates used for the PABC09 are suitable for modeling gas generation rates from degradation of cellulosic materials, but may overestimate gas generation rates from the degradation of plastics and rubber. DOE accounted for uncertainties regarding the rates of plastic and rubber degradation in the WIPP repository environment by assuming plastic and rubber degradation occurs in only 25% of the realizations. Based on the available data, the current approach for modeling microbial gas generation rates is appropriate for PA.

The available data support the assumption that the MgO backfill will adequately control brine pH and CO₂ fugacities, and thereby limit actinide solubilities in WIPP brines under inundated conditions. There are no data available regarding the carbonation rate of MgO under humid conditions in the WIPP repository, but maintenance of low CO₂ partial pressures is not important for these conditions. Because of uncertainties in the rate at which hydromagnesite will convert to magnesite in the repository environment, it is assumed for PA that the brucite-hydromagnesite reaction will buffer CO₂ fugacity at levels consistent with relatively low actinide solubilities under inundated conditions. Calculation of the EF takes into account the uncertainties associated with the rate of hydromagnesite conversion to magnesite. The current MgO emplacement plan is designed to maintain the appropriate MgO EF of 1.2 in each room of the repository. The MgO reactivity testing procedure and test results provided by DOE demonstrate that the current backfill material contains a sufficient percentage of reactive periclase plus lime to control chemical conditions in the repository, and that the testing procedure now in use would detect any MgO shipments with inadequate percentages of reactive periclase plus lime.

The assumptions related to actinide oxidation states in the WIPP repository have remained unchanged since they were developed and peer reviewed for the CCA. It is assumed that thorium(IV), americium(III), and curium(III) are the only oxidation states that will be present in the WIPP repository for these radionuclides. It is assumed that plutonium may be present in the +III or +IV oxidation states and uranium may be present in the +IV or +VI oxidation states. The available evidence indicates that neptunium is likely to be present in the +IV oxidation state in repository brines, rather than the +IV and +V oxidation states assumed for PA. Assuming that neptunium may also be present in the +V oxidation state is conservative, because of the greater solubility of neptunium(V) solids. However, because of the relatively small neptunium inventory, the assumption of higher neptunium solubilities in WIPP brines is unlikely to significantly affect PA results. Since reducing conditions will be established in the repository shortly after closure, the peer-reviewed oxidation state assumptions remain appropriate.

DOE (2009, Appendix SOTERM-2009) provided a qualitative review of actinide solubility and speciation data relevant to WIPP brines that have become available since the PABC04, but made no revisions to the FMT database. Consideration of all new geochemical data and other relevant data is required for each CRA [40 CFR 194.15(a)]. Review of the actinide solubility and aqueous speciation data available since the most recent revision of the FMT database indicates that actinide solubilities calculated using this database are adequate for use in the PABC09 calculations. However, because DOE did not use the newly available actinide solubility and aqueous speciation data related to the +III and +IV actinides to quantitatively re-evaluate the

FMT database, a substantial number of questions were raised regarding the possible effects of the new data on PA, resulting in a lengthy review process. Reviewing and updating the FMT database to take into account new aqueous speciation and solubility data prior to the CRA-2014, as was carried out for the CRA-2004, should expedite future reviews and increase confidence in the results of the dissolved actinide source term calculations.

Recent experimental investigations by DOE have indicated that borate complexation may increase aqueous concentrations of the +III and +VI actinides. The results of these experiments indicate that at WIPP-relevant pcH values in ERDA-6 brine without organic ligands, measured solubilities are approximately an order of magnitude higher than predicted by FMT calculations. However, these investigations are not complete, and +III actinide solubilities in GWB brine have not been measured at WIPP-relevant pcH values. Review of the available data indicates that borate complexation of the +III and +VI actinides is unlikely to have significant effects on PA. Disagreement between measured and predicted +III actinide solubilities in GWB brine at pcH values less than 8 indicate that the FMT database is not well parameterized for these conditions. However, the disagreement between predicted and measured concentrations in lower-pcH GWB brine will not affect PA results because the MgO backfill will maintain a higher pcH range of 8 to 10.

Recent literature data indicate that the aqueous-thorium carbonate speciation used in the FMT database may require revision. Because of the low carbonate concentrations maintained by the MgO backfill in the WIPP repository, dissolved thorium concentrations predicted using the current FMT database are adequate for PA.

DOE has not developed an aqueous speciation and solubility model for uranium(VI) and continues to use a fixed concentration of 1.0×10^{-3} M for the dissolved source term. DOE has reported the results of uranium(VI) solubility measurements in carbonate-free WIPP brines. Because of the likely importance of carbonate complexation on the solubility of uranium(VI), these results cannot be used to determine likely uranium(VI) concentrations under anticipated WIPP repository conditions. Thus continued use of a fixed concentration is appropriate.

Some inconsistencies were identified during the review of DOE's selection of +III and +IV actinide solubility data for developing the solubility uncertainty distributions. These inconsistencies resulted in decreased mean values for the actinide solubility uncertainty distributions. Re-evaluation of the uncertainty distributions for the +III and +IV actinide solubilities demonstrated that the effect on mean repository releases were unlikely to significantly affect repository performance.

The approach for calculating the colloidal actinide concentrations has remained unchanged since the CCA PAVT. This approach has been peer reviewed and was found to be adequate, if somewhat conservative. Recent literature data have identified the formation of intrinsic thorium colloids and thorium pseudocolloid formation in brines. DOE should evaluate the data regarding the formation of thorium intrinsic colloids and revise the FMT database and intrinsic thorium colloid concentration if appropriate. Although the thorium pseudocolloid formation reported in the literature is unlikely to occur because of differences in solid phase stability expected between the conditions of the experiments and WIPP repository conditions, review of the available WIPP-specific data indicates that the potential formation of pseudocolloids from MgO hydration and

carbonation products has not been thoroughly investigated. Because colloids capable of transporting actinides have been demonstrated to form from reaction of MgO in brines under some conditions, this omission introduces some uncertainty into the colloidal actinide source term model. To minimize this uncertainty, DOE should evaluate the potential formation of mineral-fragment colloids from MgO hydration and carbonation under WIPP-relevant conditions before the CRA-2014 PA.

The results of the mobile actinide source term calculations indicate that for the case using mean values of the PABC09 parameters, colloidal actinides contribute significantly to the actinide source term. Recalculation of total mobilized actinides to account for uncertainties in dissolved thorium and intrinsic thorium colloid concentrations and increases in the mean solubility uncertainty parameters for the +III and +IV actinides indicates that these changes would not significantly affect repository performance.

Distribution coefficients used to model actinide transport through the Culebra have been modified to account for estimated organic ligand concentrations that have increased in WIPP brines because of increases in the inventory for these compounds. These K_d values are likely to provide a conservative assessment of actinide transport through the Culebra.

The potential effects of heterogeneous waste loading are unlikely to significantly affect actinide solubilities, except in the case where a large proportion of the organic ligands in the inventory are placed in a single panel. DOE has accounted for this possibility in the actinide solubility calculations by assuming that the entire organic ligand inventory is dissolved in the minimum amount of brine necessary for a release from the repository. Provided that the inventory of organic ligands is adequately bounded, this approach ensures that the effects of heterogeneous waste placement are adequately accounted for in the actinide solubility calculations.

The potential production of water by microbial degradation of CPR or replacement of $\text{Fe}(\text{OH})_2 \cdot x\text{H}_2\text{O}$ by FeS during iron corrosion and water consumption by brucite hydration and possible persistence of hydromagnesite are not currently included in the repository water balance. Because of the difficulties associated with quantifying or attaching reasonable uncertainties to many of the processes that can affect the water balance, it is not practical at the present time to include these processes in the water balance calculations.

Review of the CRA-2009 (DOE 2009) and supporting information, including the results of the PABC09, indicates that DOE adequately addressed all chemistry issues relevant to repository performance. There are a number of uncertainties related to chemical processes that may affect radionuclide releases from the WIPP repository during the 10,000-year regulatory period that have been addressed for WIPP PA by making appropriately conservative, bounding assumptions. These uncertainties include:

- The rates at which plastics and rubber will degrade, including the effects of radiolytic processes on microbial degradation
- The availability of sulfate in Salado Formation minerals, including the amounts of sulfate minerals and the rates of sulfate transport to the waste in the repository, which results in uncertainties in the relative amounts of CPR degradation that may occur via sulfate reduction and methanogenesis

- Extrapolation of microbial degradation rates from short-term laboratory experiments to long-term repository conditions
- Hydromagnesite to magnesite conversion rate under repository conditions
- Oxidation states of plutonium, neptunium and uranium in the repository environment
- Effects of organic ligands on actinide solubilities and Culebra transport

Issues related to WIPP repository chemical processes that have been identified for possible additional investigation prior to the CRA-2014 include:

- Lack of rate data for brucite carbonation under humid conditions
- Review and, if appropriate, incorporation of recent literature data into the FMT geochemical modeling database for the +III and +IV actinide solubility calculations
- Development of a uranium(VI) aqueous speciation and solubility model and incorporation of this model into the FMT database
- Critical re-evaluation of the thorium-carbonate aqueous speciation and $\text{ThO}_2(\text{am})$ solubility
- Revision of the uncertainty distributions for the +III and +IV actinide solubilities using the available literature data and a consistent, well-documented method for selecting experimental data included in the uncertainty evaluation
- Evaluation of possible thorium intrinsic colloid formation
- Evaluation of the formation of pseudocolloids in WIPP brines from MgO hydration and carbonation products and potential effects on total mobilized actinides
- Evaluation of the effects of microbial degradation of CPR, MgO hydration, hydromagnesite dehydration and FeS formation on the repository water balance

These issues were qualitatively addressed during this review where it was determined that their impact on PA was minor. However, it is anticipated that a more quantitative approach for addressing these issues will expedite the review of future recertification applications.

14.0 REFERENCES

- Al Mahamid, I., C.F. Novak, K.A. Becraft, S.A. Carpenter, and N. Hakem. 1998. Solubility of Np(V) in K-Cl-CO₃ and Na-K-Cl-CO₃ solutions to high concentrations: measurements and thermodynamic model predictions. *Radiochimica Acta* 81:93-101.
- Altmaier, M., V. Neck, J. Lützenkirchen and T. Fanghänel. 2009. Solubility of plutonium in MgCl₂ and CaCl₂ solutions in contact with metallic iron. *Radiochimica Acta* 97:187-192.
- Altmaier, M., V. Metz, V. Neck, R. Müller, and T. Fanghänel. 2003. Solid-liquid equilibria of Mg(OH)₂(cr) and Mg₂(OH)₃Cl•4H₂O(cr) in the system Mg-Na-H-OH-Cl-H₂O at 25°C. *Geochimica et Cosmochimica Acta* 67:3595-3601.
- Altmaier, M., V. Neck, M.A. Denecke, R. Yin and T. Fanghänel. 2006. Solubility of ThO₂•xH₂O and the formation of ternary Th(IV) hydroxide-carbonate complexes in NaHCO₃-Na₂CO₃ solutions containing 0-4 M NaCl. *Radiochimica Acta* 94:495-500.
- Altmaier, M., V. Neck and T. Fanghänel. 2004. Solubility and colloid formation of Th(IV) in concentrated NaCl and MgCl₂ solution. *Radiochimica Acta* 92:537-543.
- Altmaier, M., V. Neck, R. Müller and T. Fanghänel. 2005. Solubility of ThO₂•xH₂O in carbonate solution and the formation of ternary Th(IV) hydroxide-carbonate complexes. *Radiochimica Acta* 93:83-92.
- André, C., and G.R. Choppin. 2000. Reduction of Pu(V) by Humic Acid. *Radiochimica Acta* 88:613-616.
- ANL (Argonne National Laboratory). 1997. *Actinide Stability/Solubility Studies in Support of the Waste Isolation Pilot Plant*. Chemical Technology Division Annual Technical Report 1997. ANL-98/13, pp. 50-52.
- Babb, S.C. 1996. *NONLIN, Ver. 2.00 User's Manual*. Sandia National Laboratories, Albuquerque, New Mexico, January 31, ERMS 230740.
- Banaszak, J.E., D.T. Reed, and B.E. Rittmann. 1998. Speciation-dependent toxicity of neptunium(V) towards *Chelatobacter heintzii*. *Environmental Science and Technology* 32:1085-1091.
- Banaszak, J.E., S.M. Webb, B.E. Rittmann, J.-F. Gaillard, and D.T. Reed. 1999. Fate of Neptunium in Anaerobic, Methanogenic Microcosm. *Scientific Basis for Nuclear Waste Management XXII* 556:1141-1149.
- Bassett, R.L. 1980. A critical evaluation of the thermodynamic data for boron ions, ion pairs, complexes, and polyanions in aqueous solution at 298.15 K and 1 bar. *Geochimica et Cosmochimica Acta* 44:1151-1160.
- Baston, G.M.N, M. Brownsword, A.J. Smith, and J.L. Smith-Briggs. 1996. *Further Near-Field Solubility Studies*. NSS/R357, AEA Technology plc, Harwell, United Kingdom.

Bernkopf, M. and J.I. Kim. 1984. *Hydrolysereaktionen und Karbonatkomplexierung von Dreiwertigem Americium in Natürlich Aquatischen System*. Report RCM-02884, Institute für Radiochemie, Tech. Univ. Munich.

Bitea, C., R. Müller, V. Neck, C. Walther and J.I. Kim. 2003. Study of the generation and stability of thorium(IV) colloids by LIBD combined with ultrafiltration. *Colloids and Surfaces A: Physicochem. Eng. Aspects* 217:63-70.

Borkowski, M. 2010. *Numerical Values for Graphs Presented in the Report LCO-ACP-08, Rev. 0 Entitled: "Actinide (III) Solubility in WIPP Brine: Data Summary and Recommendations."* LANL-CO ACRSP ACP-1002-05-17-01, Los Alamos National Laboratory, Carlsbad, New Mexico.

Borkowski, M., J.F. Lucchini, M.K. Richmann, and D.T. Reed. 2009. *Actinide (III) Solubility in WIPP Brine: Data Summary and Recommendations*. LCO-ACP-08. LANL\ACRSP Report. Los Alamos National Laboratory, Los Alamos, New Mexico. Cited by DOE (2009) as Borkowski et al. (2008).

Borkowski, M. and M. Richmann. 2009. *Comparison of Recent Thorium Thermodynamic Data with Those Used in the WIPP FMT_050405.CHEMDAT Database*. LANL-CO ACRSP ACP-0911-01-03-01, Los Alamos National Laboratory, Carlsbad, New Mexico, November 3, 2009.

Boukhalfa, H., G.A. Icopini, S.D. Reilly, and M.P. Neu. 2007. Plutonium(IV) retention by the metal-reducing bacteria *Geobacter metallireducens* GS15 and *Shewanella oneidensis* MR1. *Applied and Environmental Microbiology* 73:5897-5903.

Bousher, A. 1995. Review- unidentate complexes involving borate. *Journal of Coordination Chemistry* 34:1-11.

Brendebach, B., M. Altmaier, J. Rothe, V. Neck and M.A. Denecke. 2007. EXAFS study of aqueous Zr^{IV} and Th^{IV} complexes in alkaline $CaCl_2$ solutions: $Ca_3[Zr(OH)_6]^{4+}$ and $Ca_4[Th(OH)_8]^{4+}$. *Inorganic Chemistry* 46:6804-6810.

Bronikowski, M., O.S. Pokrovsky, M. Borkowski, and G.R. Choppin. 1999. UO_2^{2+} and NpO_2^{2+} Complexation with Citrate in Brine Solutions. In *Actinide Speciation in High Ionic Strength Media*, D.T. Reed, S. B. Clark, and L. Rao, Eds., Kluwer Academic/Plenum Publishers, pp. 177–185.

Brooks, S.C., J.K. Fredrickson, S.L. Carroll, D.W. Kennedy, J.M. Zachara, A.E. Plymale, S.D. Kelly, K.M. Kemner, and S. Fendorf. 2003. Inhibition of bacterial U(VI) reduction by calcium. *Environmental Science and Technology* 37:1850-1858.

Brush, L.H. 1990. *Test Plan for Laboratory and Modeling Studies of Repository and Radionuclide Chemistry for the Waste Isolation Pilot Plant*. SAND90-0266. Sandia National Laboratories, Albuquerque, New Mexico.

- Brush, L.H. 1995. *Systems Prioritization Method - Iteration 2 Baseline Position Paper: Gas Generation in the Waste Isolation Pilot Plant*. Unpublished report, Sandia National Laboratories, Albuquerque, New Mexico, March 17, 1995, ERMS 228740.
- Brush, L.H. 1996. *Ranges and Probability Distributions of K_{ds} for Dissolved Pu, Am, U, Th and Np in the Culebra for the PA calculations to Support the WIPP CCA*. Memorandum to M.S. Tierney, Sandia National Laboratories, Albuquerque, New Mexico, June 10, 1996, ERMS 238801.
- Brush, L.H. 2004. *Implications of New (Post-CCA) Information for the Probability of Significant Microbial Activity in the WIPP*. Sandia National Laboratories Carlsbad Programs Group, Carlsbad, New Mexico, July 28, 2004, ERMS 536205.
- Brush, L.H. 2005. *Results of Calculations of Actinide Solubilities for the WIPP Performance Assessment Baseline Calculations*. Analysis Report, Sandia National Laboratories, Carlsbad, New Mexico, ERMS 539800.
- Brush, L.H., J. Garner, and E. Vugrin. 2005. *PA Implementation of Uncertainties Associated with Calculated Actinide Solubilities*. Memorandum to Dave Kessel, Sandia National Laboratories, Carlsbad, New Mexico, February 2, 2005, ERMS 538537.
- Brush, L.H. and L.J. Storz. 1996. *Revised Ranges and Probability Distributions of K_{ds} for Dissolved Pu, Am, U, Th and Np in the Culebra for the PA calculations to Support the WIPP CCA*. Memorandum to M.S. Tierney, Sandia National Laboratories, Albuquerque, New Mexico, July 24, 1996, ERMS 241561.
- Brush, L.H., and Y. Xiong. 2003a. *Calculation of Actinide Solubilities for the WIPP Compliance Recertification Application*. Sandia National Laboratories Carlsbad Programs Group, Carlsbad, New Mexico, May 8, 2003, ERMS 529131.
- Brush, L.H., and Y. Xiong. 2003b. *Calculation of Actinide Solubilities for the WIPP Compliance Recertification Application, Analysis Plan AP 098, Rev 1*. Sandia National Laboratories, Carlsbad, New Mexico, ERMS 527714.
- Brush, L.H., and Y. Xiong. 2003c. *Calculation of Organic Ligand Concentrations for the WIPP Compliance Recertification Application*. Sandia National Laboratories, Carlsbad, New Mexico, ERMS 527567.
- Brush, L.H., and Y. Xiong. 2003d. *Calculation of Organic Ligand Concentrations for the WIPP Compliance Recertification Application and for Evaluating Assumptions of Homogeneity in WIPP PA*. Sandia National Laboratories, Carlsbad, New Mexico, ERMS 531488.
- Brush, L.H., and Y. Xiong. 2004. *Sensitivities of the Solubilities of +III, +IV, and +V Actinides to the Concentrations of Organic Ligands in WIPP Brines. Rev. 0*, Sandia National Laboratories, Carlsbad, New Mexico, December 15, 2004, ERMS 538203.

Brush, L.H., and Y. Xiong. 2005a. *Calculation of Actinide Solubilities for the WIPP Performance-Assessment Baseline Calculations. Analysis Plan AP-120, Rev. 0.* Sandia National Laboratories, Carlsbad, New Mexico, ERMS 539255.

Brush, L.H., and Y. Xiong. 2005b. *Calculation of Organic-Ligand Concentrations for the WIPP Performance-Assessment Baseline Calculations.* Sandia National Laboratories, Carlsbad, New Mexico, ERMS 539635.

Brush, L.H. and Y. Xiong. 2009. *Calculation of Organic-Ligand Concentrations for the WIPP CRA-2009 PABC.* Sandia National Laboratories, Carlsbad, New Mexico, ERMS 551481.

Brush, L.H., Y. Xiong, J.W. Garner, A. Ismail, and G.T. Roselle. 2006. *Consumption of Carbon Dioxide by Precipitation of Carbonate Minerals Resulting from Dissolution of Sulfate Minerals in the Salado Formation in Response to Microbial Sulfate Reduction in the WIPP.* Sandia National Laboratories, Carlsbad, New Mexico, ERMS 544785.

Brush, L.H., Y. Xiong, J.W. Garner, T.B. Kirchner and J.J. Long. 2008. *Sensitivity of the Long-Term Performance of the WIPP to EDTA.* Sandia National Laboratories, Carlsbad, New Mexico, ERMS 548398.

Brush, L.H., Y. Xiong, and J.J. Long. 2009. *Results of the Calculations of Actinide Solubilities for the WIPP CRA-2009 PABC.* Sandia National Laboratories, Carlsbad, New Mexico, ERMS 552201.

Bryan, C.R., and A.C. Snider. 2001a. *MgO Hydration and Carbonation at SNL/Carlsbad, Sandia National Laboratories Technical Baseline Reports, WBS 1.3.5.4, Repository Investigations, Milestone RI010, January 31, 2001.* Sandia National Laboratories, Carlsbad, New Mexico, ERMS 516749, pp. 66 to 83.

Bryan, C.R., and A.C. Snider. 2001b. *MgO Experimental Work Conducted at SNL/CB: Continuing Investigations with Premier Chemicals MgO, Sandia National Laboratories Technical Baseline Reports, WBS 1.3.5.4, Repository Investigations, Milestone RI020, July 31, 2001.*

Byrne, R.H., and S.W. Thompson. 1997. Ferric borate formation in aqueous solution. *Journal of Solution Chemistry* 26:729-734.

Choppin, G.R. 1991. Redox Speciation of Plutonium in Natural Waters. *Journal of Radioanalytical and Nuclear Chemistry Articles*, 147:109-116.

Choppin, G.R., A.H. Bond, M. Borkowski, M. Bronikowski, J.-F. Chen, S. Lis, J. Mizera, O.S. Pokrovsky, N.A. Wall, Y.X. Xia, and R.C. Moore. 2001. *Waste Isolation Pilot Plant Actinide Source Term Test Program: Solubility Studies and Development of Modeling Parameters.* Sandia National Laboratories, Albuquerque, New Mexico, April 2001, SAND99-0943.

Clayton, D. 2008. *Update to the Calculation of the Minimum Brine Volume for a Direct Brine Release.* Memorandum to L. Brush, Sandia National Laboratories, Carlsbad, New Mexico, April 2, 2008.

Clayton, D. 2009. *Update to the K_d Values for the PABC-2009*. Sandia National Laboratories, Carlsbad, New Mexico, ERMS 552395.

Clayton, D. 2010. *Update to the Actinide(III) Solubility Uncertainty Distribution*. Sandia National Laboratories, Carlsbad, New Mexico, ERMS 553405.

Clayton, D. and M. Nemer. 2006. *Normalized Moles of Castile Sulfate Entering the Repository and Fraction of MgO Lost Due to Brine Flow Out of the Repository*. Memorandum to E.D. Vugrin, Sandia National Laboratories, Carlsbad, New Mexico, October 9, 2006.

Cotsworth, E. 2004a. *CRA Completeness Comments - 3rd set - August 2004*. U.S. Environmental Protection Agency Office of Radiation and Indoor Air, Washington DC, letter (with enclosure) to R. Paul Detwiler, U.S. Department of Energy Carlsbad Field Office, September 2, 2004. Docket A-98-49, Item II-B3-74.

Cotsworth, E. 2004b. *First Set of CRA Comments (with enclosure)*. U.S. Environmental Protection Agency Office of Radiation and Indoor Air, Washington DC, letter to R. Paul Detwiler, U.S. Department of Energy Carlsbad Field Office, May 20, 2004. Docket A-98-49, Item II-B3-72.

Cotsworth, E. 2005. *EPA Letter on Conducting the Performance Assessment Baseline Change (PABC) Verification Test*. Environmental Protection Agency Office of Radiation and Indoor Air, Washington DC., letter (with enclosure) to Inés Triay, U.S. Department of Energy, Carlsbad Field Office. March 4, 2005, ERMS 538858. Docket A-98-49, Item II-B3-80.

Cotsworth, E. 2009a. *CRA-2009 First (1) Completeness Letter*. U.S. Environmental Protection Agency Office of Radiation and Indoor Air, letter to D. Moody, U.S. Department of Energy Carlsbad Field Office, May 21, 2009. Regulations.gov EDOCKET ID# EPA-HQ-OAR-2009-0330-0004.

Cotsworth, E. 2009b. *CRA-2009 Second Completeness Letter*. U.S. Environmental Protection Agency Office of Radiation and Indoor Air, letter to D. Moody, U.S. Department of Energy Carlsbad Field Office, July 16, 2009. Regulations.gov EDOCKET ID# EPA-HQ-OAR-2009-0330-0005.

Cotsworth, E. 2009c. *CRA-2009 Third Completeness Letter*. U.S. Environmental Protection Agency Office of Radiation and Indoor Air, letter to D. Moody, U.S. Department of Energy Carlsbad Field Office, October 19, 2009. Regulations.gov EDOCKET ID# EPA-HQ-OAR-2009-0330-0006.

Crawford, B., D. Guerin, S. Lott, B. McInroy, J. McTaggart, and G. Van Soest. 2009. *Performance Assessment Inventory Report – 2008*. INV-PA-08, Revision 0, Los Alamos National Laboratory Carlsbad Operations, LA-UR-09-02260, April 23, 2009.

Crawford, B.A., and C.D. Leigh. 2003. *Estimate of Complexing Agents in TRU Waste for the Compliance Recertification Application*. Los Alamos National Laboratory, Carlsbad, New Mexico, ERMS 531107.

Deng, H., S. Johnsen, Y. Xiong, G.T. Roselle, and M. Nemer. 2006. *Analysis of Martin Marietta MagChem® 10 WTS-60 MgO*. Sandia National Laboratories, Carlsbad, New Mexico. ERMS 544712.

Deng, H., M.B. Nemer, and Y. Xiong. 2007. *Experimental Study of MgO Reaction Pathways and Kinetics (Rev. 1, January 10)*. TP 06-03, Sandia National Laboratories, Carlsbad, New Mexico, ERMS 545182.

Deng, H., Y. Xiong, M. Nemer, and S. Johnsen. 2009. *Experimental Work Conducted on MgO Long-Term Hydration, 2008 Milestone Report*. Sandia National Laboratories, Carlsbad, New Mexico, ERMS 551421.

Detwiler, R.P. 2004a. *MgO Emplacement*. U.S. Department of Energy Carlsbad Field Office, letter to Elizabeth Cotsworth, U.S. Environmental Protection Agency Office of Radiation and Indoor Air, Washington DC, October 20, 2004. Docket A-98-49, Item II-B2-38.

Detwiler, R.P. 2004b. *Partial Response to Environmental Protection Agency (EPA) May 20, 2004 Letter on CRA, Enclosure 1*. U.S. Department of Energy Carlsbad Field Office, Letter to Elizabeth Cotsworth, U.S. Environmental Protection Agency Office of Radiation and Indoor Air, Washington, DC, August 16, 2004. Docket A-98-49, Item II-B2-35.

Detwiler, R.P. 2004c. *Partial Response to Environmental Protection Agency (EPA) September 2, 2004, Letter on Compliance Recertification Application*. U.S. Department of Energy Carlsbad Field Office, Letter to Elizabeth Cotsworth, U.S. Environmental Protection Agency Office of Radiation and Indoor Air, Washington, DC, December 23, 2004. Docket A-98-49, Item II-B2-40.

Detwiler, R.P. 2004d. *Response to EPA May 20, 2004, Letter on CRA*. U.S. Department of Energy Carlsbad Field Office, letter to Elizabeth Cotsworth, U.S. Environmental Protection Agency Office of Radiation and Indoor Air, Washington, DC, September 29, 2004. Docket A-98-49, Item II-B2-37.

Díaz Arocas, P., and B. Grambow. 1998. Solid-Liquid Phase Equilibria of U(VI) in NaCl Solutions. *Geochimica et Cosmochimica Acta* 62:245-263.

Ding, M., J.L. Conca, C. den Auwer, R.I. Gabitov, N.J. Hess, P. Paviet-Hartmann, P.D. Palmer, V. LoPresti, and S.D. Conradson. 2006. Chemical speciation of heterogeneously reduced Pu in synthetic brines. *Radiochimica Acta* 94:249-259.

Dodge, C.J., A.J. Francis, J.B. Gillow, G.P. Halada, C. Eng, and C.R. Clayton. 2002. Association of uranium with iron oxides typically formed on corroding steel surfaces. *Environmental Science and Technology* 36:3504–3511.

DOE (U.S. Department of Energy) 1996. *Title 40 CFR Part 191 Compliance Certification Application for the Waste Isolation Pilot Plant*, DOE/CAO-1996-2184, October 1996, Carlsbad Field Office, Carlsbad, New Mexico.

DOE (U.S. Department of Energy) 2004. *Title 40 CFR 191 Parts B and C Compliance Recertification Application*. U.S. Department of Energy Carlsbad Field Office, March 2004.

DOE (U.S. Department of Energy) 2009. *Title 40 CFR 191 Parts B and C Compliance Recertification Application*. U.S. Department of Energy Carlsbad Field Office, March 2009.

DOE (Department of Energy). 2010. *EPA-Provided Comment: Stakeholder Comment Received at the May 12, 2010 Stakeholder Meeting in Albuquerque. DOE Response*.

Ekberg, C., Y. Albinsson, M.J. Comarmond and P.L. Brown. 2000. Studies on the complexation behavior of thorium(IV). 1. Hydrolysis equilibria. *Journal of Solution Chemistry* 29:63-86.

EPA (Environmental Protection Agency) 1997a. *Compliance Application Review Documents for the Criteria for the Certification and Recertification of the Waste Isolation Pilot Plant's Compliance with the 40 CFR Part 191 Disposal Regulations: Final Certification Decision. CARD 23: Models and Computer Codes*. U.S. Environmental Protection Agency Office of Radiation and Indoor Air. Washington, DC. Docket A-93-02, Item V-B-2.

EPA (Environmental Protection Agency) 1997b. *Compliance Application Review Documents for the Criteria for the Certification and Recertification of the Waste Isolation Pilot Plant's Compliance with the 40 CFR Part 191 Disposal Regulations: Final Certification Decision CARD 24: Waste Characterization*. U.S. Environmental Protection Agency Office of Radiation and Indoor Air. Washington, DC. Docket A-93-02, Item V-B-2.

EPA (U.S. Environmental Protection Agency) 1997c. *Compliance Application Review Documents for the Criteria for the Certification and Recertification of the Waste Isolation Pilot Plant's Compliance with the 40 CFR Part 191 Disposal Regulations: Final Certification Decision. CARD 44: Engineered Barrier*. EPA Air Docket A-93-02, Item V-B-2. U.S. Environmental Protection Agency Office of Radiation and Indoor Air. Washington, DC.

EPA (U.S. Environmental Protection Agency) 1998a. *Final WIPP Certification Decision Response to Comments, Criteria for the Certification of the Waste Isolation Pilot Plant's Compliance with 40 CFR Part 191 Disposal Regulations: Certification Decision*. Office of Radiation and Indoor Air, Washington DC. Docket No. A-93-02, Item V-C-1.

EPA (U.S. Environmental Protection Agency) 1998b. *Technical Support Document for Section 194.14: Assessment of K_d s used in the CCA*. U.S. Environmental Protection Agency Office of Radiation and Indoor Air, Washington DC. Docket A-93-02, Item V-B-4.

EPA (U.S. Environmental Protection Agency) 1998c. *Technical Support Document for Section 194.23: Parameter Justification Report*. Environmental Protection Agency Office of Radiation and Indoor Air, Washington, DC. Docket A-93-02, Item V-B-14.

EPA (U.S. Environmental Protection Agency) 1998d. *Technical Support Document for Section 194.24: EPA's Evaluation of DOE's Actinide Source Term*. Environmental Protection Agency Office of Radiation and Indoor Air, Washington, DC. Docket A-93-02, Item V-B-17.

EPA (U.S. Environmental Protection Agency) 1998e. *Technical Support Document Overview of Major Performance Assessment Issues*. Environmental Protection Agency Office of Radiation and Indoor Air, Washington, DC. Docket A-93-02, Item V-B-5.

EPA (U.S. Environmental Protection Agency) 2001a. *Approval of Elimination of Minisacks*. Environmental Protection Agency Office of Radiation and Indoor Air, Washington, DC. Docket A-98-49, II-B3-15.

Environmental Protection Agency (EPA) 2001b. *MgO Minisack Review*. U.S. Environmental Protection Agency Office of Radiation and Indoor Air, Washington, DC. ERMS 519362 (US EPA 2001a, enclosure).

EPA (U.S. Environmental Protection Agency) 2006a. *Criteria for the Certification and Recertification of the Waste Isolation Pilot Plant's Compliance With the Disposal Regulations: Recertification Decision*. *Federal Register* 71:18010-18021, April 10.

EPA (Environmental Protection Agency) 2006b. *Technical Support Document for Section 194.23: Review of the 2004 Compliance Recertification Performance Assessment Baseline Calculation*. Office of Radiation and Indoor Air, Docket No. A-98-49, Item II-B1-3, March 2006.

EPA (U.S. Environmental Protection Agency) 2006c. *Technical Support Document for Section 194.24: Evaluation of the Compliance Recertification Actinide Source Term and Culebra Dolomite Distribution Coefficient Values*. Office of Radiation and Indoor Air, Docket No. A-98-49, Item II-B1-16, March 2006.

EPA (U.S. Environmental Protection Agency) 2006d. *Technical Support Document for Section 194.24: Review of the Baseline Inventory Used in the Compliance Recertification Application and the Performance Assessment Baseline Calculation*. Office of Radiation and Indoor Air, Docket No. A-98-49, Item II-B1-9, March 2006.

Fanghänel, T., T. Könecke, H.T. Weger, P. Paviet-Hartmann, V. Neck and J.I. Kim. 1999. Thermodynamics of Cm(III) in Concentrated Salt Solutions: Carbonate Complexation in NaCl Solution at 25 C. *Journal of Solution Chemistry* 28:447-462.

Felicione, F.S., K.P. Carney, and C.C. Dwight. 2001. Results from the Gas Generation Experiments at Argonne National Laboratory-West. *Sandia National Laboratories Technical Baseline Reports, WBS 1.3.5.4, Repository Investigations Milestone R1020, July 31, 2001*. Sandia National Laboratories, Carlsbad, New Mexico, ERMS 518970, pp. 2-1 to 2-5.

Felmy, A.R., H. Cho, D.A. Dion, Y. Xia, N.J. Hess and Z. Wang. 2006. The aqueous complexation of thorium with citrate under neutral to basic conditions. *Radiochimica Acta* 94:205-212.

Felmy, A.R., R.C. Moore, Z. Wang, D. Rai, and D.A. Dixon. 2000. Understanding actinide oxidation/reduction reactions: relevance to the WIPP repository. *219th American Chemical Society Meeting, San Francisco, March 26-30*.

- Felmy, A.R., D. Rai, and R.W. Fulton. 1990. The solubility of $\text{AmOHCO}_3(\text{c})$ and the aqueous thermodynamics of the system $\text{Na}^+\text{-Am}^{3+}\text{-HCO}_3^-\text{-H}_2\text{O}$. *Radiochimica Acta* 50:193-204.
- Felmy, A.R., D. Rai and M.J. Mason. 1991. The solubility of hydrous thorium(IV) oxide in chloride media: development of an aqueous ion-interaction model. *Radiochimica Acta* 55:177-185.
- Felmy, A.R., D. Rai, J.A. Schramke, and J.L. Ryan. 1989. The solubility of plutonium hydroxide in dilute solutions and in high-ionic-strength chloride brines. *Radiochimica Acta* 48:29-35.
- Felmy, A.R., D. Rai, M.S. Sterner, M.J. Mason, N.J. Hess and S.D. Conradson. 1997. Thermodynamic models for highly charged aqueous species: solubility of Th(IV) hydrous oxide in concentrated NaHCO_3 and Na_2CO_3 solutions. *Journal of Solution Chemistry* 26:233-248.
- Fiedor, J.N., W.D. Bostick, R.J. Jarabek, and J. Farrell. 1998. Understanding the mechanism of uranium removal from groundwater by zero-valent iron using X-ray photoelectron spectroscopy. *Environmental Science and Technology* 32:1466-1473.
- Fox, B. 2008. *Parameter Summary Report for the CRA-2009*. Rev. 0, Sandia National Laboratories, Carlsbad, New Mexico, ERMS 549747.
- Fox, B. and D. Clayton. 2010. *Analysis Package for EPA Unit Loading Calculations: CRA-2009 Performance Assessment Baseline Calculation*. Sandia National Laboratories, Carlsbad, New Mexico, ERMS 552912.
- Francis, A.J., and C.J. Dodge. 2008. Bioreduction of uranium(VI) complexed with citric acid by *clostridia* affects its structure and solubility. *Environmental Science and Technology* 42:8277-8282.
- Francis, A.J., C.J. Dodge, J.B. Gillow, and H.W. Papenguth. 2000. Biotransformation of uranium compounds in high ionic strength brine by a halophilic bacterium under denitrifying conditions. *Environmental Science and Technology* 34:2311-2317.
- Francis, A.J., and J.B. Gillow. 1994. *Effects of Microbial Processes on Gas Generation Under Expected Waste Isolation Pilot Plant Repository Conditions*. Progress Report through 1992. Sandia National Laboratories, Albuquerque, New Mexico, SAND93-7036, WPO 26555.
- Francis, A.J., and J.B. Gillow. 2000. *Progress Report: Microbial Gas Generation Program*. Unpublished memorandum to Y. Wang, January 6, 2000. Brookhaven National Laboratory, Upton, New York, ERMS 509352.
- Francis A.J., J.B. Gillow, and M.R. Giles. 1997. *Microbial Gas Generation Under Expected Waste Isolation Pilot Plant Repository Conditions*. Sandia National Laboratories, Albuquerque, New Mexico, SAND96-2582.

Frederickson, J.K., J.M. Zachara, D.W. Kennedy, M.C. Duff, Y.A. Gorby, S.-M. W. Li, and K. Krupka. 2000. Reduction of U(VI) in goethite (α -FeOOH) suspensions by a dissimilatory metal-reducing bacterium. *Geochimica et Cosmochimica Acta* 64:3085-3098.

Garner, J. and C. Leigh 2005. *Analysis Package for PANEL: CRA-2004 Performance Assessment Baseline Calculation*. ERMS 540572. Sandia National Laboratories.

Giambalvo, E.R. 2002a. *Recommended Parameter Values for Modeling An(III) Solubility in WIPP Brines*. Memorandum to L.H. Brush, July 25, 2002, ERMS 522982.

Giambalvo, E.R. 2002b. *Recommended Parameter Values for Modeling Organic Ligands in WIPP Brines*. Memorandum to L.H. Brush, July 25, 2002, ERMS 522981.

Giambalvo, E.R. 2002c. *Recommended Parameter Values for Modeling An(IV) Solubility in WIPP Brines*. Memorandum to L.H. Brush, July 26, 2002, ERMS 522986.

Giambalvo, E.R. 2002d. *Recommended Parameter Values for Modeling An(V) Solubility in WIPP Brines*. Memorandum to L.H. Brush, July 26, 2002, ERMS 522990.

Giambalvo, E.R. 2002e. *Recommended μ^0/RT Values for Modeling the Solubility of Oxalate Solids in WIPP Brines*. Memorandum to L.H. Brush, July 31, 2002, ERMS 523057.

Giambalvo, E.R. 2003. *Release of FMT Database FMT_021120.CHEMDAT*. Memorandum to L.H. Brush, March 10, 2003, ERMS 526372.

Gillow, J.B., and A.J. Francis. 2001a. Re-evaluation of Microbial Gas Generation Under Expected Waste Isolation Pilot Plant Conditions: Data Summary Report, January 24, 2001, *Sandia National Laboratories Technical Baseline Reports, WBS 1.3.5.4, Repository Investigations Milestone RI010, January 31, 2001*. Sandia National Laboratories, Carlsbad, New Mexico, ERMS 516749, pp. 19–46.

Gillow, J.B., and A.J. Francis. 2001b. Re-evaluation of Microbial Gas Generation Under Expected Waste Isolation Pilot Plant Conditions: Data Summary and Progress Report (February 1 - July 13, 2001), *Sandia National Laboratories Technical Baseline Reports, WBS 1.3.5.4, Repository Investigations Milestone RI020, July 31, 2001*. Sandia National Laboratories, Carlsbad, New Mexico, ERMS 518970, pp. 3-1 to 3-21.

Gillow J.B., and A.J. Francis. 2002a. Re-evaluation of Microbial Gas Generation Under Expected Waste Isolation Pilot Plant Conditions: Data Summary and Progress Report (July 14, 2001 - January 31, 2002), January 22, 2002. *Sandia National Laboratories Technical Baseline Reports, WBS 1.3.5.3, Compliance Monitoring; WBS 1.3.5.4, Repository Investigations, Milestone RI110, January 31, 2002*. Sandia National Laboratories, Carlsbad, New Mexico, ERMS 520467, pp. 2.1-1 to 2.1-26.

Gillow, J.B., and A.J. Francis. 2002b. Re-evaluation of Microbial Gas Generation Under Expected Waste Isolation Pilot Plant Conditions: Data Summary and Progress Report (February 1–July 15, 2002), January 18, 2002. *Sandia National Laboratories Technical Baseline Reports, WBS 1.3.5.3, Compliance Monitoring; WBS 1.3.5.4, Repository Investigations, Milestone RI130,*

July 31, 2002. Sandia National Laboratories, Carlsbad, New Mexico, ERMS 523189, pp. 3.1-1 to 3.1-A10.

Gillow, J., and A.J. Francis. 2003. *Microbial Gas Generation Under Expected Waste Isolation Pilot Plant Repository Conditions*. Final Report, Revision 0, October 6 Draft, ERMS 532877.

Gitlin, B.C. 2006. U.S. Environmental Protection Agency, Office of Air and Radiation, Washington, DC. Letter to D.C. Moody, U.S. Department of Energy, Carlsbad Field Office, Carlsbad, New Mexico. April 28, 2006. Docket A-98-49, Item II-B3-96.

Grambow, B., E. Smailos, H. Geckeis, R. Müller, and H. Hentschel. 1996. Sorption and Reduction of Uranium(VI) on Iron Corrosion Products under Reducing Saline Conditions. *Radiochimica Acta* 74:149-154.

Gu, B., L. Liang, M.J. Dickey, X. Yin, and S. Dai. 1998. Reductive precipitation of uranium (VI) by zero-valent iron. *Environmental Science and Technology* 32:3366-3373.

Hansen, C.W., L.H. Brush, M.B. Gross, F.D. Hansen, B. Thompson, J.S. Stein, and B-Y Park 2003a. *Effects of Supercompacted Waste and Heterogeneous Waste Emplacement on Repository Performance, Rev. 0*. Sandia National Laboratories Carlsbad Programs Group, Carlsbad, New Mexico, October 7, 2003.

Hansen, C.W., L.H. Brush, M.B. Gross, F.D. Hansen, B-Y Park, J.S. Stein, and B. Thompson 2003b. *Effects of Supercompacted Waste and Heterogeneous Waste Emplacement on Repository Performance, Rev. 1*. Sandia National Laboratories Carlsbad Programs Group, Carlsbad, New Mexico, October 17, 2003, ERMS 532475.

Hansen, C. and C. Leigh. 2003. *A Reconciliation of the CCA and PAVT Parameter Baselines*. Revision 3, Sandia National Laboratories, Carlsbad, New Mexico, April 11, 2003, ERMS 528582.

Haschke, J.M., T.H. Allen, and L.A. Morales. 2000. Reaction of Plutonium Dioxide with Water: Formation and Properties of PuO_{2+x} . *Science* 287:285-287.

Hobart, D.E., C.J. Bruton, F.J. Millero, I-M. Chou, K.M. Trauth, and D.R. Anderson. 1996. *Estimates of the Solubilities of Waste Element Radionuclides in Waste Isolation Pilot Plant Brines: A Report by the Expert Panel on the Source Term*. Sandia National Laboratories, Albuquerque, New Mexico and Livermore, California, SAND96-0098, March.

Hobart, D.E., and R.C. Moore. 1996. *Analysis of Uranium (VI) Solubility Data for WIPP Performance Assessment WBS 1.1.10.1.1*. Sandia National Laboratories, May 28, 1996, ERMS 239856.

Hua, B., J. Xu, J. Terry, and B. Deng. 2006. Kinetics of uranium(VI) reduction by hydrogen sulfide in anoxic aqueous systems. *Environmental Science and Technology* 40:4666-4671.

Icopini, G.A., J. Boukhalfa, and M.P. Neu. 2007. Biological reduction of Np(V) and Np(V) citrate by metal-reducing bacteria. *Environmental Science and Technology* 41:2764-69.

- Icopini, G.A., J.G. Lack, L.E. Hersman, M.P. Neu and H. Boukhalfa. 2009. Plutonium(V/VI) reduction by the metal-reducing bacteria *Geobacter metallireducens* GS-15 and *Shewanella oneidensis* MR-1. *Applied and Environmental Microbiology* 75:3641-3647.
- Ismail, A.E., M.B. Nemer, G.T. Roselle and Y. Xiong. 2008. *Iron, Lead, Sulfide and EDTA Solubilities*. Test Plan TP 08-02, Rev. 0, Sandia National Laboratories, Carlsbad, New Mexico.
- Kanney, J.F., A.C. Snider, T.W. Thompson, and L.H. Brush. 2004. *Effect of Naturally Occurring Sulfate on the MgO Safety Factor in the Presence of Supercompacted Waste and Heterogeneous Waste Emplacement*. Sandia National Laboratories Carlsbad Programs Group, Carlsbad, New Mexico, March 5, 2004.
- Kanney, J.F. and E.D. Vugrin, 2006. *Updated Analysis of Characteristic Time and Length Scales for Mixing Processes in the WIPP Repository to Reflect the CRA-2004 PABC Technical Baseline and the Impact of Supercompacted Mixed Waste and Heterogeneous Waste Emplacement*. Memorandum to D.S. Kessel, Sandia National Laboratories, Carlsbad, New Mexico, August 31, 2006.
- Kelly, T.E. 2010. *Fourth WIPP Completeness Letter*. U.S. Environmental Protection Agency, Letter to D. Moody, U.S. Department of Energy, February 22, 2010.
- Khalili, F.K., V. Symeopoulos, J.F. Chen and G.R. Choppin. 1994. Solubility of Nd in brine. *Radiochimica Acta* 66/67:51-54.
- Kim, J.I., M. Bernkopf, C. Lierse and F. Koppold. 1984. Hydrolysis reactions of Am(III) and Pu(VI) ions in near-neutral solutions. In *Geochemical Behavior of Disposed Radioactive Waste*, Eds. G.S. Barney, J.D. Navratil, and W.W. Schultz, Washington, D.C. ACS Symposium Series 246:115-134
- Kirchner, T. 2008. *Generation of the LHS Samples for the AP-137 Revision 0 (CRA09) PA Calculations*. Sandia National Laboratories, Carlsbad, New Mexico, ERMS 547971.
- Kirchner, T. 2010. *Sensitivity of the CRA-2009 Performance Assessment Baseline Calculation Releases to Parameters*. Sandia National Laboratories, Carlsbad, New Mexico, ERMS 552960.
- Kirchner, T., and E. Vugrin, 2006. *Uncertainty in Cellulose, Plastic, and Rubber Measurements for the Waste Isolation Pilot Plant Inventory*. Sandia National Laboratories, Carlsbad, New Mexico. ERMS 543848.
- Könnecke, T., T. Fanghänel, and J.I. Kim, 1997. Thermodynamics of trivalent actinides in concentrated electrolyte solutions: Modelling the chloride complexation of Cm(III). *Radiochimica Acta* 76:131-135.
- Krumhansl, J.L., Kelly, J.W., Papenguth, H.W., and R.V. Bynum. 1997. *MgO Acceptance Criteria*. Unpublished memorandum to E.J. Nowak, December 10, 1997. Sandia National Laboratories, Albuquerque, New Mexico, ERMS 248997.

Lambert, S.J. 1992. Geochemistry of the Waste Isolation Pilot Plant (WIPP) site, southeastern New Mexico, USA. *Applied Geochemistry* 7:513-531.

Larson, K.W. 1996. *Brine-Waste Contact Volume for Scoping Analysis of Organic Ligand Concentration*. Unpublished memorandum to R.V. Bynum, Sandia National Laboratories, Albuquerque, New Mexico, March 13, 1996, ERMS 236044.

Leigh, C. 2003. *Estimate of Cellulosics, Plastics, and Rubbers in a Single Panel in the WIPP Repository in Support of AP-107, Supersedes ERMS 530959*. Unpublished Analysis Report. Sandia National Laboratories, Carlsbad, New Mexico, ERMS 531324.

Leigh, C.D. 2005. *Organic Ligand Masses TRU Waste Streams from TWBID Revision 2.1 Version 3.13 Data Version D4.15, Revision 1*. Memorandum to L.H. Brush, Sandia National Laboratories, April 18, 2005, ERMS 539550.

Leigh, C., J. Kanney, L. Brush, J. Garner, R. Kirkes, T. Lowry, M. Nemer, J. Stein, E. Vugrin, S. Wagner, and T. Kirchner. 2005a. *2004 Compliance Recertification Application Performance Assessment Baseline Calculation*. Sandia National Laboratories, Carlsbad, New Mexico, ERMS 541521.

Leigh, C.D., J.R. Trone and B. Fox. 2005b. *TRU Waste Inventory for the 2004 Compliance Recertification Application Performance Assessment Baseline Calculation*. Sandia National Laboratories, Carlsbad, New Mexico. ERMS 541118.

Lichtner, P.C. 2007. *Interim Report on Geochemical Interactions at the WIPP Disposal Site*. Los Alamos National Laboratory LA-UR-07-6165, October 15, 2007.

Lin, M.R., P. Paviet-Hartmann, Y. Xu, and W.H. Runde. 1998. Uranyl Compounds in NaCl Solutions: Structure, Solubility and Thermodynamics. *American Chemical Society, Division of Environmental Chemistry, Preprints of Extended Abstracts*. 216th ACS National Meeting, Boston Massachusetts, August 23-27, 38:208.

Lovley, D.R., and E.J.P. Phillips. 1992. Reduction of uranium by *desulfovibrio desulfuricans*. *Applied and Environmental Microbiology* 58:850-856.

Lucchini, J.F., M. Borkowski, M.K. Richmann, and D.T. Reed. 2005. *Interactions and Stability of Hypochlorite, Hydrogen Peroxide and Uranium(VI) in Brine*. LA-UR-05-7009, poster presentation at Migration 05 Conference, Avignon, France, September 18-23, 2005.

Lucchini, J.F., H. Khaing, M. Borkowski, M.K. Richmann, and D.T. Reed. 2010. *Actinide (VI) Solubility in Carbonate-free WIPP Brine: Data Summary and Recommendations*. LCO-ACP-10, LANL\ACRSP Report. Los Alamos National Laboratory, Los Alamos, New Mexico. Cited in the text of DOE (2009) as Lucchini et al. 2009 and as Lucchini et al. 2008 in the reference list.

Madic, C. 2000. Plutonium Chemistry: Toward the End of PuO₂'s Supremacy? *Science* 287:243-244.

Marcinowski, F. 2004. U.S. Environmental Protection Agency Office of Radiation and Indoor Air, Washington DC, letter to R. Paul Detwiler, U.S. Department of Energy Carlsbad Field Office, March 26, 2004.

Meinrath, D., and J.I. Kim. 1991. Solubility products of different Am(III) and Nd(III) carbonates. *European Journal of Solid State and Inorganic Chemistry* 28:383-388.

Meinrath, D., and H. Takeishi. 1993. Solid-liquid equilibria of Nd³⁺ in carbonate solutions. *Journal of Alloys and Compounds* 194:93-99.

MFG. 2000. *Evaluation of the Reported Presence of Oxidized Plutonium in the STTP Experiments and in Plutonium Oxide Solid*. Prepared for the U.S. Environmental Protection Agency Office of Radiation and Indoor Air by MFG Inc., Boulder, Colorado, in association with TechLaw Inc., Lakewood, Colorado and Monitor Scientific, Denver, Colorado.

Millero, F.J. 1999. Modeling the Effect of Ionic Interactions on Radionuclides in Natural Waters, in *Actinide Speciation in High Ionic Strength Media*, D.T. Reed, S. B. Clark, and L. Rao, Eds., Kluwer Academic/Plenum Publishers, pp. 39 to 61.

Moody, D.C. 2006. U.S. Department of Energy, Carlsbad Field Office, Letter to E.A. Cotsworth, U.S. Environmental Protection Agency, requesting a reduction in the MgO EF from 1.67 to 1.2. April 10, 2006. ERMS 543262.

Moody, D.C. 2009a. *Response to Environmental Protection Agency Letter dated May 21, 2009 Regarding Compliance Recertification Application*. U.S. Department of Energy, Carlsbad Field Office, Letter to E. Cotsworth, Office of Radiation and Indoor Air, Environmental Protection Agency, August 24, 2009. Regulations.gov EDOCKET ID# EPA-HQ-OAR-2009-0330-0007.

Moody, D.C. 2009b. *Response to Environmental Protection Agency May 21, 2009, and July 16, 2009, Letters on Compliance Recertification Application*. U.S. Department of Energy, Carlsbad Field Office, Letter to E. Cotsworth, Office of Radiation and Indoor Air, Environmental Protection Agency, September 30, 2009. Regulations.gov EDOCKET ID# EPA-HQ-OAR-2009-0330-0008.

Moody, D.C. 2009c. *Response to Environmental Protection Agency May 21, 2009 and July 16, 2009 Letters on the 2009 Compliance Recertification Application*. U.S. Department of Energy, Carlsbad Field Office, Letter to E. Cotsworth, Office of Radiation and Indoor Air, Environmental Protection Agency, November 25, 2009. Regulations.gov EDOCKET ID# EPA-HQ-OAR-2009-0330-0011.

Moody, D.C. 2010a. *Response to Environmental Protection Agency January 25, 2010 Email Regarding the Follow-Up Questions from the May 21, 2009 Letter on the 2009 Compliance Recertification Application*. U.S. Department of Energy, Carlsbad Field Office, Letter to M. Flynn, Office of Radiation and Indoor Air, Environmental Protection Agency, February 19, 2010. Regulations.gov EDOCKET ID# EPA-HQ-OAR-2009-0330-0014.

Moody, D.C. 2010b. *Response to Environmental Protection Agency October 19, 2009 Letter on the 2009 Compliance Recertification Application*. U.S. Department of Energy, Carlsbad Field

Office, Letter to E. Cotsworth, Office of Radiation and Indoor Air, Environmental Protection Agency, February 19, 2010. Regulations.gov EDOCKET ID# EPA-HQ-OAR-2009-0330-0014.

Moody, D.C. 2010c. *Response to the Environmental Protection Agency February 22, 2010 Letter*. U.S. Department of Energy, Carlsbad Field Office, Letter to M. Flynn, Office of Radiation and Indoor Air, Environmental Protection Agency, April 19, 2010. Regulations.gov EDOCKET ID# EPA-HQ-OAR-2009-0330-0018.

Moody, D.C. 2010d. *Response to the Environmental Protection Agency January 25, 2010 E-Mail and February 22, 2010 Letter*. U.S. Department of Energy, Carlsbad Field Office, Letter to M. Flynn, Office of Radiation and Indoor Air, Environmental Protection Agency, May 26, 2010. Regulations.gov EDOCKET ID# EPA-HQ-OAR-2009-0330-0026.

Neck, V., M. Altmaier and T. Fanghänel. 2007. Solubility of plutonium hydroxides/hydrous oxides under reducing conditions and in the presence of oxygen. *Comptes Rendus Chimie* 10:959-977.

Neck, V., M. Altmaier, T. Rabung, J. Lützenkirchen and T. Fanghänel. 2009. Thermodynamics of trivalent actinides and neodymium in NaCl, MgCl₂, and CaCl₂ solutions: solubility, hydrolysis, and ternary Ca-M(III)-OH complexes. *Pure and Applied Chemistry* 81:1555-1568.

Neck, V., R. Müller, M. Bouby, M. Altmaier, J. Rothe, M.A. Denecke, and J.I. Kim. 2002. Solubility of Amorphous Th(IV) Hydroxide-Application of LIBD to Determine the Solubility Product and EXAFS for Aqueous Speciation. *Radiochimica Acta* 90:485-494.

Neiss, J., B.D. Stewart, P.S. Nico, and S. Fendorf. 2007. Speciation-dependent microbial reduction of uranium within iron-coated sands. *Environmental Science and Technology* 41:7343-7348.

Nemer, M. 2005. *Updated Value of WAS_AREA:PROBDEG*. Sandia National Laboratories, Carlsbad, New Mexico. Memorandum to D.S. Kessel, April 20, 2005, ERMS 539441.

Nemer, M. 2008. *Procedure for Testing for the Periclase + Lime Content in Martin Marietta MgO Rev. 1*. Sandia National Laboratories, Carlsbad, New Mexico, November 17, 2008, ERMS 550455.

Nemer, M. 2009. *Adequacy of MgO Reactivity Test (EPA Re-Certification Question 1-C-2) and Interpreting MgO Reactivity Test Results Above 96 Mol %*. Sandia National Laboratories, Carlsbad, New Mexico, ERMS 551892.

Nemer, M. and D. Clayton. 2008. *Analysis Package for Salado Flow Modeling: 2009 Compliance Recertification Application Calculation*. Sandia National Laboratories, Carlsbad, New Mexico, ERMS 548607.

Nemer, M., and J. Stein. 2005. *Analysis Package for BRAGFLO: 2004 Compliance Recertification Application Performance Assessment Baseline Calculation*. Sandia National Laboratories, Carlsbad, New Mexico, ERMS 540527.

Nemer, M., J. Stein, and W. Zelinski. 2005. *Analysis Report for BRAGFLO Preliminary Modeling Results With New Gas Generation Rates Based Upon Recent Experimental Results*. Analysis Report, Sandia National Laboratories, Carlsbad, New Mexico, ERMS 539437.

Novak, C.F., 1996. *Preliminary Inorganic Model for Thorium Solubility in WIPP Brines, in Database File HMW_3Th5_960119.CHEMDAT*. Memo to E.J. Nowak, 19 January 1996, Sandia National Laboratories, Albuquerque, New Mexico. WPO #30930

Novak, C.F., I. Al Mahamid, K.A. Becraft, S.A. Carpenter, N. Hakem and T. Prussin. 1997. Measurement and thermodynamic modeling of Np(V) solubility in aqueous K₂CO₃ solutions to high concentrations. *Journal of Solution Chemistry* 26:681-697.

Novak, C.F. and R.C. Moore. 1996. *Estimates of Dissolved Concentrations for +III, +IV, +V, and +VI Actinides in a Salado and a Castile Brine under Anticipated Repository Conditions*. Memo to M.D. Siegel, March 28, 1996, Sandia National Laboratories, Albuquerque, New Mexico, CCA Ref. No. 479.

Novak, C.F., R.C. Moore and R.V. Bynum. 1996. *Prediction of Dissolved Actinide Concentrations in Concentrated Electrolyte Solutions: A Conceptual Model and Model Results for the Waste Isolation Pilot Plant (WIPP)*. SAND96-2695C, Sandia National Laboratories, Albuquerque, New Mexico, October 25, 1996, WPO 38628.

Nowak, E.J. 2005. *Recommended Change in the FMT Thermodynamic Data Base*. Memorandum to L.H. Brush, April 1, Sandia National Laboratories, Carlsbad, New Mexico, ERMS 539227.

Öhman, L.-O., and S. Sjöberg. 1985. On the insignificance of aluminum-borate complexes in aqueous solution. *Marine Chemistry* 17:91-97.

Ohnuki, T., T. Yoshida, T. Ozaki, N. Kozai, F. Sakamoto, T. Nankawa, Y. Suzuki and A.J. Francis. 2007. Chemical speciation and association of plutonium with bacteria, kaolinite clay, and their mixture. *Environmental Science and Technology* 41:3134-3139.

O'Loughlin, E.J., S.D. Kelly, R.E. Cook, R. Csencsits, and K.M. Kemner. 2003. Reduction of uranium(VI) by mixed iron(II)/iron(III) hydroxide (green rust): formation of UO₂ nanoparticles. *Environmental Science and Technology* 37:721-727.

Östholms, E., J. Bruno, and I. Grenthe. 1994. On the influence of carbonate on mineral dissolution. III. The solubility of microcrystalline ThO₂ in CO₂H₂O media. *Geochimica et Cosmochimica Acta* 58:613-623.

Oversby, V.M. 2000. *Plutonium Chemistry Under Conditions Relevant for WIPP Performance Assessment*. EEG-77, Prepared for the Environmental Evaluation Group by VMO Konsult, September 2000.

Palmer, C.E. 1996. Private communication to R. Van Bynum (SAIC/SNL) from C. Palmer (LLNL), dated February 27, 1996, reported by Hobart and Moore (1996).

Papenguth, H.W. 1996. *Parameter Record Package for Colloidal Actinide Source Term Parameters*. Memorandum to C.T. Stockman, Sandia National Laboratories, Albuquerque, New Mexico, May 7, 1996, ERMS 235850.

Papenguth, H.W. and Y.K. Behl. 1996. *Test Plan for Evaluation of Colloid-Facilitated Actinide Transport at the Waste Isolation Pilot Plant*. TP 96-01, Sandia National Laboratories, Albuquerque, New Mexico.

Peake, T. 2010. *Chemistry Comments and Questions as a Follow-Up to May 21, 2009 Completeness Letter*. U.S. Environmental Protection Agency, email to D. Moody, U.S. Department of Energy, January 25, 2010 with attachment.

Rai, D., and J.L. Ryan. 1985. Neptunium(IV) hydrous oxide solubility under reducing and carbonate conditions. *Inorganic Chemistry* 24: 247–251.

Rai, D., A.R. Felmy, D.A. Moore and M.J. Mason. 1995. The solubility of Th(IV) and U(IV) hydrous oxides in concentrated NaHCO_3 and Na_2CO_3 aqueous solutions. *Scientific Basis for Nuclear Waste Management XVIII*. Kyoto, Japan, pp. 1143–1150.

Rai, D., A.R. Felmy, S.M. Sterner, D.A. Moore, M.J. Mason and Novak. 1997. The solubility of Th(IV) and U(IV) hydrous oxides in concentrated NaCl and MgCl_2 solutions. *Radiochimica Acta* 79:239-247.

Rai, D., Y.A. Gorby, J.K. Frederickson, D.A. Moore and M. Yui. 2002. Reductive dissolution of $\text{PuO}_2(\text{am})$: the effect of Fe(II) and hydroquinone. *Journal of Solution Chemistry* 31:433-453.

Rabung, T., M. Altmaier, V. Neck and T. Fanghänel. 2008. A TRLFS study of Cm(III) hydroxide complexes in alkaline CaCl_2 solutions. *Radiochimica Acta* 96:551-560.

Rand, M., J. Fuger, I. Grenthe, V. Neck, and D. Rai. 2008. *Chemical Thermodynamics of Thorium*. OECD Nuclear Energy Agency Data Bank, Eds., OECD Publications, Issy-les-Moulineaux, France.

Rao, L.F., D. Rai and A.R. Felmy. 1996a. Solubility of $\text{Nd}(\text{OH})_3(\text{c})$ in 0.1 M NaCl aqueous solution at 25°C and 90°C. *Radiochimica Acta* 72:151-155.

Rao, L.F., D. Rai A.R. Felmy, R.W. Fulton and C.F. Novak. 1996b. Solubility of $\text{NaNd}(\text{CO}_3)_3 \cdot 6\text{H}_2\text{O}(\text{c})$ in concentrated Na_2CO_3 and NaHCO_3 solutions at 25°C and 90°C. *Radiochimica Acta* 75:141-147.

Rao, L., D. Rai, A.R. Felmy and C.F. Novak. 1999. Solubility of $\text{NaNd}(\text{CO}_3)_3 \cdot 6\text{H}_2\text{O}(\text{c})$ in mixed electrolyte ($\text{Na}-\text{Cl}-\text{CO}_3-\text{HCO}_3$) and synthetic brine solutions. In *Actinide Speciation in High Ionic Strength Media: Experimental and Modeling Approaches to Predicting Actinide Speciation and Migration in the Subsurface*. Proceedings of an American Chemical Society Symposium on Experimental and Modeling Studies of Actinide Speciation in Non-Ideal Systems. Held August 26-28, 1996 in Orlando, Florida. Eds. D.T. Reed, S.B. Clark and L. Rao. Kluwer Academic/Plenum Publishers, pp. 153-169.

Reed, D.T., J.F. Lucchini, S.B. Aase and A.J. Kropf. 2006. Reduction of plutonium(VI) in brine under subsurface conditions. *Radiochimica Acta* 94:591-597.

Reed, D.T., J.F. Lucchini, M. Borkowski, and M.K. Richmann. 2010. *Reduction of Higher-Valent Plutonium by Iron under Waste Isolation Pilot Plant (WIPP)-Relevant Conditions: Data Summary and Recommendations*. LCO-ACP-09, Rev. 0, LANL\ACRSP Report, Los Alamos National Laboratory, Los Alamos, New Mexico. Cited by DOE (2009) as Reed et al. (2009).

Reed, D.T., S.E. Pepper, M.K. Richmann, G. Smith, R. Deo, and B.E. Rittmann. 2007. Subsurface bio-mediated reduction of higher-valent uranium and plutonium. *Journal of Alloys and Compounds* 444/445:376–382.

Reed, D.T. and D.R. Wygmans. 1997. *Actinide Stability/Solubility in Simulated WIPP Brines*. Interim Report 3/21/97, Actinide Speciation and Chemistry Group, Chemical Technology Group, Argonne National Laboratory, Argonne, Illinois. WPO 44625.

Reed, D.T., D.R. Wygmans, S.B. Base, and J.E. Banaszak. 1997. *Reduction of Np(VI) and Pu(VI) by Organic Chelating Agents*. Sandia National Laboratories, SAND97-2845C.

Reyes, J. 2008. U.S. Environmental Protection Agency, Office of Air and Radiation, Washington DC, letter to D. Moody, U.S. Department of Energy Carlsbad Field Office, February 11, 2009.

Richman, M.K. 2008. *Eh/pH Diagrams for Am(III), Th(IV) and Np(V) Based on the FMT Database and Current PA Assumptions*. Letter report to D. Reed, Los Alamos National Laboratory, Carlsbad Operations, Carlsbad, New Mexico, November 21, 2008.

Rittmann, B.E., J.E. Banaszak, and D.T. Reed. 2002. Reduction of Np(V) and precipitation of Np(IV) by an anaerobic microbial consortium. *Biodegradation* 13:329–342.

Roselle, G.T. 2009. *Iron and Lead Corrosion in WIPP-Relevant Conditions: Six Month Results*. Sandia National Laboratories, Carlsbad, New Mexico.

Rothe, J., M.A. Denecke, V. Neck, R. Müller, and J.I. Kim. 2002. XAFS investigation of the structure of aqueous thorium(IV) species, colloids and solid thorium(IV) oxide/hydroxide. *Inorganic Chemistry* 41:249-258.

RSI (Institute for Regulatory Science). 2006. *Application of Magnesium Oxide as an Engineered Barrier at Waste Isolation Pilot Plant, Report of the Expert Panel*. RSI-06-01.

Runde, W., and J.I. Kim. 1995. *Untersuchungen der Übertragbarkeit von Labordaten Natürliche Verhältnisse: Chemisches Verhalten von Drei- und Fünfwertigem Americium in Salinen NaCl-Lösungen (Study of the Extrapolability of Laboratory Data to Natural Conditions: Chemical Behavior of Trivalent and Pentavalent Americium in Saline NaCl Solutions)*. RCM-01094, Institute for Radiochemistry, Technical University of Munich, Munich, Federal Republic of German, ERMS 241862.

Ryan J.L. and D. Rai. 1987. Thorium(IV) hydrous oxide solubility. *Inorganic Chemistry* 26:4140-4142.

SC&A (S. Cohen & Associates). 2000. *Implications Regarding the Efficacy of MgO Backfill Based on Preliminary Results of STTP Liter-Scale Experiment L-28*. Prepared for U.S. Environmental Protection Agency Office of Radiation and Indoor Air, September 4, 2000.

SC&A (S. Cohen & Associates). 2006. *Preliminary Review of the Degradation of Cellulosic, Plastic and Rubber Materials in the Waste Isolation Pilot Plant, and Possible Effects on Magnesium Oxide Safety Factor*. Prepared for the U.S. Environmental Protection Agency Office of Radiation and Indoor Air, August 21.

SC&A (S. Cohen & Associates). 2008a. *Review of MgO-Related Uncertainties in the Waste Isolation Pilot Plant*. Prepared for the U.S. Environmental Protection Agency Office of Radiation and Indoor Air, January 24.

SC&A (S. Cohen & Associates). 2008b. *Verification of the Waste Isolation Pilot Plant Chemistry Conceptual Models*. Prepared for the U.S. Environmental Protection Agency Office of Radiation and Indoor Air, September 19.

Schuessler, W., B. Kienzler, S. Wilhelm, V. Neck, and J.I. Kim. 2001. Modeling of Near Field Actinide Concentrations in Radioactive Waste Repositories in Salt Formations: Effect of Buffer Materials. *Materials Research Society Symposium Proceedings* 663:791-798.

Shchigol, M.B. and N.B. Burchinskaya. 1961. Properties of aluminum borates. *Russian Journal of Inorganic Chemistry* 6:1267-1271.

Silva, R.J. 1982. *The Solubilities of Crystalline Neodymium and Americium Trihydroxides*. LBL-15055. Lawrence Berkeley National Laboratory, Berkeley, California.

Slater, S.A., D.B. Chamberlain, S.A. Base, B.D. Babcock, C. Conner, J. Sedlet, and G.F. Vandegrift. 1997. Optimization of Magnetite Carrier Precipitation Process for Plutonium Waste Reduction. *Separation Science and Technology* 32:127-147.

Snider, A.C. 2001. MgO Hydration Experiments Conducted at SNL/ABQ. *Sandia National Laboratories Technical Baseline Reports, WBS 1.3.5.4, Repository Investigations, Milestone RI020, July 31, 2001*. Sandia National Laboratories, Carlsbad, New Mexico. ERMS 518970, pp. 4-1 to 4-3.

Snider, A.C. 2002. MgO Studies: Experimental Work Conducted at SNL/Carlsbad. Efficacy of Premier Chemicals MgO as an Engineered Barrier, *Sandia National Laboratories Technical Baseline Reports, WBS 1.3.5.3, Compliance Monitoring; WBS 1.3.5.4, Repository Investigations, Milestone RI110, January 31, 2002*. Sandia National Laboratories, Carlsbad, New Mexico. ERMS 520467, pp. 3.1-1 to 3.1-18.

Snider, A.C. 2003a. Hydration of Magnesium Oxide in the Waste Isolation Pilot Plant, *Sandia National Laboratories Technical Baseline Reports, WBS 1.3.5.3, Compliance Monitoring; WBS*

1.3.5.4, *Repository Investigations, Milestone RI 03-210, January 31, 2003*. Sandia National Laboratories, Carlsbad, New Mexico, ERMS 526049, pp. 4.2-1 to 4.2-6.

Snider, A.C. 2003b. *Verification of the Definition of Generic Weep Brine and the Development of a Recipe for this Brine*. Unpublished Analysis Report, Sandia National Laboratories, Carlsbad, New Mexico, April 8, 2003, ERMS 527505.

Snider, A.C., and Y. L. Xiong. 2002. Carbonation of Magnesium Oxide, *Sandia National Laboratories Technical Baseline Reports, WBS 1.3.5.3, Compliance Monitoring; WBS 1.3.5.4, Repository Investigations, Milestone RI130, July 31, 2002*. Sandia National Laboratories, Carlsbad, New Mexico, ERMS 523189, pp. 4.1-1 to 4.1-28.

SNL (Sandia National Laboratories). 1997. *Chemical Conditions Model: Results of the MgO Backfill Efficacy Investigation*. Prepared for the U.S. Department of Energy, Carlsbad Area Office, April 23, 1997. Docket No. A-93-02, II-A-39.

Sonderholm, L., P.M. Almond, S. Skanthakumar, R.E. Wilson and P.C. Burns. 2008. The structure of the plutonium oxide nanocluster $[\text{Pu}_{38}\text{O}_{56}\text{Cl}_{54}(\text{H}_2\text{O})_8]^{14-}$. *Angew. Chem. Int. Ed.* 47:298-302.

Stein, C.S. 1985. *Mineralogy in the Waste Isolation Pilot Plant (WIPP) Facility Stratigraphic Horizon*. SAND-85-0321, Sandia National Laboratories, Albuquerque, New Mexico, September 1985.

Stein, J. 2005. *Estimate of Volume of Brine in Repository That Leads to a Brine Release*. Memorandum to L.H. Brush, April 13, Sandia National Laboratories, Carlsbad, New Mexico, ERMS 539372.

Stein, J., and M. Nemer. 2005. *Analysis Plan for Updating the Microbial Degradation Rates for Performance Assessment*. AP-116, Sandia National Laboratories, Carlsbad, New Mexico, ERMS 538596.

Stein, J.S., and W.P. Zelinski. 2004. *Effect of Increased Iron Surface Area from Supercompacted AMWTP Waste on Long-Term Repository Conditions as Modeled in Performance Assessment of the WIPP*. Sandia National Laboratories Carlsbad Programs Group, Carlsbad, New Mexico.

Storz, L. 1996. *Estimate of the Amount of $\text{Ca}(\text{OH})_2$ Contained in the Portland Cement Fraction of the Waste for Disposal in the WIPP*. Memorandum to Y. Wang, Sandia National Laboratories, Albuquerque, New Mexico, ERMS 240351, June 24, 1996.

Suzuki, Y., S.D. Kelly, K.M. Kemner, and J.F. Banfield. 2003. Microbial populations stimulated for hexavalent uranium reduction in uranium mine sediment. *Applied and Environmental Microbiology* 69:1337-1346.

TEA (Trinity Engineering Associates). 2000. *Review of Comments and Issues Raised by the Environmental Evaluation Group in Report EEG-77 - "Plutonium Chemistry Under Conditions*

Relevant for WIPP Performance Assessment,” Prepared for the U.S. Environmental Protection Agency Office of Radiation and Indoor Air, November 30, 2000.

TEA (Trinity Engineering Associates). 2001. *Actinide Solubility Technical Exchange Meeting Report, Albuquerque, New Mexico, May 24, 2001.* Prepared for the U.S. Environmental Protection Agency Office of Radiation and Indoor Air, June 8, 2001.

TEA (Trinity Engineering Associates). 2002. *DOE-EPA Repository Chemistry Meeting, Carlsbad, New Mexico, November 19-20, 2002.* Prepared for the U.S. Environmental Protection Agency Office of Radiation and Indoor Air, December 5, 2002.

TEA (Trinity Engineering Associates) 2004. *Review of Effects of Supercompacted Waste and Heterogeneous Waste Emplacement on WIPP Repository Performance. Final Report.* Prepared for U.S. Environmental Protection Agency, Office of Radiation and Indoor Air, Washington, DC, March 17, 2004.

Telander, M.R., and R.E. Westerman. 1993. *Hydrogen Generation by Metal Corrosion in Simulated Waste Isolation Pilot Plant Environments: Progress Report for the Period November 1989 through December 1992.* SAND92-7347, Sandia National Laboratories, Albuquerque, New Mexico, ERMS 223456.

Telander, M.R., and R.E. Westerman. 1997. *Hydrogen Generation by Metal Corrosion in Simulated Waste Isolation Pilot Plant Environments.* SAND96-2538, Prepared for Sandia National Laboratories, Albuquerque, New Mexico by Pacific Northwest National Laboratory, Richland, Washington.

Triay I.R. 2002. December 10, 2002 Letter to Frank Marcinowski related to AMWTF planned change request.

Triay, I.R. 2005. *Partial Response to Environmental Protection Agency (EPA) September 2, 2004, Letter on Compliance Recertification Application.* U.S. Department of Energy Carlsbad Field Office, letter to Elizabeth Cotsworth, U.S. Environmental Protection Agency Office of Radiation and Indoor Air, Washington, DC, January 19, 2005.

Vance, R.E., R.W. Mathewes, and J.J. Clague. 1992. 7000-year record of lake-level change on the northern Great Plains: a high-resolution proxy of past climate. *Geology* 20:879-882.

Villareal, R. 1996. *Test Plan for the Actinide Source-Term Waste Test Program (STTP).* MST5-TP-TST1-013/1, Sandia National Laboratories, July 16, 1996.

Villareal, R., J.M. Bergquist, and S.L. Leonard. 2001. *The Actinide Source Term Waste Test Program (STTP) Final Report, Volume I.* Los Alamos National Laboratory, LA UR 01 6822.

Vugrin, E.D., M.B. Nemer, and S. Wagner, 2006. *Uncertainties Affecting MgO Effectiveness and Calculation of the MgO Effective Excess Factor.* Revision 0, Sandia National Laboratories, Carlsbad, New Mexico.

Vugrin, E.D., M.B. Nemer, and S. Wagner, 2007. *Uncertainties Affecting MgO Effectiveness and Calculation of the MgO Effective Excess Factor*. Revision 1, Sandia National Laboratories, Carlsbad, New Mexico. ERMS 546377.

Wall, D. 2001. *Technical Baseline Migration Parameter Report*. Sandia National Laboratories Document, Revision 0, September 28, 2001. Sandia National Laboratories, Carlsbad, New Mexico.

Wall, N.A., 2005. *Preliminary Results for the Evaluation of Potential New MgO*. Sandia National Laboratories, Carlsbad, New Mexico. ERMS 538514.

Wall, N.A., and D. Enos. 2006. *Iron and Lead Corrosion in WIPP-Relevant Conditions, Test Plan TP 06-02*. Revision 1, Sandia National Laboratories, Carlsbad and Albuquerque, New Mexico. April 24, 2006.

Wall, N.A. and S.A. Mathews. 2005. Sustainability of humic acids in the presence of magnesium oxide. *Applied Geochemistry* 20:1704-1713.

Wall, N.A., and D.E. Wall. 2004. *Discussion on the Influence of Organic Ligands on the Solubility of U(VI)*. Memorandum to the WIPP Record Center, November 30, 2004, Sandia National Laboratories, Carlsbad, New Mexico, ERMS 537938.

Wang, Y. and L.H. Brush. 1996. *Estimates of Gas-Generation Parameters for the Long-Term WIPP Performance Assessment*. Unpublished memorandum to M.S. Tierney, Sandia National Laboratories, Albuquerque, New Mexico, January 26, 1996, WPO 31943.

Wang, Y., L.H. Brush, H. Gao, and J.S. Stein. 2003. Re-evaluation of Microbial Gas Generation Rates for Long-Term WIPP Performance Assessment. *Sandia National Laboratories Technical Baseline Reports, WBS 1.3.5.3, Compliance Monitoring; WBS 1.3.5.4, Repository Investigations, Milestone RI 03-210, January 31, 2003*. Sandia National Laboratories, Carlsbad, New Mexico, pp. 3.1-1 to 3.1-12.

Wang, Z., R.C. Moore, A.R. Felmy, M.J. Mason, and R.K. Kukkadapu. 2001. A study of the corrosion products of mild steel in high ionic strength brines. *Waste Management* 21:335-341.

Weiner, R.F. 1996. *Oxidation State Distribution in the WIPP*. Presentation at Technical Exchange Meeting on June 27, 1996, Sandia National Laboratory, Albuquerque, New Mexico.

Wilson, C., D. Porter, J. Gibbons, E. Oswald, G. Sjoblom, and F. Caporuscio. 1996a. *Conceptual Models Peer Review Report*, Prepared for the U.S. Department of Energy, Carlsbad, New Mexico, July 1996, Docket No. A-93-02 Item II-G-1.

Wilson, C., D. Porter, J. Gibbons, E. Oswald, G. Sjoblom, and F. Caporuscio. 1996b. *Conceptual Models Supplementary Peer Review Report*, Prepared for the U.S. Department of Energy, Carlsbad, New Mexico, December 1996, Docket No. A-93-02 Item II-G-12.

Wilson, C., D. Porter, J. Gibbons, E. Oswald, G. Sjoblom, and F. Caporuscio. 1997a. *Conceptual Models Second Supplementary Peer Review Report*, Prepared for the U.S. Department of Energy, Carlsbad, New Mexico, January 1997, Docket No. A-93-02 Item II-G-21.

Wilson, C., D. Porter, J. Gibbons, E. Oswald, G. Sjoblom, and F. Caporuscio. 1997b. *Conceptual Models Third Supplementary Peer Review Report*, Prepared for the U.S. Department of Energy, Carlsbad, New Mexico, April 1997, Docket No. A-93-02 Item II-G-22.

Wolery, T.J., and D.C. Sassani. 2007. *Analysis of Sulfate Reduction Modeling by Brush et al. (2006)*. Prepared by Lawrence Livermore National Laboratory and Sandia National Laboratories, September 4, 2007.

WTS (Washington TRU Solutions LLC). 2003. *Specification for Prepackaged MgO Backfill*. Unpublished Specification, D-0101, Rev. 5. Washington TRU Solutions LLC, Carlsbad, New Mexico.

WTS (Washington TRU Solutions) 2005. *Specifications for Prepackaged Backfill*. Waste Isolation Pilot Plant Procedure D-0101, Revision 7, May 2005.

Xia, Y., L. Rao, A.R. Felmy, and D. Rai. 2001. Determining the Distribution of Pu, Np, and U Oxidation States in Dilute NaCl and Synthetic Brine Solutions. *Journal of Radioanalytical and Nuclear Chemistry* 250:27-37.

Xiong, Y.-L. 2004. *A Correction of the Molecular Weight of Oxalate in FMT_021120.CHEMDAT and Incorporation of Calcium Oxalate Monohydrate (Whewellite) Into CHEMDAT With Its Recommended Dimensionless Standard Chemical Potential (μ^0/RT) Value*. Memorandum to L.H. Brush, June 8, 2004, Sandia National Laboratories, Carlsbad, New Mexico, ERMS 535813.

Xiong, Y. 2009. *Release of FMT_090720.CHEMDAT*. E-mail to Jennifer Long, July 22, 2009, Sandia National Laboratories, Carlsbad, New Mexico, ERMS 539304.

Xiong, Y., and A.C. Snider. 2003. *Carbonation Rates of the Magnesium Oxide Hydration Product Brucite in Various Solutions*. Sandia National Laboratories Technical Baseline Reports, WBS 1.3.5.4, Repository Investigations, Milestone RI 03-210, January 31, 2003. Sandia National Laboratories, Carlsbad, New Mexico, ERMS 526049, pp. 4.3-1 to 4.3-11.

Xiong, Y. L.H., Brush, A. Ismail, and J.J. Long. 2009a. *Uncertainty Analysis of Actinide Solubilities for the WIPP CRA-2009 PABC*. Sandia National Laboratories, Carlsbad, New Mexico, ERMS 552500.

Xiong, Y., H. Deng, M.B. Nemer and S. Johnsen. 2009b. *Thermodynamic Data for Phase 5 ($Mg_3Cl(OH)_5 \cdot 4H_2O$) Determined from Solubility Experiments*. Memorandum to L.H. Brush, May 8, 2009, Sandia National Laboratories, Carlsbad, New Mexico, ERMS 551706.

Xiong, Y., E.J. Nowak, and L.H. Brush. 2004. *Updated Uncertainty Analysis of Actinide Solubilities for the Response to EPA Comment C-23-16*. Sandia National Laboratories, Carlsbad, New Mexico, ERMS 538219.

Xiong, Y., E.J. Nowak, and L.H. Brush. 2005. *Updated Uncertainty Analysis of Actinide Solubilities for the Response to EPA Comment C-23-16, Rev. 1 (Supersedes ERMS 538219)*. Sandia National Laboratories, Carlsbad, New Mexico, ERMS 539595.

Xiong, Y., H. Deng, M. Nemer and S. Johnsen. 2010a. Experimental Determination of the Solubility Constant for Magnesium Chloride Hydroxide Hydrate ($Mg_3Cl(OH)_5 \cdot 4H_2O$, Phase 5) at Room Temperature, and Its Importance to Nuclear Waste Isolation in Geological Repositories in Salt Formations. *Geochimica et Cosmochimica Acta*, in press, accepted May 19, 2010, accessed June 8, 2010 at www.sciencedirect.com/science/journal/00167037.

Xiong, Y., L.H. Brush, J. W. Garner and J.J. Long. 2010b. *Response to Three EPA Comments Pertaining to Comparisons of Measured and Predicted Dissolved and Colloidal Th(IV) and Am(III) Concentrations*. Revision 1. (Supersedes ERMS 553409.) Sandia National Laboratories, Carlsbad, New Mexico, ERMS 553595.

Yamazaki, H., B. Lagerman, V. Symeopoulos, and G.R. Choppin. 1992. Solubility of Uranyl in Brine. *Proceedings of the Third International High Level Radioactive Waste Management Conference*, Las Vegas, Nevada, American Nuclear Society, La Grange Park, and American Society of Engineers, New York, pp. 1607–1611.

Zhang, P., J. Hardesty, and H. Papenguth. 2001. *MgO Hydration Experiments Conducted at SNL-ABQ*. Sandia National Laboratories Technical Baseline Reports, WBS 1.3.5.4, Compliance Monitoring; WBS 1.3.5.4, Repository Investigations, Milestone RI010, January 31, 2001. Sandia National Laboratories, Carlsbad, New Mexico, ERMS 516749, pp. 55-65.